UNDERSTANDING IMMUNE DEFICIT IN ALCOHOL RELATED LIVER DISEASE WITH THE DEVELOPMENT OF A HUMAN 3D ORGANOID MODEL

by

LAURA ELIZABETH HARFORD

A thesis submitted to the University of Birmingham for the degree of
DOCTOR OF PHILOSOPHY

Centre for Liver and Gastrointestinal Research
Institute of Immunology and Immunotherapy
School of Medical and Dental Sciences
University of Birmingham
March 2023

Acknowledgements

I consider it a true privilege to have been surrounded by such incredible people throughout this journey. This thesis has been built with the kindness of others, without whom this project would not have been possible.

I would like first to thank Trish Lalor for her supervision and support. You offered advice and guidance, while helping us to grow. Thank you to Janet Lord for her expertise and insight, which helped to shape some of the most interesting findings of this project. To the members of the Lord and Lalor labs - in particular Kirsty, John, Lozan, Nic and Beth - thank you for always being there whenever help was needed. I would also like to thank Simon and the whole Hirota lab, who paved the way for me to incorporate new technology into my PhD. To members of the CLGR past and present - there are too many people to thank individually, but I wanted to extend particular gratitude to Reenam, Ellie, Janine, Scott, Gary, Dan, Marco, and Paul for your support and generosity. To Emma, Panda and Alex for making this happen. To Graham, for your guidance and encouragement.

To my amazing family and friends, I am grateful for you every day. To Mark, Jenny and Jen. To all of my parents and my sister, who have supported me unwaveringly and unconditionally every step of the way. To Ren, who has never let me go a single day without smiling.

I would like to thank the Wellcome Trust for funding this project, the incredible NHS staff who supported it and the patients who so generously consented to being a part of it. Thank you to MIDAS; Robin, Steve, Graham, Eva and Vikki for the opportunity to complete this work.

Abstract

The UK is in the midst of a liver disease epidemic. Deaths are rising, and yet awareness and treatment options remain limited. In patients with alcohol related liver disease (ARLD), outcomes are particularly poor, and patients are highly susceptible to infection. In this project we aimed to understand how the peripheral immune phenotype changes in patients with both chronic and acute ARLD, and how this is influenced by crosstalk with a damaged liver. We were able to analyse blood samples from patients with different stages of ARLD, and investigate changes in peripheral blood cell composition. We saw striking differences in neutrophil number and phenotype, which also translated to reduced phagocytic ability – particularly in patients with acute alcoholic hepatitis. Utilising progenitor cells from both cirrhotic and healthy primary liver tissue, we developed a human 3D organoid model to generate cells which we were able to expand and differentiate to both a ductal-like and hepatocyte-like state. Differentiated organoids showed expression of key detoxification enzymes and liver markers, as well as ability to form lipid droplets. We saw some differences between ARLD and donor derived organoids, including altered expression of albumin and complement genes. The model showed limited responses to alcohol exposure, however ductal organoids induced an increase in NETosis in healthy neutrophils and both ductal and hepatocyte-like organoids exhibited strong neutrophil chemotactic properties. We have therefore generated a human tissue derived model which can support the study of liver-neutrophil crosstalk in ARLD, and have evidence which may contribute to explanations of reduced neutrophil functionality and increased sepsis risk in these patients.

Table of Contents

Table of Contents *4*

List of Figures *7*

List of Tables *10*

Abbreviations *11*

Chapter 1 – Introduction *13*

1.1 Liver architecture and function **13**

1.2 Liver regeneration and the progenitor population **18**

1.3 The liver as a central immune hub **20**

1.3.1 Immune cell recruitment 20

1.3.2 Immune tolerance 21

1.3.3 Endotoxin interactions in the liver 22

1.3.4 Synthesising tools for systemic immune function 24

1.4 The liver as a "detox" organ **25**

1.4.1 Metabolism of alcohol 26

1.5 Alcohol Related Liver Disease **28**

1.5.1 Symptoms and Diagnosis 28

1.5.2 Stages of ARLD 29

1.5.3 Challenges with predicting progression 33

1.6 Treatment and management of ARLD **34**

1.6.1 Treatments in alcoholic hepatitis 35

1.6.2 Treatments for late-stage ARLD 37

1.7 Immunocompromise and Infection in Alcohol-Related Liver Disease **39**

1.8 The role of Neutrophils in ARLD **41**

1.9 Modelling liver disease **44**

1.9.1 Modelling the liver environment in 2D culture 45

1.9.2 Modelling liver disease *in vivo*: the pros and cons of mouse models 48

1.9.3 The promise of 3D *in vitro* models 50

1.9.4 Organoids – the next step in *in vitro* modelling 51

1.10 Aims of this thesis **53**

Chapter 2 – Methodology *54*

2.1 Patient groups and ethical approval **57**

2.2 Calculation of clinical scores **59**

2.3 Analysis of phenotype and function of cells in peripheral blood **60**

2.3.1 Full blood count 60

2.3.2 Measurement of phagocytic ability of peripheral blood neutrophils 60

2.3.3 Measurement of oxidative burst in human neutrophils 61

2.3.4 Production of Neutrophil Extracellular Traps (NETs) by human neutrophils 63

2.4 Imaging of human liver tissue **67**

2.4.1 Immunohistochemistry in human liver sections 67

2.4.2 Immunofluorescent staining of human liver sections 69

2.5 Analysing gene expression in whole tissue 72
2.5.1 RNA extraction 72
2.5.2 cDNA synthesis 73
2.5.3 Analysis of gene expression using quantitative PCR (qPCR) 75

2.6 Human Liver Organoid Culture 77
2.6.1 Isolation of progenitor cells from fresh human liver tissue for 3D organoid culture 77
2.6.2 Isolating hepatic organoids from cryopreserved tissue 81
2.6.3 Maintenance culture of hepatic organoids (expansion period) 83
2.6.4 Cryopreservation and subsequent re-establishment of organoid cultures 84
2.6.5 Differentiation into hepatocyte-like organoids 85

2.7 Investigating phenotype and function of primary human liver derived organoids 86
2.7.1 Analysis of hepatic progenitor cell phenotype using flow cytometry 86
2.7.2 Removal of organoids from Matrigel for downstream applications 87
2.7.3 Monitoring organoid growth over time 88
2.7.4 Acute stimulation of organoids with ethanol and LPS 89
2.7.5 Treatment with fatty acids to assess formation of lipid droplets 90
2.7.6 Analysing organoid gene expression via qPCR 90
2.7.7 qPCR arrays to investigate expression of multiple pathway components 90
2.7.8 Analysis of fibrosis associated gene changes with NanoString technology 91
2.7.9 Immunofluorescent staining of whole organoids 91
2.7.10 IL-8 ELISA 92
2.7.11 Quantification of multiple analytes in organoid supernatant using Proteome Profilers 94
2.7.12 Assessing chemotactic potential of organoid media via neutrophil migration 95
2.7.13 Investigating Organoid-neutrophil co-culture 96

2.8 In Silico analysis of sequencing data 97
2.8.1 Differential gene analysis 97
2.8.2 Clustering of differential gene analysis data 98

Chapter 3 – What are we trying to model? 99

3.1 Introduction 99

3.2 Results 102
3.2.1 Analysis of peripheral blood from ARLD patient cohorts 102
3.2.2 Neutrophil function in AH and cirrhosis 111
3.2.3 Characterising the local tissue environment in healthy and diseased livers 113

3.3 Discussion 126
3.3.1 Considerations in our patient cohort (blood) 126
3.3.2 Cellular and biochemical components of peripheral blood 129
3.3.3 Changes in neutrophil number and function 133
3.3.4 Characterising whole liver tissue 135
3.3.5 Summary 139

Chapter 4 – Developing an Organoid Model 141

4.1 Introduction 141

4.2. Results 143
4.2.1 Adapting protocols for organoid isolation from normal and cirrhotic liver specimens 143
4.2.2 Confirmation of ductal-like phenotype in culture 152
4.2.3 Differentiation into hepatocyte-like organoids 155

4.3 Discussion 164
4.3.1 Understanding organoid phenotype 164
4.3.2 Overcoming culture challenges 168

4.3.3 Adapting published protocols 172
4.3.4 Limitations of source material 175
4.3.5 Summary 176

Chapter 5 – Modelling injury in 3D cultures 178

5.1 Introduction 178

5.2 Results 180
5.2.1 Selecting appropriate injurious stimuli 180
5.2.2 Understanding organoid response to injury 186
5.2.3 Do supernatants from hepatic organoids influence neutrophil function? 199

5.3 Discussion 205
5.3.1 Alcohol metabolism 205
5.3.2 Inflammatory responses to injury 209
5.3.3 Neutrophil – liver crosstalk 214
5.3.4 Conclusions 218

Chapter 6 – General Discussion 220
6.1 Modelling ARLD *in vitro*: where do we stand? 221
6.2 Organoid technology in liver research: how far have we come? 224
6.3 Capturing liver disease in a dish: where could we go? 227
6.4 "How much do you know about your liver?" 233

Chapter 7 – Future work 234
7.1 The next steps 234
7.2 Looking further ahead 236
7.3 Final thoughts 238

Supplementary data 240

References 243

List of Figures

Figure 1.1: The structure of the liver lobule 14
Figure 1.2: Modification of ethanol by liver enzymes. 27
Figure 1.3: Stages of progression in Alcohol Related Liver Disease (ARLD 30
Figure 2.1: Gating strategy for PHAGOTEST and PHAGOBURST neutrophil function assays. 63
Figure 2.2: Density gradient from centrifuged Leukocyte Rich Layer.....65
Figure 2.3: Quantifying immunohistochemical staining using FIJI software.....71
Figure 2.4 Isolation of progenitor cells from whole human liver. 80
Figure 2.5: Timeline for isolation, expansion and differentiation of 3D organoids.....85
Figure 2.6: Analysis of hepatic progenitor cell phenotype using flow cytometry. 87
Figure 3.1: Alcoholic hepatitis is associated with a reduction in hematocrit and altered red blood cell phenotypes. 105
Figure 3.2: Comparison of peripheral blood cellular composition in healthy donors and patients across the ARLD spectrum. 106
Figure 3.3: Comparison of white blood cell number in healthy donors and patients across the ARLD spectrum 108
Figure 3.4: Markers of leukocyte activation status and immune response are elevated in alcoholic hepatitis. 109
Figure 3.5: Correlations between immature granulocytes and clinical indicators of alcoholic hepatitis. 110
Figure 3.6: Neutrophil phagocytosis is impaired in AH.....112
Figure 3.7: Histochemical staining of human liver specimens 114
Figure 3.8: Increased ductular reactivity in ALD livers indicated by staining with progenitor cell markers. 116
Figure 3.9: Patterns of regeneration are not consistent across explanted ALD livers. 117
Figure 3.10: Hepatic TLR4 is not altered at the mRNA level in alcohol-related cirrhosis. 118
Figure 3.11: Changes in gene expression in ALD livers. 119
Figure 3.12: CD45+ immune cells localise to areas of fibrosis in ALD cirrhotic livers.....120
Figure 3.13: Neutrophils are found in the parenchyma during acute alcoholic hepatitis. 121
Figure 3.14: Selection of parenchymal cell types from whole liver single cell sequencing to identify differentially expressed genes in ALD.....122

Figure 3.15: Cluster analysis of data from whole liver single cell sequencing to identify differentially expressed genes in ALD hepatocytes. 123
Figure 3.16: Cluster analysis of data from whole liver single cell sequencing to identify differentially expressed genes in ALD cholangiocytes. 124
Figure 4.1: Schematic illustrating the organoid generation process and experimental outputs. 143
Figure 4.2: Hepatic progenitor cell isolation gives rise to 3D organoid cultures. 145
Figure 4.3: Cryopreserved human liver tissue can be used as a source of hepatic progenitor cells...146
Figure 4.4: Organoids derived from donor and ALD livers grow at similar rates 148
Figure 4.5: Passaging of organoid cultures requires varied split ratios to avoid overcrowding 149
Figure 4.6: Commercially available murine hepatic organoid culture medium cannot be adapted for human hepatic organoid culture. 151
Figure 4.7: Organoids show expression of progenitor cell markers in culture. 153
Figure 4.8: The presence of hepatocyte marker HNF4**α** suggests bipotential progenitor phenotype. 154
Figure 4.9: Differentiation medium causes structural changes in ductal-like organoids resulting in a more hepatocyte-like morphology. 156
Figure 4.10: Changes in expression of hepatocyte markers show differentiation from a ductal-like to a hepatocyte-like phenotype. 159
Figure 4.11: Expression of hepatocyte markers in organoids compared to 2D and 3D cell line cultures. 160
Figure 4.12: Differentiated organoids exhibit hepatocyte functions such as lipid storage. 161
Figure 4.13: Albumin expression differs with differentiation state and tissue origin. 162
Figure 5.1: Ductal and hepatocyte-like organoids express alcohol metabolizing enzymes, which may be altered in the presence of ethanol 182
Figure 5.2: Single dose of ethanol does not alter expression of CYP2E1 or EpCAM in differentiated organoids. 183
Figure 5.3: Common housekeeping gene Cycle threshold (Ct) values are not altered with treatment or differentiation state. 184
Figure 5.4: Exposure to ethanol and LPS does not alter organoid morphology or size, but may induce some release of cell damage marker adenylate kinase. 185
Figure 5.5: Chemokine production by Ductal-like organoids in response to treatment with ethanol and LPS. 187

Figure 5.6: Chemokine production by hepatocyte-like organoids in response to treatment with ethanol and LPS. 188
Figure 5.7: Both ductal and hepatocyte-like organoids produce IL-8 under basal and stimulated conditions. 189
Figure 5.8: Acute treatment with ethanol and LPS does not cause changes to key organoid markers. 191
Figure 5.9: Donor liver derived organoids show a robust genomic response to treatment which is not recreated in cirrhotic liver derived organoids. 194
Figure 5.10: Diminished response to treatment is not due to increased senescence markers in ALD compared to donor derived organoids. 195
Figure 5.11: Differentiated organoids express the genes for several complement proteins 197
Figure 5.12: Organoid expression of complement proteins changes with differentiation and is altered in disease 198
Figure 5.13: Organoids are able to induce neutrophil chemotaxis. 200
Figure 5.14: Neutrophil phagocytosis is not altered by incubation with basal or conditioned organoid medium. 202
Figure 5.15: Ductal - but not hepatocyte-like - organoids induce NETosis in healthy and diseased human neutrophils. 204
Figure S.1: Isotype Matched Control (IMC) images for Immunohistochemical staining of Cytokeratin 19, SOX9 and EpCAM in human liver. 240
Figure S.2: Isotype Matched Control (IMC) images for Immunohistochemical staining of CD45 and TLR4 in human liver. 241
Figure S.3: Isotype Matched Control (IMC) images for Immunofluorescent staining of whole tissue and organoids. 242

List of Tables

Table 2.1: Reagent list detailing supplier and catalogue numbers of reagents used throughout this project. 56
Table 2.2: Inclusion and Exclusion criteria for ARLD patient groups. 58
Table 2.3: Table of antibodies detailing antibody target, host species and isotype, supplier, clone and catalogue number 70
Table 2.4: Conditions for cDNA synthesis from isolated RNA. 74
Table 2.5: Conditions for qPCR reaction in a Roche LightCycler® 480 II. 75
Table 2.6: Table of TaqMan Assay IDs utilised for qPCR analysis in whole liver tissue and 3D organoids. 76
Table 2.7: Organoid media composition. 82
Table 3.1: Summary of clinical and demographic data for blood sample donors. 104

Abbreviations

AH	Alcoholic Hepatitis
ALD	Alcoholic Liver Disease
ACLF	Acute-on-Chronic Liver Failure
ADF	Advanced DMEM/F12
ADH	Alcohol Dehydrogenase
ALP	Alkaline Phosphatase
ALT	Alanine Aminotransferase
APP	Acute Phase Protein
APR	Acute Phase Response
ARLD	Alcohol Related Liver Disease
AST	Aspartate Aminotransferase
AUD	Alcohol Use Disorder
BEC	Biliary Epithelial Cells
BMI	Body Mass Index
BMP-7	Bone morphogenetic protein 7
BSEP	Bile salt export pump
CAID	Cirrhosis Associated Immune Dysfunction
CCL(n)	Chemokine (C-C motif) Ligand (n)
CK19	Cytokeratin 19
CRP	Cre-Reactive Protein
CT	Computerised Tomography
CXCL(n)	Chemokine (C-X-C motif) ligand (n)
CYP	Cytochrome P450
DAMP	Damage Associated Molecular Pattern
DAPI	4’,6-diamidino-2-phenylindole
DAPT	N-[N-(3,5-Difluorophenacetyl-L-alanyl)]-(S)-phenylglycine t-butyl ester
DMEM	Dulbecco's Modified Eagle Medium
DMSO	Dimethyl Sulfoxide
ECM	Extracellular Matrix
EDTA	Ethylenediaminetetraacetic Acid
EGF	Epithelial Growth Factor
EpCAM	Epithelial Cellular Adhesion Molecule
FACS	Fluorescence-Activated Cell Sorting
FCS	Foetal Calf Serum
FFPE	Formalin Fixed Paraffin Embedded
FGF	Fibroblast Growth Factors
G-CSF	Granulocyte Colony-Stimulating Factor
GAHS	Glasgow Alcoholic Hepatitis Score
GI	Gastrointestinal
HCC	Hepatocellular Carcinoma
HGF	Hepatocyte Growth Factor
hiPSCs	human induced Pluripotent Stem Cells

HRP	Horseradish Peroxidase
HSCs	Hepatic Stellate Cells
ICAM-1	Intercellular Adhesion Molecule 1
IDA	Industrial Denatured Alcohol
IHC	Immunohistochemistry
IL-(n)	Interleukin (n)
KC	Kupffer Cell
Lgr5	Leucine-rich repeat-containing G-protein coupled receptor 5
LPS	Lipopolysaccharide
LDL	Low Density Lipoprotein
LSEC	Liver Sinusoidal Endothelial Cell
MBL	Mannose Binding Lectin
MCP1	Monocyte Chemoattractant Protein 1
MELD	Model for End-Stage Liver Disease
MRP2	Multidrug Resistance-Associated Protein 2
NAC	N-acetylcysteine
NAD	Nicotinamide Adenine Dinucleotide (oxidised)
NADH	Nicotinamide Adenine Dinucleotide (reduced)
NAFLD	Non-Alcoholic Fatty Liver Disease
NET	Neutrophil Extracellular Trap
NFκB	Nuclear Factor kappa-light-chain-enhancer of activated B cells
NHS	National Health Service
PAMP	Pathogen Associated Molecular Pattern
PBS	Phosphate Buffered Saline
PCR	Polymerase Chain Reaction
PFA	Paraformaldehyde
PHH	Primary Human Hepatocytes
PMA	Phorbol Myristate Acetate
PRR	Pattern Recognition Receptor
QEHB	Queen Elizabeth Hospital Birmingham
ROS	Reactive Oxygen Species
RPMI	Roswell Park Memorial Institute
SAA	Serum Amyloid A
SOX9	Sex-determining region Y-box 9 (SOX9)
STOPAH	STeroids Or Pentoxifylline for Alcoholic Hepatitis
TBS	Tris Buffered Saline
TLR	Toll-Like Receptor
TNFα	Tumour Necrosis Factor Alpha
UKELD	United Kingdom Model for End-Stage Liver Disease
US	Ultrasound
VAP-1	Vascular Adhesion Protein 1
VCAM-1	Vascular Cell Adhesion Molecule 1

Chapter 1 – Introduction

While mortality rates in the UK have decreased for many major disease groups from cancer to diabetes, the number of deaths due to liver disease has increased 400% since 1970(1). With the population in the midst of a liver disease epidemic, we still lack mechanistic understanding and treatments for many common liver conditions and are now battling with rising incidence due to increases in obesity and alcohol consumption(1). There are many contributing factors to this high mortality rate, and the umbrella term of "liver disease" covers many different conditions affecting several different subgroups of patients. This thesis will focus on Alcohol Related Liver Disease (ARLD) and how this presents in both an acute and chronic setting. Here I begin by introducing the liver and its functions in both health and disease, and discuss some of the challenges faced in both modelling and treating the different presentations of ARLD.

1.1 Liver architecture and function

Possibly one of our most underappreciated biological workhorses, the liver performs over 500 essential functions that span from immune regulation to lipid metabolism(2). As the largest internal organ, it is formed of two lobes that receive over a litre of blood per minute via both the portal vein (~75%) and hepatic artery (~25%)(3). This high throughput of blood, particularly from the portal vein which supplies blood from the gastrointestinal tract, places the liver in a unique position where it is constantly exposed to immune and metabolic stimuli(4). After entering the portal area, blood moves through the liver microvasculature - the hepatic sinusoids - and drains from the hepatic central vein(5). The cellular functional unit within the liver (referred to as liver 'lobules') consists predominantly of hepatocytes (around

60%), alongside biliary epithelial cells (BEC), Kupffer cells, liver sinusoidal endothelial cells (LSEC), and hepatic stellate cells (HSCs)(6).

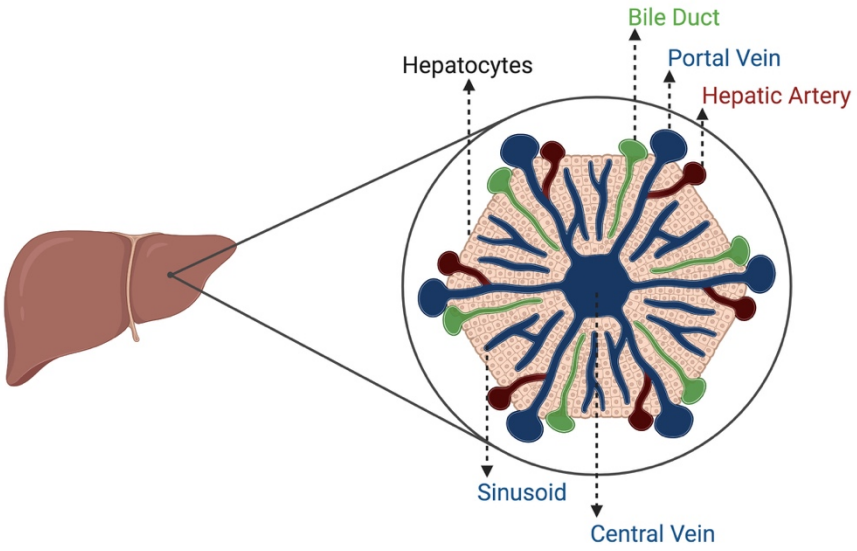


Figure 1.1: The structure of the liver lobule. This diagram illustrates the liver lobule, which is the functional unit within the liver. It is a hexagonal structure which consists predominantly of hepatocytes, organised around a branch of the central vein. Blood enters via the portal vein (from the gastrointestinal tract) and hepatic artery, moves through the hepatic sinusoids (lined with hepatic sinusoidal endothelial cells), and drains via the central vein. Bile that is produced by the hepatocytes is secreted into the bile canaliculi (lined with biliary epithelial cells) and drains into the bile ducts. Image generated in BioRender.

As the main parenchymal cells of the liver, hepatocytes are responsible for the majority of its functions(7). They contain a plethora of highly efficient enzymes involved in the metabolism of xenobiotics, sugars and lipids, alongside producing proteins required for a range of essential biological functions(7, 8). These processes respond to systemic signalling to meet the nutritional requirements of the body**.** Within hepatocytes, lipids can be stored, synthesised and oxidised to maintain energetic and functional homeostasis. Dysregulation of this process can lead to an accumulation of lipids within hepatocytes known as steatosis, which is the precursor to several liver diseases(9). Hepatocytes are also involved in regulation of blood glucose levels, as sugars that have been released by digestion are transported to the liver and converted to glycogen for storage. In response to blood insulin levels, hepatocytes either increase these stores or break them down and release them as glucose during fasting(8). These cells are also responsible for the production and secretion of bile and albumin. Alongside being essential for digestion, bile is the main mechanism for the removal of toxic substances, as well as bile salts and bilirubin which are waste products from red blood cell breakdown(10). Albumin accounts for 10% of liver protein synthesis, and an impressive 75% of plasma protein in humans(11). Albumin also has a number of essential roles - including maintaining oncotic pressure, reduction of oxidative damage, and immunomodulation – all of which are impaired in liver disease due to reduced synthesis and altered function(12, 13).

Kupffer Cells (KCs) are the liver resident macrophages and patrol the liver sinusoids. They are the most abundant tissue resident macrophages in the body and have key roles in both health and disease(14, 15). Under homeostatic conditions, Kupffer cells play a vital role in immunological tolerance within the liver and can release a number of anti-inflammatory

cytokines such as IL-10(16-18). Portal blood carries with it many potential immune stimulants from the digestive system, such as antigens from commensal bacteria or food particles. As expert phagocytes, Kupffer cells act as a clean-up crew to remove these alongside other particles and damaged erythrocytes(14). When activated, KCs can contribute to inflammation via a number of mechanisms, including cytokine release and production of reactive oxygen species (ROS)(19). These are highly reactive oxygen containing molecules that are essential for many biological functions, but can also cause tissue damage and pathogenic inflammation(20). Kupffer cells show high phenotypic plasticity in response to the liver environment and altered KC phenotype is associated with a number of liver diseases in both a pro-inflammatory and anti-inflammatory capacity(21). While KC activation can allow for effective wound healing and immune responses, pro-inflammatory behaviour can further contribute to liver injury(21).

Liver sinusoidal endothelial cells (LSEC) are the second most common cell type in the liver and make up around 50% of the non-parenchymal cell portion(22). These cells line the sinusoids, forming the capillary like circulatory system that is woven throughout the liver. As well as having characteristic endothelial barrier function, these cells play a very active role in immune regulation, and express a number of scavenger receptors that are able to take up and present antigens(23). In disease, they promote angiogenesis and vasoconstriction which contributes to pathology(24). Closely associated with LSEC, stellate cells account for a small percentage of liver cells (5-10%), and their primary function is the storage of retinoids within lipid droplets(25). When activated, these cells transition into proliferative myofibroblasts and are responsible for huge quantities of extracellular matrix (ECM) production. While this process is

advantageous in regards to short term injury repair, dysregulation leads to excess ECM protein deposition and the development of fibrosis(26). This is a hallmark of chronic liver injury, and similarly to the pro-inflammatory state of Kupffer cells, demonstrates how long-term activation of protective processes can evolve into a disease perpetuating environment. The crosstalk between these cell types is essential for homeostasis, with LSEC actively maintaining stellate cell quiescence in healthy conditions(27).

Cholangiocytes or biliary epithelial cells (BEC) are a heterogeneous, dynamic population of cells that line the bile ducts and account for around 5% of liver cells(28). Whilst comparatively much lower in number than hepatocytes, they are responsible for bile transport and modification, without which we lose many essential functions of the liver(29). A number of diseases are related to bile duct dysfunction (known collectively as cholangiopathies), however altered bile duct proliferation is seen across the spectrum of liver diseases. There are various mechanisms via which cholangiocytes proliferate in response to injury, and this increase in biliary cells is commonly referred to as a "Ductular Reaction"(30). This term was first used in the 1950s to describe the altered proliferation of cholangiocytes in disease(31, 32). In 2004, Roskams *et al* defined this phenomenon as "a reaction of ductular phenotype, possibly but not necessarily of ductular origin, in acute and chronic liver disease"(33, Table 1), with the word "reaction" referring to the involvement of surrounding cells. Within this process, hepatic progenitor cells or even mature hepatocytes can expand into duct-like cells. This demonstrates how an already heterogeneous biliary population becomes even more complex in the context of liver injury. We are still lacking knowledge on how these cells contribute to inflammation and disease. Biliary cells have been shown to regulate immune

responses via secretion of cytokines and chemokines, influence the activation of ECM depositing cells, and even contribute to the senescent secretome(28). They are also able to directly bind and recognise bacterial products, giving them an essential role in pathogen responses within the liver(34).

Key points:

- The liver is an extremely complex organ with a wide range of essential functions
- Most of these are undertaken by hepatocytes, however crosstalk between multiple cell types is essential for homeostasis
- Dysregulation of beneficial processes such as inflammation and wound healing can contribute to disease pathology

1.2 Liver regeneration and the progenitor population

The remarkable regenerative capacity of the liver after injury has been a concept studied since the legends of Prometheus in ancient Greece, and yet is still not fully understood(35). The widely used rat hepatectomy model shows that even after surgical removal of 60% of liver tissue, the remaining liver is able to regenerate to its full mass within 5-7 days(36). Even in the cases of patients who are living liver donors, a study showed that liver mass was largely recovered within three months(37). While we refer to this process as regeneration, it is in fact better described as hepatocyte hyperplasia, where we see an increase in liver mass from replicating hepatocytes rather than true regeneration from a stem cell population(38). While hepatocytes are generally quiescent in healthy liver, serial transplantation models have shown that these cells have replicative capacity on par with hematopoietic stem cells after injury(39).

However, when injury or disease hinders hepatocyte replication, we see an activation of progenitor driven regeneration(40). Historically, nomenclature regarding hepatic stem cell function and phenotype has been poorly defined. “True” liver stem cells - sometimes referred to in the literature as “Oval cells”(41)- were described based on morphological changes to the nucleus in response to injury in rat livers. While these are now accepted as the source of liver progenitors in rats, more recent research is moving away from this terminology in humans(42). It is generally accepted that there is a population of bi-potential progenitors, which have the ability to differentiate into either biliary epithelial cells or hepatocytes, and are generally classified by markers such as EpCAM, SOX9 and Cytokeratin 19 (CK19)(43). However, there is a crossover between these markers and the normal biliary cell population, suggesting that within the heterogeneous collection of cholangiocytes, there exist more plastic progenitors that are able to differentiate in to hepatocyte-like cells(44). They are believed to originate from within the Canals of Hering, the interface between the hepatic canaliculi and biliary tree, and expand rapidly in response to injury(45). To add to this challenging topic however, it has even been demonstrated that injured hepatocytes can also dedifferentiate and contribute to the bipotential progenitor cell pool(46), or that circulating stem cells from blood and bone marrow can also differentiate to hepatocytes within the liver(47-49). It is believed that in large part, these progenitor cells give rise to the “ductular reactions” seen in disease, although these responses vary depending on the type of liver injury(50). Understanding this phenomenon has remained a challenge since animal models do not capture the complexity or heterogeneity of the processes seen in humans. While these cells clearly have an essential role in regeneration and replacing lost liver mass, they are also associated with fibrogenesis, immune cell recruitment and inflammatory cytokine release(50-

52). The ability to isolate these progenitor cell populations from human liver to use in *in vitro* investigative models is therefore attractive. Their plasticity and influence in disease makes them an interesting research tool, and therefore much of the work in my thesis considers the isolation and culture of such cells in the context of alcohol-related injury.

Key points:

- Whilst most liver regeneration is due to hepatocyte proliferation, there is a bi-potential progenitor population that can differentiate into hepatocytes or cholangiocytes
- "Ductular Reactions" are a phenomenon seen in most liver diseases, which includes expansion of these progenitor cells, and are also associated with disease pathogenesis

1.3 The liver as a central immune hub

In earlier sections, I have highlighted the unique site of antigen exposure within the liver and the potential for many hepatic cells to contribute to inflammatory responses. It is next important to understand the scale of the influence that the liver has on both local and systemic immune function, and how this is altered in ARLD.

1.3.1 Immune cell recruitment

The liver contains a large and diverse population of resident immune cells, which play a vital role in tissue homeostasis and infection control(53). However, the liver is also uniquely designed to enable further infiltration of circulating immune cells in response to injury or infection. From an architectural perspective, the arrangement of hepatic sinusoids results in slow blood flow, which encourages immune cell interaction with LSEC(23). These cells also lack a basement membrane and tight junctions, which would usually obstruct migrating cells,

and are highly permeable due to specially adapted fenestrations – allowing efficient communication between the tissue and circulating blood cells(22, 54). The release of chemokines such as CXCL8 (IL-8), CCL2 and CCL20 by both parenchymal and non-parenchymal cells of the liver recruits immune cells from the periphery(55), and expression of adhesion molecules such as VAP-1 and VCAM-1 encourages immune trafficking(56, 57). Alongside more traditional antigen presenting cells like KCs and dendritic cells, LSEC and hepatocytes are also able to present antigens to circulating immune cells and induce activation and inflammatory responses(58). Collectively, these features make the liver highly effective at capturing and retaining immune cells from the peripheral blood, supporting swift and effective responses to injury. Unfortunately, dysregulation of these processes result in excessive recruitment of pro-inflammatory cells that can contribute to local tissue damage, and an increased immune presence in the liver is a hallmark of both acute and chronic liver disease(59).

1.3.2 Immune tolerance

In order to maintain homeostasis, immune responses within the liver are tightly regulated to ensure active immune surveillance and clearance of pathogens, whilst maintaining tolerance to self-antigens and stimuli from the gastrointestinal (GI) tract. An example of this is the increased tolerance of liver transplants compared to other organs, demonstrated with porcine liver allographs in the 1960s(60). Impressively, both animal model and patient studies have shown that liver transplants can induce tolerance in recipients when they receive a second organ allograft from the same donor, which also demonstrates the strong influence that liver signalling has on systemic immunity(61).The liver has a complex baseline expression

of pro (such as interferon gamma) and anti-inflammatory (such as IL-10) cytokines, and these carefully moderate the responses of both resident and circulating immune cells(62).

The cells of the liver can induce adaptive tolerance via a number of mechanisms. A combination of direct (via antigen presentation and costimulatory molecules) and indirect (via release of anti-inflammatory cytokines such as IL-10) interaction with T cells can result in changes such as induction of regulatory T cells (Tregs) and removal of activated $CD8^+$ T cells(63). This activity is furthered by hepatic dendritic cells, which have also been shown to have an immature phenotype that promotes tolerance(64). As highlighted above, the influence of this anti-inflammatory behaviour is not limited to the liver microenvironment. Overall, this promotion of tolerance enables the liver to withstand continuous exposure to immune stimuli from the GI tract, and protect the body from excessive inflammation. Loss of these functions in liver injury can therefore result in a systemic increase in inflammation, which can contribute to pathogenesis(62).

1.3.3 Endotoxin interactions in the liver

One of the main initiators of immune activation is the recognition of either Pathogen Associated or Damage Associated Molecular Patterns (PAMPs and DAMPs respectively), by Pattern Recognition Receptors (PRRs)(65). PAMPs (including bacterial products like Lipopolysaccharide (LPS)) and DAMPs (stress associated endogenous antigens such as extracellular DNA) are conserved patterns which are frequently associated with infection and injury. Toll-like receptors (TLRs) are one of the most important and extensively studied families of PRRs, and recognise a wide range of both PAMPs and DAMPs(66). Binding of ligand

to these receptors initiates a downstream signalling cascade, activating transcription factors such as NFκB and inducing production of pro-inflammatory cytokines(66). Varied expression of TLRs is found throughout the parenchymal and non-parenchymal cells of the liver, although expression at the mRNA level in multiple cell types does not necessarily translate to responses *in vivo*(67). Of particular note, hepatocytes express TLRs 1-10 at a translational level, but respond predominantly to stimulation of TLR2 and TLR4 (by lipoproteins(68) and LPS respectively(69)). TLR4 is expressed on most hepatic cells, and is of particular interest due to both its unusual signalling in the liver compared to other tissues and the increased influence of LPS in patients with ARLD(70). Ordinarily, TLR4 signalling would elicit a strong inflammatory response, including production of cytokines such as TNFα and IL-8(71). However, in a healthy liver, activation of this receptor often has the opposite effect and induces anti-inflammatory actions, including downregulation of antigen presentation in LSEC and production of cytokines such as IL-10(72). This allows for a level of tolerance to LPS, which the main component of the outer membrane of gram negative bacteria and is therefore one of the antigens to which the liver is most commonly exposed from commensal gut bacteria(73). This molecule, also known as endotoxin, is also found on pathogenic gram-negative bacteria, and it is therefore essential that both the liver parenchyma and resident immune cells have a high level of tolerance to accommodate gut derived LPS while still being able to mount an effective response to infection. Hepatocytes, LSEC and Kupffer cells have all been demonstrated to have a role in clearance of LPS from circulation(74-76), possibly via the LDL receptor(77), which contributes to local and systemic tolerance. In ARLD however, we see a sensitisation to LPS in the liver, which leads to inflammation and damage within the tissue(78). When combined with the alcohol-induced increase in LPS exposure from the gut (as discussed in Section 1.7), this

molecule plays a significant role in disease pathogenesis, and is therefore included in the experimental models discussed in this thesis.

1.3.4 Synthesising tools for systemic immune function

Hepatocytes are responsible for the production of many of the proteins found in our serum. Amongst these are several key immune regulators, including components of the "acute phase response" (APR). The APR is a systemic, non-specific immune response to injurious stimuli that includes fever, changes in the vasculature, and alterations in liver function that result in the production of acute phase proteins (APPs) to promote pathogen clearance and destruction(79). Of these proteins, some of the most significant include C-reactive protein (CRP), Serum Amyloid A (SAA) and components of the complement system, which all contribute to systemic alterations in immune function(80). The complement system is comprised of over 50 different proteins, of which hepatocytes synthesise 80-90% of the total pool(81, 82). In the presence of PAMPs, compliment proteins sequentially activate each other during the "complement cascade", resulting in opsonisation of bacteria, formation of a membrane attack complex (lysis of pathogens) and increased inflammation. This occurs via one of three pathways depending on the way the proteins are activated; the classical pathway, alternative pathway, and mannose binding lectin (MBL) pathway(83). Dysregulation of this pathway is associated with a number of liver diseases, and so a delicate balance is essential in order to protect against both pathogens and uncontrolled inflammation(82). Furthermore, the complement system has been implicated in every stage of ARLD(84). Alongside proteins that are produced as part of the APR (positive APPs), there is a compensatory reduction in other liver proteins (negative APPs)(79). This shifts the balance within hepatocytes and results

in lower production of essential proteins such as albumin, which is a further consequence of sustained inflammation(85, 86).

This role in synthesising immune proteins further emphasises how liver health is integral to systemic immune function, and therefore how liver disease and injury impacts our susceptibility to infection.

Key points:

- The liver is an immune organ that can regulate both local and systemic immune responses
- In disease and injury, we see loss of regulation and production of essential proteins, whilst simultaneously seeing overactivation of pro-inflammatory pathways

1.4 The liver as a "detox" organ

The liver is probably most recognised for its ability to "detox". Hepatocytes are the centre for the modification and removal of both exogenous and endogenous toxins, and contain an arsenal of enzymes capable of metabolising a wide range of molecules(87). Unfortunately, many of these processes create highly reactive metabolites, and leave the liver vulnerable to damage. As a result, hepatotoxicity is the most common reason for drug recall, and the liver is the organ that suffers most dramatically from alcohol misuse(88).

The majority of drugs are modified in the liver by enzymes of the Cytochrome P450 (CYP) family, with CYP3A4/5 being responsible for over a third of these interactions(89). CYP enzymes catalyse the oxidation of compounds, rendering them more water soluble and easier for the body to excrete(90). In doing so however, they can release a number of highly reactive

metabolites which can cause local tissue damage and inflammation(91). To mediate this, the liver is also equipped with anti-oxidant molecules such as glutathione which can protect from oxidative injury(92). The liver also has the highest expression of alcohol dehydrogenase (ADH) in the body which oxidises a range of alcohols, including those produced endogenously by gut bacteria, alongside having roles in steroid and bile metabolism(93).

1.4.1 Metabolism of alcohol

Beverage alcohol (ethanol) is absorbed into the blood stream within 10 minutes of consumption, and peak blood alcohol levels occur between 30 and 90 minutes later(94). Despite expression of ADH in the gut, the GI tract is responsible for only a small percentage of ethanol metabolism (known as first pass metabolism), and the rest of the responsibility falls to the liver(95). Ethanol is predominantly metabolised by ADH1, which converts ethanol to acetaldehyde by the oxidisation of NAD^+ to NADH(93) (Figure 1.2). Acetaldehyde is highly toxic and can form mutagenic protein adducts, so it is rapidly converted to acetate by acetaldehyde dehydrogenase(96). ADH1a is by far the most efficient enzyme with regards to ethanol breakdown and is responsible for around 75% of this process. However, it is limited by a low capacity for alcohol (with a Km of only 1mM) and thus when exposed to high blood alcohol levels, ADH1Aa quickly reaches its maximum(93). In this instance, the enzyme Cytochrome P450 2E1 (CYP2E1) can contribute to clearance. Under normal circumstances CYP2E1 is only responsible for 10-25% of alcohol metabolism, but it has a 10-fold higher capacity for ethanol – making this a more relevant mechanism in the context of binge alcohol exposure(93), albeit a less efficient one(97). Unfortunately, the metabolism of ethanol by CYP2E1 produces increased reactive oxygen species alongside acetaldehyde, which can lead to local tissue

damage and inflammation. There is evidence that with repeated and chronic alcohol exposure levels of CYP2E1 expression within the liver are increased, resulting in a higher proportion of the more damaging mechanisms of ethanol metabolism and increased inflammation(97, 98).

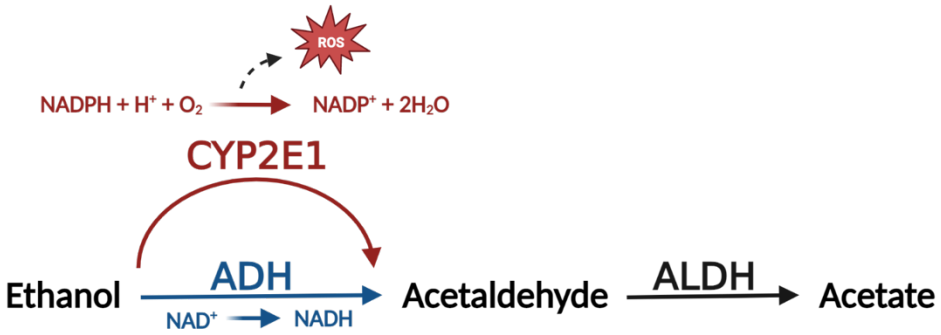


Figure 1.2: Modification of ethanol by liver enzymes. In the liver, beverage alcohol (ethanol) is metabolised predominantly by alcohol dehydrogenase (ADH) enzymes, which reduce NAD^+ to NADH and form the toxic intermediate acetaldehyde, which is then metabolised to acetate by acetaldehyde dehydrogenase (ALDH). In response to high ethanol concentrations, Cytochrome P450 2E1 (CYP2E1) is also capable of metabolising ethanol, however results in a higher production of reactive oxygen species (ROS) which can induce inflammation and cause local tissue damage. Image generated in BioRender and adapted from Zakhari et al (99).

1.5 Alcohol Related Liver Disease

In 2020, alcohol was the direct cause of 8,974 deaths in the UK(100). Of these, alcoholic liver disease accounted for 77.8% of them(100), and liver disease is now the biggest cause of death in people aged 35-49 years old in the UK(101). In this section I will highlight the presentation and diagnosis of ARLD, and the multiple stages of disease progression.

1.5.1 Symptoms and Diagnosis

The liver's inherent ability to regenerate and repair presents a challenge with regards to diagnosing patients with ARLD. In many cases, disease can go undetected for decades as the liver continues to perform its usual functions and patients remain asymptomatic despite underlying ongoing injury(102). However, when liver failure does occur, the systemic impact leads to a multitude of complications. Patients with early stage disease often present with abdominal pain at most(103). However, as injury develops, loss of liver function results in jaundice (yellowing of the skin and eyes) from accumulation of bilirubin, gastrointestinal bleeding due to reduced production of clotting factors, ascites (fluid retention) due to portal hypertension, and hepatic encephalopathy (neurological symptoms) due to loss of blood detox functions(103-107).

There is no single test for liver disease, and diagnoses are made based on cumulative results from blood tests, physical examinations, patient histories and liver biopsies(108). Blood tests measure levels of liver derived molecules such as albumin and bilirubin, alongside the presence of liver enzymes such as aspartate aminotransferase (AST) and alanine aminotransferase (ALT)(109). These enzymes are usually contained within hepatocytes and

are released into the blood stream due to hepatocyte damage; ALT is a more specific predictor of this as it is predominantly found in the liver, whereas AST is also found in several other tissues(109). Conversely, blood albumin levels reduce due to loss of hepatocyte function and protein production. Assessment of alcohol consumption behaviour is a key indicator of ARLD as opposed to other liver disease aetiologies, and non-invasive scans to assess degree of liver scarring can then be performed in patients who are considered high risk(110). The only way to achieve a definitive diagnosis for most stages of ARLD is with a biopsy, however they are rarely performed due to the increased risk of invasive procedures in this patient group, and the likelihood that it will not affect management of the condition(108). For ARLD patients with alcoholic hepatitis in particular, surgery overall is considered to be a considerably higher risk(111).

1.5.2 Stages of ARLD

There are several stages of ARLD, and levels of severity within each of those stages also. Liver injury starts with steatosis, then progresses to steatohepatitis, followed by fibrosis and eventually cirrhosis, which is also often the precursor to hepatocellular carcinoma (HCC)(112).

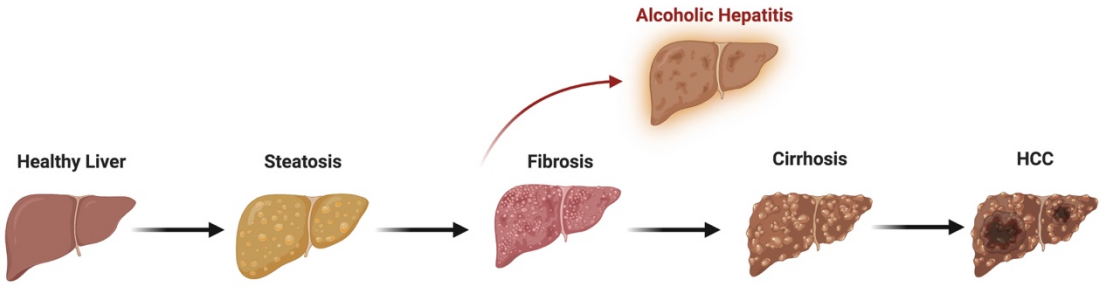


Figure 1.3: Stages of progression in Alcohol Related Liver Disease (ARLD). *Excessive alcohol consumption first results in an accumulation of fat within the liver known as steatosis. Chronic exposure causes inflammation and development of fibrosis (scarring and deposits of extracellular matrix proteins). Patients can also suffer from acute alcoholic hepatitis – a severe inflammatory condition that usually occurs on a background of liver injury. Continued damage can result in cirrhosis and development of hepatocellular carcinoma (HCC). Image created in BioRender.*

Steatosis

The liver plays an important role in lipid metabolism. Production of NADH during ethanol processing inhibits fatty acid breakdown and encourages the storage of triglycerides which leads to steatosis – the accumulation of fat within hepatocytes(113). Steatosis is present in 90% of those who drink heavily, but can be reversed with a period of abstinence(97). Steatosis is not exclusive to ALD, and is also associated with obesity and high fat diets (as seen in Non-Alcoholic Fatty Liver Disease or NAFLD)(114). According to the British Liver Trust, around 63% of adults in the UK are considered overweight or obese, and around one third of them are predicted to have early stage NAFLD(101). It has been long established that increased weight is a risk factor for ARLD(115), and the combined effects of raised BMI and alcohol consumption have been shown to notably increase mortality from liver disease(116). At this stage diagnosis is unlikely as patients are often completely asymptomatic or only presenting with mild abdominal discomfort, and can still have normal liver function tests(103). Progression from steatosis often requires a "second hit", such as an infection or additional metabolic challenge(117).

Alcoholic Hepatitis (AH)

A portion of ARLD patients (around 10-35%) will develop acute alcoholic hepatitis (AH) – a clinical syndrome presenting as severe, acute, highly inflammatory liver failure(118). The term AH is often used interchangeably in the literature with alcoholic steatohepatitis (ASH), which more accurately describes the histological features in these patients, showing steatosis alongside hepatocyte damage and immune infiltration (predominantly by neutrophils)(119). This is accompanied by characteristic morphological changes such as hepatocyte ballooning (the swelling of damaged cells before death) and the presence of cytokeratin deposits known as Mallory-Denk bodies(120). In these patients, diagnosis is usually made based on factors such as bilirubin levels higher than 85μm/L, an AST level higher than the ALT level, an increase in white blood cell count (particularly neutrophils) and a relevant patient history(121).

According to a 2018 meta-analysis, the average recorded 28 day mortality rate for AH is around 30%, and this has not improved since 1971(122). AH can often develop in the context of an alcohol binge or after a longer period of particularly heavy drinking, but typically occurs on the background of some level of underlying chronic liver injury(123). Symptoms are usually severe with rapid onset, and indicators of liver failure (such as jaundice) can also be accompanied by features of systemic inflammatory response syndrome (SIRS)(124). Despite extensive liver damage and continued heavy drinking, many patients continue on to develop fibrosis and cirrhosis without suffering from this acute inflammatory condition.

Fibrosis

Fibrosis is defined as the deposition of extracellular matrix (ECM), which is indicative of a chronic wound healing response(125). This is a hallmark of late stage liver disease irrespective of the aetiology, although fibrosis patterns do vary with disease types. In ALD fibrosis starts with perivenular (around the veins) and/or pericellular (around the cells) matrix deposits(126). These patterns are also prognostic, where the level of fibrosis directly relates to disease severity(127, 128). Whilst historically fibrosis was seen as irreversible damage, we now know that it is a much more dynamic process than previously thought; fibrosis regression has been documented in a number of liver diseases, although evidence in ARLD is mixed(129). The mechanisms of fibrosis are largely driven by activated hepatic stellate cells (HSCs). HSCs also produce additional leukocyte chemoattractants and contribute to their own continued activation, which results in the deposition of large quantities of ECM proteins and causes changes in the vasculature, altered liver structure, and loss of function(130).

Cirrhosis and HCC

Without intervention, continued exposure to injury eventually results in progression to cirrhosis. This stage is defined by "marked distortion of hepatic architecture by extensive fibrosis, typically in a chicken-wire pattern, formation of regenerating nodules and abnormal sinusoidal blood flow"(119, p.169). Incredibly, patients can still be asymptomatic at this stage with a condition known as "compensated" cirrhosis, where despite considerable damage the liver is still performing its necessary functions. Patients can then "decompensate" and show symptoms of liver failure such as ascites, hepatic encephalopathy, and jaundice(131). At this stage, patients can also present with acute-on-chronic alcoholic hepatitis, which is

accompanied by systemic inflammation and multi-organ failure(132). While reports on incidence vary, a small proportion of patients (around 3%) with ALD cirrhosis will progress to liver cancer(133-135). Despite this seemingly low relative incidence, 90% of primary liver cancers (usually hepatocellular carcinoma (HCC)) occur on a background of chronic liver disease and cirrhosis, and a third of these are due to ARLD specifically(136). Cirrhosis itself is considered a pre-neoplastic lesion, and CYP2E1 is a key driver in the development of cancer largely due to its production of ROS(137).

1.5.3 Challenges with predicting progression

Steatosis is present in almost all heavy drinkers, and yet a much lower percentage go on to develop severe disease(138). Identifying patients who are more likely to develop severe liver disease is challenging, and many factors have been attributed to increased susceptibility including age, sex, ethnicity, BMI and even the type of alcohol consumed(119) - this further highlights the need for effective models of liver disease that can account for interpatient variability and help to find new ways to identify those who are most at risk. An essential point to note is that the UK government considers “Higher Risk Drinking” (i.e. likely to already be suffering from health damage due to alcohol use) as regularly drinking more than 35 units per week for women and 50 units per week for men(139); this equates to roughly 3.5-5 bottles of wine per week (at 14% alcohol by volume). The damaging effects of alcohol are easily underestimated, and currently around a quarter of the UK adult population are predicted to be drinking at an “increased” or “higher” risk level. Furthermore, the stigma regarding alcohol dependency can lead to poor reporting from patients and undiagnosed progression to liver disease. A recent review discussed the impact of this stigma on healthcare in ARLD, as patients

are less likely to come forward to ask for support or may underplay their condition for concern of altered treatment(140). Later stage diagnosis creates more challenges in regards to treatment and intervention, but this also highlights the need for more systematic improvements in healthcare for these patients.

Key points:

- ARLD progresses from lipid accumulation through to severe scarring and loss of liver function – a process which is largely driven by immune cell involvement
- Up to a third of patients also suffer with alcoholic hepatitis - a severe, acute inflammatory condition with high mortality

1.6 Treatment and management of ARLD

As highlighted above, by the time many patients present with symptoms they are already at a stage of disease where treatment options are extremely limited. According to the British Liver Trust, around three quarters of people in the UK are diagnosed at a point when it is too late for lifestyle changes or intervention(101). At all stages of ARLD, the first step is the removal of the injurious stimuli with alcohol abstinence(119). In early disease this can lead to almost complete reversal of damage, but can also improve liver function considerably even in late stages(141, 142). Abstinence can however be challenging in cohorts where patients are suffering from alcohol use disorder (AUD), and alcohol withdrawal syndrome can lead to dramatic effects including seizures and even death(143). There are pharmacological agents which can support patients during this stage, however these are often also associated with hepatotoxicity and therefore unsuitable or untested in patients who have already progressed to later stage disease(119). In all patients, alcohol abstinence is most effective if supplemented with lifestyle changes that include improved nutrition and psychological

support from healthcare professionals(144). A meta-analysis by Heckley *et al* showed that abstinence in chronic drinkers reduced their chances of liver cancer by 6-7% per year, with around 23 years needed to reduce the chances to those of a non-drinker (although estimates ranged from 14-70 years)(145).

1.6.1 Treatments in alcoholic hepatitis

Patients who present with AH are at high risk of infection, acute kidney injury (AKI) and multi-organ failure, and therefore the primary concerns are often reduced alcohol intake, early detection and treatment of infection, and nutritional intervention(146). Currently the only accepted pharmaceutical intervention is corticosteroids, however these have a number of limitations and their use is controversial as less than half of patients are eligible for treatment and outcomes are mixed(147). There have been a number of trials investigating steroid treatment in AH, one of the largest of which to date (STOPAH) showed no significant reduction in mortality after 28 days in groups treated with the glucocorticoid Prednisolone, but did see an expected increase in infections(148). While steroids are able to reduce immediate dangers of extreme systemic inflammation they increase the already high risk of infection. It is therefore essential to confirm that there is no presence of infection before starting a steroid course(144). The Lille model of treatment has improved outcomes by identifying "null responders" to steroids after 7 days of treatment which allows early cessation and avoids unnecessary immunocompromise(149). A meta-analysis of five different randomised controlled trials by Metharin *et al,* further showed a significant improvement in 28 day mortality with steroid treatment, although this was predominantly in patients who were classified as "responders"(150). These conflicting results show that trials on steroid use are

still inconclusive overall, and there are few options if they are not effective or for those patients who are considered ineligible.

Other anti-inflammatory tools and pathways have been considered as a means to manage disease in patients with AH. As the cytokine Tumour Necrosis Factor α (TNFα) is a significant contributor to many of the inflammatory processes in AH, there were investigations into the use of anti-TNF therapy due to these drugs showing promise in the treatment of sepsis(151, 152). Successful trials with the TNFα inhibitor Pentoxifylline in AH offered hope that this mechanism could improve outcomes for these patients(153). However, the STOPAH trial also investigated treatment with Pentoxifylline and showed no improvement in 28-day mortality(148). Furthermore, trials of two different anti-TNF therapies (Etanercept and Infliximab) resulted in considerably poorer outcomes for treated patients versus controls and had to be terminated due to infection risk(154). This emphasises the delicate balance required between regulation and activation of the immune response in AH, along with the complexities of treating it. Some trials have tried to address these challenges by combining multiple agents as dual therapies. Small trials combining N-acetylcysteine (NAC – an antioxidant which reduces the presence of ROS) with Prednisolone showed increased survival compared to Prednisolone alone(155). Several small trials have also shown promise for the use of G-CSF (Granulocyte – Colony Stimulating Factor) in AH, including in patients who have not responded to steroid treatment(156, 157). While results do appear to be positive, a 2020 meta-analysis of 7 different studies highlights that there is still conflicting data on this treatment and so further investigation is required(158).

1.6.2 Treatments for late-stage ARLD

While there have been many different treatments trialled for late-stage ALD, so far none have been able to significantly alter the end point of disease(159). This likely reflects the complexity of the condition and need to manage inflammation, fibrosis and altered regeneration as well as any systemic complications of chronic disease. Currently, the most effective treatment is a liver transplant(119). Historically, this has been a controversial issue due to the stigma surrounding AUD, concerns regarding relapse and shortage of donor livers(160). However, over the last few decades we have seen a change in approach to ALD transplants and outcomes have been shown to be comparable to other disease aetiologies(161). Generally, a 6 month period of sobriety is required before patients are able to be placed on the transplant waiting list, however recent evidence may suggest that the "6 month rule" is not actually associated with better survival or lower relapse, and that early liver transplant in ALD could potentially be more beneficial(162, 163). The current NHS estimate is a 3-4 month wait for a liver transplant(164), although this can be shorter for those who have more severe disease, or who are willing to accept more "high risk" donor livers (depending on factors such as donor health, age, and cause of death). Despite this, the issue remains that the demand for organs for all types of chronic liver disease still far outweighs the ones that are available. Even with recent advances with normothermic perfusion technology, many livers cannot be made viable for transplant(165). The annual report on liver transplantation for 2020-21 showed that 6 months after going on the waiting list, 65% of patients had been transplanted, 28% were still waiting, 5% had died and 2% had been removed(166). It is also important to consider those who do not meet the strict criteria for being placed on the transplant list; alongside alcohol abstinence, UK patients must have a 50% likelihood of survival in 5 years' time after transplant,

which is challenging for many ALD patients where alcohol associated co-morbidities such as kidney, GI and heart issues can influence overall health(167).

There is an undeniable unmet medical need for treatments at all stages of liver disease and the situation is particularly challenging for those with ARLD. Although liver transplantation has a 5-year survival rate of nearly 85%, this is not a sustainable treatment especially with increasing levels of ARLD in the UK population(166). This unmet need is the basis for our project where we wish to develop primary human cell models to understand the interplay between the immune system and hepatotoxicity in ARLD. In the next sections I will therefore consider the impact of alcohol on the immune system and also how ARLD can be modelled for preclinical research into new treatments and biomarkers.

Key points:

- Abstinence underpins the treatment for any stage of ARLD
- Pharmacological interventions are available but have limited utility
- Transplant is the only treatment for late stage disease, and while well tolerated, there are not enough available livers to meet demand

1.7 Immunocompromise and Infection in Alcohol-Related Liver Disease

Despite the extreme consequences of loss of liver function ranging from bleeding disorders to hepatic encephalopathy, the cause of death in up to 50% of patients with cirrhosis is infection(168) – an issue that is even more prominent in patients with alcoholic cirrhosis(169). Considering the huge increase in both local and systemic immune cell activation during liver damage, it seems counterintuitive that these patients would be unable to effectively clear infections. However, patients with cirrhosis have an immune deficit that is ideal for opportunistic pathogens, and patients frequently suffer from spontaneous bacterial peritonitis, urinary tract infections and pneumonia(170). Cirrhosis Associated Immune Dysfunction (CAID) is a well-established condition in patients with end stage liver disease, independent of aetiology, and is characterised by an increase in inflammation in parallel with a decrease in immune function(171). There are added complications to this condition in ARLD due to the effects of alcohol on the gut and directly on immune cells, and these patients see higher incidences of bacterial, fungal and viral infections than in other chronic liver diseases(172).

Endotoxemia (defined as an excess of bacterial products such as LPS in the blood) is a common complication of liver disease, and circulating LPS levels are predicative of mortality and poor responses to steroid treatment in AH(173). Alcohol causes mucosal damage and leads to "leaky gut" syndrome – an increase in gut permeability resulting in the presence of commensal bacterial products in the portal blood(174). This is worsened by bacterial overgrowth and dysbiosis, and changes in the gut microbiome are an established feature of ARLD(175, 176). One study identified a decrease in beneficial commensal bacteria and an increase in more

harmful opportunistic pathogens in patients with AUD. The gut microbiota of these patients also showed altered functionality, with an increase in genes related to alcohol metabolism, which in turn resulted in an increased presence of toxic metabolites such as acetaldehyde(177). Interestingly, this study also showed differences between patients with AUD with and without liver cirrhosis, suggesting the influence of liver function on the microbiome alongside alcohol itself(177). Samuelson *et al* also showed that mouse models of alcoholic gut dysbiosis led to increased susceptibility to *Klebsiella pneumoniae* infection, highlighting the fact that systemic immunological responses are also affected by alcohol, in part explaining increased incidence of pulmonary infections in patients with AUD(178). In a patient cohort with community acquired pneumonia, those with chronic liver disease were around 10 years younger than average, and patients with AUD have been shown to be 10 times more likely to develop pneumococcal pneumonia(179, 180).

Gram negative bacteria are responsible for around 75% of the infections in ALD patients(181). Infections increase mortality four-fold in patients with cirrhosis(182), and can trigger acute-on-chronic liver failure (ACLF)(183). In a study by Fernandez *et al,* bacterial infections were present in 37% of cases of ACLF at diagnosis and developed in around half of the remaining patients within 4 weeks; those with infections had a significantly poorer prognosis(184). As discussed previously, the presence of LPS from the membrane of gram-negative bacteria is well tolerated in the liver - however the significant increase in exposure from the damaged gut and bacterial infections can elicit a robust response. Immune responses are activated not only by the PAMPs from commensal and pathogenic bacteria and fungi, but also from the DAMPs arising from gut and liver cellular damage. This leads to a systemic increase in

circulating inflammatory cytokines and immune cell activation(185). Despite this, high levels of immunosuppressive cytokines are present in ARLD(186). Studies in liver disease have suggested that endotoxemia also contributes to altered monocyte function and downregulation of HLA-DR (required for antigen presentation)(187), making it particularly relevant in ARLD where LPS exposure is high.

1.8 The role of Neutrophils in ARLD

In health, invading pathogens are rapidly contained by our innate immune response, and the first responders to infectious challenge are usually neutrophils(188). These cells are essential to maintain a strong defence against pathogens, and loss of function is associated with severe risk of infection(189). Their involvement in ARLD has been known for decades, due to their extensive liver infiltration in AH(190). However, their complex role in both infection control and repair is becoming increasingly apparent, and they are an essential piece of the puzzle regarding our understanding of immunocompromise in liver disease.

Neutrophils are our most abundant white blood cell, making up 50-70% of the circulating leukocyte population**,** and respond swiftly and intensely to immune challenges(188). Not only are they phagocytic, they are equipped to perform a range of other antimicrobial functions such as NETosis(191) (a process whereby they eject their DNA in order to entrap bacteria), production of ROS, and the ability to release a store of azurophilic granules which can both modulate the immune response and damage bacteria(192). They are derived from myeloid precursors in the bone marrow, and are continually released into the circulation to account for their short half-life. While reports on this vary, estimations from labelling experiments

suggest a circulation half-life of around 4-8 hours(193). They circulate in the periphery performing immune surveillance, and in the instance that they encounter a stimulus, they swiftly migrate to sites of injury and contribute to infection control and wound repair(194). The bone marrow therefore contains a substantial reservoir of these cells in order to rapidly replace cells lost in immune responses, and estimations in mice show a capacity for 10-fold increase in circulating granulocytes in response to infection(195). Alcohol consumption has a direct effect on the bone marrow, and patients with chronic alcohol use exhibit bone marrow damage which effects granulocyte differentiation, altering neutrophil responses to infection(196). Patients admitted with AUD often have granulocytopenia (low circulating numbers of granulocytes), and the effects of alcohol on the bone marrow mean that the neutrophils that replenish the systemic pool are often at an earlier stage of differentiation and not functionally mature(197). Neutrophils also have complex roles once they arrive in the liver. High levels of hepatic neutrophil infiltration is a marker of poor prognosis in patients with acute liver failure, and blood Neutrophil/Lymphocyte ratio is often used as a prognostic tool which correlates strongly with poor outcome(198). Neutrophil recruitment to the liver itself is unique, and differs not only from other organs but also shows variation within the liver. While the classical recruitment cascade takes place in the post-capillary venules, selectin-independent migration occurs in the sinusoids(199). Here, alternative adhesion molecules such as VAP-1 and ICAM-1 are constitutively expressed(200, 201), and upregulated in response to injury. The attenuation of acute liver damage and reduced hepatic neutrophil infiltration in ICAM-1 knockout mice supports the role of infiltrating neutrophils as a contributor to liver damage(202). NETS have also been associated with poor outcome in acute

liver failure, with markers of NETs found to be 30% higher in patients who died or required urgent liver transplant(203).

There is conflicting data about whether neutrophils are over or under stimulated in AH. It appears that while patient neutrophils have a higher level of baseline activation they are less responsive to infection. Mookerjee *et al* showed that neutrophil function is altered in acute-on-chronic alcoholic liver disease, but that this effect was reversible with the removal of endotoxin. In these patients, there was a higher baseline of ROS production, but significantly lower phagocytic ability compared to healthy controls(204). This pattern of simultaneous over and under activation mimics the neutrophil phenotype seen in sepsis, where these cells show functional impairment and pro-inflammatory behaviour(205). Acute binge alcohol consumption in healthy volunteers has also been shown to reduce NET production in response to PMA(206), and *in vitro* addition of serum from stable cirrhotic patients also induces neutrophil dysfunction(207). Alongside downregulation of pro-inflammatory cytokines such as TNFα and IL-8, one study investigating *in vitro* alcohol treatment of neutrophils also showed a reduction in the production of hepatocyte growth factor (HGF) which would suggest a role in liver regeneration(208). Lu *et al* showed that in liver injury, injection of activated (but not non-activated) neutrophils reduced liver injury in a mouse model(209). Alongside this, they also showed *in vitro* that activated neutrophils polarised macrophages to a more anti-inflammatory state(209). This influence over macrophage phenotype was also shown to be triggered by neutrophil production of ROS(210). Neutrophils also exhibit prolonged survival in drug induced liver injury, where they upregulate pro-resolution genes(211). In the context of sterile injury, neutrophils have even been shown to contribute to the repair of liver tissue, and

then “reverse migrate” back out of the liver(212). This demonstrates the importance of understanding neutrophil roles in ARLD, and how to balance their pro-inflammatory and pro-resolution functions in response to liver signalling.

1.9 Modelling liver disease

So far, I have discussed the complexity of the liver, and highlighted how its function is reliant on the cross talk between a wide range of different cell types. Both parenchymal and non-parenchymal cells are essential, alongside the influence of more transient interactions such as those from peripheral immune cells that pass through the livers highly developed vasculature. I have also considered changes in liver function during injury, and how exposure to ethanol may compromise immune functions. Due to the intricate 3D structure of this organ and the importance of spatial orientation on cell function, recreating the complexity of these interactions in an *in vitro* model of the liver has proven difficult to date(213). Since the mid 1900s, there have been increasingly complex models both *in vitro* and *in vivo* that have helped to answer many questions regarding the liver in health and disease(213), however there are still considerable gaps in our knowledge. Recent advances in technology have highlighted deficiencies of earlier models and the field is moving forward quickly. However, we are still in need of a representative model of the liver that is both functionally accurate and achievable in the lab. Recreating the multifaceted interactions within the liver requires consideration of temporal and spatial responses, whilst balancing practicality and accuracy. Importantly, studies of 3D models demonstrating retained phenotype in culture show that it is also necessary to use cells that represent those in a human liver which may have been exposed to injury, inflammation, and fibrosis for many years(214).

1.9.1 Modelling the liver environment in 2D culture

As hepatocytes are the predominant cell type in the liver, modelling *in vitro* is usually centred around these cells and primary human hepatocytes remain the "gold standard" of liver modelling. The successful perfusion isolation of adult rat hepatocytes in the late 1960s provided cells that could be cultured for up to 8 days(215), and drove considerable progress in the field. However, it was still over a decade before this technique was effectively translated to achieve the isolation of high quantities of viable hepatocytes from human liver(216) and issues with functionality became swiftly apparent(217). Alterations in the phenotype of cultured rat hepatocytes had been previously noted, alongside suggestions that loss of their cell to cell contacts was a potential cause(218). The pursuit of an effective model of the complex *in vivo* environment of the liver began, and new *in vitro* methods included co-culture with rat epithelial cells(219) or increasing contact with the extracellular matrix by employing "sandwich" culture(220). When isolated and utilised for studies short term, PHHs retain function and phenotype effectively(221). However, the three key limitations of this model are de-differentiation, lack of proliferation and difficult to obtain source material from both healthy and diseased donors. The de-differentiation process occurs quickly when placed in 2D culture. Cell to cell contact has been shown to be important for effective polarisation of PHH in culture, which is essential for function(222). Furthering this, the content and configuration of the matrix on which these cells are grown greatly effects how this polarisation is maintained(223). When plated on collagen I coated plastic tissue culture plates, rat hepatocytes showed de-differentiation into fibroblast like cells after 72 hours whereas those in sandwich culture maintained cuboidal cell type(224). More recently, global proteomic analysis has shown a selective de-differentiation profile when hepatocytes are cultured as a

monolayer(225). Expression changes during de-differentiation predicted a decrease in metabolic associated factors and transcription regulators such as HNF4α, but activation of inflammatory regulators such as NFκB and production of pro-inflammatory cytokines. Alongside issues with maintaining phenotype, achieving high numbers of PHH can be challenging. Source material is often difficult to access, and sizeable wedges are required for effective perfusion. Alongside this, hepatocyte isolation from diseased tissue gives highly variable results, with ALD livers resulting in the poorest yields(221). This issue is furthered by the difficulties expanding these cells in culture. Mature hepatocytes are inherently quiescent, and *in vivo* studies have shown that the liver needs to be "primed" in order to respond effectively to mitogens(226). Despite the livers impressive ability to regenerate in response to injury(227), initiating this process *in vitro* has proven difficult and requires alterations such as small molecule intervention or transduction with HPV oncogenes(228). When combined with the complex isolation procedure, this can result in limited cell quantity for experiments.

Due to availability, simplicity and ease of culture, immortalised hepatocyte cell lines are commonplace in liver research. These cell lines are obtained either by isolating from primary human liver cancers, or by "immortalising" primary hepatocytes using techniques such as overexpression of viral oncogenes(229). The mutations acquired by these cells allow them to proliferate indefinitely, making them a valuable *in vitro* tool as they can be expanded quickly and simply with a stable and consistent phenotype. Commonly used cell lines such as HepG2 and Hep3b are derived from human hepatomas(230). These cells retain hepatocyte-like morphology and several key functions such as albumin production(230). Despite being derived from a hepatoma, HepG2 cells have also been shown to be more representative of *in vivo*

gluconeogenesis and hepatokine expression than an immortalised cell line derived from healthy cells(231). However, these cell lines have been shown to lack a number of important functions, particularly those related to toxicity and xenobiotic metabolism. Whilst they have been used in toxicology studies for a number of years, they are limited by very low or even a total lack of expression of certain drug metabolising enzymes and transporters when compared to primary hepatocytes(232). Westerink *et al* showed that whilst HepG2 have physiological levels of phase II enzymes they lack a large proportion of Cytochrome P450 (CYP) enzymes – a particular issue when looking at alcohol induced liver injury(233). In order to utilise these cell lines to study alcohol metabolism and overcome this deficiency, there is often a requirement to use plasmid transfection or retroviral infection in order to cause CYP2E1 or ADH overexpression(234). Other cell lines such as HepaRG have shown levels of CYP induction more similar to isolated PHH and show a particularly representative phenotype in the context of toxicology studies(235, 236), as well as in modelling effects of ethanol exposure on liver steatosis(237). However, despite their promise for studying xenobiotic metabolism, HepaRG cells were shown to have similar limitations to HepG2 cells when it came to predicting drug hepatotoxicity(238). Alongside this, these cells behave similarly to liver bipotent progenitor cells and require stimulation with DMSO to induce differentiation into hepatocyte-like cells. In this instance, a heterogeneous population is formed where only around 50% of cells are differentiated(239). Cell lines offer a consistent and convenient way of investigating many elements of liver disease, however the above features limit the extent to which they truly represent patient biology. In recent years, differentiation of human induced pluripotent stem cells (hiPSCs) has also provided a new source of hepatocyte-like cells that maintain the genetic properties of the patient from which they were derived. While these show many hepatocyte-

like functions and have been utilised for studies in response to ethanol exposure(240), there is evidence that they represent a more foetal than adult hepatocyte phenotype(241) and improvements are still needed for them to be considered as effective as isolated PHHs(242).

1.9.2 Modelling liver disease *in vivo*: the pros and cons of mouse models

Murine models of disease are still relied on heavily across the field of biomedical research. Genetic conservation between human and mouse is high(243), and there are undoubtable advantages of investigating disease in a whole-body system. As discussed previously, the liver's central positioning and input from the gut and peripheral circulation mean that the study of hepatocytes alone *in vitro* captures only a small part of the systemic effects of liver injury. However, considerations should be made for obvious differences between human and mouse, from size difference to stress induced by housing(244). Historically, there have been dramatic examples of drugs such as Fialuridine that have shown no adverse reaction in mice, but caused fatal liver failure in humans – highlighting clear limitations of animal models in this context(245). However, murine models remain an essential tool for the study of chronic liver disease. The ability to modify and "humanise" mice is exemplified by Xu *et al* who were able to demonstrate Fialuridine toxicity in chimeric mice with humanised livers(246).

Regarding their application to alcoholic liver disease, we are yet to develop a mouse model that recapitulates all elements of human disease. The classic progression of ALD as discussed previously includes development of steatosis, inflammation and progression to fibrosis. In current mouse models, development of significant steatosis requires administration of a high fat diet alongside alcohol consumption, and representative fibrosis requires addition of

secondary liver injuries such as carbon tetrachloride(247). One of the most commonly used models has traditionally been the Lieber-Decarli liquid diet(248). However, while this does result in steatosis even long term application yields low levels of inflammation and liver injury(249). When combined with binge alcohol dosing, this can be improved to show high levels of blood alcohol, injury and inflammation(250), which is also advantageous as it is more representative of patient behaviour where acute-on-chronic liver damage is often seen. However, the minimal extent of fibrosis and functional compromise does not recapitulate that seen in human disease, and animal welfare must be considered when developing longer, more complex models. Furthering this, the impact of alcohol exposure can differ between male and female mice(251), and behaviour regarding alcohol consumption can be another limitation of mouse models. Differences have been shown between "alcohol avoiding" and "alcohol preferring" strains, as well as a lack of increasing dependency as seen in humans and the cessation of ethanol consumption in response to rising blood levels of acetaldehyde(252).

Regarding alcohol metabolism, the main ethanol oxidising enzymes ADH and CYP2E1 are both expressed in mice, although there is only one ADH gene in mice (Adh1) compared to three in humans (ADH1A, 1B, 1C)(253) and alcohol is metabolised at five times the rate(93). The ability to genetically manipulate mice has led to the creation of several transgenic mice strains that are particularly helpful for the study of alcohol metabolism such as $CYP2E1^{-/-}$ and $Adh1^{-/-}$ (253). Despite other rodent models such as rats showing better development of fibrosis, this feature is one of the key reasons that mice are often chosen as the preferred model for liver disease(254). However, the inability to develop the full spectrum of disease, the short

duration of many models and welfare concerns around using rodents in such severe injury models means that many investigators prefer to use human cellular tools.

1.9.3 The promise of 3D *in vitro* models

Limitations of 2D liver culture became apparent very soon after successful hepatocyte isolation. The move to "sandwich culture"(220) and understanding the influence of surrounding matrix(223) caused swift improvement in hepatocyte viability and function. Development of more complex 3D cultures began with the formation of spheroids. It was first noted that isolated rat liver cells spontaneously aggregated when plated on non-adherent culture flasks(255), and that these spheroids maintained hepatocyte viability and function many weeks after initial formation. This was later shown with PHHs(256) and has since been demonstrated as an effective *in vitro* model of a range of liver diseases(257). Spheroids have also provided an improved method of culture for immortalised cell lines. HepG2 cells cultured as 3D spheroids showed increased hepatocyte like properties when compared to monolayer culture(258) although it has been suggested that this is due to length of time in culture as opposed to 3D arrangement(259). This has also been shown with HepaRG cells where 3D spheroid culture improved CYP enzyme activity and sensitivity to hepatotoxic drugs when compared to 2D monolayers(260). It has also provided the opportunity to increase the complexity of the liver model by introducing heterogeneity and non-parenchymal cell types - PHH spheroid co-culture with Kupffer cells, liver sinusoidal endothelial cells and hepatic stellate cells showed improved hepatocyte function when compared with PHH spheroids alone(261).

1.9.4 Organoids – the next step in *in vitro* modelling

Following on from this, one of the most significant developments in the world of 3D modelling has been the development of organoid technology. Whilst nomenclature is yet to be standardised in this new and fast moving field, the most common definitions describe organoids as 3D structures grown from stem cells that are capable of self-organisation and self-renewal, as well as being functionally similar to the organ from which they are derived(262). These stem cells can be pluripotent stem cells or isolated tissue progenitor cells that can self-organise into complex structures when placed within the correct environmental cues representative of their stem cell niche(263). Success with this technique has been shown across a huge range of tissues, from the brain(264) to snake venom glands(265) and it has also shown great promise as a new *in vitro* model of the liver.

Previous work from Sato *et al* had shown effective growth of small-intestinal organoids utilising the Lgr5+ stem cell population found in the bottom of intestinal crypts(266). This group was then able to identify a subset of similar Lgr5+ bi-potential progenitor cells in adult mouse livers, which were activated in response to injury(267). Isolation of these cells and plating within Matrigel (a commercially available ECM for 3D culture) resulted in 3D organoid structures that were representative of bile ducts and expressed low levels of mature hepatocyte markers. Changes in media cues enabled differentiation of these structures into heterogeneous organoids containing biliary-like and hepatocyte-like cells, which showed evidence of mature hepatocyte phenotype including binucleation, albumin production and LDL uptake. Later work showed the ability to isolate these progenitor cells from adult human liver, enabling growth and differentiation of organoids that were genetically stable for over

one year in culture(214). Importantly, these cells can be expanded repeatedly before differentiation, offering an increase in patient derived cell yield. Alongside this, when derived from patients with the single polymorphism liver disease α1-antitrypsin deficiency, organoids retained disease phenotype. This was also shown with structural bile duct defects when organoids were isolated from a patient with Alagille syndrome(214). While patient variability can add a level of complexity to studies, the imprinted phenotype in progenitor cell derived organoids offers a unique means by which to study human disease processes *in vitro*. Using the same isolation protocol, liver organoids have also been isolated from patients with cirrhosis in order to investigate the inflammatory effects of ductular reactions(52). Given the possibility of such a model to investigate the pathophysiological mechanisms in alcohol related disease, and the potential to consider interplay with immune cells, we wished to develop the approach here in Birmingham. Therefore, in my thesis I have adapted methodology for isolating hepatic organoids from both healthy human liver and diseased specimens. I have also analysed the nature of the systemic immune cells, particularly neutrophils from patients with AH. I then combined these approaches to investigate the influence of organoid conditioned medium on neutrophil activation and began to show how this form of 3D culture can be combined with other cell types to build a more complex picture of liver injury.

Key points:

- Modelling the complexity of the liver is challenging, but promise has been shown with 3D models
- A human hepatic organoid model derived from bi-potential progenitor cells has been developed, and can be used to recreate disease phenotypes

1.10 Aims of this thesis

This introduction section has described some of the complexities of the liver in health and disease, along with the challenges faced with studying them. This project focused on utilising the Centre for Liver and Gastrointestinal Research's privileged access to human tissue and blood samples to try and develop an *in vitro* model of alcohol related liver disease, whilst simultaneously improving our understanding of the influence of ARLD on neutrophil behaviour.

The aims of this project were as follows:

1. To describe the phenotype and function of peripheral neutrophils in patients with both acute and chronic ARLD
2. To develop a 3D human organoid model with cells derived from both healthy and cirrhotic primary human liver tissue
3. To expose this model to injurious stimuli such as ethanol and bacterial products in order to recreate the diseased liver environment
4. To investigate the crosstalk between neutrophils and hepatic organoids

Chapter 2 – Methodology

All statistical analysis and graphical data presentation was completed using GraphPad Prism unless otherwise specified. Table 2.1 provides details on reagents and kits used throughout this project. Separate tables are provided for antibodies (Table 2.3), Taqman Gene arrays (Table 2.5) and organoid media components (Table 2.6).

Item	Company	Cat. Number
β mercaptoethanol	Sigma-Aldrich	M6250-500ML
Accutase™	Merck Life Science	A6964-100ML
96 Well Black Flat Bottom TC-Treated Microplates	Corning	3916
Advanced DMEM-F12 (ADF)	Thermo Fisher Scientific	11540446
Antigen Unmasking Solution - Citrate-Based	Vector Labs	H-3300
Antigen Unmasking Solution - Tris-Based	Vector Labs	H-3301
Applied Biosystems™ High-Capacity cDNA Reverse Transcription Kit	Thermo Fisher Scientific	4368814
BD™ CompBead	BD Biosciences	552843
BLOXALL®	2B Scientific	SP-6000-100
Bovine Serum Albumin Fraction V	Thermo Fisher Scientific	15260037
Casein	Vector Labs	2C0803
CellTracker™ Green	Thermo Fisher Scientific	C2925
Collagenase D	Sigma-Aldrich	11088858001
Corning® Cell Recovery Solution	Thermo Fisher Scientific	11543560
Corning® Matrigel® Membrane Matrix	Thermo Fisher Scientific	11573620
Corning™ Costar™ Flat Bottom Cell Culture Plates	Thermo Fisher Scientific	10065370
CytoSelect™ Cell Migration Assay	2B Scientific	CBA-104
Dako Fluorescence Mounting Medium	Agilent Technologies	S302380-2
Dextran	Sigma-Aldrich	31392
DNase 1	Sigma-Aldrich	4716728001
DPX Mountant	Cell-Path	SEA-1300-00A
DRAQ5™ Fluorescent Probe Solution	Thermo Fisher Scientific	62251
Dulbecco's Modified Eagle Medium (DMEM)	Thermo Fisher Scientific	41965-039
DuoSet® Ancillary Reagent Kit 2	Bio-Techne Ltd	DY008
Earls Balanced Salt Solution (EBSS)	Thermo Fisher Scientific	11540616
Ethanol	Thermo Fisher Scientific	20821.33
Foetal calf serum (FCS)	Thermo Fisher Scientific	10500064
Gibco™ Penicillin-Streptomycin-Glutamine	Thermo Fisher Scientific	12090216
Goat serum	Sigma-Aldrich	G9023
Haematoxylin (Mayer's)	PRC	PRC/R/42
HBSS (containing no calcium or magnesium)	Thermo Fisher Scientific	14170088
HBSS containing calcium and magnesium	Sigma-Aldrich	H6648-500ML
HCS LipidTOX™ Red neutral lipid stain	Invitrogen	H34476
Human IL-8/CXCL8 DuoSet® ELISA	Bio-Techne Ltd	DY208-05
Hybri-Max™ Dimethyl sulfoxide (DMSO)	Merck Life Science	D2650
ImmPACT® DAB Peroxidase (HRP) Substrate	Vector Labs	SK-4105
ImmPRESS® HRP Horse Anti-Mouse IgG Polymer Detection Kit	2B Scientific	MP-7402-15
ImmPRESS® HRP Horse Anti-Rabbit IgG Polymer Detection Kit	2B Scientific	MP-7401-15
Industrial Denatured Alcohol	pfm medical	PRC/R/101
Lambda DNA	Thermo Fisher Scientific	SD0011
Lipopolysaccharide (LPS)	Sigma-Aldrich	L4391-1MG
Lonza ToxiLight Non-Destructive Cytotoxicity BioAssay Kit	2B Scientific	CBA-104
nCounter Fibrosis Panel	NanoString	XT-CSO-HFIB2-12
Nuclease-free water	Promega	P119C
Oleic acid	Sigma-Aldrich	O1383-1G

Palmitic acid	Sigma-Aldrich	P5585-10G
Paraformaldehyde (PFA)	Thermo Fisher Scientific	J61899.AK
Percoll®	GE healthcare	17-0891-01
PHAGOBURST™	Celonic	341058
PHAGOTEST™	Celonic	341060
Phorbol 12-myristate 13-acetate (PMA)	Sigma-Aldrich	P1585
Phosphate buffered saline (PBS)	Thermo Fisher Scientific	BR0014G
Pierce™ Rapid Gold BCA Protein Assay Kit	Thermo Fisher Scientific	A53225
Primocin®	invivogen	ant-pm-1
Proteome Profiler™ Human Chemokine Array Kit	Bio-Techne Ltd	ARY017
Quick Start™ BSA Standard	Bio-Rad	5000206
Radioimmunoprecipitation assay (RIPA) buffer	Millipore	20-188
Red cell lysis buffer	Sigma-Aldrich	R7757-100ML
Ribolock RNase Inhibitor	Thermo Fisher Scientific	EO0382
RNase-Free DNase Set	QIAGEN	79254
RNeasy® Mini Kit	QIAGEN	74104
Roswell Park Memorial Institute (RPMI) 1640 Medium	Thermo Fisher Scientific	31870-025
SYTOX™ Green Nucleic Acid Stain	Thermo Fisher Scientific	S7020
TaqMan® Array for the Human Complement Pathway	Thermo Fisher Scientific	10460735
TaqMan® Universal Master Mix II (no UNG)	Thermo Fisher Scientific	4440040
TaqMan® Universal Master Mix II (with UNG)	Thermo Fisher Scientific	4440038
Tris Buffered Saline	Agilent Technologies	K800721-2
Triton™ X-100	Sigma-Aldrich	T8787
Trypan blue	Sigma-Aldrich	T8154
Tween ®20	Sigma-Aldrich	P1379-1L
Xylene	pfm medical	UN 1307

Table 2.1: Reagent list detailing supplier and catalogue numbers of reagents used throughout this project.

2.1 Patient groups and ethical approval

This study involved the use of both blood and tissue samples from human patients. All patient biomaterials were collected with approval of local ethical committees (local research ethics committee approval reference 06/Q2702/61 Immune Regulation, 18-WA-0214 Liver Inflammation and 19-WA-0129 Liver fibrosis) and written informed patient consent. Peripheral blood samples were taken from healthy volunteers, patients admitted to the Queen Elizabeth Hospital Birmingham (QEHB) gastrointestinal ward with acute alcoholic hepatitis (AH), cirrhotic patients with ALD who were under assessment and abstinent from alcohol (ALD-A), and patients with cirrhosis who were still actively drinking (ALD-D). The inclusion and exclusion criteria for each patient group was adapted from Thursz *et al*(148) and is described in Table 2.2. Human liver samples were taken from either explanted material from patients who had undergone liver transplantation for chronic disease, normal resected liver tissue, or from donor organs that were deemed unfit for transplant and donated for research. All work involving primary blood or liver samples was completed in a category two biosafety cabinet.

Patient Group	Inclusion Criteria	Exclusion Criteria
Abstinent ALD Cirrhotic **(ALD-A)**	• Abstinent from drinking >6 months • Known liver cirrhosis, established by biopsy, CT or US.	• Evidence of hepatitis B, hepatitis C, HCC or biliary obstruction • Current malignancy
Actively Drinking ALD Cirrhotic **(ALD-D)**	• Known liver cirrhosis, established by biopsy, CT or US. • Not abstinent from alcohol	• Evidence of hepatitis B, hepatitis C, HCC or biliary obstruction • Current malignancy
Alcoholic Hepatitis **(AH)**	• Ongoing alcohol use prior to admission (>80g/day in men, >50g/day in women) • Bilirubin >50mmol/l • Any ongoing infection controlled for at least 48 hours of antibiotics prior to entering the study • <4 weeks since admission to hospital	• >2months abstinence • >3months prior jaundice • Evidence of hepatitis B, hepatitis C, HCC or biliary obstruction • Current malignancy • Serum creatinine >500 • Untreated sepsis • AST>500, ALT>300

Table 2.2: Inclusion and Exclusion criteria for ARLD patient groups. Patients were selected based on the above criteria by clinical colleagues. Patients who were ALD cirrhotic were selected from cancer screening clinics, and patients with alcoholic hepatitis were selected from those admitted to the gastrointestinal ward at the Queen Elizabeth Hospital Birmingham. Patients were consented and blood samples collected by Dr Reenam Khan and processed in the Centre for Liver and Gastrointestinal Research (CLGR). Inclusion and exclusion criteria were adapted from those described by Thursz et al(148).

2.2 Calculation of clinical scores

Severity of disease in patients was assessed by calculating values for Model for End-Stage Liver Disease (MELD) Score(268), United Kingdom Model for End-Stage Liver Disease (UKELD) Score(269), and Glasgow Alcoholic Hepatitis Score (GAHS)(270), using online calculators which employ the following equations/parameters:

MELD score:

$$9.57 \times \ln(creatinine) + 3.78 \times \ln(total\ bilirubin) + 11.2 \times \ln(INR) + 6.43$$

UKELD score:

$$[(5.395 \times \ln(INR)) + (1.485 \times \ln(creatinine)) + (3.130 \times \ln(bilirubin)) - (81.565 \times \ln(sodium))] + 435$$

GAHS:

A score was calculated by assigning values to the values indicated in the table below, for a maximum possible score of 12.

	Score assigned		
	1	**2**	**3**
Age	<50	⩾50	–
WBC count (10^9/L)	<15	⩾15	–
Urea (mmol/L)	<5	⩾5	–
INR	<1.5	1.5–2.0	>2.0
Bilirubin (μmol/L)	<125	125–250	>250

Alcohol intake:
Alcohol units consumed per week were estimated using the online Unit Calculator from Alcohol Change UK(271) using clinical data provided.

2.3 Analysis of phenotype and function of cells in peripheral blood

2.3.1 Full blood count

A complete blood count was taken from peripheral whole blood using the Sysmex XN-1000 haematology analyser. EDTA anticoagulated blood was collected from the patient groups described in Table 2.2 and analysed on the Sysmex XN-1000 according to manufacturer's instructions. To ensure the sample was well mixed it was left on a rotator for approximately 5 minutes at a low speed to minimize activation of the immune cells. The vacutainer was inserted into the machine, which extracts 88µl of blood for analysis. A complete blood count was then conducted via flow cytometric analysis. Calibration of the instrument was maintained by ensuring that a quality control sample (provided by Sysmex) was processed before each clinical sample.

2.3.2 Measurement of phagocytic ability of peripheral blood neutrophils

The phagocytic ability of peripheral blood neutrophils was measured using the CELONIC PHAGOTEST™ kit according to manufacturer's instructions. Briefly, 5ml of whole blood was collected in a Heparin containing vacutainer and was left slowly rocking at room temperature for a maximum of 30 minutes. From this vacutainer, 100µl of blood was dispensed into each of two Falcon™ round bottomed lidded test tubes and placed on ice. In order to measure phagocytosis by fluorescence, 20µl of FITC-labelled *E.coli* was then added to each tube and vortexed for 5 seconds. One tube was then left on ice as a "0°C control", and the other was incubated in a 37°C water bath for 10 minutes. After 10 minutes, the tube was then removed from the water bath and immediately placed back on ice where ice-cold quenching solution

was added to both tubes in order to inhibit fluorescence of any non-phagocytosed bacteria. Both samples were then washed by adding 3ml of pre-cooled wash buffer and centrifuging for 5 minutes at 250g, 4°C. As this pellet was quite unstable, supernatant was carefully removed and discarded using a Pasteur pipette, which was also used to gently resuspend the pellet. This step was then repeated. In order to lyse red blood cells and fix the neutrophils, 2ml of lysing solution was added to each tube, which were vortexed for 5 seconds and left to incubate at room temperature in the dark for 20 minutes. To remove the red blood cell lysate, the tubes were then centrifuged for 5 minutes at 250g, 4°C and the supernatant was discarded. The fixed cells were washed with 3ml of wash buffer as above, followed by incubation with a DNA staining dye on ice for 10 minutes. This allowed the exclusion of any remaining non-phagocytosed bacteria via cytometry as it is possible to separate these from leukocytes based on DNA content. The mean fluorescence intensity (MFI) in the FITC channel of each sample was measured using the CyAn™ ADP Analyzer. Approximately 10,000 neutrophils were counted per sample and analysed using the gating strategy demonstrated in Figure 2.1.

2.3.3 Measurement of oxidative burst in human neutrophils

To assess the ability of peripheral blood neutrophils to produce reactive oxygen species (ROS) in response to different stimuli, we measured oxidation of the fluorogenic substrate dihydrorhodamine 123 using the CELONIC PHAGOBURST™ Kit. This was completed as per the manufacturer's instructions using heparinised whole blood from the patient groups described in Table 2.2. 5ml of whole blood was collected in a heparin containing vacutainer and was left slowly rocking at room temperature for a maximum of 30 minutes. From this vacutainer, 100µl of blood was dispensed into each of four Falcon™ round bottomed lidded test tubes and

placed on ice. The following reagents were then added on ice to each tube:

Tube 1: 20μl wash buffer for "negative control"

Tube 2: 20μl pre-cooled *E.coli* bacteria

Tube 3: 20μl PMA working solution (1:200 dilution) for "high stimulation control"

Tube 4: 20μl fMLP working solution (1:200 dilution) for "low stimulation control"

All four tubes were vortexed for 5 seconds and incubated in a 37°C water bath for 10 minutes. After this incubation, 20μl of the substrate solution was then added to all tubes, the samples were vortexed again and returned to the water bath for another 10 minutes. It should be noted that this substrate addition should happen "*in situ*" without removing the tubes from the water bath, however due to additional safety measures introduced after the COVID-19 pandemic tubes were briefly returned to the biosafety cabinet. To lyse red blood cells and fix the neutrophils, 2ml of lysing solution was added to each tube, which were then vortexed for 5 seconds and left to incubate at room temperature in the dark for 20 minutes. After this, cells were centrifuged for 5 minutes at 250g, 4°C and the supernatants were discarded. The fixed cells were then washed with 3ml of wash solution and centrifuged again at 4°C, 250g for 5 minutes. In order to distinguish the neutrophils from any remaining bacteria during flow cytometric analysis (based on DNA content), the cells were incubated in a DNA staining solution on ice for 10 minutes whilst protected from light. The mean fluorescence intensity (MFI) in the FITC channel of each sample was measured using the CyAn™ ADP Analyzer. Approximately 10,000 neutrophils were counted per sample and analysed using the gating strategy demonstrated in Figure 2.1.

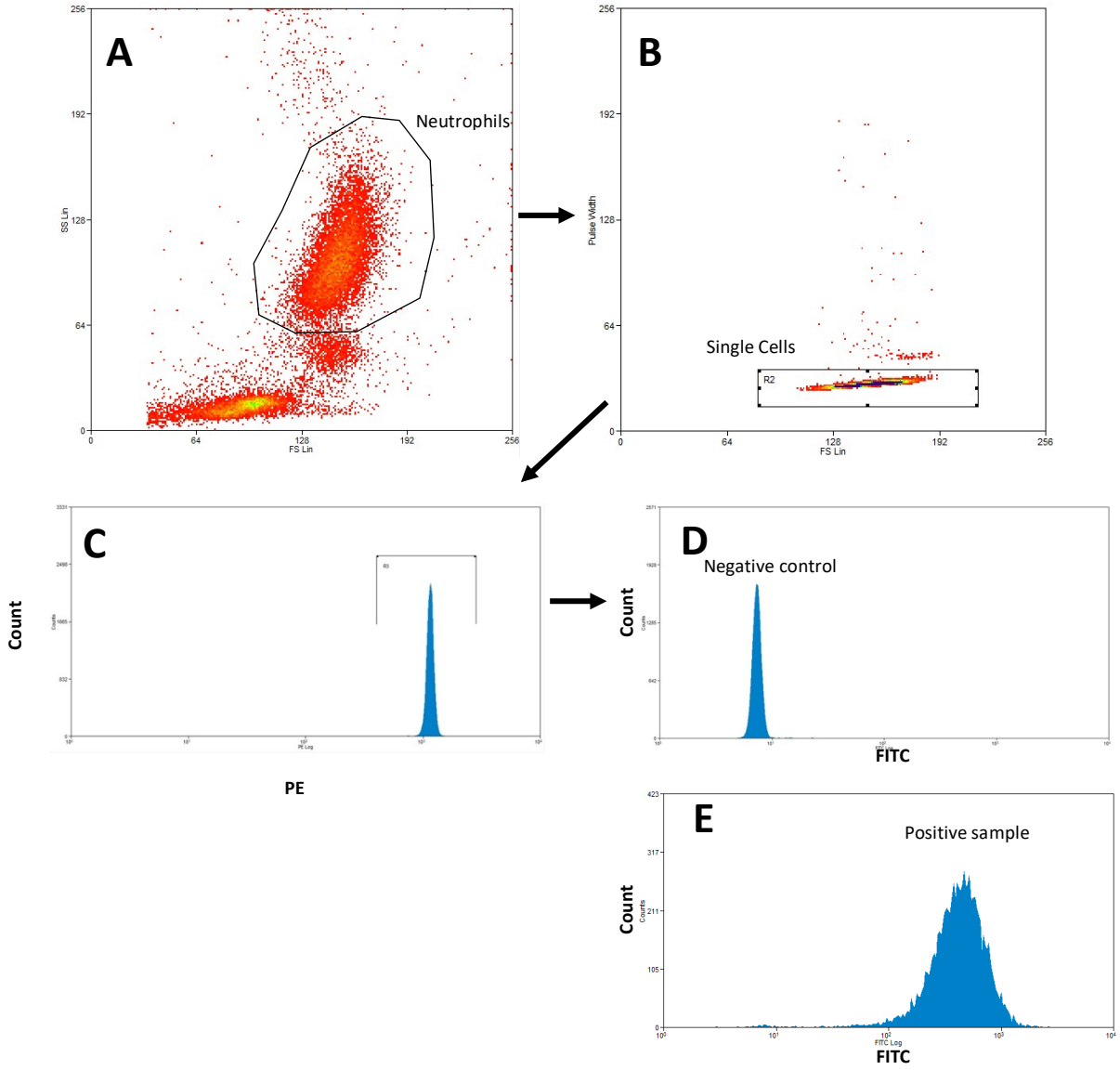


Figure 2.1: Gating strategy for PHAGOTEST and PHAGOBURST neutrophil function assays. Heparinised whole blood samples were processed as described in sections 2.3.2 and 2.3.3 for PHAGOTEST/PHAGOBURST assays respectively. Measurement of FITC fluorescence using a CyAn™ ADP Analyzer was used to assess the amount of internalised FITC-labelled E.coli bacteria/production of reactive oxygen species (ROS) with the above gating strategy. Neutrophils were selected based on size and granularity assessed by forward scatter and side scatter respectively (A), and forward scatter and pulse width were used to select for single cells and exclude cell clumps (B). Any contamination by residual E.coli was excluded using PE dye to stain for DNA content, and selecting only human cells based on high DNA content/PE expression (C). Negative controls were used to establish a baseline of FITC expression (D) and FITC expression due to phagocytosed bacteria/ROS could then be measured (E) and mean fluorescence intensity (MFI) calculated for each sample.

2.3.4 Production of Neutrophil Extracellular Traps (NETs) by human neutrophils

As a measure of activation, we quantified the production of NETs by neutrophils that were isolated from peripheral blood samples based on the protocol published by Hazeldine *et al*(272). Patient samples were always paired in the same experiment with a healthy donor. 20ml of blood was collected in EDTA containing vacutainers from each volunteer and then transferred to a 50ml falcon tube. In order to minimise red blood cell contamination, 3.3ml of Dextran was added (at a 1:6 ratio) and the tube was gently inverted to mix and left to separate for 30-40 minutes at room temperature. This results in a leukocyte rich layer (LRL) top of a red blood cell layer. Once this incubation was complete, a Percoll gradient was prepared in two 15ml falcon tubes by first adding 5ml of 56% Percoll, and then gently layering 2.5ml of 80% Percoll underneath. Up to 7ml of the LRL was then gently added on top of each Percoll gradient using a 3ml Pasteur pipette, and the tubes were centrifuged at 500g for 20 minutes with no break or acceleration. After this step, the plasma and lymphocyte layers were discarded, and the neutrophil layer was gently collected using a 3ml Pasteur pipette (see Figure 2.2).

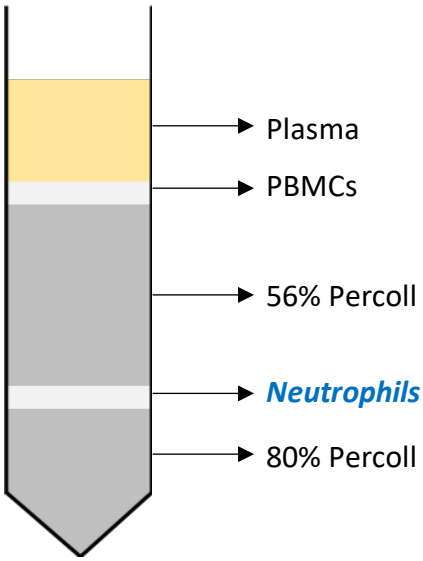


Figure 2.2: Density gradient from centrifuged Leukocyte Rich Layer. After addition of dextran to whole blood to create a Leukocyte Rich Layer (LRL), the sample was added to a Percoll density gradient containing 80% and 56% Percoll. After centrifuging at 500g for 20 minutes without break or acceleration, a visible neutrophil layer was formed at the interface of the two Percoll densities. The above layers containing plasma and peripheral blood mononuclear cells (PBMCs) was discarded and neutrophils collected using a Pasteur pipette.

These cells were then added to a new 15ml falcon containing 5ml of PBS and washed by centrifuging for 10 minutes at 250g. The resulting pellet was then resuspended in 10ml of PBS and a cell count was performed using haemocytometer. To exclude dead cells and allow effective counting of high concentration samples, 10µl of isolated neutrophils was diluted with 30µl of medium and 10µl of Trypan blue for a final dilution of 1:5. The volume containing 1 million cells were then added to a separate Eppendorf for each of the following conditions:

Tube 1: Untreated control (RPMI)

Tube 2: DMSO treated control (DMSO in RPMI)

Tube 3: PMA treated control (25nM PMA in RPMI)

Tube 4: Untreated organoid media control

Tube 5: Treated organoid media (Organoid media + 100mM Ethanol + 100ng/ml LPS)

Tubes 6-10: Organoid supernatants*

**Organoid supernatants were diluted in matched treated or untreated media. Ductal supernatants were diluted 1:3, differentiated supernatants were diluted 1:2.*

These Eppendorfs were then centrifuged at 250g for 5 minutes, and the cells were resuspended in 1ml of the appropriate media from the conditions above. The cells were then plated at least in triplicate in a 96 well tissue culture plate by adding 200μl of each sample per well (resulting in 200,000 neutrophils per well). The plate was then incubated for 3 hours at 37°C. After this incubation, the supernatant was removed from each well and transferred to a separate 0.5ml Eppendorf tube, which were then centrifuged in a pre-cooled centrifuge at 4°C, 2200g for 10 minutes to remove any cell debris. 100μl of cell-free supernatant from each tube was then added to a well in a flat bottomed black 96 well plate. In order to stain the extracellular DNA, SYTOX™ green dye was diluted 1:500 in RPMI media and 10μl was added to each well using a multichannel pipette. To allow quantification of total extracellular DNA, an 8-step standard curve of lambda DNA concentration, from 0-1000ng/ml was also included on the plate. The samples were then incubated in the dark for 10 minutes, and read immediately using a BioTek Synergy™ 2 plate reader at an excitation of 485 nm and emission 530 nm. Total DNA concentration was calculated using the standard curve for each experiment.

2.4 Imaging of human liver tissue

2.4.1 Immunohistochemistry in human liver sections

Immunohistochemical (IHC) analysis was performed on both Formalin Fixed Paraffin Embedded (FFPE) and snap frozen acetone fixed sections of human liver. FFPE sections were dewaxed and rehydrated by submerging them for 3x 3 minutes in xylene, 3x 3 minutes in industrial denatured alcohol (IDA) and 2x 3 minutes in water. Antigens that had been masked during the fixation and embedding process were then retrieved using either Tris-based (pH 9) or Citrate based (pH 6) antigen unmasking solution (antigen dependent). Before use, the unmasking solution was first diluted 1:100 in 1L of water and preheated in the microwave for 10 minutes. Dewaxed and rehydrated FFPE sections were then added and microwaved on high for 30 minutes, followed by 10 minutes to cool, and around 5 minutes under cold running water. Frozen sections were prepared for staining by thawing at room temperature for 10-20 minutes.

Prepared sections were then encircled using a wax pen and washed three times by submerging the slides in either PBS + 0.1% Tween (0.1% PBST) or TBS + 0.1% Tween (0.1% TBST) (primary antibody dependent) for 5 minutes on a rocking platform. The slides were then placed in a humidified chamber and incubated for 15 minutes with BLOXALL® Endogenous Peroxidase and Alkaline Phosphatase Blocking Solution on a rocking platform at room temperature. After this, the slides were washed again and incubated for 20 minutes on a rocking platform in a 2x casein solution (in dH_2O) in order to block non-specific protein binding. To further reduce non-specific background staining, the slides were incubated while rocking at room temperature for 20 minutes with serum from the host species of the secondary antibody (included in the

ImmPRESS® peroxidase (HRP) polymer kits). Primary antibodies were then added at the concentrations indicated in figure legends and left rocking at 4°C overnight or for 1 hour at room temperature. After this incubation, the slides were washed and then incubated with the secondary antibody from the appropriate ImmPRESS® peroxidase (HRP) polymer kit for 30 minutes while rocking at room temperature. The sections were then washed twice and stained with an ImmPACT® DAB Peroxidase (HRP) substrate kit as per the manufacturer's instructions. After staining had developed, the slides were washed with water for 5 minutes with gentle agitation and nuclei were counterstained with Meyers haematoxylin for approximately 30 seconds. After another 5 minute wash in water with gentle agitation, warm water was used to develop the haematoxylin staining for approximately 3 minutes. The sections were then dehydrated and cleared by reversing the protocol above (2x 3 minutes in water, 3x 3 minutes in IDA and 3x 3 minutes in xylene). Sections were then mounted by adding one drop of DPX mountant to a 25mm x 40mm coverslip, which was then slowly lowered on to the tissue section in order to avoid bubbles. This mountant was left to dry overnight before imaging.

In order to collect representative images and quantify staining, stained slides were imaged using a ZEISS Axio Scan .Z1 Slide Scanner at a 10x magnification. From these images, five random fields of view were selected using on the Zen Black software. To avoid bias, this was done by randomly selecting 5 areas across the thumbnail image on the same magnification. Images were created from view and converted to a .TIFF (Tagged Image File) format for quantification in FIJI image analysis software. This was completed using the thresholding function as shown in Figure 2.3.

2.4.2 Immunofluorescent staining of human liver sections

All immunofluorescence staining (IF) was completed on snap frozen acetone fixed liver sections. Sections were left to thaw at room temperature for 10-20 minutes and then encircled with a wax pen. These were then washed three times by submerging the slides in either 0.1% PBST or 0.1% TBST (primary antibody dependent) for 5 minutes on a rocking platform. To reduce non-specific staining, the slides were incubated for 20 minutes on a rocking platform with a blocking solution consisting of 2 x casein and 10% serum from the host species of the secondary antibody. After this incubation, the primary antibody was added at the dilutions indicted in Table 2.3 and the slides were incubated while rocking either overnight at 4°C or for 1 hour at room temperature. After this the slides were washed three times and incubated with the appropriate secondary antibody while rocking at room temperature for 30 minutes, and protected from direct light from this point onwards. The sections were then washed 3 times and nuclei were counterstained with DAPI for three minutes while rocking. The slides were then washed a final 3 times and mounted by adding 2 drops of DAKO fluorescence mounting media to each section and covering with a 25mm x 40mm coverslip. The sections were left to dry overnight at room temperature and then stored at 4°C until imaging. All IF slides were imaged using a ZEISS LSM780 or LSM880 confocal microscope, and image analysis was completed using ZEISS ZEN Blue or ZEN Black software.

Antibody	Species/isotype	Supplier	Clone	Cat No.	Dilution
Albumin	Goat/IgG	Bethyl Laboratories	Polyclonal	A80-229A	1:100
CD45	Rabbit/IgG	Abcam	Polyclonal	ab10558	1:400
Cytokeratin 19	Rabbit/IgG	Abcam	EP1580Y	ab52625	1:200
EpCAM	Mouse/IgG1	Progen	HEA125	61004	1:50
HNF4α	Rabbit/IgG	Cell Signalling	C11F12	3113S	1:5000
Neutrophil Elastase	Rabbit/IgG	Abcam	EPR7479	ab219585	1:2000
SOX9	Rabbit/IgG	Abcam	EPR14335-78	ab185966	1:250
TLR4	Mouse/IgG2b	Abcam	76B357.1	ab22048	1:200
Isotype controls					
Isotype control	Mouse/IgG2bκ	eBioscience™	eBMG2	15227377	AD
Isotype control	Rabbit/IgG	Abcam	EPR25A	ab172730	AD
Isotype control	Rabbit/IgG	Abcam	Polyclonal	ab37415	AD
Isotype control	Mouse/IgG1κ	Thermo Fisher	P3.6.8.1	14-4714-85	AD
Secondary Antibodies					
Goat anti-Mouse Alexa Fluor™ 647	Goat/IgG1	Invitrogen	Polyclonal	A21240	1:500
Donkey anti-Goat Alexa Fluor™ 488	Donkey/IgG	Invitrogen	Polyclonal	A11055	1:500
Goat anti-Mouse Alexa Fluor™ 488	Goat/IgG1	Invitrogen	Polyclonal	A21121	1:500
Goat anti-rabbit Alexa Fluor™ 594	Goat/IgG	Invitrogen	Polyclonal	A11037	1:500
DAPI	-	Invitrogen	-	D1306	1:50,000

Table 2.3: Table of antibodies detailing antibody target, host species and isotype, supplier, clone and catalogue number. Dilution of isotype control antibodies was assay dependent (AD).

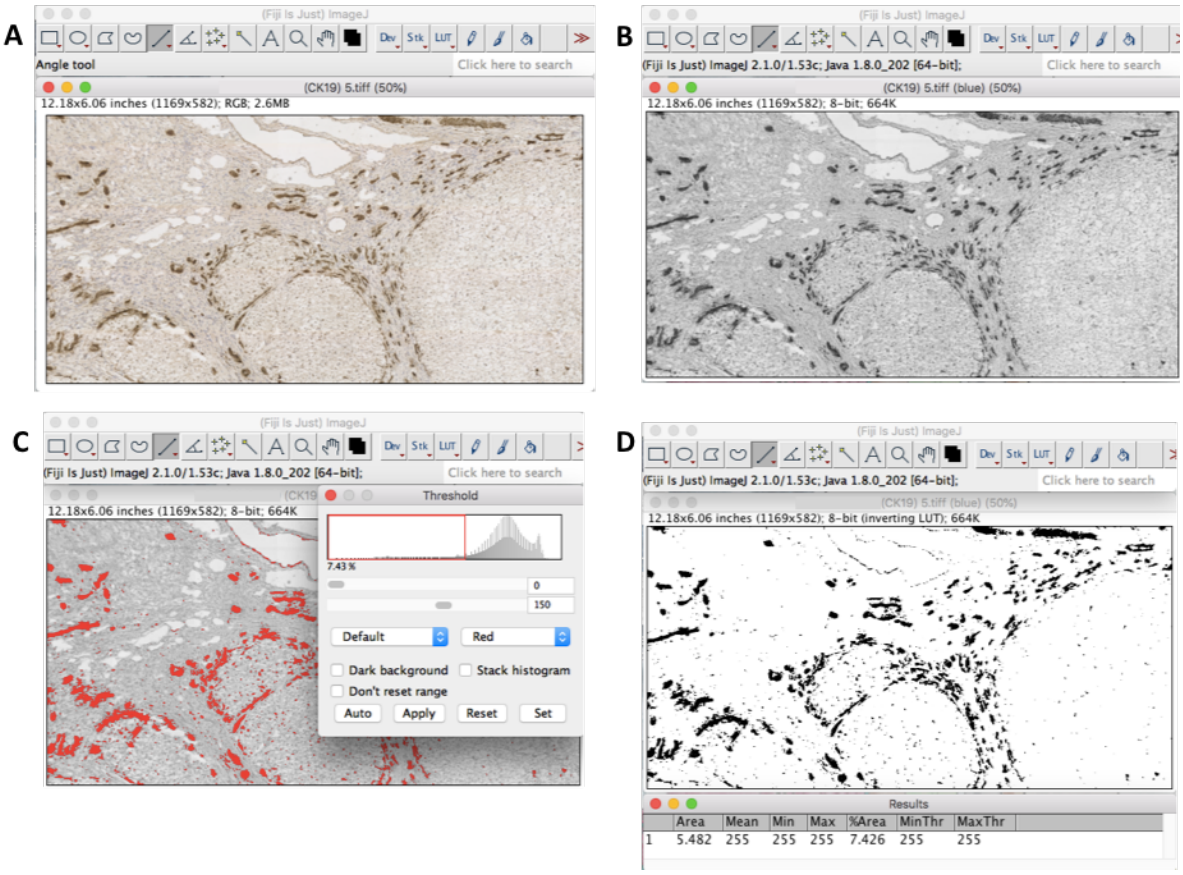


Figure 2.3: Quantifying immunohistochemical staining using FIJI software. Example image analysis process from an ALD liver section stained for Cytokeratin 19. Representative images selected randomly using ZEN Blue software are uploaded to FIJI as a .TIFF file (A). The image is then split into separate red, green and blue colour channels, with the blue channel being used for the next stages of analysis and show in panel(B). Using the threshold function, it is then possible to isolate areas of staining whilst selecting out areas of non-specific background staining, which is done manually to select a suitable threshold for the stain (area of selection shown in red) (C). This threshold can then be applied, and a measurement taken of the total percentage area of staining as shown in panel (D) where measured area is shown in black and %Area measurement is shown below the image. Using a macro plug in for the software, this can be batch processed to reduce bias when thresholding.

2.5 Analysing gene expression in whole tissue

2.5.1 RNA extraction

Whole tissue data in this project was predominantly generated using banked RNA extracted from human liver samples by Dr Emma Shepherd. RNA extraction was performed using a Qiagen RNeasy Plus Mini Kit as per the manufacturer's instructions. Prior to using the kit, working solutions of the kit components were prepared as follows: four volumes of absolute ethanol were added to buffer RPE, and 10µl/ml of β-Mercaptoethanol was added to the RLT buffer in order to improve the stability of the RNA (this solution was replaced once a month). 30mg of snap-frozen tissue was lysed in 600µl of RLT buffer using a gentleMACS™ Tissue Dissociator. 600µl of ethanol was then added to the sample, which was mixed and transferred to a RNeasy spin column. This was centrifuged for 30 seconds at 10,000rpm, and the flow-through was discarded from this and every subsequent step until the elution in RNase free water. On-column DNase digestion was then performed by adding 350µl of Buffer RW1 to the column and centrifuging for 30 seconds at 10,000rpm, followed by addition of 80µl of DNase (diluted 1:8 with buffer RDD) and incubating for 15 minutes at room temperature. A further 350µl of Buffer RW1 was then added to the column, which was centrifuged again for 30 seconds at 10,000rpm. The column was then washed twice with 500µl of Buffer RPE; first by centrifuging for 30 seconds at 10,000rpm then for 2 minutes at 10,000rpm. In order to further dry the membrane and ensure no carry over of ethanol, the column was then removed and added to a new 2ml collection tube which was centrifuged at full speed for 1 minute. The column was then placed in a 1.5ml collection tube and 30µl of RNase-free water was added directly onto the membrane. This was centrifuged for 1 minute at 10,000rpm in order to elute

the RNA and the concentration of RNA (ng/μl) was measured using an Implen™ NanoPhotometer™. This concentration was noted for cDNA synthesis.

2.5.2 cDNA synthesis

All cDNA was synthesised using Applied Biosystems™ High-Capacity cDNA Reverse Transcription Kit according to manufacturers' instructions. Each 20μl reaction contained 6.8μl of cDNA Master Mix and up to 13.2μl of RNA. Where RNA yields were high enough, 2μg of RNA was added to each 20μl reaction alongside nuclease free water to bring the total volume up to 13.2μl. However, in many instances this was not achievable from low yield organoid samples. In these cases, the maximum concentration possible was added within the limitation of the 13.2μl total volume. This was combined with 6.8μl of cDNA Master Mix (Table 2.4A) to give a final volume of 20μl, and cDNA was synthesised using a SensoQuest labcycler under the conditions as shown in Table 2.4B. Each time cDNA was synthesised, a No Enzyme Control (NEC) and No Template Control (NTC) were also made using the same protocol as for cDNA synthesis, except for using nuclease free water to replace the Reverse Transcriptase and RNase Inhibitor (NEC) or RNA (NTC). Synthesised cDNA was stored at -20°C.

A

cDNA Master Mix	
Component	**Volume (µl)**
10x RT Buffer	2
25x dNTP Mix (100mM)	0.8
10x RT Random Primers	2
MultiScribe™ Reverse Transcriptase	1
RNase Inhibitor	1

B

cDNA Synthesis		
Step	**Cycles**	**Time (Mins)**
1	25	10
2	37	120
3	85	5
4	4	Hold

Table 2.4: Conditions for cDNA synthesis from isolated RNA. For each 20µl cDNA synthesis reaction, 6.8µl of cDNA Master Mix was added using the component volumes listed in (A). cDNA was then synthesised using a SensoQuest Labcycler using the protocol conditions listed in (B).

2.5.3 Analysis of gene expression using quantitative PCR (qPCR)

mRNA expression was investigated in both whole liver and organoid samples using qPCR. Experiments were completed in a 384 well plate format with a total reaction volume of 10µl/well. This reaction contained 5µl of TaqMan® Universal Master Mix II (no UNG), 0.5µl of the desired Taqman assay (Table 2.6) and 4.5µl of cDNA in nuclease free water. Where possible 25ng of cDNA was added per well (with the volume of nuclease free water adjusted accordingly to give a total volume of 4.5µl) although this was limited by the concentration of cDNA made. The PCR was performed using a Roche LightCycler® 480 II machine under the conditions shown in Table 2.5 and analysis was completed using the LightCycler® 480 software. Relative expression to housekeeping genes (assay dependent) was calculated with samples with a Ct value lower than 35 cycles. Relative expression to housekeeping genes (in triplicates of each sample) was calculated by device software using the following equations:

$$\Delta \boldsymbol{CT} = (Average\ Ct\ for\ Gene\ of\ Interest) - (Average\ Ct\ for\ Housekeeping\ Gene)$$

$$\boldsymbol{Relative\ Expression\ of\ Gene\ of\ Interest} = 2^{-\Delta Ct}$$

qPCR conditions			
Step	**Cycles**	**Time (mm:ss)**	**Temperature (°C)**
Polymerase activation	1	10:00	95
Denature	40	00:15	95
Anneal/extend		1:00	60

Table 2.5: Conditions for qPCR reaction in a Roche LightCycler® 480 II.

Target	Assay ID
ABCB11 (BSEP)	Hs00994811
Albumin	Hs006090411_m1
β-Actin	Hs01060665_g1
CYP2C19	Hs00426380
CYP2E1	Hs00559367_m1
CYP3A4	Hs00604506
EPCAM	HS00901885_m1
GAPDH	Hs99999905_m1
HNF4A	Hs00230853_m1
Human complement C3	Hs00163811_m1
Human complement C5	Hs00156197_m1
Human complement C8A	Hs00175098_m1
Human complement MBL2	Hs00175093_m1
KRT19	Hs00761767_s1
KRT7	Hs00559840_m1
SRSF4	Hs00194538_m1
TLR4	Hs00152939_m1
CDKN2A (P16)	Hs00923894
CDKN1A (P21)	Hs00355782

Table 2.6: Table of TaqMan Assay IDs utilised for qPCR analysis in whole liver tissue and 3D organoids.

2.6 Human Liver Organoid Culture

Organoid protocols were developed and adapted from protocols described by Huch *et al*(214) and Fernando *et al*(273), alongside in-house protocols from the Centre for Liver and Gastrointestinal Research (University of Birmingham) and Dr Simon Hirota (University of Calgary).

2.6.1 Isolation of progenitor cells from fresh human liver tissue for 3D organoid culture

Organoid cultures were established from approximately 2cm^3 human liver tissue using an adapted version of the protocol published by Huch *et al* (214) and Fernando *et al*(273) (Figure 2.4). Cubes of liver were cut (avoiding the liver capsule) from a slice of either explanted ALD liver, normal resected tissue or donor liver. Cubes were then stored in Dulbecco's Modified Eagle Medium (DMEM) at 4°C until isolation. Ideally isolations took place within 48 hours of the organ being explanted, but organoid cultures were also grown successfully when isolated within 72 hours. All of the reagents were kept on ice throughout the isolation protocol, apart from those used for enzyme digestion. When isolating from tissue samples, the following items were prepared in advance:

- A 48 well tissue culture plate was pre-warmed to 37°C at least two hours before plating the isolated cells, ideally the night before. This allows the Matrigel to set instantly on contact with the plate and help maintain the domed structure.
- A 100µl aliquot of Matrigel was thawed on ice, in the fridge at 4°C for at least two hours before plating isolated cells, ideally the night before. As Matrigel begins to solidify at room temperature it is essential to keep this on ice at all times, and thawing time cannot be reduced by incubating at higher temperatures.

- **Wash buffer** (DMEM containing 1% FBS) was prepared and precooled on ice.
- **Digestion buffer** (Earls Balanced Salt Solution (EBSS) containing 2.5mg/ml collagenase D and 0.1mg/ml DNase 1) was prewarmed to 37°C.
- An aliquot of Accutase enzymatic digestion solution was prewarmed to 37°C.

Importantly, before any contact with cells throughout this protocol, pipette tips were pre-coated in ice cold PBS containing 2% FBS (PBS2) in order to prevent sample loss due to cells adhering inside the pipette tip. This step also allowed precooling of pipette tips before handling Matrigel.

The cube of tissue (Figure 2.4A) was removed from the DMEM and minced in a sterile petri dish until pieces were approximately 1-3mm^3 (Figure 2.4B). Once minced the sample was transferred to a 50ml tube, 20ml of wash buffer was added and sample was washed twice by centrifuging at 4°C, 300g for 5 minutes (Figure 2.4C). After this, the supernatant was discarded and pelleted tissue was incubated in pre-warmed digestion buffer for 30 minutes at 37°C, with occasional agitation by hand. 20ml of ice-cold wash buffer was added to stop digestion, and the sample was filtered through a 70μm nylon cell strainer into a clean 50ml falcon tube (Figure 2.4D). After centrifugation at 4°C, 300g for 5 minutes, the cell pellet was resuspended in 10ml of fresh wash buffer and left on ice (Fraction A). During this time, any tissue that remained in the 70μm nylon cell strainer was digested for a second time using Accutase. The strainer was placed in a well of 6 well plate with the lip of the filter resting on the edge of the well. 7.5-10ml of Accutase was added and tissue was incubated at 37°C for 10 minutes (Figure 2.4E). At the end of this incubation the tissue was washed through using 5ml of ice-cold wash buffer. This cell suspension (Fraction B) was then collected from the well with a Pasteur

pipette, centrifuged and resuspended as with Fraction A. The two fractions were then combined and filtered through a new 70μm nylon cell strainer. After a final wash the resulting pellet was resuspended in 10ml of Advanced DMEM-F12 (ADF). This cell suspension was centrifuged again at 4°C, 300g for 5 minutes. The supernatant was then removed and the pellet was resuspended in 35ml ADF + 13.5ml Percoll (density 1.130g/ml) + 1.5ml 10x PBS in order to remove unwanted cells and debris. This suspension was centrifuged at 4°C, 100g for 10 minutes and then washed three times in 10ml of ADF by centrifuging at 4°C, 300g for 5 minutes.

To prepare cells for resuspension in Matrigel, the resulting pellet was resuspended in 1ml of ADF, transferred to a 1.5ml Eppendorf tube, and centrifuged at 4°C, 300g for 5 minutes. This was done twice - once with the hinge of the Eppendorf facing downwards, and then again with the hinge of the Eppendorf facing upwards. The supernatant was then removed, leaving around 25μl on the pellet, which was then pipetted up and down 3-5 times. This facilitated partial resuspension of the cells to minimise bubble formation after addition of Matrigel. The cells were then resuspended in 75μl Matrigel. 25μl of Matrigel-cell suspension was added to the centres of 3-4 wells in a pre-warmed 48-well tissue culture plate using pre-cooled pipette tips. The plate was inverted and the Matrigel was left to solidify at 37°C for 30 minutes (Figure 2.4F-G). Once the Matrigel had solidified, cells were fed with 250μl per well of "Expansion Medium" as described by Huch *et al*(214), the components of which are listed in Table 2.6. This media was supplemented with 100ng/ml Noggin, 100ng/ml Wnt, and 10μM Y27632 for the first three days post-isolation. These cultures were not passaged until two weeks post-isolation.

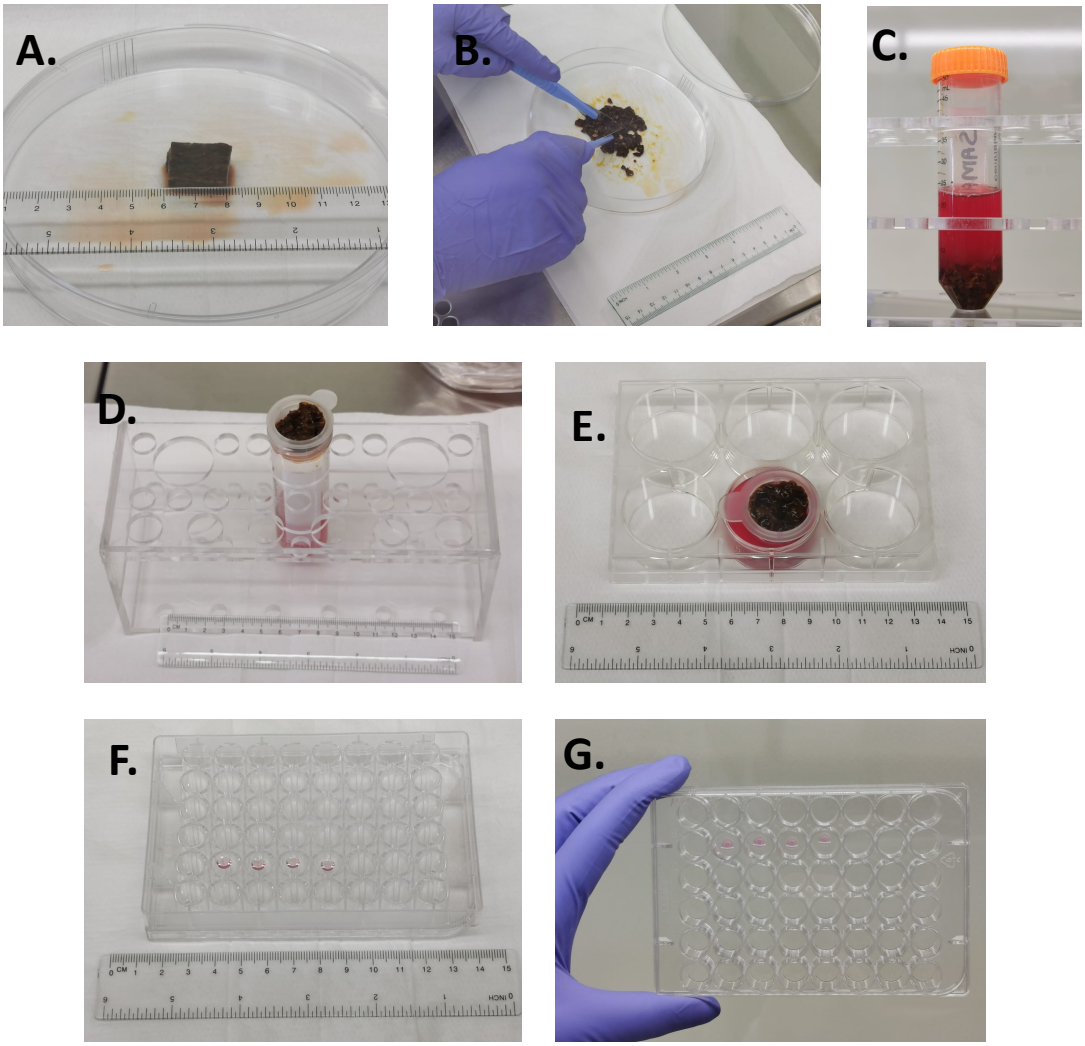


Figure 2.4 Isolation of progenitor cells from whole human liver. Cubes of liver (A) are minced (B), washed and incubated with a collagenase D/DNase enzyme digest solution (C). The cell suspension is then filtered through a cell strainer (D) and the remaining tissue is digested a second time with Accutase (E). After further washing and clean up steps, the cell pellet is resuspended in Matrigel and plated in a pre-warmed 48 well plate. This plate is then inverted (F) and incubated at 37℃ to set the Matrigel dome. Once the domes have solidified (G) 250µl of supplemented Expansion Media was added per well, as described in Table 2.6.

2.6.2 Isolating hepatic organoids from cryopreserved tissue

Pieces of fresh liver tissue approximately 10mm x 3mm x 3mm were cut and added to a 2ml cryovial, with 1-2ml of "Freezing Medium" consisting of ADF + 10% FBS + 5% DMSO. These vials were then frozen slowly in an alcohol-free freezing container for 24 hours, and stored long term in liquid nitrogen. To isolate cells from these samples, they were removed from liquid nitrogen and thawed rapidly at 37°C. Tissue pieces were allowed to settle to the bottom of the vial, and freezing medium was carefully aspirated. The tissue was then washed with 1ml of "Recovery Media" described by Tsai *et al*(274) as detailed in Table 2.6. The contents of the cryovial were then transferred to a 1.5ml Eppendorf using a widened pipette tip. The tissue pieces were allowed to settle and as much liquid was removed as possible, followed by the addition of 500µl of fresh recovery media. To dissociate the tissue pieces, the sample was minced using fine nosed dissecting scissors within the Eppendorf. A PBS2 coated widened pipette tip was then used to transfer the contents to a 50ml Falcon tube, with any leftover cells being washed from the Eppendorf with an additional 1ml of recovery media and added to the Falcon tube. The tissue was again left to settle, the supernatant was removed and the tissue pieces were incubated for 30 minutes in digestion buffer as listed in 2.6.1. From this point onwards, the protocol followed the same steps as when isolating from fresh whole tissue (Section 2.6.1).

When the Matrigel-cell suspension was plated and solidified, 250µl of recovery media was supplemented with 10µM of Y27632 and added to the wells. This media was replaced with recovery media alone for a further 48 hours, and then finally replaced with standard Expansion Media. These cultures were not passaged until two weeks post-isolation.

Expansion

Reagent	Concentration	Company	Cat. number
A-83-01	5 μM	Merck Life Science	SML0788
B27	1X	Thermo Fisher	17504044
EGF	50 ng/nl	Peprotech	AF-100-15
FGF10	100 ng/ml	Peprotech	100-26
Forskolin	10 μM	STEMCELL Technologies	72112
Gastrin	10 nM	Merck Life Science	G9020
HEPES pH7	10 mM	Sigma-Aldrich	H0887
HGF	25 ng/ml	Peprotech	100-39H
N-Acetylcysteine (NAC)	1.25 mM	Sigma	A9165-5G
N2	1X	Thermo Fisher	11520536
Nicotinamide	10 mM	Sigma	72345-50G
R-Spondin 1	500 ng/ml	Peprotech	120-38
Additional supplements post-isolation:			
Noggin	100 ng/ml	Peprotech	120-10C
Wnt	100 ng/ml	Bio-Techne Ltd	5036-WN-010
Y27632	10 μM	Peprotech	1293823

Differentiation

Reagent	Concentration	Company	Cat. number
A-83-01	500 nM	Merck Life Science	SML0788
B27	1X	Thermo Fisher	17504044
BMP7	25ng/ml	Peprotech	120-03P
DAPT	10 μM	Abcam	ab120633
Dexamethasone	30 μM	Sigma-Aldrich	D2915
EGF	50 ng/ml	Peprotech	AF-100-15
FGF19	100 ng/ml	Peprotech	100-32
Gastrin	10 nM	Merck Life Science	G9020
HEPES pH7	10 mM	Sigma-Aldrich	H0887
HGF	25 ng/ml	Peprotech	100-39H
N2	1X	Thermo Fisher	11520536

Recovery

Reagent	Concentration	Company	Cat. number
Thiazovivin	2.5μM	Peprotech	1227180
SB431542	100nM	Peprotech	3014193
CHIR99021	4μM	Peprotech	2520691
Y27632	10μM	Peprotech	1293823

Table 2.7: Organoid media composition. All organoid media was made from Advanced DMEM F-12 (ADF) supplemented with 5mM Penicillin, Streptomycin and Glutamine (PSG) alongside additional components as listed for Expansion, Differentiation(214) and Recovery Media(274). Media was prepared in small batches and stored at 4℃ for no more than 2 weeks. Aliquots of media were warmed as needed to feed organoid cultures, and Primocin antimicrobial reagent (100μg/ml) was added to prevent growth of contaminants(273).

2.6.3 Maintenance culture of hepatic organoids (expansion period)

Culture protocols were adapted from Huch *et al*(214) and Fernando *et al*(273). Organoid media was changed every 2-3 days by aspirating the media from each well and replacing it with 250µl of fresh, prewarmed Expansion Media. After the initial 2-week period post isolation, organoid cultures were passaged approximately once every 7 days at a split ratio of 1:2 – 1:12. Confluence was assessed based on organoid crowding, including the number and size of 3D structures within the Matrigel droplet as demonstrated in Figure 4.5 (Chapter 4). This protocol required the sample and all reagents to be kept on ice and all tips to be coated with PBS2. Media was aspirated and replaced with 1ml of ice-cold ADF. Matrigel domes and organoid structures were then mechanically dissociated via pipetting up and down with a P1000 pipette tip, and the contents of the plate were transferred to a 50ml falcon tube. The cells were centrifuged twice at 4°C, 300g, for 5 minutes, then the supernatant was removed and the cells were resuspended in 1ml of ADF. This cell suspension was then pipetted up and down 30 times in order to further dissociate organoid structures and transferred into a 1.5ml Eppendorf, which was centrifuged at 4°C, 300g for 5 minutes. This was done twice - once with the hinge of the Eppendorf facing downwards, and then again with the hinge of the Eppendorf facing upwards. After removing the supernatant, the pellet was resuspended in the appropriate volume of Matrigel for the desired number of wells (25µl/well); e.g. to split 2 wells at a 1:6 ratio, the pellet would be resuspended in 300µl of Matrigel for plating in 12 wells. Organoids where then plated as described in 2.6.1 and 250µl of Expansion Media was added per well. This media was supplemented with 10µM Y27632 for the first three days post passage, then changed every 2-3 days thereafter.

2.6.4 Cryopreservation and subsequent re-establishment of organoid cultures

To cryopreserve cultured organoids for storage, organoid structures were dissociated and removed from the Matrigel by following the steps in Section 2.6.3. After washing twice (4°C, 300g for 5 minutes), supernatant was removed and replaced with 1ml of "freezing medium" consisting of ADF + 10% FBS + 5% DMSO. The equivalent of 2-3 confluent wells were stored per cryovial and topped up with freezing medium to a total volume of 1ml per vial. For example, freezing 10 confluent wells would give 5 cryovials each containing 200µl of cell suspension, followed by the addition of 800µl of freezing medium. The cryovials were then frozen slowly in an alcohol-free freezing container for 24 hours and stored long term in liquid nitrogen.

In order to culture these cells, samples were removed from liquid nitrogen and thawed rapidly with the addition of 1ml of prewarmed "thawing media" (at 37°C) consisting of ADF + 1% Bovine Serum Albumin (BSA) + 15mM HEPES buffer, as adapted from protocols published by STEMCELL Technologies(275). This cell suspension was then transferred using a PBS2 coated pipette into a 15ml falcon tube containing 2ml of room temperature thawing media. The cryovial was then washed out with an additional 1ml of thawing media and added to the 15ml falcon tube. This tube was centrifuged at 4°C, 300g for 5 minutes, and the resulting pellet was resuspended in 1ml of ice cold ADF and transferred to a 1.5ml Eppendorf. Cells were washed twice and plated in Matrigel as described in section 2.6.1. Once the Matrigel had solidified, 250µl of Expansion Media supplemented with Y27632 (10mM) was added to each well.

2.6.5 Differentiation into hepatocyte-like organoids

The protocols above generate progenitor-derived ductal-like organoids. These were further differentiated into hepatocyte-like organoids as described by Huch *et al*(214). In order to encourage differentiation into mature hepatocytes, cultures were passaged and then "primed" with the addition 25ng/ml of BMP7 for 7-10 days. After this period, the organoid cultures were passaged again and plated for the final time. Since differentiated organoids do not proliferate, this passage step was used to set up the final experimental plates. The cultures were supplemented with BMP7 for a further 2-4 days, and then the media was replaced with "Differentiation Media" as described in Huch *et al*(214). The components and concentrations of this media are shown in Table 2.6.

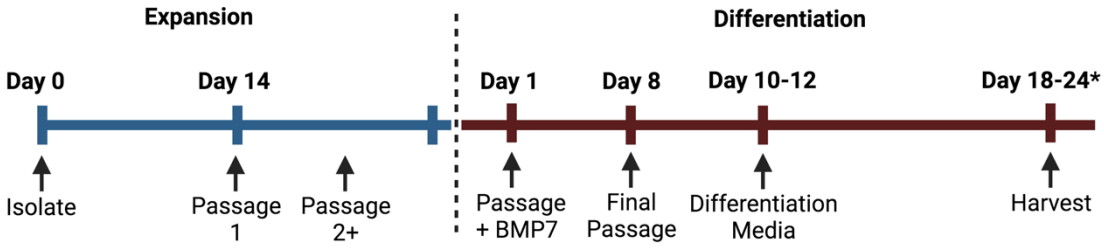


Figure 2.5: Timeline for isolation, expansion and differentiation of 3D organoids. Hepatic progenitor cells were isolated from human liver tissue as described in 2.6.1 and plated in Matrigel. After 2 weeks these were passaged for the first time as described in 2.6.3, and then continually passaged approximately every 7 days. To differentiate, cultures were passaged and BMP7 was added for 7 days. Organoids were then passaged again, left in Expansion Media plus BMP7 for 2-4 days and then Expansion Media was replaced with differentiation media. Organoids were harvested either 8 or 12 days after switch to differentiation media. Figure created in BioRender.

2.7 Investigating phenotype and function of primary human liver derived organoids

2.7.1 Analysis of hepatic progenitor cell phenotype using flow cytometry

To confirm the presence of $EpCAM^+$ progenitor cells in our tissue isolates, the final pellets from one ALD and one donor sample isolated as described in 2.6.1 were fixed in 4% PFA at room temperature for 1 hour. These were then washed three times in 10ml of PBS by centrifuging at 250g for 3 minutes, resuspended in FACS buffer (PBS + 2% FBS), and distributed evenly between round bottom tubes. Samples were centrifuged at 420g for 5 minutes and supernatant was gently poured out leaving approximately 100µl in the tube. Anti-EpCAM antibody was added to one tube, leaving the other as an unstained control, and incubated at room temperature for 30 minutes. The sample was then washed in FACS buffer at 420g for 5 minutes, and incubated with a fluorescent secondary antibody for 30 minutes. Sample was then washed in 1ml of buffer twice, and then resuspended in 300µl. This was then filtered through a cell strainer, and analysed using a Fortessa Flow Cytometer using the gating strategy indicated in Figure 2.6. Compensation beads were used to optimise fluorescence compensation.

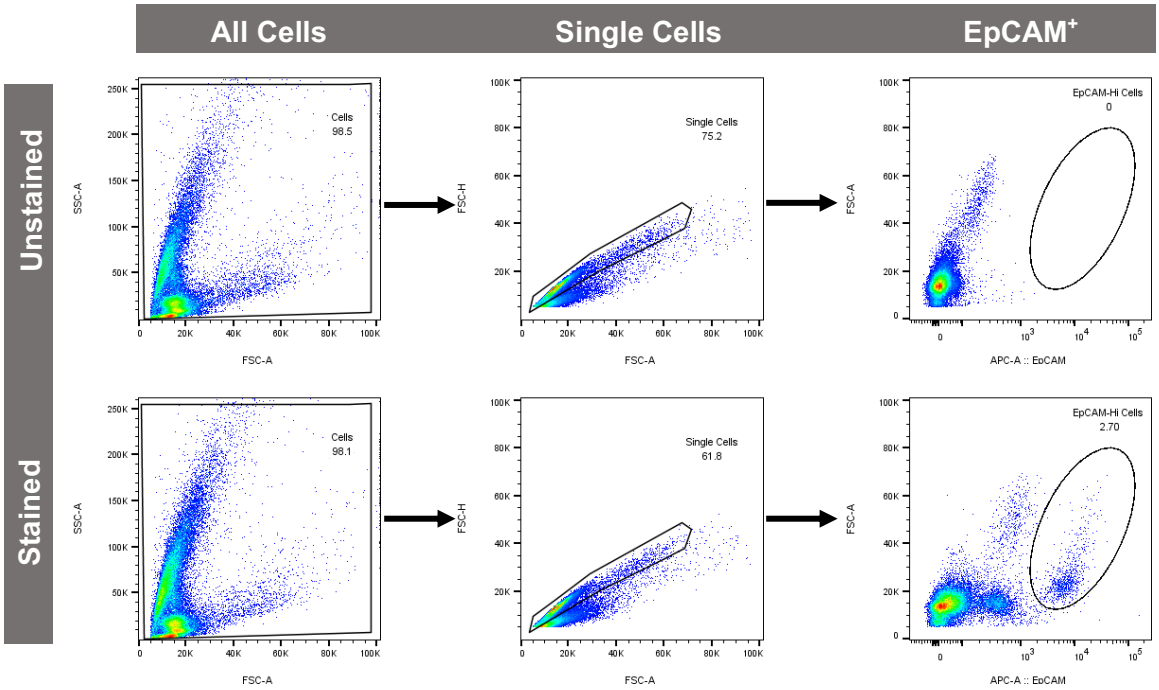


Figure 2.6: Analysis of hepatic progenitor cell phenotype using flow cytometry. Fixed cells from whole liver isolations as described in 2.6.1 were stained for EpCAM⁺ progenitor cells compared to an unstained control. Single cells were selected using Forward Scatter Height vs Forward Scatter Area (FSC-H vs FSC-A), removing cell clumps. EpCAM⁺ cells were then selected based on high expression of APC fluorescence.

2.7.2 Removal of organoids from Matrigel for downstream applications

The Matrigel dome surrounding organoids needed to be depolymerised and removed in order to complete phenotypical and functional analysis of the cells. Culture media was gently aspirated and was replaced with 200µl of Corning® Cell Recovery Solution, which was used as per the manufacturer's instructions. The cultures were gently pipetted up and down to break up the Matrigel with a P1000 pipette tip (for RNA or protein extraction) or a sterile Pasteur pipette (for whole organoid imaging). The plate was then left rocking at 4°C for approximately 20-30 minutes. After this, the contents of the plate were transferred to a 15ml

falcon tube and centrifuged at 4°C for 3 minutes at 250g (for RNA and protein), or 100g (for imaging) in order to separate the depolymerised Matrigel. This supernatant was removed with a P1000 pipette tip and replaced with 3ml of ice-cold PBS to wash off residual Matrigel and cell recovery solution. The cell pellet was gently resuspended with a P1000 pipette tip or Pasteur pipette and centrifuged at 250g or 100g again as above. This wash step was then repeated 1-2 times depending on the stability of the pellet, as Matrigel carry over results in a less defined pellet at the bottom of the tube and therefore requires an extra wash step for removal. The final pellet was then resuspended as appropriate for the desired downstream application.

2.7.3 Monitoring organoid growth over time

To compare growth rates of donor liver and cirrhotic liver-derived organoids, the increase in total protein concentration was monitored over the course of 10 days. Two wells of organoids were taken every 2-3 days post passage (including immediately after plating on day 0). The organoids were removed from Matrigel as described in Section 2.7.2 and lysed in 250µl of 1x RIPA (Radioimmunoprecipitation assay) buffer. Samples were snap frozen in liquid nitrogen and then stored at -80°C for batch analysis. To perform this analysis, lysates were thawed on ice and then sonicated at a frequency of 20 kHz for two 10 second periods with the samples remaining on ice throughout the protocol. Total protein was then immediately quantified using a Pierce™ Rapid Gold BCA Protein Assay Kit as per the manufacturer's instructions. Briefly, a BSA standard (2mg/ml) was diluted in RIPA buffer to give concentrations of 2,000, 1,500, 1,000, 750, 500, 250, 125, 25, and 0µg/ml. The standards, alongside RIPA buffer (as a background control) and the protein lysates were added in duplicate to a low adhesion 96 well

plate with 20µl per well. The appropriate amount of Pierce™ Rapid Gold Working Reaction was then prepared for the number of samples at a ratio of 50:1 for kit reagents A:B. The working reaction was mixed thoroughly, rapidly added to the plate and incubated at room temperature for 5 minutes. Absorbance at 480nm was read using a BioTek Synergy™ HT plate reader. Average absorbance values for replicate wells from each condition were calculated and background was subtracted from all values. Total protein concentrations were then calculated using the known values from the standard curve. Growth rate was assessed by the percentage increase in total protein between each sample at day 0, 2, 4, 7, and 9.

2.7.4 Acute stimulation of organoids with ethanol and LPS

In order to recreate the hepatocellular toxic response to ethanol in patients with ARLD, we exposed organoids to a range of alcohol concentrations in the presence or absence of LPS. Responses were explored in both ductal-like and hepatocyte-like organoids derived from both healthy and cirrhotic tissue. Stocks of 1M Ethanol were diluted in organoid media in order to give final in-well concentrations between 1-200mM, and the cultures were incubated for 24 hours at 37°C alongside untreated controls. Ductal organoids were treated at high-confluency (approximately 6 days post-passage) and hepatocyte-like organoids were treated on either the 8th or 11th day of culture (assay dependent) in differentiation media. For dual injury with LPS, a stock LPS concentration of 1mg/ml was diluted in the appropriate organoid culture medium to give a final in-well concentration of 100ng/ml LPS. After 24 hours, supernatants from each condition were collected, snap frozen in liquid nitrogen and stored at -80°C. Organoids were collected for RNA isolation (Section 2.7.6) or immunofluorescent staining (Section 2.7.9).

2.7.5 Treatment with fatty acids to assess formation of lipid droplets

To assess whether differentiated organoids were able to form lipid droplets under lipogenic conditions, cultures of hepatocyte-like donor-derived organoids were fed with media supplemented with 0.4mM Oleic acid, and 0.2mM Palmitic acid for 24 hours. Wells were then washed twice with 1ml PBS and fixed in PFA for 1hr 20 minutes. Organoids were then washed three times in PBS by centrifuging for 3 minutes at 100g, and resuspended in LipidTOX™ non-specific lipid dye. Organoids were transferred to a chamber slide and imaged on a ZEISS LSM880 confocal microscope with Airyscan by Pantelitsa Papakyriacou.

2.7.6 Analysing organoid gene expression via qPCR

To isolate RNA, organoids first needed to be removed from the Matrigel as described in 2.7.2**.** Once washed in PBS, the final pellet was resuspended in 350µl of RLT lysis buffer (which was increased to 600µl if the lysed sample was highly viscous), snap frozen in liquid nitrogen and stored at -80°C. Stored samples were thawed on ice and lysed further by passing the sample through a needle 10 times. One unit of 70% ethanol (either 350µl or 600µl depending on the volume of RLT buffer used for initial lysis) was added to the sample before proceeding with RNA isolation, cDNA synthesis and qPCR as described in Sections 2.5.1-2.5.3.

2.7.7 qPCR arrays to investigate expression of multiple pathway components

In order to check if (and which) complement proteins were expressed by liver organoids, we used the TaqMan® Array for the Human Complement Pathway. This array contains lyophilised TaqMan assays for 28 complement pathway associated genes and 4 endogenous control genes in a 96 well plate format. The plate design allows for a single sample plated in triplicate,

however we used this opportunity to investigate three different samples plated singly. A total of 12.5ng of cDNA (in nuclease free water) was added to each well along with 5µl of TaqMan® Universal Master Mix II (with UNG) to give a total reaction volume of 10µl. The samples were added to the plate using a multichannel pipette, mixed several times by pipetting to allow for reconstitution of the lyophilised TaqMan assays, and then transferred to a white Roche LightCycler® compatible 96 well plate. The PCR was completed using Roche LightCycler® 480 II machine under the conditions shown in Table 2.4, with an additional UNG activation step at the start for two minutes at 50°C. I assessed the variability of the endogenous housekeeping genes across the three samples and chose TBP as the gene against which to calculate relative expression.

2.7.8 Analysis of fibrosis associated gene changes with NanoString technology

RNA was isolated from organoid cultures as described in 2.7.6 and purity was confirmed via TapeStation. Samples were loaded onto an nCounter Fibrosis Panel by Ellie Northall, and the NanoString panel was run by Birmingham Tissue Analytics. Data was analysed in nCounter software by Dr Emma Shepherd and displayed as a heatmap of differential gene change in response to treatment, with minimum cut-off of 2-fold gene change.

2.7.9 Immunofluorescent staining of whole organoids

Throughout this protocol (adapted from protocols provided by Dr Simon Hirota), organoids were handled using a 3ml Pasteur pipette to avoid the collapse of 3D structures. To prepare the organoids for staining, they were first removed from their Matrigel dome as described in section 2.7.2 and then fixed in a 15ml falcon tube in 1ml of 4% Paraformaldehyde (PFA) for at

least 30 minutes at room temperature. Organoids were then washed three times in 10ml of PBS by centrifuging at 100g for 3 minutes, removing supernatant and gently resuspending the structures in fresh PBS with a Pasteur pipette. After the last wash, cells were permeabilised with 0.2% Triton-X for 10 minutes whilst rocking at room temperature. The tube was then centrifuged at 100g for 1 minute to collect the organoids at the bottom of the tube and the supernatant was removed. The structures were washed 3 times in PBS + 0.2% Tween (0.2% PBST) by adding 5ml of PBST, rocking at room temperature for 3 minutes and then centrifuging for 1 minute at 100g. In order to reduce non-specific staining, the organoids were blocked in a solution containing 2x casein and 10% serum from the secondary antibody host species for 20 minutes. Primary antibodies were then added at the dilutions indicated in Table 2.3 and samples were incubated on a rocking platform for 1 hour at room temperature or overnight at 4°C. The structures were then washed 3 times in 0.2% PBST and incubated with the appropriate secondary antibodies for 30 minutes at room temperature, whilst rocking and protected from light. After this incubation the organoids were washed another three times and the nuclei were counterstained with DAPI for 5 minutes while rocking at room temperature**.** After a final 3 washes, organoids were mounted in an ibidi 8-well μ-slide using DAKO fluorescence mounting medium and imaged using a ZEISS LSM780 or LSM880 confocal microscope. Image analysis was completed using ZEISS ZEN Blue or ZEN Black software.

2.7.10 IL-8 ELISA

IL-8 concentrations in organoid supernatants were measured using a Human IL-8/CXCL8 DuoSet® ELISA and ancillary reaction kit as per the manufacturer's instructions. Briefly, a high-binding plate was coated with 100μl of IL-8 capture antibody overnight at room temperature.

The next day the content of each well was aspirated and washed three times with 400µl of wash buffer. At the end of the wash step the plate was blotted firmly against absorbent tissue to prevent any carry over of liquid between steps. Non-specific binding was then blocked with 300µl of block buffer for 1 hour at room temperature, followed by another three washes. Standards were prepared using a 1:2 serial dilution (from 2000pg/mL to 31.3pg/mL) of a reconstituted IL-8 protein standard. 100µl per well of these standards were added to the plate in duplicate along with diluent and media only controls in order to subtract background binding. 100µl per well of organoid supernatant was then added in triplicate either neat or at a 1:10 dilution, the plate was covered with an adhesive strip and then incubated for 2 hours at room temperature. After this incubation, the plate was washed three times and 100µl per well of detection antibody was added for a further 2 hours at room temperature. After another three washes, 100µl of Streptavidin-HRP was added to each well and incubated for 20 minutes at room temperature. From this point, the plate was protected from direct light. The plate was then washed as above one final time, and 100µl of substrate solution (provided) was added to each well for 20 minutes. This reaction was stopped by adding 5µl of stop solution and gently tapping to encourage mixing. The plate was read immediately at 450nm and 540nm using a BioTek Synergy™ HT plate reader, and the values for the second reading were subtracted. The averaged values for the standard curve were interpolated using a Sigmoidal, 4PL, X is concentration analysis in GraphPad Prism, and used to calculate the concentration of IL-8 in each condition.

2.7.11 Quantification of multiple analytes in organoid supernatant using Proteome Profilers

In order to investigate the range of chemokines and cytokines produced by treated and untreated organoids, we analysed supernatants using Human Proteome Profiler™ Arrays as per the manufacturer's instructions. One membrane (containing the capture antibodies) was added to each well of the assay dish provided, with the identification number facing upwards. 2ml of array buffer 4 was added to block non-specific binding, and the dish was incubated while rocking for 1 hour at room temperature. During this incubation, samples were prepared by adding array buffer 4 to give a total volume of 1.5ml alongside 15µl of the provided antibody detection cocktail, and left to incubate at room temperature for 1 hour. Array buffer 4 was then aspirated from each well and replaced with the prepared sample mixtures. This was left to incubate on the membranes overnight at 4°C while rocking. The next day, membranes were removed using tweezers and placed in separate 50ml falcon tubes containing 20ml of wash buffer. Each membrane was washed three times while rocking for 10 minutes, and the dish was washed and dried thoroughly with deionised water. After the third wash, the membranes were returned to the dish and incubated with 2ml of streptavidin-HRP at room temperature while rocking for 30 minutes. Each membrane was washed an additional three times. In order to image the blots, excess buffer was removed from each membrane with absorbent paper. The membranes were placed on a flat piece of clingfilm where 1ml of Chemi reagent mix was added to each membrane. After 1 minute, excess reagent was removed with absorbent paper and the blots were placed between two halves of a plastic sheet protector. This was then smoothed over to ensure no air bubbles remained and the blots were imaged using a Bio-Rad ChemiDoc™ MP Imaging System. Images of the blots were quantified using Fiji image analysis software to calculate the mean pixel intensity (MPI) of each

dot, and values were normalised to the positive control values from the corner of each blot. To calculate the MPI, images were converted to 8-bit TIFFs and inverted to a negative image (in order to more clearly select the areas of interest). Using a circular selection tool, each dot was selected and the MPI within that area was measured. The negative control blot was also measured to give a background reading, which was subtracted from all other values.

2.7.12 Assessing chemotactic potential of organoid media via neutrophil migration

The chemotactic properties of organoid supernatant were analysed using a CytoSelect™ Cell Migration Assay as per the manufacturer's instructions. Briefly, 30ml of healthy donor blood was collected in EDTA containing vacutainers, and neutrophils were isolated as described in section 2.3.4. The resulting pellet was then gently washed in HBSS (containing no calcium or magnesium) by centrifuging for 10 minutes at 250g. Cells were then resuspended in 10ml of HBSS and counted using a haemocytometer, after which they were centrifuged again at 250g for 10 minutes and resuspended at $3x10^6$ cells per ml in HBSS containing calcium and magnesium.

The Cell Migration assay plate was prepared during the above incubation periods. The plate was removed from the fridge and warmed up at room temperature for 10 minutes. Under sterile conditions, the 3μm membrane chamber was removed from the plate and 150μl of either organoid supernatant or controls were added to the wells of the "feeder tray". The membrane chamber was then carefully replaced (ensuring no bubbles were trapped underneath) and 100μl of neutrophil cell suspension was added on top of the membrane in each well. The plate was then incubated at 37°C for 2 hours to allow neutrophils to migrate towards the chemoattractant in the feeder tray. At the end of the incubation, the media was

aspirated from the top half of the membranes and the chamber was moved from the feeder tray to a "cell harvesting" tray containing 150µl per well of pre-warmed Cell Detachment Solution and incubated at 37°C for 30 minutes. The chamber was then gently tilted from side to side to detach any cells that may remain on the underside of the membrane, and removed. From each well, 75µl of sample from both the feeder tray and the harvesting tray were then combined in a clean 96 well plate and 50µl of pre-prepared Lysis Buffer/CyQuant® solution was added and the plate was incubated at room temperature for 20 minutes. To quantify migration, 150µl from each well was then transferred to a 96 well black bottomed imaging plate and fluorescence was read at 480nm/520nm using a BioTek Synergy™ 2 fluorescence plate reader.

2.7.13 Investigating Organoid-neutrophil co-culture

A pilot experiment was performed to assess neutrophil-organoid co-cultures. Primary neutrophils were isolated by Dr Marco Rink, and stained with CellTracker™ Green (1:1000 dilution) for 40 minutes at 37°C. Simultaneously, organoids in culture were stained with DRAQ5™ Fluorescent Probe Solution (1:2000 dilution). Stained neutrophils were washed once in 10ml of HBSS and resuspended in organoid media at a concentration of 2 million/ml. Organoid media was removed from organoid wells and replaced with 250µl of neutrophil suspension, and co-cultures were incubated at 37°C for 1.5 hours. Co-cultures were then imaged using a ZEISS LSM880 confocal microscope by Dr Marco Rink, and images were rendered to give a 3D visualisation of neutrophil migration using Imaris software by Dr Scott Davies.

2.8 In Silico analysis of sequencing data

2.8.1 Differential gene analysis

Differential gene analysis of single cell RNA sequencing data was performed by Dr Paul Horn, utilising publicly available data published by Ramachandran *et al*(276). In order to compare gene changes between healthy donor liver (n=5) and ALD cirrhotic liver (n=2), a raw cell count matrix was first obtained from gene omnibus (GEO accession GEO136103). All subsequent analyses steps were performed in R using a workflow based on Amezquita *et al*(277). Quality control was then performed and droplets not containing a cell were filtered out from the dataset. Cells with gene counts below 300 and with more than 30 % mitochondrial RNA were then removed. Genes expressed in fewer than 3 cells were removed for computational efficiency. Logarithmic normalisation of counts was performed using cluster-wise sum factors (`quickCluster` and `computeSumFactors` functions in `scran`) and the `logNormCounts` function in the `scater` package.

After performing principal component analysis on top variable genes, shared nearest neighbour graph-based clustering and UMAP visualisation enabled the removal of all clusters derived from circulating blood cells which had contaminated the sample. Feature selection, principal component analysis and graph-based clustering was then re-done using only liver resident cells to remove bias. Stability of the clustering was verified by bootstrap analysis, followed by cell type annotation-based reference annotation from the human primary cell atlas implemented in the package `SingleR`. We then selected the cluster designated Epithelial Cells and repeated normalisation, clustering and UMAP visualisation. Populations of cholangiocytes and hepatocytes were identified based on the presence of the markers

EpCAM/KRT19 and Albumin/TTP respectively. Genes that were present in both healthy and diseased samples were then compared, and those with a positive or negative 2-fold change in disease were analysed further.

2.8.2 Clustering of differential gene analysis data

To assess how differential gene expression in disease could be an indication of altered function, differential gene analysis data was clustered using Cytoscape software. C2 curated gene sets including CP canonical pathways (version 7.2) from the Human Molecular Signatures Database (MSigDB)(278, 279) were used for enrichment analysis. Based on differentially expressed genes with a minimum 2-fold change, gene set overrepresentation analysis was performed using ClusterProfiler to identify pathways associated with gene expression changes. The returned pathways were then clustered according to the gene overlap to indicate overarching patterns. These were utilised to create an enrichment map to show altered gene sets. Appropriate node cut off was set (P-value 0.05) and Edge cut off (percentage overlap) was adjusted to achieve visually distinct sub-clusters of gene sets. This network was then clustered using MCL cluster in ClusterMaker function of Cytoscape. Clusters were named with AutoAnnotate and names adjusted where appropriate. Singleton clusters were not displayed.

Chapter 3 – What are we trying to model?

3.1 Introduction

In 2020 there was a 20% increase in alcohol specific deaths, and liver disease is now the largest cause of death in people aged 35-49 years old in the UK - a majority of which is due to alcohol(280, 281). Around 90% of those who drink heavily have steatosis(97), and this can progress to alcoholic steatohepatitis, fibrosis and eventually cirrhosis – severe loss of liver function and structure where symptoms persist even if patients cease to consume alcohol(112). Throughout these stages, patients can also develop alcoholic hepatitis (AH), which is a severe, highly inflammatory acute liver failure associated with multi-organ failure and high mortality. AH patients present with high serum bilirubin (and therefore jaundice) and liver enzymes in their blood, alongside high white blood cell counts(282). Unless patients are presenting with AH or being treated for an unrelated condition, cirrhosis can remain asymptomatic and undiagnosed. Furthermore, late-stage disease diagnosis is up to 12 times higher in patients with ARLD compared to other aetiologies(283). At this point, often the only treatment available for these patients is a liver transplant, however they must often be abstinent for 6 months before they are able to join the transplant list in most UK centres. Patients who are diagnosed with cirrhosis are also regularly monitored for liver cancer, as incidence is high in these groups(119). With regards to our study, we were able to collect peripheral blood samples from patients who had been admitted to the hospital with AH, alongside cirrhotic patients from the cancer screening clinic who were both abstinent (ALD-A) and continuing to drink (ALD-D). Our ALD-A cohort also contains samples from patients who

were attending a pre-transplant clinic, and are often decompensated – meaning disease is symptomatic and the liver is no longer able to effectively perform its functions(284).

Across the spectrum of ARLD, we consistently see an immunocompromised phenotype where patients are at a higher risk of infection - whether in acute or chronic disease(285). Cirrhosis itself is known to cause immune deficits, and the added complications of alcohol toxicity lead to increased exposure to bacterial products and immune cell dysfunction(286). The immune role of the liver is well established, but many gaps remain in our knowledge of how to manage this immune-liver crosstalk in patients. Unexpected complications of immune-modulating treatments have highlighted the delicate balance that must be struck in order to support patients with alcohol related liver failure, and also emphasises the unmet medical need regarding treatment options for these groups(148, 154). In particular, changes in neutrophil number, phenotype and function are one of the most significant contributors to systemic inflammation and immunocompromise in these patients(287). In this project, we used our patient samples to further investigate how circulating cell parameters differed between cohorts. In order to improve our experimental models of liver injury, we also need to understand the architectural and immune differences in the local liver environment at each stage of disease. For this thesis in particular, this also informs how this tissue may perform as a source material for a primary human liver organoid model. In particular, the presence of bi-potential progenitor cells as described by Huch *et al* would allow us to pursue published protocols for 3D primary cell organoids culture(214).

Therefore, the specific aims of this chapter were to:

- Characterise the peripheral immune cell populations at different stages of ARLD
- Compare neutrophil phenotype and function in health and disease
- Understand the histopathological consequences of ARLD
- Identify populations of progenitor cells in donor and ALD livers that could provide source material for a 3D organoid liver model

3.2 Results

3.2.1 Analysis of peripheral blood from ARLD patient cohorts

Before using cells in our mechanistic models it was necessary to understand the nature of the injury I was trying to recreate. For this purpose, I was able to access peripheral blood samples from patients across the ARLD spectrum to compare to healthy donors. The demographic information for our samples is summarized in Table 3.1. Here it is clear that there is a wide range in ages across all cohorts, and that our healthy donors were younger on average than all patient groups, but particularly those with cirrhosis. We also noted that patients who were admitted with the more severe injury of acute alcoholic hepatitis were on average younger than both the abstinent and drinking cirrhotic patients by around 10 years. While we were not able to collect full biochemical data from our healthy volunteers, the values from our patient groups can be compared to the QEHB pathology lab reference values shown in Table 3.1. As expected, there were marked increases in serum liver injury markers such as ALT, AST, ALP, CRP and bilirubin in our alcoholic hepatitis cohort. These were notably higher than in our cirrhotic patient groups, and while we still see many values outside of the normal ranges indicating persistent injury even in abstinent patients, the averages from this cohort were within the recommended range for many of these markers. Reflecting the inflammatory nature of the condition, we see a striking increase in CRP in AH patients compared to other disease groups which indicates the production of immune mediators by the liver. This is also reflected by reduced production of albumin, which is most notable in AH but also seen in cirrhotic patients and is indicative of impaired protein synthesis. This was also reflected in the INR values, with all patient groups above the normal reference range with the most significant increase again seen in the AH patients, suggesting impaired coagulation and increased bleed

risk. There are several established scoring systems that take these biochemical values into account to assess disease severity and prognosis. For patients with AH, the Glasgow Alcoholic hepatitis Score (GAHS) averaged at 8.1 which suggests high disease severity in our cohort overall, as significant risk of mortality is seen with a score of 9 and above. Similar systems are used to assess severity in cirrhotic patients. As expected our abstinent cirrhotic patients had the highest MELD (Model for End stage Liver Disease) score, likely because many of these patients were attending the transplant clinic for ALD (and were therefore at advanced stage disease). Comparatively, cirrhotic patients who were still drinking and not listed for transplant had a predictably lower score, as they were likely to have less advanced disease on average. Interestingly the UKELD (UK model for End stage Liver Disease) score was very similar for both cirrhotic cohorts (Table 3.1).

Neutrophil/Lymphocyte (N/L) and Lymphocyte/Monocyte (L/M) ratios were also notably different between healthy control samples and patient cohorts, which is suggestive of poor prognosis and susceptibility to infection respectively(288). These differences were again most marked in our AH patients, and higher in drinking compared to abstinent patients. In both patient groups who were not abstinent we recorded a weekly estimated alcohol consumption above the recommended intake for an adult in the UK(139), but this was strikingly high in patients with acute alcoholic injury (Table 3.1).

	Data presented as **mean (range)**			
	Healthy Volunteers (HC)	**Alcoholic Hepatitis (AH)**	**Cirrhotic Abstinent (ALD-A)**	**Cirrhotic Drinking (ALD-D)**
Demographic data				
Sample number	28	29	35	11
Age	37 (27)	48 (45)	58 (41)	61 (30)
Sex (M/F)	10/18	18/11	19/16	7/4
Clinical data				
ALT(U/L)	***0-55***	58.5 (189)	22.9 (51)	27.18 (27)
AST (U/L)	***5-34***	142.6 (252)	27.8 (43)	41.7 (67)
ALP (U/L)	***30-130***	191.4 (470)	107.5 (261)	135.9 (163)
Urea (mM/L)	***2.5-7.8***	5.7 (35.4)	6.3 (18.7)	5.7 (15.1)
Albumin (g/L)	***35-50***	24.76 (33)	37.74 (24)	38 (22)
CRP (mg/L)	***0-5***	44.07 (135)	4.72 (36)	7.125 (17)
Bilirubin (μm/L)	***<21***	247.5 (520)	32.3 (200)	18.27 (29)
Sodium (mM/L)	***133-146***	133.9 (22)	138.6 (19)	136.9 (12)
Creatinine (μm/L)	***64-104***	65.14 (220)	72.89 (115)	73.18 (60)
Clinical scores				
INR	***1***	1.7 (1.7)	1.2 (0.9)	1.2 (0.5)
MELD	-	-	10.4 (20)	9.1 (7)
UKELD	-	-	49.7 (18)	49.6 (9)
GAHS	-	8.1 (6)	-	-
N/L ratio	2.2 (2.9)	7.2 (33.2)	3.5 (20.5)	5.1 (10.1)
L/M ratio	4.5 (5.7)	1.3 (3.5)	3.4 (8.1)	1.8 (1.82)
Mean estimated alcohol consumption (units/week)	***14***	176.5 (385)	-----	50.9 (131.3)

Table 3.1: Summary of clinical and demographic data for blood sample donors. Peripheral blood samples were collected from healthy control donors (HC), patients with alcoholic hepatitis (AH), abstinent cirrhotic patients (ALD-A), and patients with cirrhosis who are still actively drinking (ALD-D). Anonymised demographic and clinical data was sourced from electronic patient records or calculated from complete blood counts. Age is rounded to nearest whole year. Data is listed as mean (range), where values in red are above the reference/HC range, and values in blue are below the reference/HC range. For clinical values that were not collected from healthy volunteers, reference ranges from the QEHB pathology labs are listed in bold italics.

Next, I looked specifically at the cellular components in patient blood using the Sysmex analyser. Anaemia and altered red cell count is a common feature of liver disease, and in particular elevated red cell size and an increase in immature red blood cells (RBCs) is often found in patients with AH and ARLD(289). Figure 3.1 confirms this pattern in our acute patient group, with significant elevations in Mean Corpuscular Volume (MCV - red blood cell size) and numbers of reticulocytes in AH compared to healthy controls and abstinent cirrhotic patients. This was accompanied by reduced haematocrit (proportion of RBCs in blood) although red cell parameters in our cirrhotic patients were not significantly different from healthy controls. Similarly Figure 3.2 confirms a trend towards a reduced total red blood cell count in all disease groups, with AH counts being significantly lower compared to both healthy and cirrhotic samples. Platelet counts also appeared lower in all disease groups, and were significantly different in both AH and abstinent cirrhotic patients when compared to healthy controls.

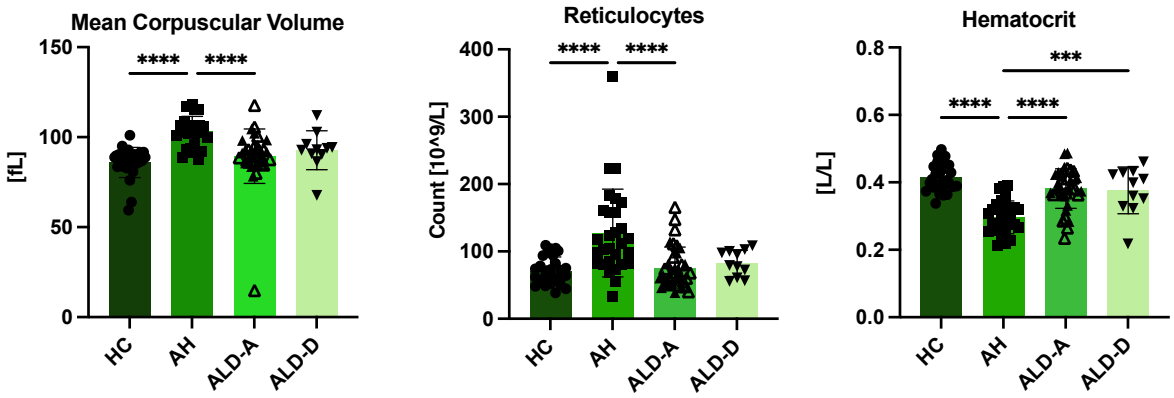


Figure 3.1: Alcoholic hepatitis is associated with a reduction in hematocrit and altered red blood cell phenotypes. Peripheral blood samples were taken from healthy control donors (HC), patients with alcoholic hepatitis (AH), abstinent cirrhotic patients (ALD-A), and patients with cirrhosis who are still actively drinking (ALD-D). ALD-A patients from pre-transplant clinic and cancer screening clinic are represented by an unfilled and filled triangle respectively. Analysis of Mean Corpuscular Volume (red blood cell (RBC) size), reticulocyte (immature RBC) count, and Hematocrit (RBC proportion) was performed by Laura Harford, Dr Reenam Khan or Dr Lozan Sheriff using an automated Sysmex XN-1000 analyzer. Column data represent mean +/- SD values for group and black symbols indicate individual data points. Data are from n=11-35 samples per group. Statistical comparison was performed using one-way ANOVA or Kruskal-Wallace test with multiple comparisons depending on normality of the data, where P values are P≤0.05 (*), P≤0.01 (**), P≤0.001 (***), P≤0.0001 (****).

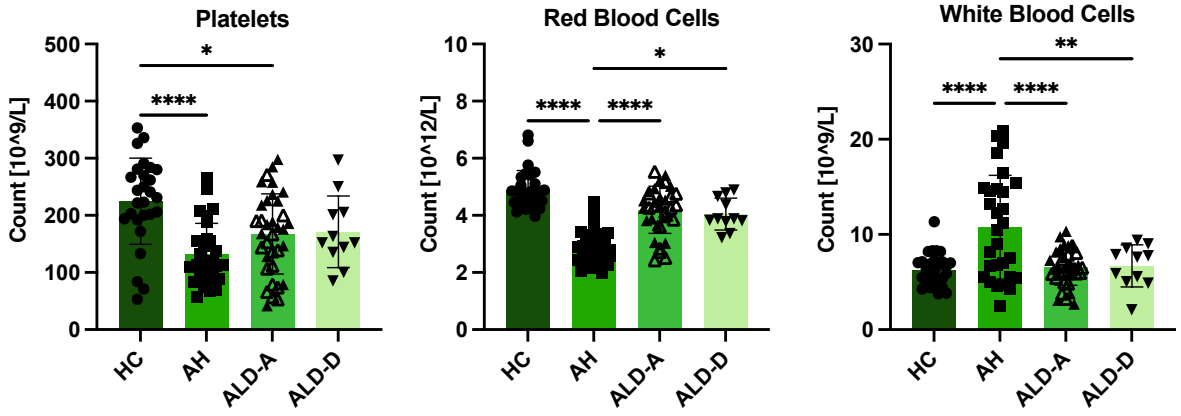


Figure 3.2: Comparison of peripheral blood cellular composition in healthy donors and patients across the ARLD spectrum. Peripheral blood samples were taken from healthy control donors (HC), patients with alcoholic hepatitis (AH), abstinent cirrhotic patients (ALD-A), and patients with cirrhosis who are still actively drinking (ALD-D). ALD-A patients from pre-transplant clinic and cancer screening clinic are represented by an unfilled and filled triangle respectively. Absolute counts for platelets, red blood cells and white blood cells were performed by Laura Harford, Dr Reenam Khan or Dr Lozan Sheriff using an automated Sysmex XN-1000 analyzer. Column data represent mean +/- SD values for group and black symbols indicate individual data points. Data are from n=11-35 samples per group. Statistical comparison was performed using one-way ANOVA or Kruskal-Wallace test with multiple comparisons depending on normality of the data, where P values are P≤0.05 (*), P≤0.01 (**), P≤0.001 (***), P≤0.0001 (****).

We also noted a significant elevation in total white blood cell (WBC) count in AH which was not present in the cirrhotic samples (Figure 3.2). Interestingly, despite an overall increase in circulating WBCs we saw a significant decrease in peripheral lymphocyte number in AH and cirrhotic patients who were still drinking**.** As shown in Figure 3.3A, this high WBC number is accounted for predominantly by a significant increase in neutrophils. While we also saw increases in monocytes and other granulocytes such as basophils and eosinophils, the relative proportion of these cells is considerably smaller. These changes are most significant in AH, although ALD-D patients also showed significant changes in lymphocyte and monocyte number compared to healthy controls. Of particular note, AH patient blood had a high increase in immature granulocytes (Figure 3.3). Furthermore, patients with AH had a higher Neutrophil Reactivity Index suggesting increased neutrophil activation, but this was not

mirrored in measurements of neutrophil granularity which was only notably different in abstinent cirrhotic patients (Figure 3.4). This increased immune activity is also seen with a higher count of Reactive Lymphocytes in AH patients which was not present in healthy controls or cirrhotic groups.

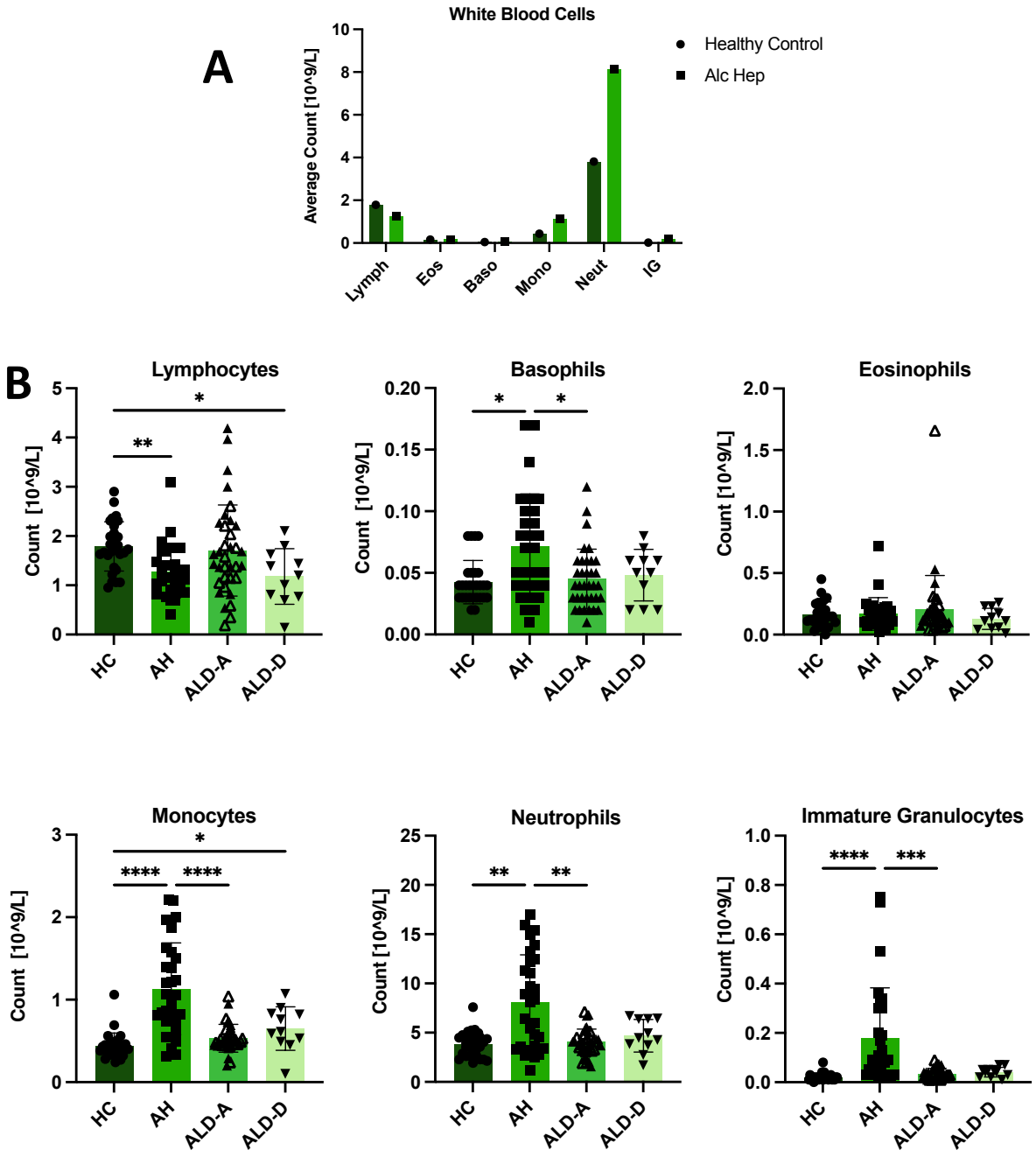


Figure 3.3: Comparison of white blood cell number in healthy donors and patients across the ARLD spectrum. Peripheral blood samples were taken from healthy control donors (HC), patients with alcoholic hepatitis (AH), abstinent cirrhotic patients (ALD-A), and patients with cirrhosis who are still actively drinking (ALD-D). ALD-A patients from pre-transplant clinic and cancer screening clinic are represented by an unfilled and filled triangle respectively. Absolute counts of lymphocytes, eosinophils, basophils, monocytes, neutrophils and immature granulocytes were performed by Laura Harford, Dr Reenam Khan or Dr Lozan Sheriff using an automated Sysmex XN-1000 analyzer. The average count (A) and absolute counts (B) are displayed. Column data represent mean +/- SD values for group and black symbols indicate individual data points. Data are from n=11-35 samples per group. Statistical comparison was performed using one-way ANOVA or Kruskal-Wallace test with multiple comparisons depending on normality of the data, where P values are P≤0.05 (*), P≤0.01 (**), P≤0.001 (***), P≤0.0001 (****).

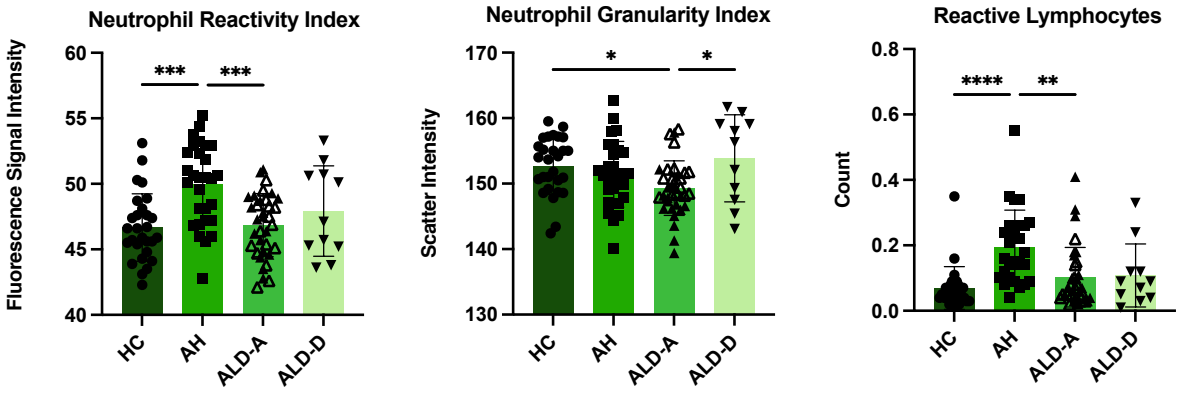


Figure 3.4: Markers of leukocyte activation status and immune response are elevated in alcoholic hepatitis. Peripheral blood samples were taken from healthy control donors (HC), patients with alcoholic hepatitis (AH), abstinent cirrhotic patients (ALD-A), and patients with cirrhosis who are still actively drinking (ALD-D). ALD-A patients from pre-transplant clinic and cancer screening clinic are represented by an unfilled and filled triangle respectively. Analysis of Neutrophil Reactivity Index, Neutrophil Granularity Index, and Reactive Lymphocytes was performed by Laura Harford, Dr Reenam Khan or Dr Lozan Sheriff using an automated Sysmex XN-1000 analyzer. Column data represent mean +/- SD values for group and black symbols indicate individual data points. Note that y axes are clipped at indicated values to permit clear visualization of individual sample symbols. Data are from n=11-35 samples per group. Statistical comparison was performed using one-way ANOVA or Kruskal-Wallace test with multiple comparisons depending on normality of the data, where P values are P≤0.05 (*), P≤0.01 (**), P≤0.001 (***), P≤0.0001 (****).

An important finding as shown in Figure 3.5 was that the immature granulocyte count in AH correlated with several markers of prognosis and severity, including GAHS, bilirubin and NLR. Whilst I was unable to statistically confirm this association within the available timeframe, the patients within our AH cohort with the highest IG count also appeared to be those with some of the more severe co-morbidities. As indicated in Figure 3.5, the 5 mortalities that occurred during this study were patients with some of the highest IG counts. Interestingly, if I considered IG percentage as opposed to total count, values were only significant when compared to bilirubin (P=0.012) and NLR (P=0.0099) (data not shown).

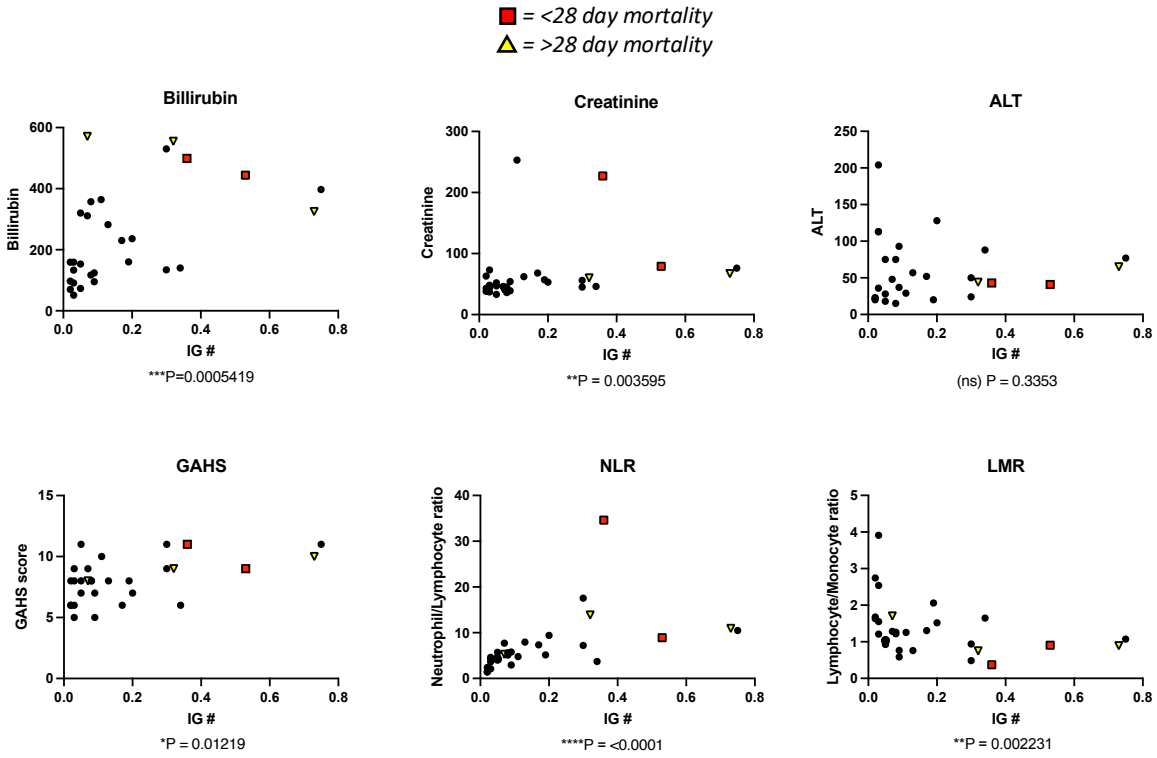


Figure 3.5: Correlations between immature granulocytes and clinical indicators of alcoholic hepatitis. Peripheral blood samples were taken from patients with alcoholic hepatitis (AH) and correlated with clinical measurements. Absolute counts for immature granulocytes alongside neutrophils, monocytes and lymphocytes were performed by Laura Harford, Dr Reenam Khan or Dr Lozan Sheriff using an automated Sysmex XN-1000 analyzer, and used to calculate neutrophil/lymphocyte ratio (NLR) and lymphocyte/monocyte ratio (LMR). Peripheral blood levels of bilirubin, creatinine and alanine aminotransferase (ALT) were obtained from patient clinical records. Glasgow Alcoholic Hepatitis Score (GAHS) was calculated based on patient clinical records. Correlation was calculated using Spearman's rank correlation coefficient. Column data represent mean +/- SD values for group and symbols indicate individual data points. Red squares indicate patient mortality within 28 days of admission, yellow triangles indicate patient mortality more than 28 days after admission. n=29 samples where P values are P≤0.05 (*), P≤0.01 (**), P≤0.001 (***), P≤0.0001 (****).

3.2.2 Neutrophil function in AH and cirrhosis

In order to investigate neutrophil function in ARLD, we isolated primary neutrophils from patients with AH and abstinent cirrhotic patients, alongside healthy controls. We were then able to assess their responses to different immune stimuli. Despite Sysmex data suggesting higher neutrophil reactivity in AH (Figure 3.4), we observed reduced effectiveness when responding to microbial challenges both in this group and to a lesser extent in cirrhotic patients (Figure 3.6). The production of reactive oxygen species (ROS) in response to fMLP, *E. coli* and PMA was not significantly affected in patients with acute or chronic injury, however there is a slight trend towards lower production in disease (Figure 3.6A). Conversely, there was a notable reduction in phagocytosis of opsonised *E.coli* in abstinent ALD patients, with a trend for further impairment in patients with AH (Figure 3.6B). To further investigate antimicrobial responses in patients with AH specifically, we measured the production of Neutrophil Extracellular Traps (NETs) by isolated neutrophils in response to incubation with PMA. Both AH and healthy donor neutrophils showed similar NET production in response to PMA, which could be measured by total fluorescence of stained NETs and by confocal microscopy (3.6C-E). Despite Sysmex data suggesting that AH neutrophils showed a higher level of activation, we saw no difference in baseline production of NETs in unstimulated cells. Overall, we saw changes in neutrophil number and function in all assessed disease groups, but this was considerably more prominent in AH than chronic ALD cohorts.

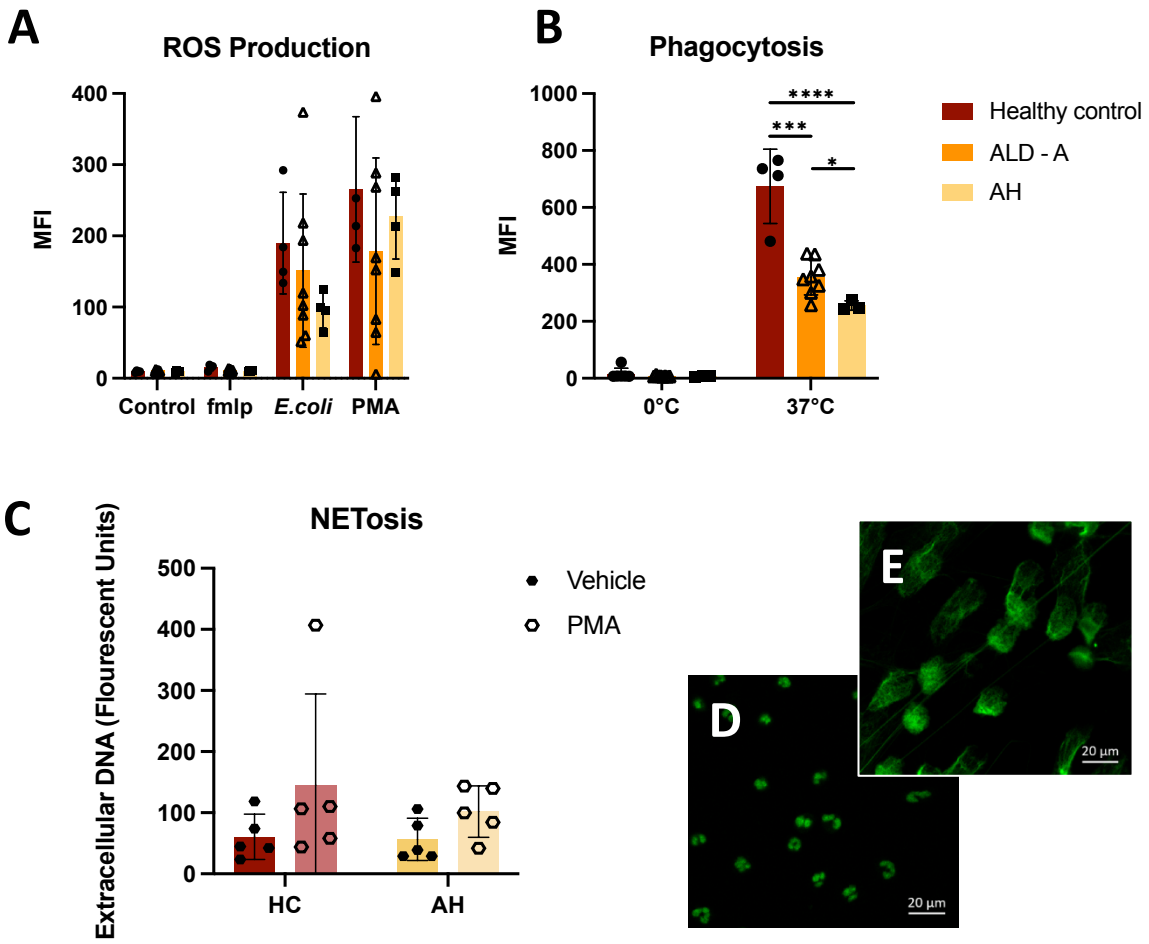


Figure 3.6: Neutrophil phagocytosis is impaired in AH. Peripheral blood samples were taken from healthy control donors (HC), patients with alcoholic hepatitis (AH), and abstinent stable cirrhotic patients (ALD-A) awaiting transplant in heparin containing vacutainers. Production of ROS (Reactive Oxygen Species) (A) and phagocytosis (B) were measured using PHAGOBURST/PHAGOTEST respectively and analyzed using flow cytometry. For PHAGOBURST, 100µl of whole blood was incubated with 20µl of wash buffer (control), fMLP, E. coli or PMA for 10 minutes at 37℃, followed by a further 10 minute incubation with dihydrorhodamine-123. For PHAGOTEST, 100µl of whole blood was incubated with 20µl of fluorescently labelled opsonized E. coli for 10 minutes at 37℃. Samples were fixed and fluorescence intensity was measured within 1 hour. NETosis was measured in isolated neutrophils from healthy donors or patients with AH. These were incubated for 3 hours with either vehicle (DMSO) or PMA, and production of extracellular DNA was measured by fluorescence (C). Experiment conditions were duplicated on coverslips for fluorescent images, and cells treated with vehicle (D) or PMA (E) were stained with SYTOX™ Green and imaged by confocal microscopy. Column data represent mean +/- SD values for group and symbols indicate individual data points. Staining completed by Dr Reenam Khan and Laura Harford. Statistical comparison was performed using unpaired t-test where P values are P≤0.05 (*), P≤0.001 (***), P≤0.0001 (****).

3.2.3 Characterising the local tissue environment in healthy and diseased livers

Before isolating organoids from tissue, we assessed expression and localisation of key markers in both healthy donor tissue and explanted ALD livers using microscopy and qPCR. When analysing chromogenic staining, explanted ALD livers demonstrated presence of fibrosis and immune cell aggregates, which were not seen in donor livers (Figure 3.7). As the ALD explants were from end stage cirrhotic livers, we also saw notable changes in liver architecture, with areas of regeneration encapsulated by bridging fibrosis. Immune cell aggregates also suggest leukocyte infiltration due to inflammatory cues from the damaged liver.

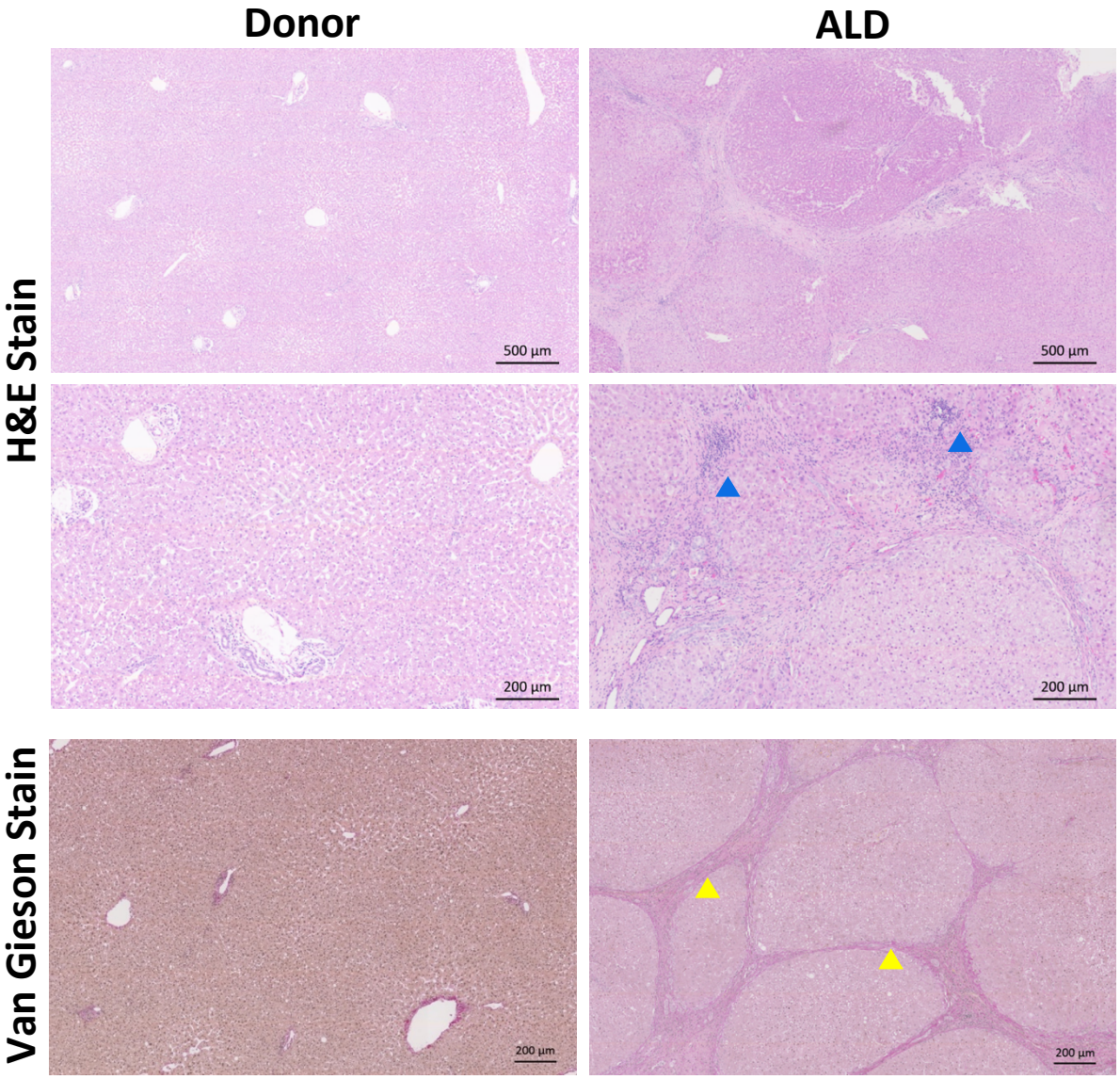


Figure 3.7: Histochemical staining of human liver specimens. *Representative images showing chromogenic staining of formalin fixed paraffin embedded human liver sections. 5µm sections of liver tissue from either donor or ALD livers were stained with Haematoxylin and Eosin (H&E) or Van Gieson stain using in house protocols. Representative fields of view were captured using a ZEISS Axio Scan .Z1 microscope slide scanner, and scale bars are as indicated on individual panels. Blue arrows indicate immune cell aggregates and yellow arrows indicate areas of bridging fibrosis.*

Next, we used immunohistochemistry to investigate the presence of established progenitor cell markers in healthy and diseased tissue. In donor livers, we observed $EpCAM^+$ staining on bile ducts dispersed across the tissue and predominantly in portal areas (Figure 3.8). This pattern of staining changes strikingly in ALD liver tissue, with a high proportion of $EpCAM^+$ cells within regenerative nodules, as well as on a notably higher number of bile ducts. Quantification of this staining confirmed a significant increase in disease. Cytokeratin 19 (CK19) staining also increases significantly in ALD tissue. In donor livers, we saw an expression pattern of CK19 on biliary cells that was similar to EpCAM and suggests an expected dual positive population of cholangiocytes. However, in ALD tissue CK19 positive cells were predominantly seen within the fibrotic septa rather than within regenerating nodules. Finally, the significantly increased presence of the stem cell marker SOX9 in ALD livers also localised in similar patterns to both EpCAM and CK19 positive cells, suggesting the presence of high numbers of bi-potential progenitor cells within these tissues. Whilst we did see these patterns of progenitor cells in all investigated ALD samples, Figure 3.9 highlights that the extent of this regeneration and therefore EpCAM positive cell number is highly variable both between patients and within distinct areas of individual samples.

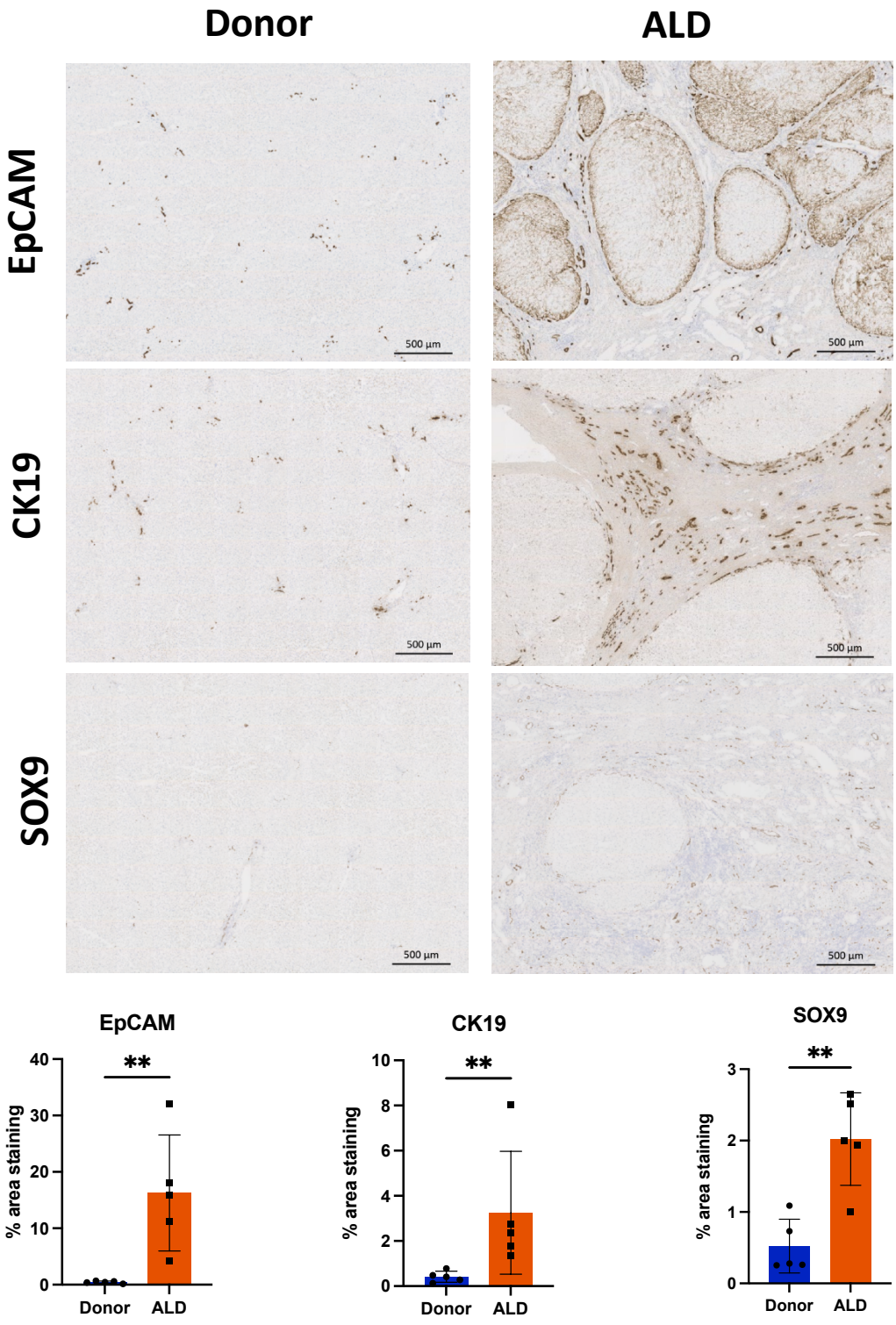


Figure 3.8: Increased ductular reactivity in ALD livers indicated by staining with progenitor cell markers. Representative images of immunochemical staining for EpCAM, CK19 and SOX9 in 5µm human liver sections from donor and alcoholic liver disease (ALD) samples. Percentage area of staining is shown adjacent to the corresponding images and was quantified for n=5 livers for each condition using FIJI software. Data are mean ±SD values from 5 fields of view per sample. Each data point indicates an individual liver. Statistical comparison of staining in healthy vs ALD liver was performed using unpaired t test where P values are P≤0.05 (*), P≤0.01 (**). Scale bar is 500um.

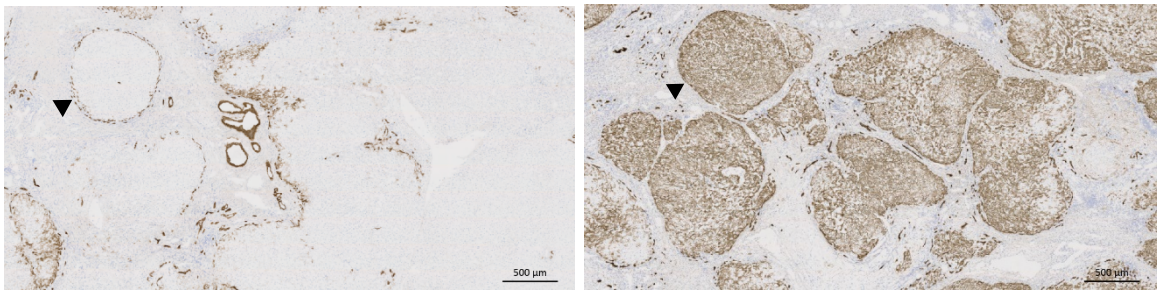


Figure 3.9: Patterns of regeneration are not consistent across explanted ALD livers. Representative images of immunohistochemical staining of EpCAM in 5µm sections from two different human explanted ALD livers. Regenerative nodules are indicated with black arrows. Scale bar represents 500µm.

We also saw protein expression of the PRR TLR4 on these ductal cells, and while this increased with the increased ductal cell number in disease, it was not significantly higher at the mRNA level (Figure 3.10) in whole tissue samples. However increased expression of progenitor cell markers in ALD tissue was further confirmed at the mRNA level using qPCR, alongside hepatocyte markers HNF4α and albumin (Figure 3.11). Markers of hepatocytes were not altered in disease, and despite high expression of several progenitor markers associated with regeneration, we also saw significantly increased expression of the senescence marker P16 (but not P21) in ALD tissue.

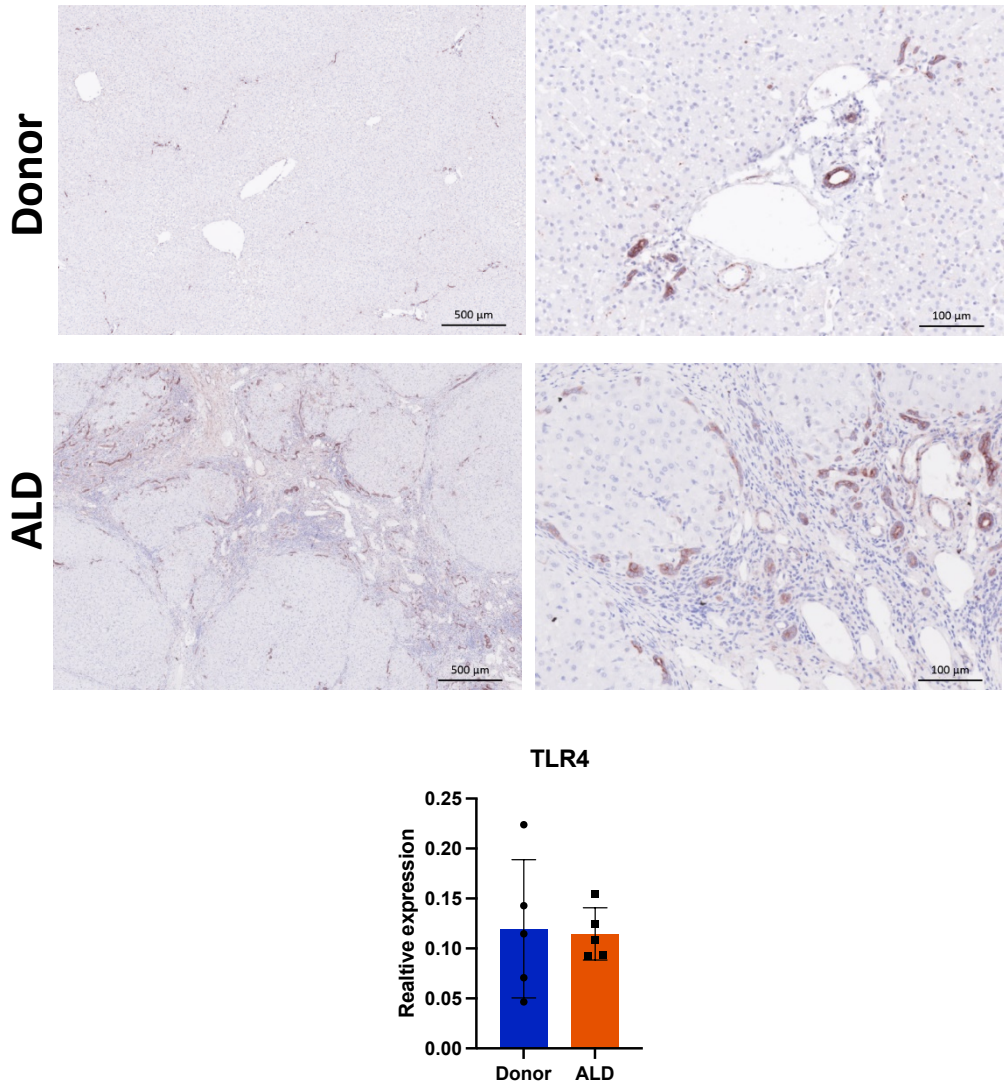


Figure 3.10: Hepatic TLR4 is not altered at the mRNA level in alcohol-related cirrhosis. Representative images of immunohistochemical staining for TLR4 in 5µm human tissue sections from donor and ALD livers. Expression of TLR4 in donor and ALD explant human liver tissue was also assessed by qPCR. Values were generated from n=5 livers for both donor and ALD and represent mean relative expression ±SD compared to SRSF4 housekeeping gene. Each data point represents an individual. Unpaired t-test suggested no significant alteration in mRNA expression in diseased compared to donor livers.

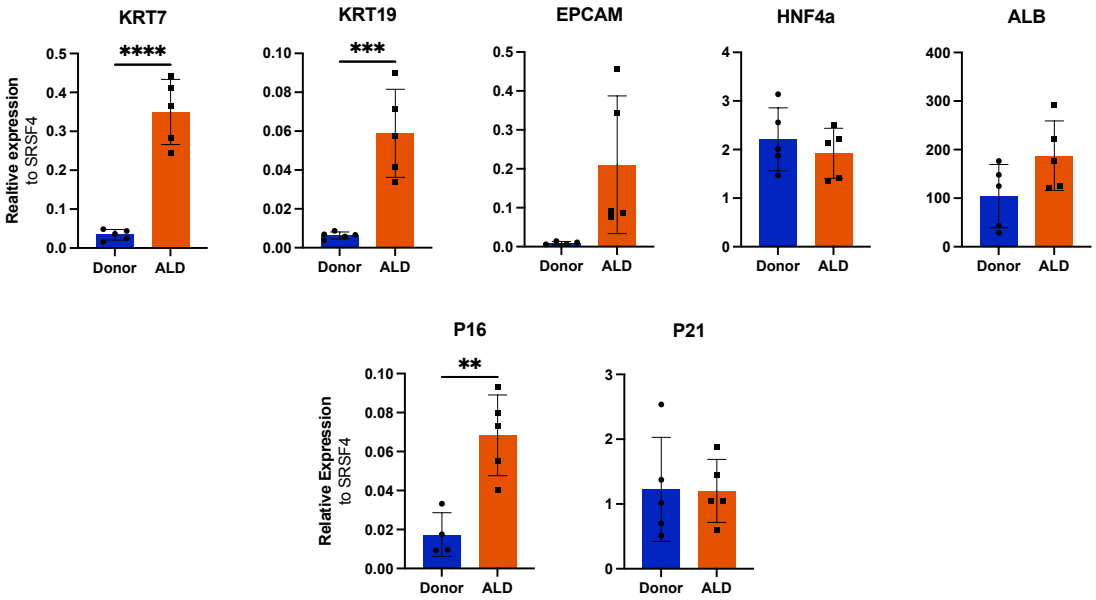


Figure 3.11: Changes in gene expression in ALD livers. Expression of indicated genes in donor and ALD explant human liver tissue were assessed by qPCR. Values were generated from n=4-5 livers for both donor and ALD and represent mean relative expression ±SD compared to SRSF4 housekeeping gene. Each data point represents an individual liver. Unpaired t-test suggested significant alteration in mRNA expression in diseased compared to donor livers where P values are P≤0.01 (**), P≤0.001 (***), P≤0.0001 (****).

We noted a strong presence of CD45+ leukocytes in both donor and ALD tissue, with no significant difference in percentage staining across representative fields of view. However, the localisation of these cells changed notably in disease, where they became associated with areas of fibrosis (Figure 3.12). Despite these high numbers of CD45+ leukocytes in the tissue, our staining suggests that this was not due to neutrophil infiltration. Hepatic neutrophil infiltration is a hallmark of AH, and chromogenic staining shows high numbers of polymorphonuclear cells within the parenchyma of a liver biopsy sample from an AH patient (Figure 3.13A) alongside other classic pathologies such as ballooning hepatocytes and Mallory-Denk Bodies. In contrast to this, neutrophil elastase staining in donor and ALD tissue showed almost no specific positive staining in any fields of view (where antibody functionality could be confirmed on small areas of infiltration – inset image) (Figure 3.13B).

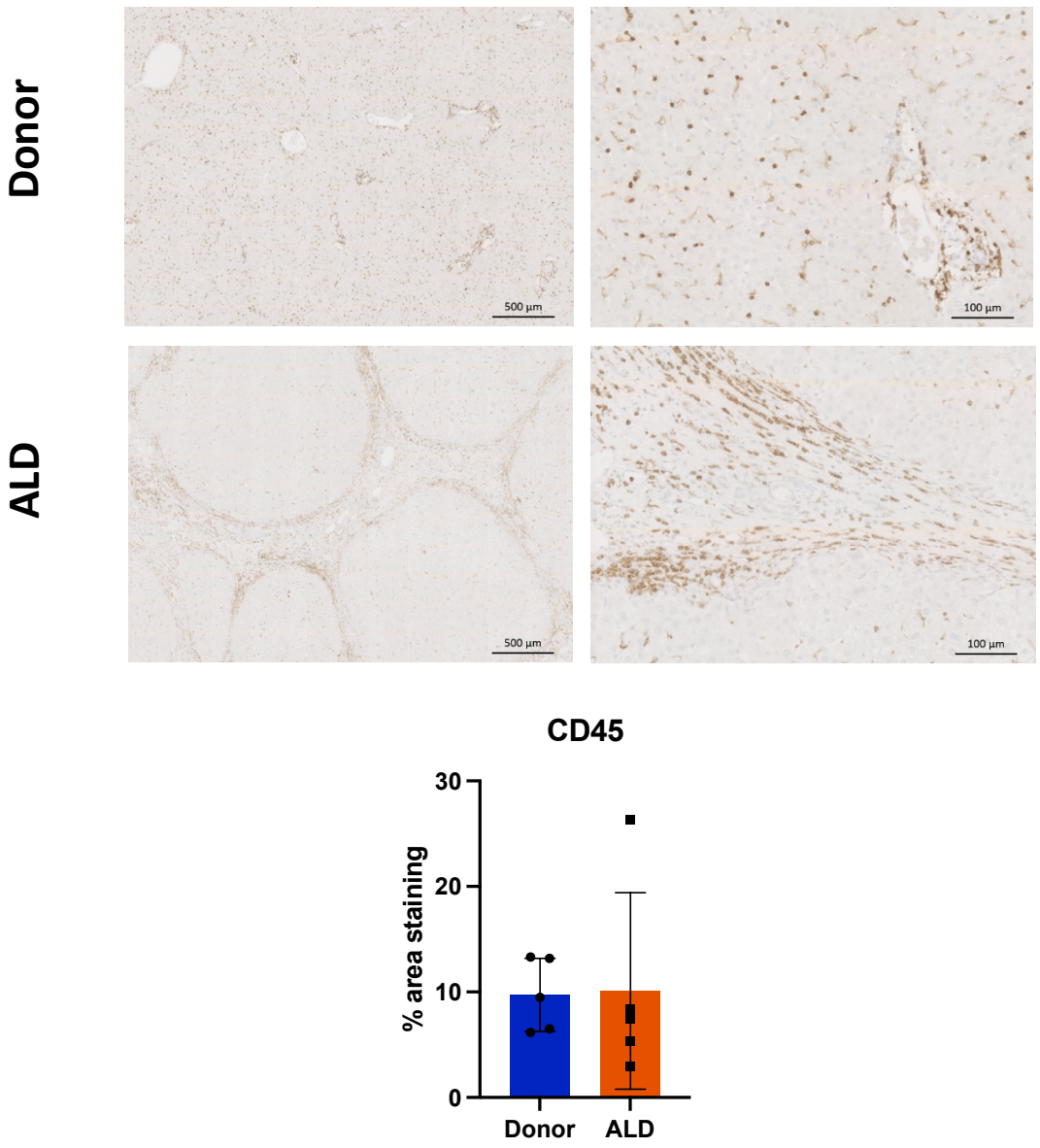


Figure 3.12: CD45+ immune cells localise to areas of fibrosis in ALD cirrhotic livers. Representative images of immunochemical staining for CD45+ cells (leukocytes) in 5µm human liver sections from donor and alcoholic liver disease samples. Percentage area of staining was quantified for n=5 livers for each condition using FIJI software. Data are mean ±SD values from 5 fields of view per sample. Each data point indicates an individual liver. Statistical comparison of staining in healthy vs ALD liver with unpaired t-test showed no significant difference. Scale bars are as indicated in individual images.

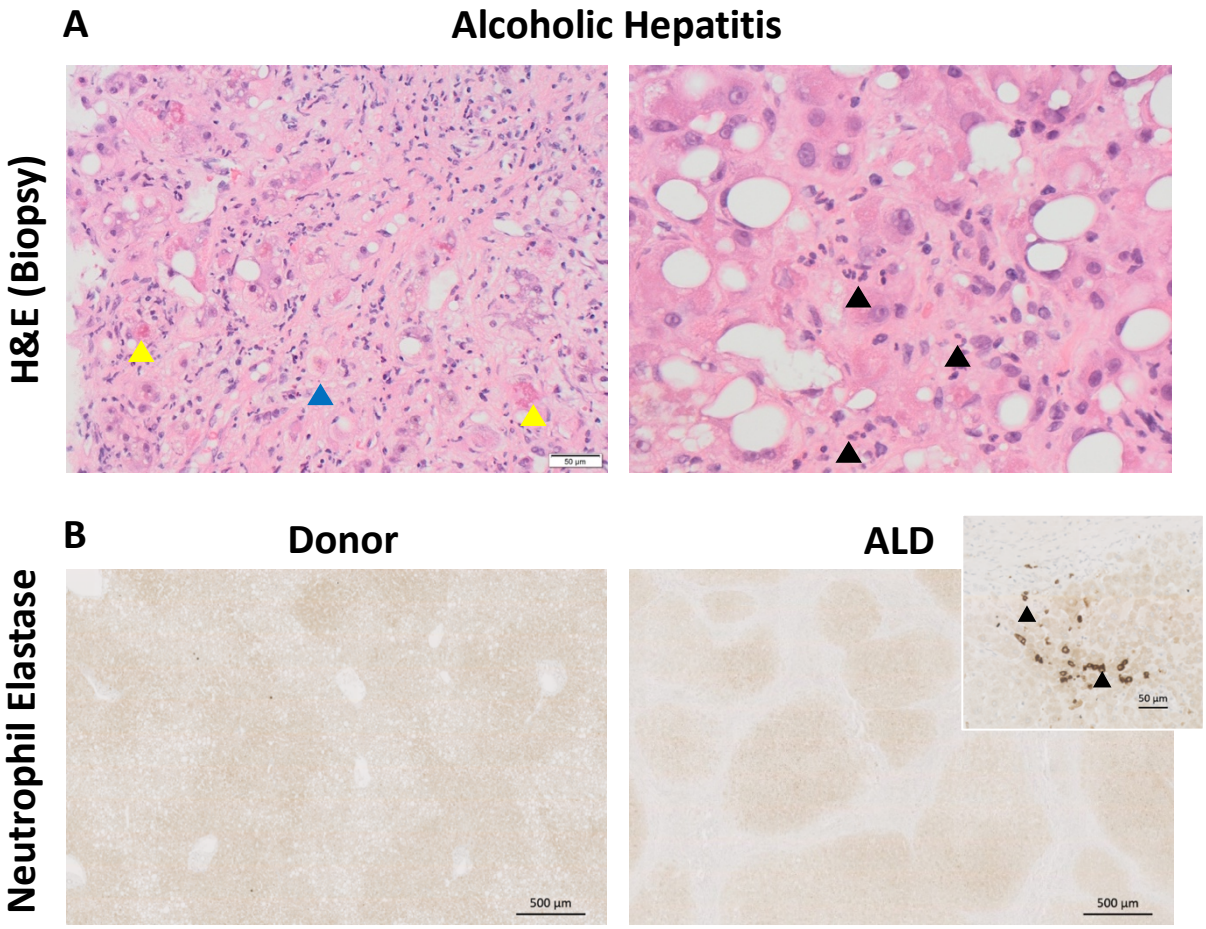


Figure 3.13: Neutrophils are found in the parenchyma during acute alcoholic hepatitis. Representative images showing chromogenic or immunohistochemical staining of 5µm sections of formalin fixed paraffin embedded human liver tissue. Sections of liver tissue from alcoholic hepatitis biopsy samples (A) were stained with Haematoxylin and Eosin using in house protocols. Yellow, blue and black arrows indicate examples of Mallory-Denk Bodies, ballooning hepatocytes, and infiltrating multinucleated cells (neutrophils) respectively. Sections from donor or ALD explanted livers were stained using an anti-human neutrophil elastase antibody using immunohistochemistry (B). Representative fields of view were captured using light microscopy and magnification is shown by scale bars on individual panels. Inset image in (B) shows positive neutrophil staining for comparison (indicated by black arrows). Images in (A) courtesy of Dr. Rachel Brown, Pathology department, QEHB.

Further phenotyping of both hepatocytes and cholangiocytes from donor and ALD livers was conducted using publicly available single cell RNA sequencing data(276). Analysis was performed by Dr Paul Horn (Centre for Liver and Gastrointestinal Research - CLGR) who compared gene expression data between 5 donor and 2 ALD livers, specifically within cholangiocyte and hepatocyte clusters (Figure 3.14). Cluster analysis was then performed on genes where differential expression was 2-fold or higher indicating which pathways were likely to be altered in diseased hepatocytes (Figure 3.15) and cholangiocytes (3.16). Of particular note, we saw changes in TLR4/inflammatory signalling, myeloid cell differentiation, mitochondrial activation and cell adhesion/spreading in hepatocytes from the ALD samples.

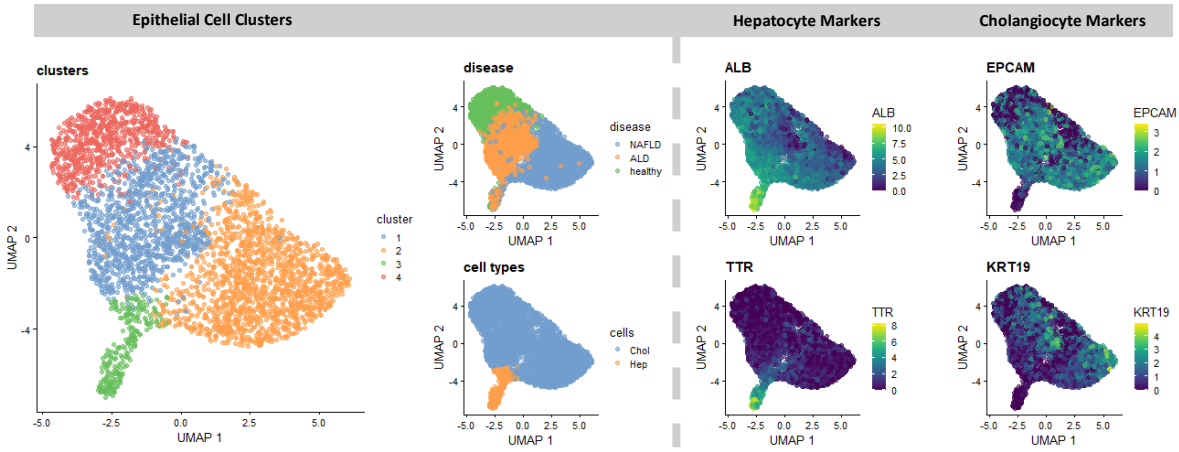


Figure 3.14: Selection of parenchymal cell types from whole liver single cell sequencing to identify differentially expressed genes in ALD. Whole liver single cell sequencing datasets published by Ramachandran et al(276) were reanalysed by Dr Paul Horn. Raw data was stratified based on disease type, and then cell type by the markers indicated. Hepatocytes were identified by expression of Albumin (ALB) and transthyretin (TTR), and cholangiocytes by EpCAM (EPCAM) and Cytokeratin 19 (KRT19). n=2 ALD, 5 donor livers. A raw cell count matrix was first obtained from gene omnibus (GEO accession GEO136103). All subsequent analyses steps were performed in R using a workflow based on Amezquita et al(277).

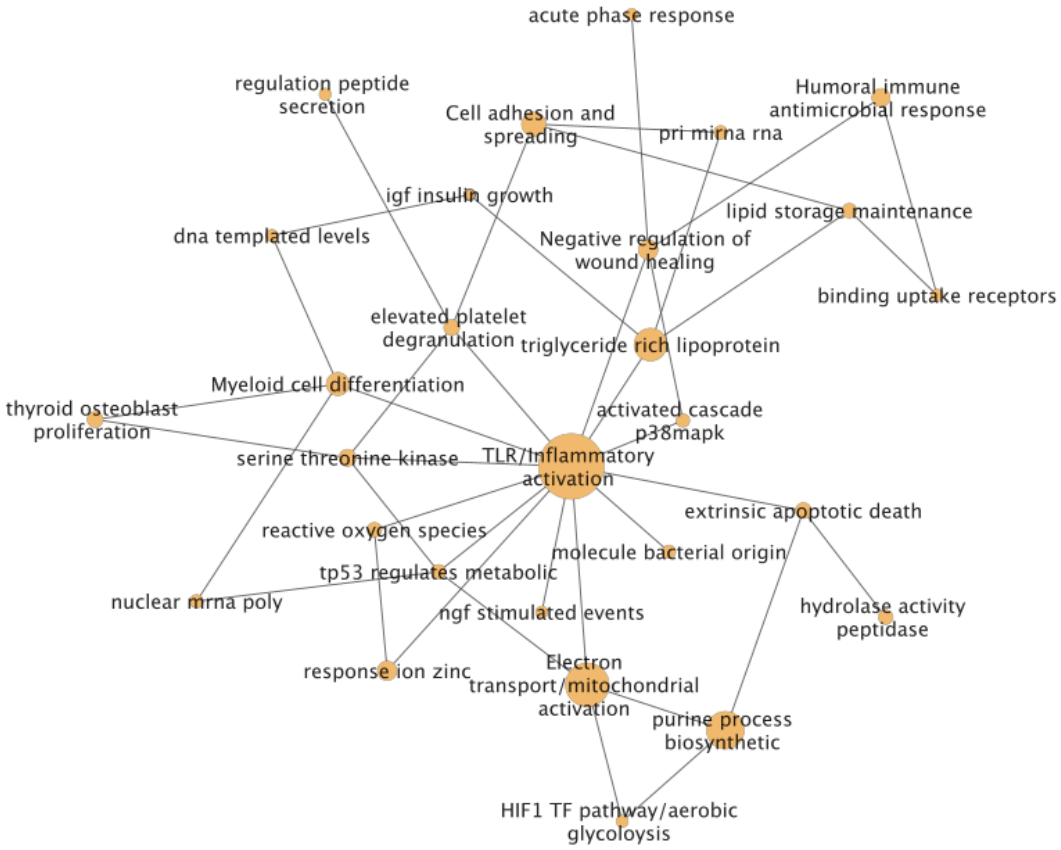


Figure 3.15: Cluster analysis of data from whole liver single cell sequencing to identify differentially expressed genes in ALD hepatocytes. Differential gene expression was assessed between donor and ALD derived hepatocytes based on published single cell sequencing data(276). Where differential gene expression between donor and disease was 2-fold or higher, cluster analysis was performed to identify pathways that were altered in disease. Node size indicates the number of gene clusters associated with the indicated pathways. Connected nodes share minimum of 35% gene similarity, but relative distance between nodes holds no value. n=2 ALD, 5 donor livers. Singleton nodes are not displayed.

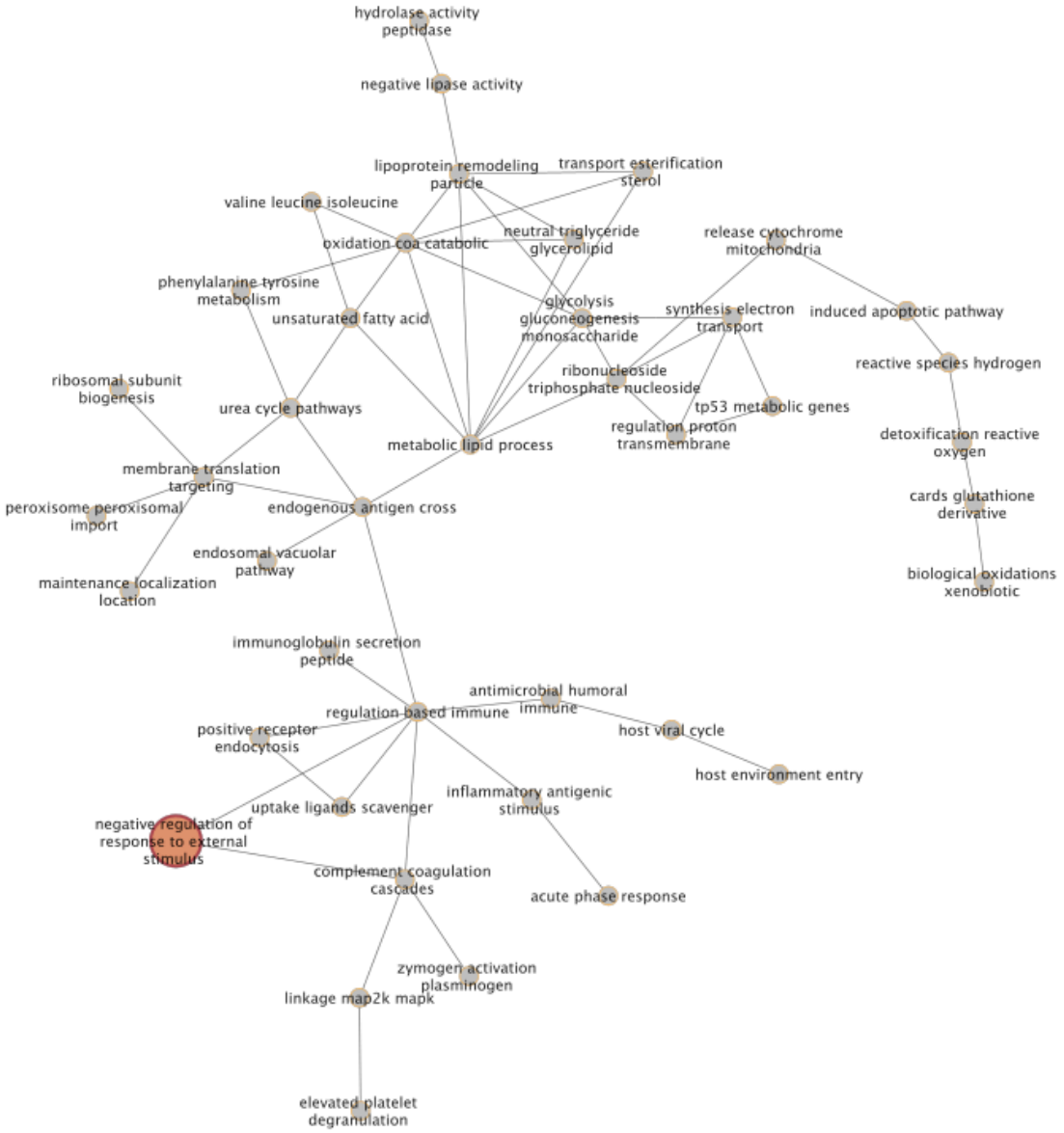


Figure 3.16: Cluster analysis of data from whole liver single cell sequencing to identify differentially expressed genes in ALD cholangiocytes. Differential gene expression was assessed between donor and ALD derived hepatocytes based on published single cell sequencing data(276). Where differential gene expression between donor and disease was 2-fold or higher, cluster analysis was performed to identify pathways that were altered in disease. Node size indicates the number of gene clusters associated with the indicated pathways. Connected nodes share minimum of 37.5% gene similarity, but relative distance between nodes holds no value. n=2 ALD, 5 donor livers. Singleton nodes are not displayed.

Overall these findings highlight some of the key changes in peripheral blood leukocytes and red cells in patients with ARLD. We see altered immune cell interactions within the liver, the presence of fibrosis, and altered neutrophil infiltration in the liver in acute injury. The increased presence of hepatic progenitor cells and "ductular reactions" in ALD explanted livers support our aim to isolate and culture these cells in a 3D organoid system, even when working with more challenging cirrhotic samples. Differential gene analysis between donor and ALD derived hepatocytes further highlighted our target pathways of interest, and support our intention to model the liver-immune crosstalk *in vitro.*

3.3 Discussion

3.3.1 Considerations in our patient cohort (blood)

By assessing changes in the peripheral blood count of our patients, we were able to understand the differences in baseline immune cell number in health and disease. While the healthy controls were age matched where possible in functional experiments, a limitation of this group is that cases were significantly younger, especially when comparing to cirrhotic patient groups. It is well established that there are immune changes with age(290) which should be considered when drawing conclusions between our healthy donors and older cirrhotic cohorts. However, the most significant immune cell changes were in AH patients where ages were notably closer matched, so in this instance the age difference with healthy controls is likely less influential. We had double the number of female vs male patients in our patient groups, which was matched in our healthy controls**.** This fits with the literature regarding the impact of alcohol injury, which is more significant in female patients(291). This is even the case in animal models, where a more significant alcohol injury is seen in female mice in the context of ethanol binge(251). Interestingly, this does not translate to number of deaths proportionally, since alcohol related deaths in the UK are twice as high in males as females(292). It should be noted that data on other factors known to impact susceptibility to ARLD (such as such has ethnicity) (119, 293) was not collected from our cohorts.

Patients in both ALD-A and ALD-D cohorts were in late stage liver disease with established cirrhosis. It should be noted that in the ALD-A group, there was a combination of patients who are awaiting transplant with more severe disease, and those who had more stable compensated cirrhosis. In the Birmingham transplant centre, patients who are pre-transplant

have been abstinent for at least 6 months, and often present with symptoms due to decompensation. When grouped as our abstinent ALD cohort we see considerable crossover in most read outs, but it should be noted that there is an argument for investigating these as two different control groups. As our numbers are relatively small in the context of patient cohort studies, we may well be overlooking more significant differences between our two ALD-A clinics. For the purpose of this study, they offer an abstinent cirrhotic control that allows us to assess the additive effects of alcohol.

While we had a number of strict requirements regarding eligibility for our study (Section 2.1), there was a very wide range in disease severity. One requirement in our AH patients was a blood bilirubin concentration of at least 50μm/L, but our results ranged from 51-571μm/L. Alongside this and possibly most importantly to note, due to both our inclusion criteria and the challenges and ethical implications of consenting decompensated patients, we did not receive samples from the patients with the most severe AH and therefore do not capture the full spectrum of disease. Due to factors such as the neurological effects of hepatic encephalopathy or intubation in patients who have progressed to SIRS and organ failure, many patients are unable to give informed consent. Despite this, the significant differences we measure even when excluding these cases emphasises the impact of acute hepatitis on peripheral immune cell constituents.

In our AH cohort, diagnosis was based on the biochemical analysis described in Table 3.1 and patient history. Although biopsy is the only definitive diagnosis for AH, this was performed very rarely in our patients. As supported by high INR scores in Table 3.1 these patients have a

high risk of bleeding events, and therefore it is standard practice to diagnose AH without biopsy as this procedure increases risk without altering treatment options. Another element that should be considered especially in the case of AH patients in our cohorts is the approach to antibiotic treatment operational within QEHB. As spontaneous bacterial peritonitis (SBP) and pneumonia are common and patients often present with potential infection, antibiotics are often prescribed. It should therefore be noted that we don't see a rate of infection as high as might be expected in an AH patient cohort elsewhere, but it is likely that this, alongside inability to collect samples from the most severe cases, probably contributes to reduced incidence of infection in our cohort. We noted that our AH patients reported a weekly alcohol consumption around 170 units per week with a maximum of more than 350 units per week. This equates to above 100g of alcohol a day which is in keeping with that reported for patients with AH in many centres(294). When assessing weekly alcohol intake, we relied on self-reporting across all cohorts. This causes an issue with standardisation as reports are often given as a non-specific description such as "glass of wine" rather than in units or absolute volumes. The units consumed per week were then calculated based on assumed conversions such as a "glass" of spirit to be a standard double (50ml), but there is likely a wide range of error in these estimations. Alongside this, conversations regarding alcohol consumption can be challenging(295) and not always an accurate representation of alcohol intake. Blood alcohol levels are only taken as confirmation in pre-transplant patients or if reports are not representative of drinking behaviours which may have caused decompensation. It should be noted that AH can actually occur after several weeks of abstinence(123) but this was not the case in any patients included in this study. Our values for consumption are therefore in keeping with the severity of disease noted in our biochemical assessments.

3.3.2 Cellular and biochemical components of peripheral blood

The output from the Sysmex analyser offers many detailed insights into the peripheral blood makeup of our ARLD cohorts. Many of the patterns we see support published data for patients with AUD and cirrhosis(108), and help us to build a picture of the immunological differences with and without alcohol as an additional factor. Readouts such as Low HCT (red blood cell proportion) and high MCV (red blood cell size) are not diagnostic but are characteristic of AH. Significant reduction of HCT is most commonly caused by folic acid deficiency, however as this deficiency is present in up to 80% of people with AUD, reduced HCT can be indicative of the condition(296). This is easily treated with administration of folic acid, and its association with alcohol consumption is reflected by the notably higher values in abstinent patients compared to AH. Interestingly our control group of cirrhotic patients who are still drinking did not fit with this trend, although it is possible that this would be seen when comparing it to the abstinent group if the cohort sizes were similar. Malnutrition and poor intestinal absorption alongside a weak anti-folate mechanism of ethanol all contribute to this deficiency and therefore reduction in HCT(297). Whilst not used as a clinical diagnostic marker, MCV has also been shown to be elevated in patients with AUD in a number of studies(298) and is again elevated in AH patients when compared to healthy controls and cirrhotic patients.

Our findings are also suggestive of known effects of alcohol on haematopoiesis, and the significant elevation in total white blood cell (WBC) count in AH which was not present in the cirrhotic samples is expected due to the inflammatory element of the acute injury. The bone marrow toxicity of alcohol leads to altered production of immune cells, and often an increase in the number of immature blood cells(196). We see this reflected in our results in the high

numbers of reticulocytes (immature red blood cells), and immature granulocytes (IGs) in patients with AH. This is one of the key findings in this patient cohort, as IGs have been previously identified as a predictor of progression to sepsis in burn-injured patients(299). Furthermore, a clinical study of patients with SIRS showed that an IG% of <2% had over 90% specificity at excluding sepsis(300). This has a number of exciting applications in the context of our patient cohort. While our patient numbers are relatively low, correlation of IG# and % with several prognostic markers of AH is promising for its ability to predict severity (although correlation with IG# may be skewed by overall increases in neutrophil number). Furthermore, one of the greatest challenges in AH is the poor response to and high risk of current treatments. As highlighted in Chapter 1, patients must be carefully selected for steroid treatment since these drugs can lead to severe complications in the presence of infection. IG% could therefore potentially offer a quicker indication of infection in AH compared to blood cultures, or as a biomarker for those who may be more prone to sepsis and would respond poorly to steroid treatment. This readout is easy to collect rapidly, and could also potentially identify patients who may benefit from prophylactic antibiotic treatment. Additionally, Piotrowski *et al*(288) showed that lymphocyte/monocyte ratio (LMR) was particularly useful when predicting onset of infection in patients with cirrhosis. While we did not see enough infections in our cohort to validate this, the addition of IG to these estimates may have clinical benefits.

One of the rationales behind our patient group selection was to assess the additive effect of active drinking in patients with cirrhosis. This allowed us to assess the effect of alcohol on systemic immune function, especially in the case of the ALD-A vs ALD-D group. While numbers

are lower in our ALD-D cohort, we appear to see injury patterns and readouts that are intermediate between ALD-A and AH. Although our numbers are not significant, the values in the ALD-D cohort seem to demonstrate an additive effect of alcohol on top of cirrhosis, but also that cirrhosis alone is enough to cause systemic change even in abstinence.

A reduction in circulating platelets is also common in patients with liver disease, and contributes to their increased risk of bleeding incidents. It is well established that ethanol supresses thrombopoiesis(301) and that chronic liver disease is associated with thrombocytopaenia and sequestration of platelets in the spleen(302). Altered platelet behaviour is also seen with platelet trafficking to the liver during injury, where they can regulate leukocyte recruitment and activation(303). This is in keeping with the increased INR values we saw in the clinical data (Table 3.1). Interestingly, we also saw a significant increase in basophils in AH. While little evidence is reported on basophils in human liver disease, there is an interesting link demonstrated in data from mouse models showing that in response to *Listeria monocytogenes* infection, basophils are recruited to the liver and mediate Kupffer cell proliferation and liver repair(304). A similar behaviour has also been demonstrated by neutrophils during liver injury where they could induce macrophages to switch to a more reparative phenotype(210). This could suggest a more general role for granulocytes in resolution of liver inflammation. Basophils are often overlooked due to the fact that they make up such a small fraction of the granulocyte population, but they may be influential *in vivo* in liver injury. It should also be acknowledged that when referring to isolated neutrophils during our functional assays, there is likely to be some basophil contamination. Therefore, while we know our isolated neutrophil purity is high (which has been tested after isolations

using the Sysmex analyser) we can't exclude the potential for an impact of other granulocytes. The high numbers of immature granulocytes that we see in AH and ALD-A could also potentially contribute to the reduced neutrophil function that we see in Figure 3.6, as immature neutrophils have been shown to perform these antibacterial functions less effectively than mature neutrophils in patients with sepsis and SIRS(305). However, immature granulocytes only account for a small percentage even in AH patients, and so understanding what signalling is changing neutrophil behaviour overall is important.

Considering the significant increase in total white blood cell count, the decrease in lymphocytes in patient groups who were consuming alcohol is an interesting finding in keeping with what has been previously reported(306). This study also reports that there was only an increase in the $CD4^+/CD8^+$ ratio in patients with advanced fibrosis. This finding, along with the increased activity we see in reactive lymphocytes in AH could suggest interesting changes in lymphocyte subsets in these patients, and activation of both innate and adaptive responses to alcohol injury. Alongside this, Neutrophil/Lymphocyte ratio has been shown to be predictive of sepsis progression in patients who receive living donor liver transplants(307), and highlighted as a possible mechanism to identify patients who may respond better to steroid treatment(198). This data collectively shows many potential applications and benefits of utilising the outputs from the Sysmex analyser as additional markers in ARLD patients who may be at risk of infection.

3.3.3 Changes in neutrophil number and function

In Chapter 1, I discussed the influence of neutrophil activity in liver disease and infection. Our Sysmex data demonstrates the dramatic increase in neutrophil number in acute injury, and our findings are suggestive of some neutrophil dysfunction in AH. We have demonstrated altered neutrophil responses in acute and chronic liver disease, with our most significant findings being in AH. While the reduction in phagocytosis is in keeping with other publications, our results do not recreate published findings of increased ROS production at baseline(204) (although do suggest that there may be a slight deficiency in ROS production with stimulation). Mookerjee *et al* also showed a more prominent response to fMLP (which we did not replicate) which they attributed to neutrophil priming(204). While not significant, we see patterns of lower ROS production particularly in response to *E. coli*, and combined with the significant reduction in phagocytosis this does suggest less effective antimicrobial responses.

The more intricate changes in ROS production, especially at baseline or in response to weak stimuli such as fMLP may be easier to quantify with different techniques. The PHAGOBURST protocol was limited in the way we collected the data, as this was a measure of total conversion of a substrate by ROS at a single end point, and may have missed important variation over time. We had hoped to investigate the production of these molecules and general oxidative metabolism in more detail using Seahorse technology. Traditionally used to assess metabolic activity, measures of oxygen consumption rate can be utilised to study neutrophil ROS production with this platform(308). These studies would allow not only a temporal but also a dose dependent measure of neutrophil responses in donor and AH samples. I did perform some initial pilot studies with healthy blood, but the logistical

challenges of selecting and consenting patients, collecting samples and then transferring isolated neutrophils (which are already prone to activation) to a Seahorse facility was not something we were able to overcome within the time constraints of the project. Moving forward, this technique may offer valuable insight into the more intricate production of ROS in ARLD, and therefore not only the mechanisms of inflammation but also more effective treatment protocols for pharmaceutical interventions such as NAC. There are varied results from trials that add this anti-oxidant therapy alongside steroid treatment, but overall there appears to be no notable improvement(309). However, understanding patterns of ROS production by neutrophils in patients with ARLD may highlight alternative strategies for this type of treatment.

Unfortunately, both the PHAGOBURST and PHAGOTEST reagents were discontinued before our intended sample number of AH patients could be reached. However, the significant decrease in measured phagocytosis even at low numbers strongly suggests that these differences are substantial. It should be noted however that the quantity of *E.coli* was not normalised to neutrophil cell number, which considering the significantly higher numbers of neutrophils in AH could influence the outcome if not at saturating levels. As neutrophil numbers in ALD patients were similar to healthy controls and we also saw a significant reduction in phagocytosis in these patients, this could suggest that what we see in AH is a legitimate loss of function. This would support an explanation for sepsis risk in severe injury. As these protocols were designed to be completed in whole blood, it is difficult to normalise for neutrophil cell number. Repeating these studies with isolated neutrophils could help to confirm the functional changes we see.

Unlike the other antimicrobial effects we studied, we found no significant difference in NET production at baseline or in response to stimuli in AH vs control. Bukong *et al*(206) demonstrated that alcohol treatment on neutrophils *ex vivo* induced spontaneous NETosis, but impaired responses to PMA. In this case, we might expect to see a higher baseline level of NETosis in our AH samples which was not recreated. It should be noted that there are technical limitations to this set of experiments that were confirmed after completion. While there is an increase in NET production with PMA treatment, the fold change is much lower than would be expected. We believe now that this was due to an under-seeding of cells within the wells of the plate due to insufficient centrifugation, but experiments could not be repeated within the time constraints of the project.

Overall what we see in peripheral blood samples is altered systemic immune composition across all versions of ARLD we assessed. Notably, changes in AH are more significant and here we demonstrated altered neutrophil phenotype and function. It is possible that this is due to alcohol induced changes in hemopoiesis, resulting in fewer mature and fully functional cells. Significantly increased number but lower phagocytic ability in our patients fits with the highly inflammatory but poorly responsive phenotype in AH.

3.3.4 Characterising whole liver tissue

When introducing this work, I described the challenges with modelling the liver. This chapter provided an opportunity to evaluate the primary human liver tissue which we are privileged to access in order to understand the environment that we hope to recreate, and assess whether we would be able to isolate the progenitor cell population needed to develop our

organoid model(214). We demonstrate expected structural differences between healthy and cirrhotic liver tissue, showing increased immune infiltration, fibrosis and regenerative nodules as well as huge variation between samples. The histological findings supported the biochemical characterisation of our cirrhotic samples, but the interpatient variation is an important consideration for our model, and discussed in more detail in Chapter 4.

The significant increase in EpCAM, CK19 and SOX9 at a protein level indicates an increased pool of hepatic progenitor cells(43) in our explanted diseased samples. The staining patterns of EpCAM in particular within the regenerative nodules may suggest a level of hepatocyte regeneration from this pool, as is often seen in disease when high hepatocyte replication is no longer sufficient to replace lost liver mass(310). As evidenced by Figure 3.9 however, this is not universal across all samples and may impact the pool of cells from which we are isolating. Notably we observed high numbers of ductular reactions in cirrhotic livers even in the absence of alcohol (as transplant patients will have been abstinent for at least 6 months). The balance of these signs of regeneration in contrast to the expression of senescence markers (such as cell cycle inhibitor P16) is interesting, but also in keeping with the induction of senescence associated with liver disease(311).

We also noted an overall change in the immune landscape in our ALD liver samples. We observed clear immune infiltration (which was not due to neutrophils as demonstrated in Figure 3.13), shifts in leukocyte localisation and changes in TLR4 staining patterns. There is evidence that ductular reaction expansion is mediated by the LPS – TLR pathway(312) which would explain the increase we appear to see on ductal cells, and also why this would be

activated in patients with late stage ARLD where altered exposure to LPS is likely. There are several studies implicating TLR4 in alcohol injury, and therefore understanding its location in whole liver tissue is important for our model(313). TLR4 was expressed at low level by hepatocytes, but also by cholangiocytes and immune cells. This may explain why we see no significant relative difference in mRNA expression in whole liver tissue samples, but it is clear from differential gene expression between donor and ALD liver single cell sequencing that there are alterations in this pathway in disease (Figure 3.15). Genes relating to TLR4 and inflammatory signalling were the most commonly altered when performing cluster analysis on hepatocyte data, and emphasises the importance of this pathway in ARLD.

The localisation of immune cells within areas of fibrosis in disease is well established, and can contribute to the inflammatory liver environment(314). We saw clear changes in leukocyte localisation in ALD livers, with cells becoming much more scar associated. While CD45 is a non-specific leukocyte marker it is likely that a majority of these cells are lymphocytes, which account for most of the infiltrating cells in chronic alcoholic cirrhosis(315), and may also account for the reduction seen in peripheral blood samples. The difference between this chronic inflammation and the dramatic acute inflammatory response in AH is demonstrated by the images of neutrophil infiltration gifted to us by Dr Rachel Brown. These images show distinctive features of the acute injury response, including high numbers of polymorphonuclear cells localising around dying hepatocytes (known as satelitosis(316)). As highlighted in Chapter 1, the liver is well adapted to encourage leukocyte infiltration, both in its architecture and capacity for cell signalling. Patients with AH have shown increased hepatic expression of CXC family chemokines such as IL-8 (CXCL8), Groα (CXCL1) and CXCL5, which

correlated with neutrophil infiltration and poor prognosis(317). There is also an upregulation of adhesion molecules such as vascular cell adhesion molecule 1 (VCAM-1) on hepatic endothelium in response to inflammation, further encouraging recruitment and infiltration of lymphocytes which already have increased contact due to slow blood flow in liver sinusoids(318). Patterns of hepatic chemokine expression have been shown to change in chronic vs acute ARLD in line with the altered immune infiltrate(319). Interestingly, neutrophil sequestration in the liver sinusoids is associated with endotoxemia, which is common in AH, as a result of interactions with hyaluronan as opposed to "classic" adhesion molecules(320). Furthermore, this sequestration could be induced by activation of endothelial TLR4(321)– further emphasising the links between the TLR4 signalling pathway and neutrophil behaviour in the liver.

This again highlights important liver-immune crosstalk for us to capture in our 3D model, particularly in the case of trying to recreate acute injury. It is important to note that the images of AH are from rare biopsy samples, and the tissue we receive in sufficient volumes for analysis primarily comes from cirrhotic patients. This is an important consideration for our source material, as the ALD livers are likely to be from patients with much later stage disease and without the acute effects of ethanol. This has a number of implications including the type of fibrosis and level of regeneration(322) and may impact the phenotype of cultured cells. However, AH very often occurs on a background of chronic injury, and so comparing donor and diseased tissue in this model has clinical relevance. The level of liver progenitor markers has also been shown to correlate with mortality in patients with AH(323), so understanding how they change in ALD tissue is important if isolating them to model acute injury.

Alongside TLR4 inflammatory pathways, the differential gene analysis performed by Dr Paul Horn reinforces our interest in many other key pathways (Figures 3.14 – 3.16). In hepatocytes, there was indication of changes in pathways involved in the acute phase response, myeloid differentiation, antimicrobial peptides and reactive oxygen species amongst many others. This is in keeping with what we would predict in an ALD cirrhotic environment; increases in acute phase proteins such as those in the complement cascade are strongly associated with ARLD(84) and the notable changes in the TLR/inflammatory signalling pathways are in keeping with our TLR4 staining in cirrhotic ALD tissue (Figure 3.10), although our staining was largely localised to ductal cells. The original publication grouped several liver diseases in their analysis, therefore when stratifying for ALD livers the comparisons were made between 5 donor and only 2 ALD livers. The purpose of this analysis was simply to investigate available whole liver tissue data and see if this corroborated our aims to study the liver-immune crosstalk with a focus on neutrophils. These gene clusters support the hypothesis that altered liver function in ALD is causing systemic changes in the immune system, which are reflected in the results seen in our patient blood samples. It also highlights the importance of capturing these interactions in our model.

3.3.5 Summary

This chapter shows an expected alteration in immune cell phenotype and function in both the peripheral blood and the liver from patients with ARLD. It highlights the inability of peripheral neutrophils to respond effectively to bacterial stimuli in ARLD, and also their change in localisation and recruitment into the liver parenchyma in response to acute alcohol injury. We have also identified our bi-potential progenitor cells of interest both in cirrhotic and ALD livers,

and noted changes in number and localisation which are important to consider when analysing how they respond in culture. As we developed our liver model, it was important to have identified key features of ARLD that need to be captured by our system. Understanding the differences in neutrophil behaviour is also important in this context, as being able to see the systemic differences associated with altered liver tissue environment in acute and chronic disease is key to understanding what we are trying to replicate in the next chapter.

Chapter 4 – Developing an Organoid Model

4.1 Introduction

As I have discussed in previous chapters, the complexity of the human liver makes it notoriously difficult to model. Its unique architecture, blood supply and location within the body all contribute to its ability to perform over 500 functions – from lipid metabolism to generation of proteins for blood clotting(2). Traditional 2D culture methods lose hepatocyte function, and animal models fail to recreate the diversity of human disease (217, 249). Both *in vitro* and *in vivo* models of ARLD are particularly challenging, and this contributes to our lack of understanding of mechanisms and hence treatment options for this disease.

This chapter describes my efforts to utilise recent advances in 3D culture technology to develop an *in vitro* organoid model from primary human liver tissue. Organoids are stem cell derived 3D structures that resemble the tissue from which they originate in phenotype and function(262). Following on from work with Lgr5+ stem cells(267), Huch *et al* developed a liver organoid protocol utilising the bi-progenitor stem cell population found within the liver(214). These cells can differentiate into cholangiocytes or hepatocytes depending on the cues they receive *in vivo,* and this characteristic can be utilised to culture ductal-like and hepatocyte-like organoids *in vitro*. Huch *et al* demonstrated a phenotypic and functional shift from ductal-like organoids (expressing common stem cell and cholangiocyte markers) to hepatocyte-like organoids (becoming quiescent and exhibiting hepatocyte functions such as albumin production) when supplied with appropriate differentiation cues.

One of my key questions for this project is whether this technique can be adapted to model alcohol related liver disease. Utilising our unique partnership with the QEHB Liver Unit, we aimed to isolate and culture organoids from both donor and ALD cirrhotic tissue. This would not only allow us to investigate inherent differences in tissue function, but to later assess whether donor and cirrhotic derived organoids reacted differently to injurious stimuli such as ethanol exposure. Importantly, although hepatocytes account for a majority of liver cells and are key to alcohol metabolism, the influence of the ductular reactive cells in disease is significant, particularly in the context of alcoholic hepatitis(52). I therefore considered it important to study both the ductal progenitor cells and differentiated hepatocyte cells in my models.

In this chapter I aimed to:

- Grow and culture organoids from both healthy and cirrhotic primary human liver tissue
- Differentiate these organoids into hepatocyte-like cells
- Confirm the phenotype and function of these organoids to understand how they might respond to alcohol injury

4.2. Results

4.2.1 Adapting protocols for organoid isolation from normal and cirrhotic liver specimens

The first step in the development of our ARLD organoid model was to adapt published protocols to generate organoids from our donor and cirrhotic tissue specimens. At the time of initial development, publications on human liver organoids were limited. Therefore, protocols published by Fernando *et al*(273) and Huch *et al*(214) were adapted for the isolation, culture, and differentiation of hepatic progenitor cells into hepatocyte-like 3D structures as indicated in Figure 4.1.

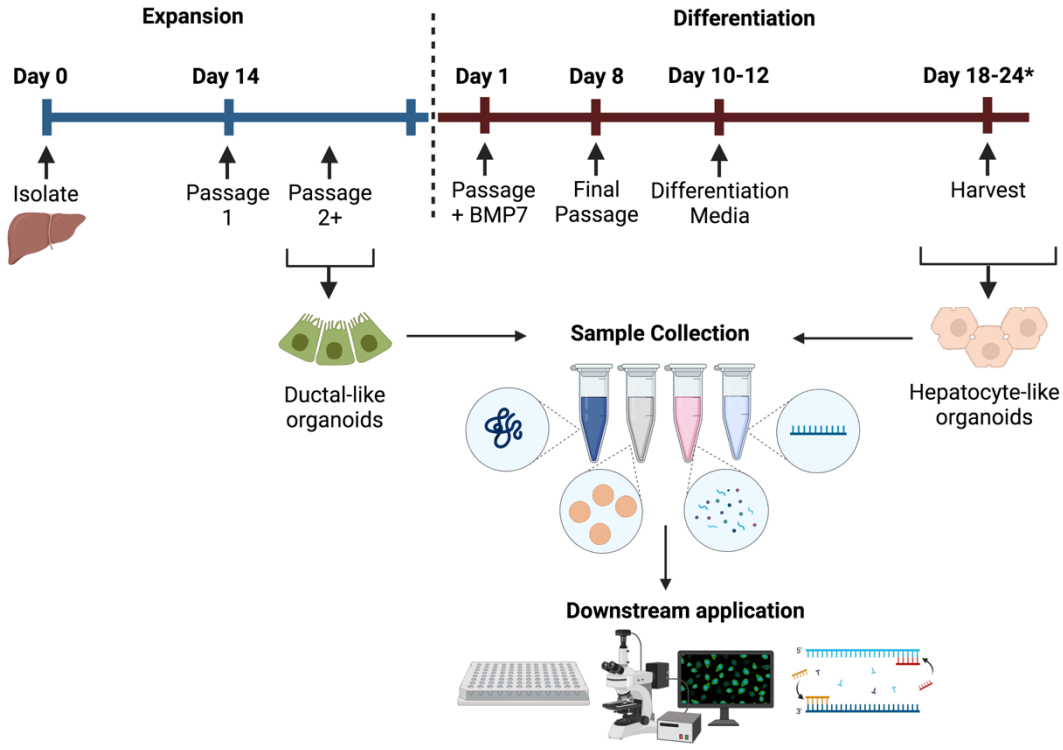


Figure 4.1: Schematic illustrating the organoid generation process and experimental outputs. Primary liver progenitor cells were isolated from ALD or donor liver tissue. These were seeded in Matrigel and passaged after two weeks. Experiments utilizing ductal-like organoids were completed from passage 2 onwards. For hepatocyte-like organoids, samples were differentiated at the time points indicated and samples were collected either 8 or 12 days post final passage. Collected samples included total protein, whole fixed organoids, supernatants and RNA. These were used for downstream outputs including ELISAs, imaging, and qPCR. Image created with BioRender.

While the original protocol from Huch *et al* (214)sorted for EpCAM$^+$ cells which were seeded in the Matrigel, it also stated that organoids could be grown from crude isolations (without selection) at a frequency that matched the expected proportion of EpCAM$^+$ cells. I chose to pursue this method of crude isolation, but also wanted to confirm that this process did indeed generate the EpCAM$^+$ cells of interest. Flow cytometric analysis was performed on the final cell pellet from representative donor and ALD liver isolations as shown in Figure 4.2. This demonstrates that in isolations from both healthy and cirrhotic tissue (Figure 4.2A and B respectively) we see EpCAM$^+$ positive cell populations that are indicative of our progenitor cells of interest, and that there were more in the ALD sample. Once seeded in Matrigel, we were able to successfully grow 3D structures from our isolates that were visible within 2-3 days (Figure 4.2C). While we did see a low percentage of progenitor cells in the total harvested cell populations in our flow cytometry analysis, it is clear from Figure 4.2C and D that organoid structures can be rapidly expanded from the progenitors with passage. Within a few days of isolation, we saw 3D structures approximately 100 microns across. After only two passages, we generated many structures over 10 times the size as indicated by the representative images in Figure 4.2C and D. Panel C also shows a considerable amount of background debris which is largely attributed to red blood cell contamination. While these are quickly removed with passage, their presence added an additional variable and challenges with imaging. Therefore, I also tested the protocol with an additional red blood cell lysis step. However, this caused poorer organoid growth and this step was omitted thereafter (data not shown).

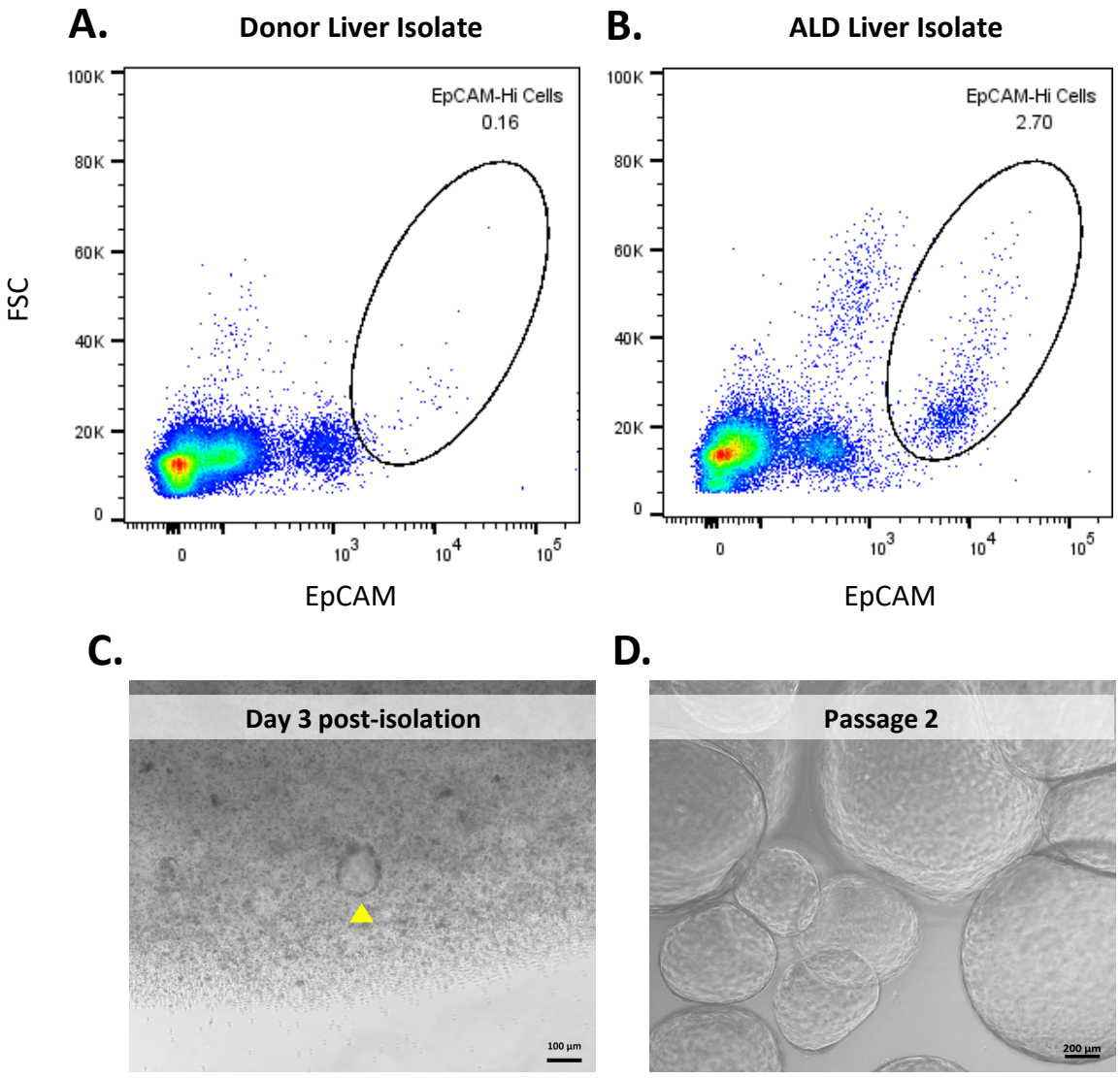


Figure 4.2: Hepatic progenitor cell isolation gives rise to 3D organoid cultures. Cells isolated from whole liver tissue were investigated for bi-potential progenitor marker EpCAM using flow cytometry. The final cell pellet retained from the liver progenitor cell isolation protocol described by Huch et al(214) was stained with an anti-EpCAM antibody followed by an APC-conjugated fluorescent secondary antibody. Fluorescence was measured using a Fortessa Flow Cytometer, and plots were generated showing EpCAM positive cells present in the isolation pellet from an exemplar donor (A) and ALD (B) liver. Post-isolation, cells are seeded within 2-4 25µl droplets of Matrigel in a 48 well plate. Cells were cultured in Expansion Medium (EM) as described by Huch et al, supplemented with 100ng/ml Noggin, 100ng/ml Wnt, and 10µM Y27632 for the first three days post-isolation, and standard EM thereafter. Cultures were passaged every 7-10 days. A representative image of an early-stage organoid structure in culture 3 days post-isolation is shown in (C) (indicated with a yellow arrow). A representative image of organoid structures from the same sample is shown in (D) after 2 passages. Images captured by phase contrast microscopy and scale bar is as indicated.

As part of their published protocol, Huch *et al*(214) stated that it is possible to cryopreserve established organoids, which can then be thawed and produce viable cultures at a later date. Cultures have also been previously established from cryopreserved whole gut tissue(274), and I wanted to investigate whether this was also possible with our human liver tissue samples. I collected small samples of fresh liver tissue which were then slowly frozen for 24 hours at -80°C and stored long term in liquid nitrogen. These were then rapidly thawed, and the isolation protocol was completed with added steps adapted from the gut organoid protocol established by Tsai *et al*(274), and detailed in Chapter 2. As shown in Figure 4.3, it was possible to grow and culture organoids from frozen liver tissue samples. Although I did not extensively compare the use of fresh vs frozen tissue, it appeared that the yield of organoids may have been slightly reduced when isolating from frozen samples, although further repeats would be necessary to ensure this is not simply due to inter-donor variability or tissue quantity.

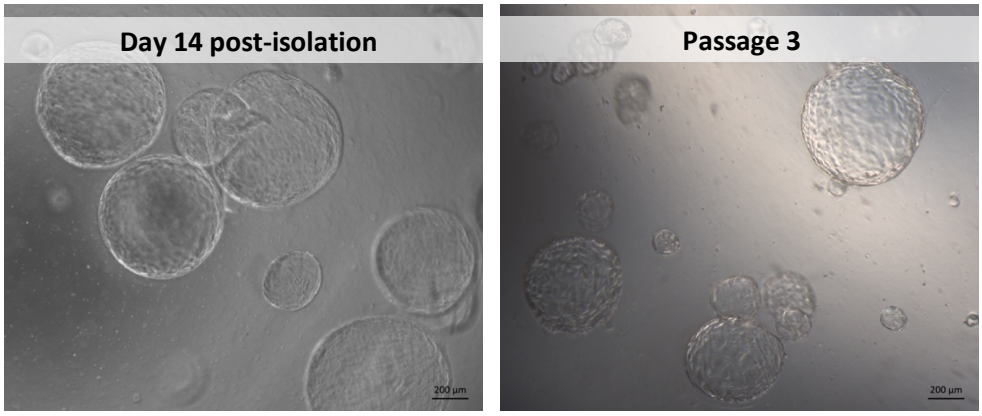


Figure 4.3: Cryopreserved human liver tissue can be used as a source of hepatic progenitor cells. Small pieces of liver approximately 5-10mm were cryopreserved in freezing medium containing 5% DMSO and 10% FBS, by slow-freezing at -80℃ and then stored in liquid nitrogen. To isolate progenitor cells, samples were rapidly thawed using the recovery medium described by Tsai et al (274) and an adapted organoid isolation protocol described by Huch et al(214), as described in Chapter 2. Representative images show 3D organoid structures 14 days post-isolation from tissue without passage, and again after 3 passages.

Once I had confirmed that my protocol allowed me to generate organoids from both donor and cirrhotic liver, I began to compare the nature of the cells from each. First, I measured total organoid protein over time to assess whether there was any difference in the growth rate of donor derived vs ALD derived ductal-like organoids. Figure 4.4 shows that although there was considerable variation between individual samples (as indicated by the error bars on panels A and B) growth rates were similar between tissue types. Growth was also investigated by simple image analysis. Here time lapse microscopy was used to film organoid size over time (Figure 4.4C). This too showed the increase in organoid size over time in agreement with our total protein measurements.

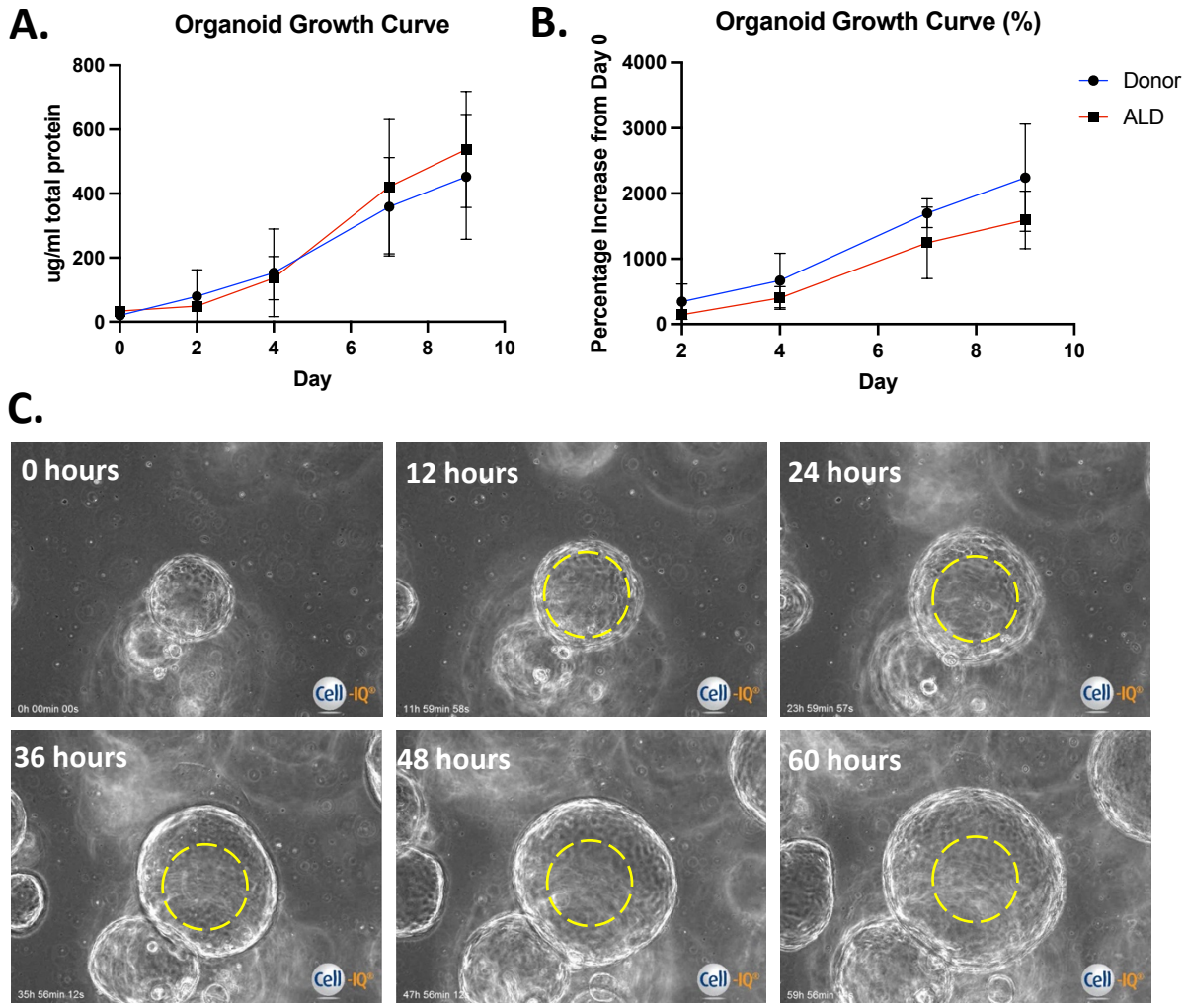


Figure 4.4: Organoids derived from donor and ALD livers grow at similar rates. Measurement of total protein (A) in organoid wells shows no notable difference between donor derived and ALD derived organoids, when comparing percentage increase over time (B). Each time point was plated in duplicate, and results were collected by removing organoid structures from Matrigel using Corning® Cell Recovery Solution. Samples were collected and measured on Day 0 (immediately after plating), 2, 4, 7 and 9. Total protein in the wells was assessed using a Pierce™ Rapid Gold BCA Protein Assay kit as per manufacturer's instructions and measured using a BioTek Synergy™ HT plate reader for n=2-3 livers per condition, where scale bars represent ±SD. Representative images (C) show increase in size of a single ductal-like organoid (isolated from normal liver tissue) over 60 hours in culture in a Cell-IQ live cell imaging system (at 37℃, in Expansion Medium). Approximate time incubated is indicated in the top left of each panel, with each image taken approximately 12 hours apart. The comparative size of the imaged organoid at 0 hours is indicated with a yellow circle at each time point.

Organoid culture confluency after plating was dictated by the crowding of organoids within the Matrigel. After observing multiple isolates, I noted that this was highly variable between individuals, but did not seem to be dependent on the nature of the starting tissue. Figure 4.5 shows representative images of organoid crowding in samples that were plated at three different split ratios from the same starting sample. In this instance, the 1:12 split shows an ideal level of confluency before passage. In other samples that looked similar to the cells in panel A and B, I observed rapid discolouration of media, and loss of Matrigel droplet integrity due to overcrowding. Choosing split ratios became easier with practice, and could be estimated based on the speed at which samples reached the level of confluency shown in panel C. This allowed me to adjust cell management accordingly depending on intended output for the experiment.

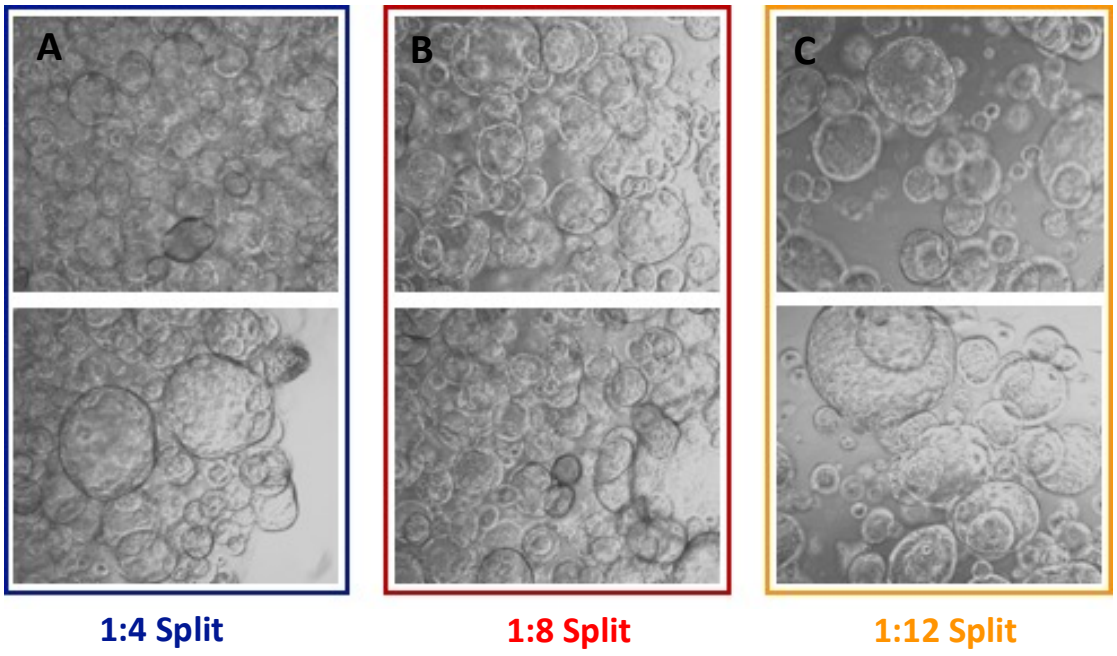


Figure 4.5: Passaging of organoid cultures requires varied split ratios to avoid overcrowding. Representative images showing confluent organoid cultures (isolated from normal liver tissue) that were passaged 1:4, 1:8 or 1:12 and imaged by brightfield microscopy on day 7 post-passage. Organoids were cultured in "Expansion Medium" detailed in Chapter 2, and samples for all split ratios were seeded from the same original culture. Scale bar is 200μm.

Although the organoids from both donor and cirrhotic tissue were growing well using these approaches, the media used for culture was complex and expensive to make. At the start of this project, there was no commercially available media for the culture of human hepatic organoids. I therefore undertook some preliminary testing to see if it was possible to adapt a commercially available medium for murine hepatic organoid culture (HepatiCult™ Organoid Growth Medium - STEMCELL Technologies) for human samples by adding 5µM of A-83-01 and 10µM of Forskolin as described by Huch *et al*(214). While it was possible to grow and culture organoids with this supplemented medium, the results were considerably poorer than when using the published "Expansion Medium" (Figure 4.6). I found that the yield of organoids was reduced and that the structures were smaller and did not survive well in long term culture. I therefore decided to continue with the published Expansion Medium recipe (Table 2.7).

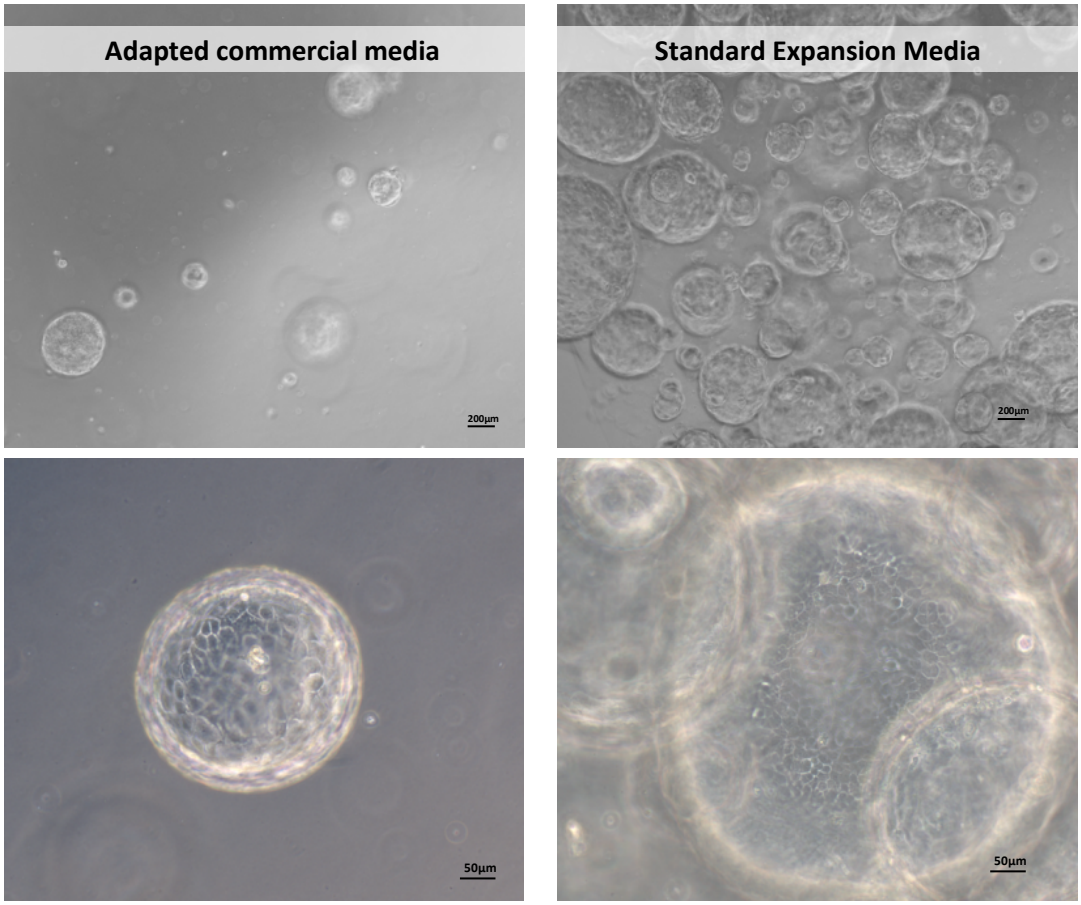


Figure 4.6: Commercially available murine hepatic organoid culture medium cannot be adapted for human hepatic organoid culture. Freshly passaged ductal-like organoids were grown in the presence of either HepatiCult™ Organoid Growth Medium (Mouse) supplemented with 5µM of A-83-01 and 10µM of Forskolin, or standard organoid Expansion Medium as described by Huch et al(214). Media was changed every 2-3 days and images were taken 7 days post passage using brightfield microscopy. Representative images show organoids in each condition at different magnifications as indicated by the scale bar.

4.2.2 Confirmation of ductal-like phenotype in culture

After proving that organoids could be cultured from both donor and ALD tissue, I next used different approaches to confirm the ductal-like phenotype of cultured organoids. In agreement with my initial FACS analysis (Figure 4.2) the presence of the key ductal marker EpCAM, alongside Cytokeratin 19 (CK19), was maintained in culture. Figure 4.7A shows representative images of EpCAM and CK19 staining in cirrhotic ALD liver tissue, indicating a dual positive population of progenitor cells. This is reflected when staining for the same markers in ductal organoids derived from an ALD liver, where most cells within the organoid were dual positive for EpCAM and CK19 (Figure 4.7B). To further confirm the bi-potential nature of these cells, I also stained for the presence of hepatocyte transcription factor HNF4α, which was present in the nuclei of ductal-like organoid cells (Figure 4.8).

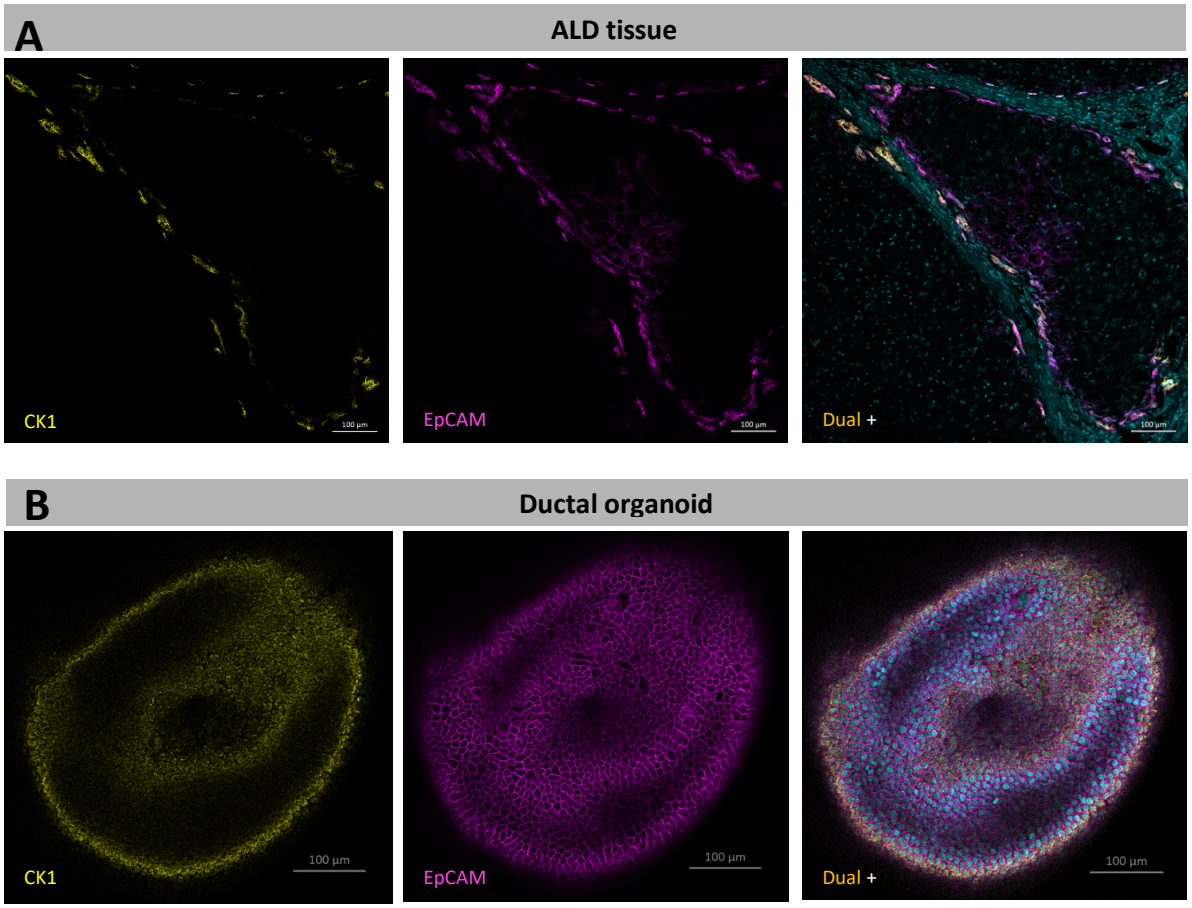


Figure 4.7: Organoids show expression of progenitor cell markers in culture. *(A) Immunofluorescent images from a representative human ALD liver stained with Cytokeratin 19 (yellow) and EpCAM (magenta) antibodies and DAPI as a nuclear counterstain (cyan). (B) Representative images of immunofluorescent staining of paraformaldehyde fixed cultured ductal organoids, from an ALD liver stained with the same antibodies. All samples were imaged using a ZEISS LSM780 confocal microscope. Scalebars are as indicated.*

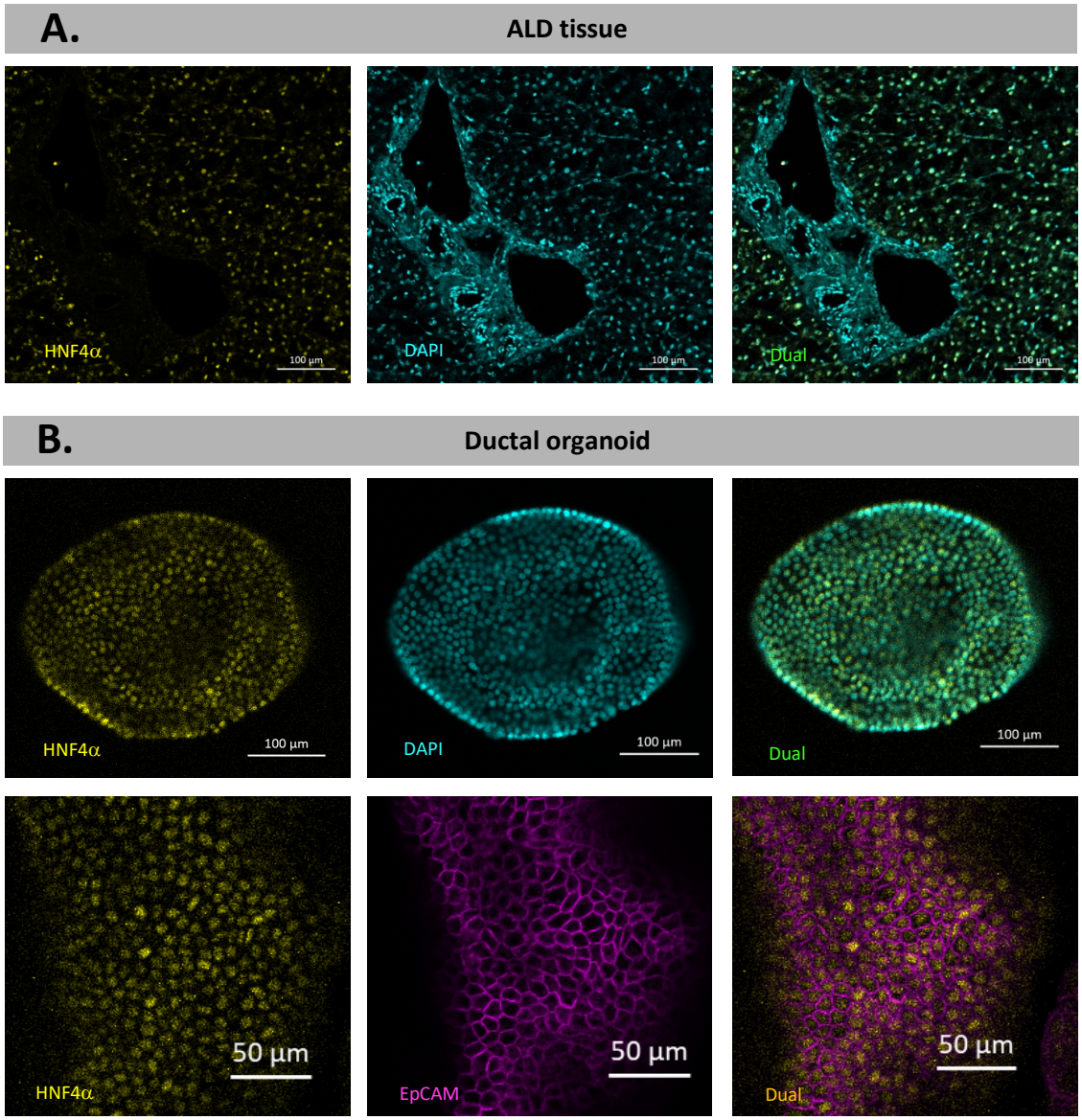


Figure 4.8: The presence of hepatocyte marker HNF4α suggests bipotential progenitor phenotype. (A) Immunofluorescent images from a representative human ALD liver stained with HNF4α (yellow) and DAPI as a nuclear counterstain (cyan). Dual positive cells are green. (B) Representative images of immunofluorescent staining of paraformaldehyde fixed cultured differentiated organoids, where the top three panels are staining with the same antibodies as in (A), and the bottom three show HNF4α (yellow) alongside co-staining for the ductal marker EpCAM (magenta). All samples were imaged using a ZEISS LSM780 confocal microscope. Scalebars are as indicated.

4.2.3 Differentiation into hepatocyte-like organoids

After confirming the ductal-like phenotype and presence of bi-potential progenitor markers, I next needed to validate whether it was possible to differentiate the organoids to become more hepatocyte-like. This process involved priming with BMP7 (known to induce hepatocyte differentiation *in vivo*(324)) and culture in differentiation media for either 8 or 12 days. After this differentiation period, I observed changes in the morphology of both the individual cells and whole organoid structures (Figure 4.9). The organoids became smaller and denser, and individual cells became more rounded. The ductal-like and hepatocyte-like cells adopted a similar shape when compared to 2D cultures of primary biliary epithelial cells (BEC) and hepatocytes respectively.

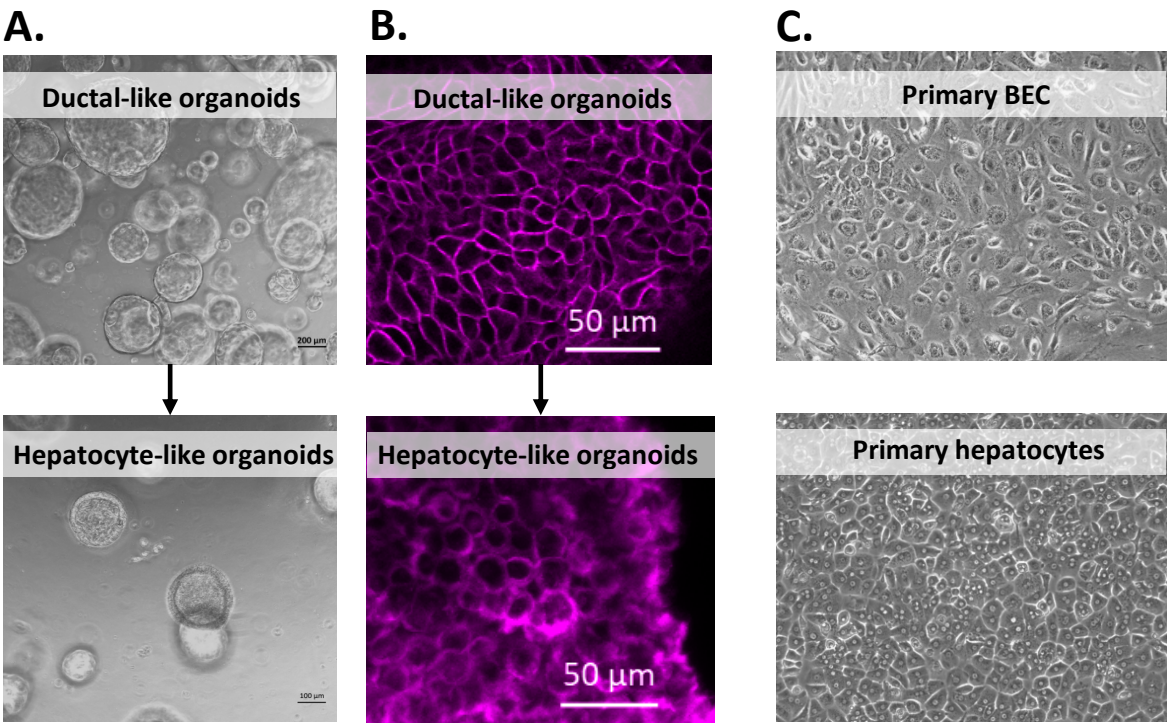


Figure 4.9: Differentiation medium causes structural changes in ductal-like organoids resulting in a more hepatocyte-like morphology. (A) shows representative brightfield microscope images of whole organoids in a ductal-like phase when cultured in Expansion Medium (scale bar 200µm), and then in a hepatocyte-like phase after 7 days of culture in differentiation medium (scale bar 100µm). (B) shows immunofluorescent images of paraformaldehyde fixed organoids again in ductal-like and hepatocyte-like states at higher magnification (scale bar 50µm), where organoids have been stained with an EpCAM antibody (magenta). (C) shows brightfield images of isolated human biliary epithelial cells (BEC) and hepatocytes and in 2D culture, courtesy of Dr Emma Shepherd.

Alongside structural changes, we saw an increase in the expression of a number of key hepatocyte markers such as Cytochrome C P450 enzymes at an mRNA level in fully differentiated organoids, with a trend towards slightly higher expression in donor derived organoids compared to ALD (Figure 4.10). This was also true for BSEP and MRP2. I also attempted to compare expression of key hepato-specific markers between organoids and samples from 2D and 3D 'spheroid' cultures of the HepG2-C3A hepatocyte cell line donated by Dr Nicholas Coltman(325) (Figure 4.11). This was to assess whether expression levels in our organoid model were comparable to other common 2D and 3D models used for liver toxicity studies. Expression of CYP3A4, 2C19 and BSEP was much higher in organoids than the HepG2 cells in 2D or 3D, whereas MRP2 was notably higher in HepG2 cells. CYP2D6 was highest in 3D spheroid culture of HepG2 cells, and CYP2E1 levels were similar when comparing donor derived organoids and 3D spheroid models, or ALD derived to 2D spheroid models (Figure 4.11).

Next, I wished to confirm hepatocyte functionality in differentiated organoids. Storage of fats within hepatocytes is relevant not only in homeostasis but also in alcohol injury, where development of steatosis is a characteristic early feature(112). Incubation of organoids with a combination of palmitic and oleic acid(326, 327) confirmed accumulation of lipid droplets within the hepatocyte cytoplasm (Figure 4.12) when organoids were stained with a lipophilic dye. Alongside this, qPCR (Figure 4.13A-B) confirmed increase in albumin gene expression by both donor derived and ALD derived organoids with differentiation, although this was notably smaller in ALD derived organoids. Here, relative albumin mRNA expression and fold change compared to ductal-like organoids were lower when the cells were derived from ALD liver. I

attempted to confirm these observations at protein level by quantifying albumin secretion into organoid supernatants using ELISAs, however due to issues with assay sensitivity I also looked at albumin protein production by immunofluorescent staining (Figure 4.13C). While technical limitations with both imaging and supernatant analysis mean that production of albumin protein requires further investigation and confirmation, changes in gene expression suggest that these cells are becoming more hepatocyte-like with differentiation.

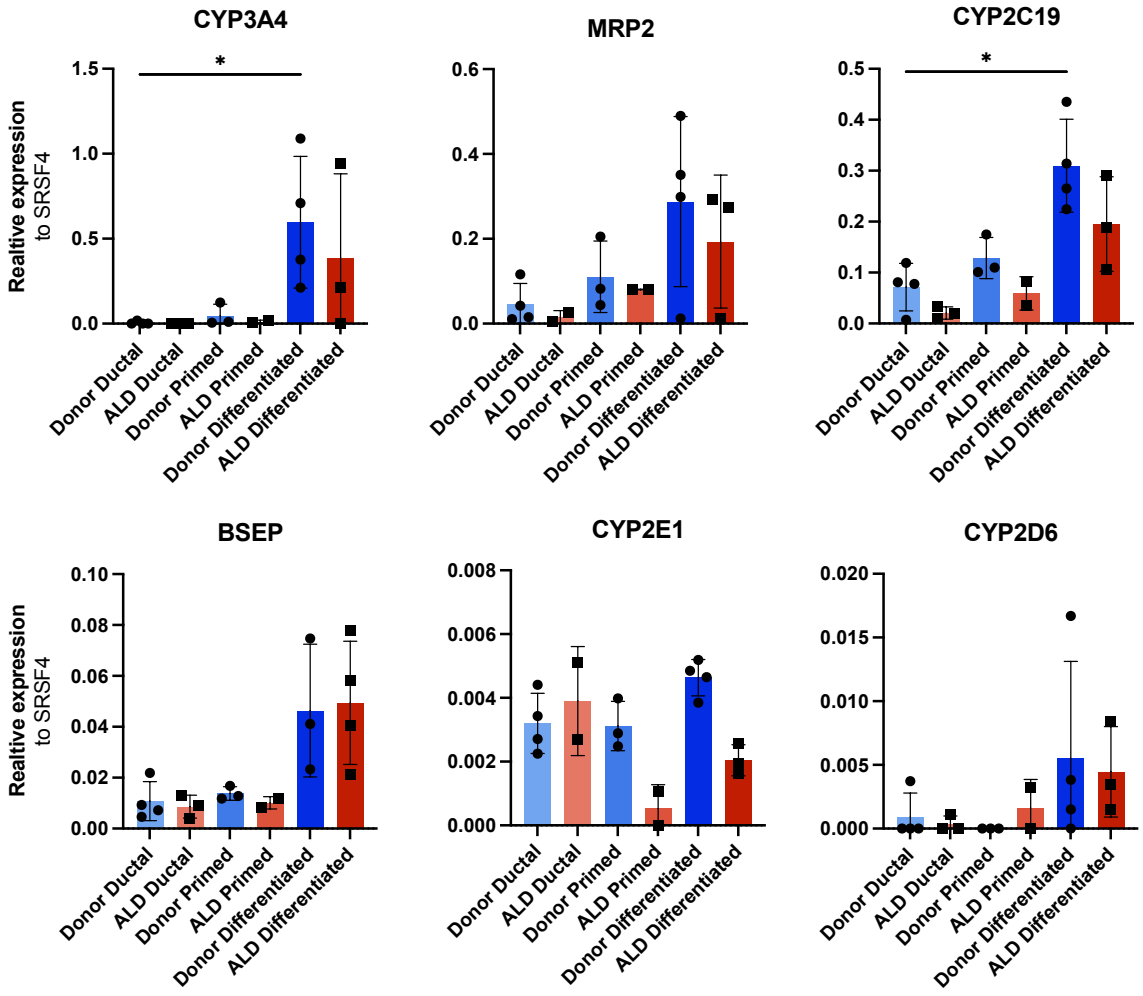


Figure 4.10: Changes in expression of hepatocyte markers show differentiation from a ductal-like to a hepatocyte-like phenotype. Gene expression of key hepatocyte markers in ductal-like, primed (+BMP7) and differentiated samples was measured via qPCR relative to SRSF4 housekeeping gene from donor (blue) and ALD (red) derived organoids. Data points represent organoids derived from individual samples for n=2-4 per group where error bars are ±SD. Statistical comparison of relative expression between ductal and differentiated organoids was performed using Mann – Whitney test where P values are P≤0.05 (*).

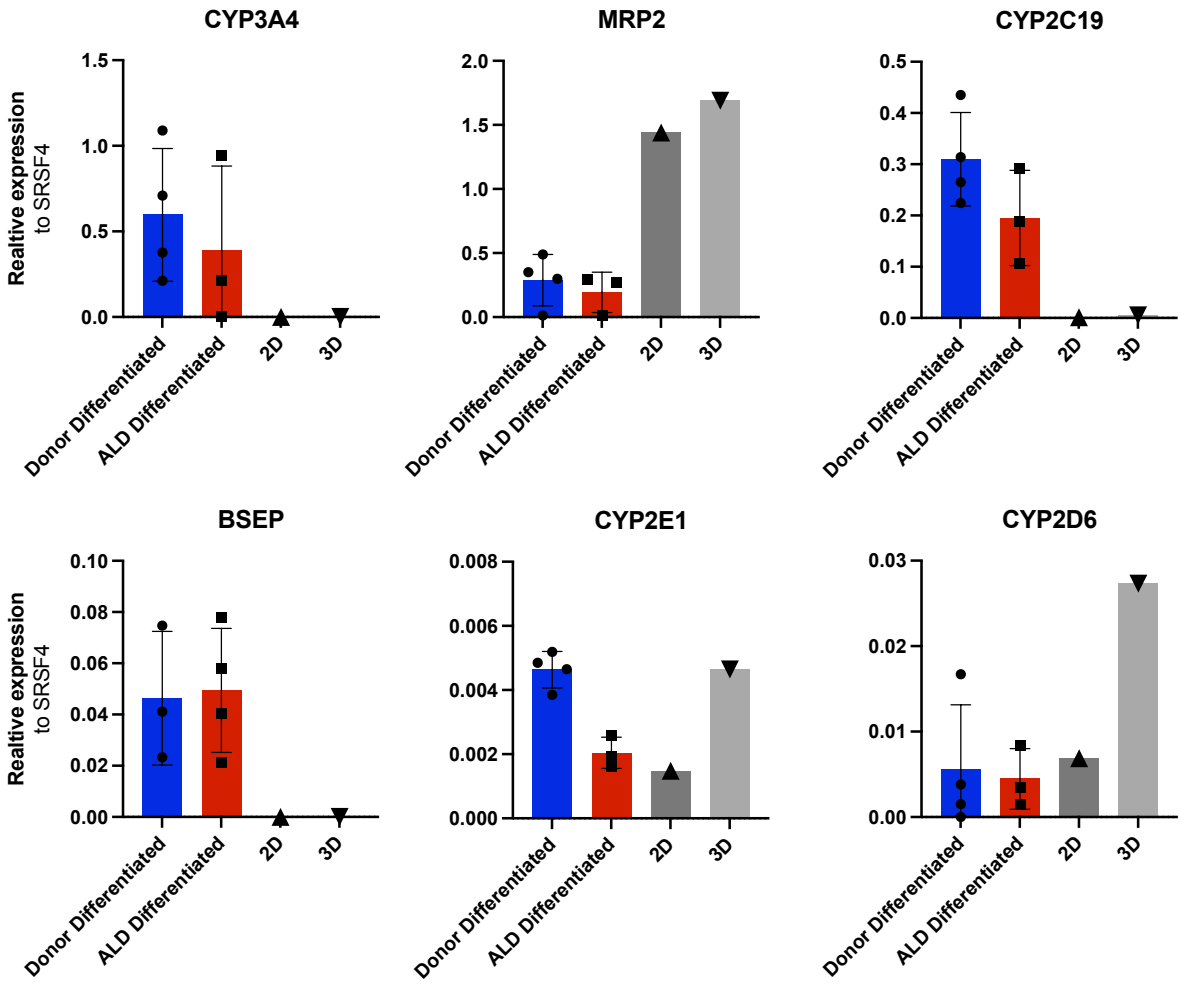


Figure 4.11: Expression of hepatocyte markers in organoids compared to 2D and 3D cell line cultures. Gene expression of key hepatocyte markers in differentiated donor and ALD derived organoids. Data points represent organoids derived from individual samples for n=2-4 per group, or single values for 2D and 3D cultures of a HepG2/C3A hepatocyte cell line where error bars are ±SD. Statistical comparison of relative expression between donor and ALD organoids was performed using Mann – Whitney test and showed no significance.

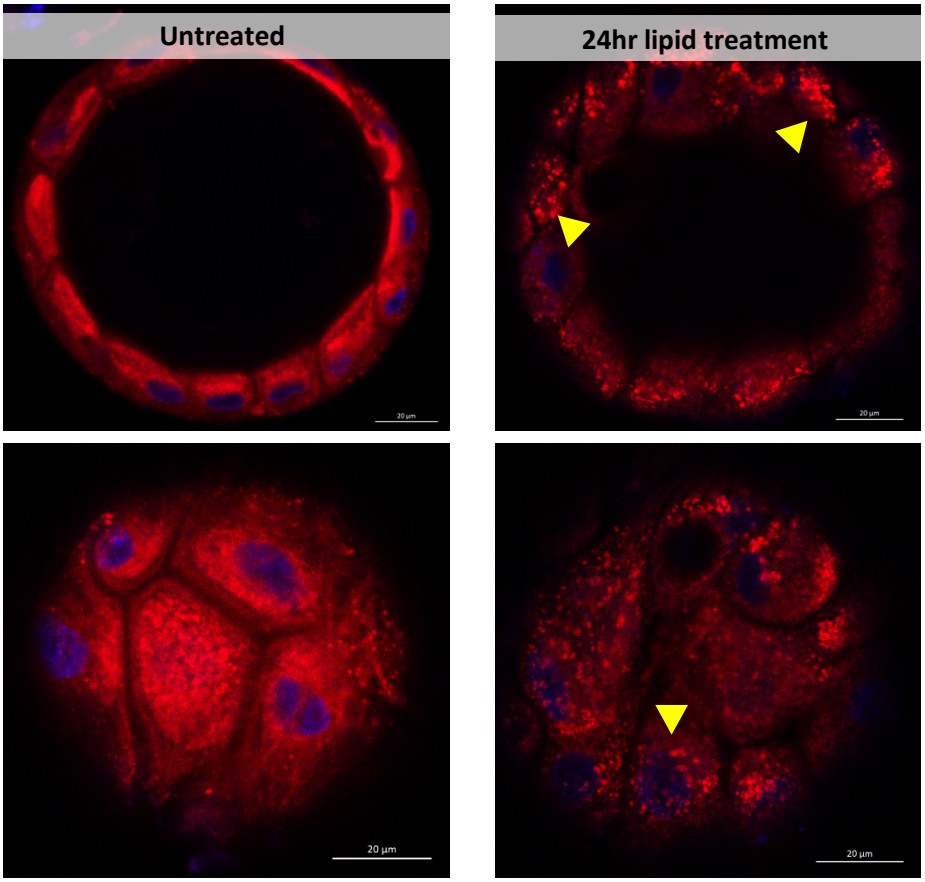


Figure 4.12: Differentiated organoids exhibit hepatocyte functions such as lipid storage. Differentiated donor derived organoids were incubated for 24 hours with an oleic acid and palmitic acid lipid mix and stained with HCS LipidTOX™ neutral lipid stain (red). Nuclei are counterstained with DAPI (blue). Confocal imaging shows arrangement of lipids in droplets within the cell cytoplasm (as indicated with yellow arrows) in treated organoids compared to untreated controls. Images taken using ZEISS LSM880 with Airyscan Fast by Pantelitsa Papakyriacou and show both central (top images) and surface (bottom images) planes of the organoid structures.

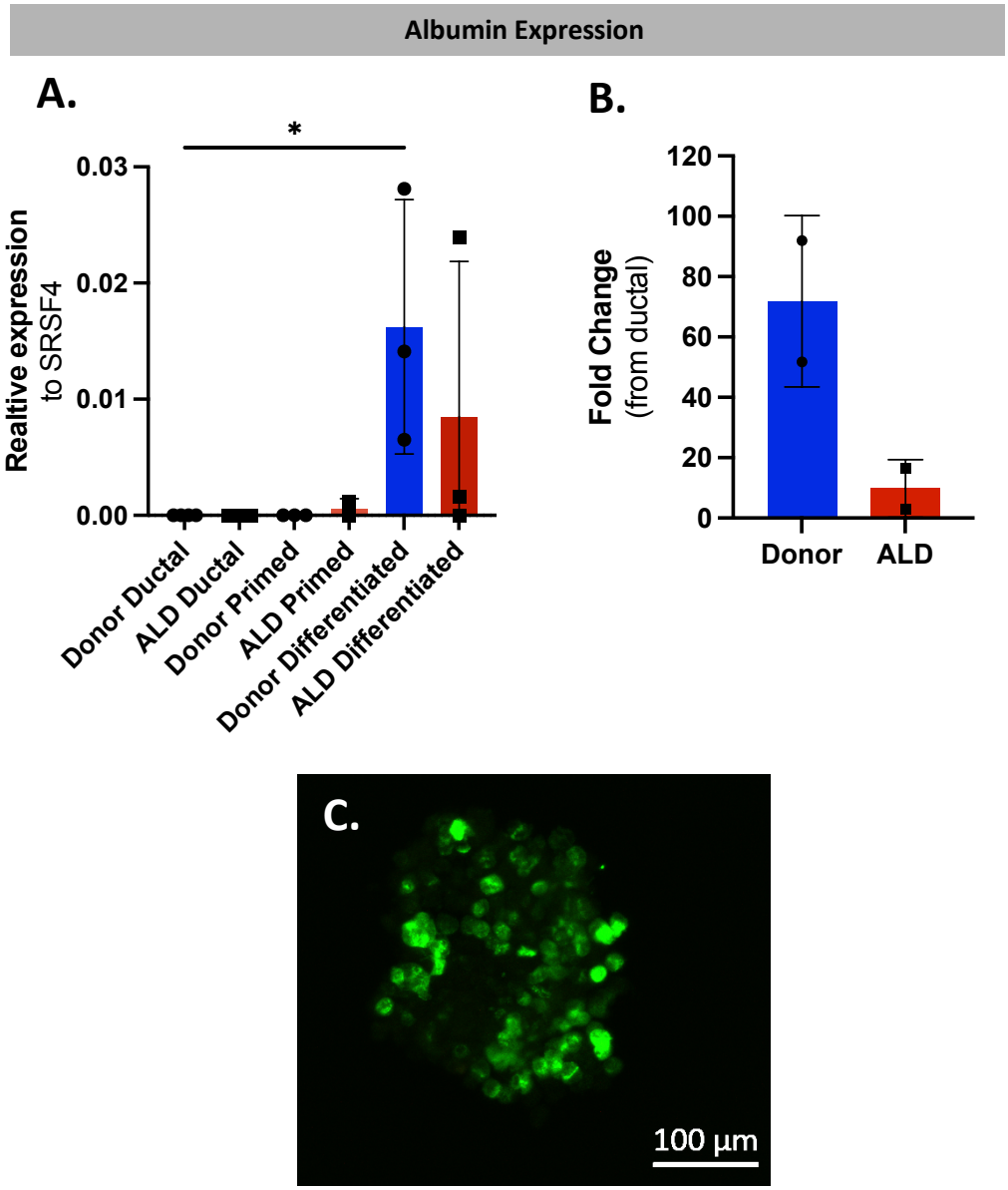


Figure 4.13: Albumin expression differs with differentiation state and tissue origin. Albumin gene expression relative to a SRSF4 housekeeping gene was assessed via qPCR in ductal, primed (+BMP7) and differentiated organoids derived from donor (blue) and ALD (red) livers, where n=2-4 per condition and each data point represents an individual sample (A). Data is also presented as fold change from ductal expression to differentiated in donor and ALD derived livers where n=2 per condition (B). Error bars are ±SD. Albumin protein expression in a representative donor derived differentiated organoid is visible with immunofluorescent staining of human albumin (green). Image taken using ZEISS LSM780 confocal microscope, scale bar is 100µm (C).

Overall, the data in this chapter confirm I was able to effectively grow, culture and differentiate hepatic organoids from both donor and ALD human livers. While growth patterns and many features of differentiation appear to be the same, ALD derived organoids seemed to trend towards lower levels of expression of some proteins – particularly in the context of albumin production. These findings allow us to progress with adapting this model for alcohol injury.

4.3 Discussion

In this chapter I have demonstrated how our model developed at a time when protocols and resources were limited. It was key to understand not only whether we could replicate the liver organoid phenotype in recently published works, but whether this was possible with both our donor and cirrhotic source material – particularly with regards to ALD livers which have historically proven challenging to isolate from(221). Furthermore, could we grow organoids that showed phenotype and functions which would make them a feasible model for alcohol injury.

4.3.1 Understanding organoid phenotype

Overall, our findings seemed to fit with those published by Huch *et al*. The patterns of growth and gene expression were in keeping with the literature, where the combined expression of ductal markers (EpCAM/CK19) and HNF4α suggest a progenitor cell phenotype, as HNF4α is not expressed in normal adult BEC, but is expressed at all stages of development (328). Limaye *et al* also showed that HNF4α expression could be found in BEC in severe liver injury, and noted the association in these cases with the appearance of ductular reactions and an intermediate hepatocyte phenotype(328). HNF4α is essential for hepatocyte differentiation(329), and our change in morphology and expression of hepatocyte associated genes with differentiation cues suggests that we were successfully pushing these cells towards a hepatocyte-like phenotype.

We saw increased expression of a number of genes which are characteristic of mature hepatocytes, and associated with key functions. MRP2 and BSEP are transporters found on

the apical side of differentiated hepatocytes, and key for the functional transport of toxic bile salts out of hepatocytes into the bile canaliculi(330). Cytochrome P450 enzymes and albumin are considered classic markers of mature hepatocytes, and commonly used to assess hepatocyte differentiation in *in vitro* models(331), so the increases we see in our hepatocyte-like cells is supportive of a change in phenotype. Interestingly, the increased pattern of expression seen with CYP enzymes CYP3A4, CYP2D6 and CYP2C19 was not seen with CYP2E1 - a key enzyme for ethanol metabolism. It should be noted that changes in expression in response to ethanol are due to post-translational stabilisation of protein rather than increases in mRNA expression, which may influence this result(332). Interestingly, when compared to a HepG2-C3A immortalised cell line, we see higher expression of some but not all of these enzymes (although it is important to note that this comparison was made to a single sample). While higher levels of several hepatocyte enzymes in our model might suggest better representation of liver cells, the expression of albumin at the mRNA level was hundreds of times higher in the single sample from the 3D spheroid (data not shown). This HCC cell line derivative was specifically selected for due to increased albumin production amongst other factors, particularly in 3D culture, and high expression of MRP2 has been demonstrated(333, 334) which could contribute to the differences we see compared to our organoids. It is important to highlight that here lies a key gap in our data, which is the confirmation that mRNA expression is representative of functional protein expression in our model. As we were unable to quantify actual albumin protein production it is difficult to conclude if this disparity is due to underproduction by organoids or overproduction by the 3D spheroid model, and if these levels have any physiological relevance. We were not able to overcome challenges of measuring low level soluble albumin within the timeframe of this project, and while

immunofluorescent staining of albumin in differentiated organoids suggests that mRNA expression does translate to protein production, technical issues when imaging resulted in a loss of nuclear counterstain in these images – making it difficult to draw conclusions as to the specificity of the stain. These experiments should be repeated as a priority in future work. Furthermore, mRNA expression of drug metabolising enzymes and transporters is promising, but confirming function is a key step – particularly in the case of CYP2E1 and understanding whether alcohol metabolism is taking place in our model. Addition of known substrates and measurement of metabolites would be confirmatory. For example, conversion of para-nitrophenol to para-nitrocatechol has been shown to be an effective method of assessing CYP2E1 activity(335). Similarly, assays have been developed to assess transport of fluorescent substrates by MRP2(333, 336). While there is considerable work to be completed to establish the range of activity that these organoids are capable of, the increase in gene expression and ability of differentiated organoids to metabolise lipid into droplets is supportive of hepatocyte function. The next step here would be to understand whether we can replicate steatosis due to ethanol exposure.

Alongside improved understanding of functional responses, this model would benefit from a wider and deeper investigation of gene expression. This is highlighted at multiple times throughout this project and discussed in more detail in Chapter 7, but the genes we have studied are only giving a small snapshot. As mentioned above, the markers we chose were selected due to their established use when investigating hepatocyte function *in vitro*. However these are limited, and another publication from Huch *et al* even questions the suitability of liver stem cell markers such as EpCAM(337) due to liver cell plasticity. Their 2015 publication

also shows a perhaps surprising increase in Cytokeratin 19 with liver organoid differentiation (a marker associated with ductular reactions, and a finding which we replicated)(214). The whole liver single cell sequencing data(276) analysed in Chapter 3 showed clear changes in functional pathways between ALD and donor cholangiocytes and hepatocytes. Single cell sequencing has been used for a number of organoid models(338), and investigating organoid gene expression in a similar way would allow us to understand differences between donor and ALD derived samples, and the extent of phenotypic change with differentiation.

An interesting finding was that, on average, the hepatocyte genes were expressed to a greater extent in donor derived organoids than cirrhotic, despite similar growth rates. This may be indicative of stem cell exhaustion, or representative of the loss of hepatocyte function seen in chronic liver injury. There is some evidence in mice that with a glucocorticoid induced stress model, liver progenitor "stemness" is lost due to Galectin-3 activity– a molecule which is increased in patients with alcoholic liver cirrhosis(339). This molecule had previously been associated with regenerative nodules, and while absent in normal liver, hepatocyte expression is induced in cirrhosis(340). The loss of "stemness" could perhaps induce some loss of phenotypic plasticity, and therefore make cells more "resistant" to differentiation. Galectin-3 has been proposed as a biomarker for a number of diseases including liver fibrosis(341), and its links to inflammation and liver progenitor cells would make expression in donor vs ALD derived organoids an interesting avenue of exploration. The disparity in expression of hepatocyte genes was most notable in the differences in albumin production, but was challenging to quantify particularly in the instance of fold change as albumin levels were often too low in ductal-like organoids to give a quantifiable signal by qPCR. RNA yield was low in

differentiated organoids, and an increase in the input of material would be needed to account for low ductal expression and calculate this fold increase. Furthermore, RNA quality was often lower when hepatocyte-like cell yields were particularly low, which would be improved with increased material input and reduce the risk of false results. As shown in Chapter 3, patients with late stage ARLD have reduced albumin production. An "imprinted phenotype" has been demonstrated in a number of organoid models(342), and these findings may suggest that organoids derived from cirrhotic liver have retained some characteristics of the diseased liver although further investigation is needed to confirm this. These findings are supported by Bhogal *et al* (221), who showed that when isolating primary human hepatocytes from donor and explanted livers, cells from ALD livers produced significantly lower albumin in culture than those from other cirrhotic tissues. Investigating albumin production by organoids derived from other liver diseases would provide interesting insight into this finding.

4.3.2 Overcoming culture challenges

While this project was adapted from published protocols, this was the first time an organoid model has been established within our group. I was fortunate to receive training in murine gut organoids thanks to Dr Simon Hirota at the University of Calgary, however this was not directly translatable for our human liver samples. Understanding how to handle these samples in culture and optimising elements such as split ratios, Matrigel droplet size and passage frequency was a key element of developing this model. Overcrowding in organoid wells caused unnecessary passages and stress, alongside repetitions of a time consuming and expensive passage process. Splitting too harshly resulted in difficulty recovering a confluent culture. On average, a 1:6 split ratio for both donor and ALD derived organoids was suitable

for passages every 7 days, however this was incredibly donor dependent and varied from 1:2 to 1:12. If organoid overcrowding occurred, we would see yellowing of culture medium due to increased pH and eventually collapse of the Matrigel droplet – resulting in detachment from the tissue culture dish and loss of sample. Interestingly, we also observed sensitivity to changes in plastic wear, where the stability of Matrigel droplets was dependent on culture plate supplier. This is a factor that should be considered if further optimisation of this protocol occurs, or when planning experiments during periods where consumables supply is less reliable. Similarly, stability of the Matrigel droplet could be compromised by vibrations within Category 2 biosafety cabinets, which could be circumvented with dampened tissue paper underneath the plate to absorb vibrations. There are also more general limitations of Matrigel to be noted, such as batch variation and a wide range of potential growth factor concentrations(343). Alongside alternative products such as growth factor reduced Matrigel, there has been significant advances in the options available for extracellular matrix (ECM) gels which is discussed further in Chapter 6, and should be considered for future work on this project.

At the start of this work there was no commercially available medium for human hepatic organoids and attempts to adapt available mouse medium were not successful. Huch *et al* discussed in their work that their previously established mouse liver organoid medium was not directly translatable to human liver tissue, and cultures degenerated rapidly. They discovered high levels of TGFβ signalling, and noted that addition of the TGFβ pathway inhibitor A-83-01 improved survival. Furthering this, addition of the cAMP agonist Forskolin (which has been shown to induce ductal cells *in vivo(214, 344))* increased the stem cell marker

LGR5+ and ductal marker Cytokeratin 19, and lead to long term stable culture of human organoids. As the HepatiCult™ Organoid Growth Medium (Mouse) was developed in collaboration with Huch *et al*, I had hoped to "humanise" it with the addition of A-83-01 and Forskolin, allowing use of a commercially available organoid medium. However, as shown in Figure 4.3 it resulted in poorer organoid yield and therefore the published Expansion Medium recipe was used. It is unclear if there are additional factors added to the HepatiCult™ which reduced the effectiveness with human samples, although it should be noted that this experiment was not repeated after initial testing. The protocol for making the published Expansion Medium is a limitation of this work, as it creates multiple opportunities for the introduction of both human and pipetting error. The standard Expansion Medium alone requires the addition of 14 different components, each of which are individually reconstituted, aliquoted and added to every batch (at a minimum every 2 weeks). Long term storage in freezers over periods of lab inaccessibility and changes in supplier due to product unavailability also introduce variation into a model where this is already a challenge. Human hepatocyte organoid media is now commercially available, and moving forward would improve the reliability of this organoid culture. Similarly, STEMCELL Technologies now provide a range of resources regarding the culture, cryopreservation and experimental handling of organoids. This is discussed further in Chapter 6, but highlights the exciting possibilities of this model going forward; the time dedicated to overcoming challenges in the day to day use of this model limited the ways in which we could apply it, as well as concerns regarding normalisation and reproducibility. The existence of commercially available protocols and reagents for human liver organoids means that there is much more scope to investigate how

this model responds to alcohol injury, and to understand differences between cirrhotic and donor derived samples with fewer confounding variables from the culture process.

A surprisingly complex aspect of this project was determining total cell count in order to measure growth rates. Despite many different optimisations to the protocol, I found that cells either could not be reduced to a single cell suspension or resulted in reduced growth after harsher enzymatic digestion. Eventually, this issue was circumvented to some degree by measuring the change in total protein over time. This allowed me to plot a growth curve based on total protein, that showed a similar pattern in doubling time to Huch *et al(214).* This value was not impacted by any ECM protein carryover, as control Matrigel-only droplets showed undetectable levels of protein when measured. This method was then carried forward as a crude way of normalising samples such as supernatants, but the inability to perform an exact cell count remains one of the most significant limitations of this project. This issue became more pronounced in later experiments, particularly when trying to understand differences between ALD and donor derived organoid responses to injury. Conversely, total protein normalisation may have some advantage due to the significant heterogeneity in organoid growth between samples. Due to notable donor variability, seeding cells in equal number may not result in equal cultures at an experiment endpoint. Therefore, total protein may offer value with regards to understanding differences in treatment response between samples. Generating sufficient material from differentiated organoids for downstream analysis was also challenging. Ductal-like organoids grew rapidly and were easily lysed, often yielding several hundred nanograms per microliter of RNA. However, yields were considerably lower for hepatocyte-like organoids, where not only do we actively halt proliferation with

differentiation but also see a reduction in size and increase in density. An initial concern was whether I was achieving sufficient cell lysis, however this was challenging to improve without loss of sample. If this type of model were ever to be scaled, for example in the context of drug discovery, it is important that this limitation is circumvented and protocols optimised with additional steps such as phenol-chloroform RNA extraction(345). Another element of the culture protocol that required optimisation (but is not displayed in the figures above) included understanding the impact of Matrigel droplet size and time in differentiation medium. In the early stages of this project we noticed that when differentiating organoids, a monolayer of cells appeared in the bottom of the well outside the Matrigel droplet after approximately one week in culture. These appeared to originate from organoids that had "collapsed", but it was not possible to investigate these cells separately from the organoid cultures. As we were concerned that these cells could be contaminating our results due to having a different and unknown phenotype, we tried to reduce their impact by reducing the time that organoids differentiated in culture from 12 days to 8, and plating smaller Matrigel droplets to limit organoid size and avoid collapse. As these mitigations did not improve the presence of the monolayer of cells (which did appear to remain within the culture well after removal of the organoids) we continued with the original protocol. However, it cannot be overlooked that they may have influenced qPCR and proteome results, and investigation into these cells would be beneficial if seen in future cultures.

4.3.3 Adapting published protocols

It should be noted that adaptions were made to the published protocols in order to suit our source material and resources. We chose to plate isolated progenitor cells from a crude liver

preparation rather than by sorting for EpCAM$^+$ cells, as the original publication by Huch *et al*(214) showed that this yielded proportionally similar numbers of organoids and removal of the sorting step would minimise potential for contamination of the cultures. The methods published by Huch *et al* also described a Percoll-based clean up step as part of a hepatocyte isolation, which we chose to include as it removed a large amount of debris whilst also giving a good organoid yield that matched the expected phenotype. The flow cytometry analysis of representative isolation pellets (Figure 4.2) confirmed that our adapted method of isolation did result in EpCAM$^+$ cells, and the increased percentage seen in the ALD isolation is in keeping with our immunohistochemical staining (Chapter 3). However, it appears that there may be more than one EpCAM$^+$ population. In this analysis we considered the cells with the strongest signal (EpCAM^{hi}) to be our positive population, but we are unable to differentiate between cells from ductular reactions, biliary epithelial cells and even mature hepatocytes that have developed from progenitors and are EpCAM$^+$ (346). While our results suggest that we have indeed been producing organoids from our expected population, further investigation into whether different EpCAM$^+$ cell populations alters organoid phenotype (especially in cirrhotic liver where ductular reactions result in heterogeneous populations(33)) is essential to understand the outcomes of this model.

To investigate these populations more clearly, it would be beneficial to compare the results to organoids grown from EpCAM$^+$ cells alone. During our in-house protocol for the isolation of hepatic sinusoidal endothelial cells from whole liver tissue, we include a step to remove EpCAM$^+$ cells using immunomagnetic selection(57). This method could potentially offer an efficient way to optimise our isolation protocol going forward, by selecting for EpCAM$^+$ cells

without requiring a cell-sorter. Surprisingly, no additional steps were required to get an effective isolation from highly scarred cirrhotic tissue. While the initial manual tissue dissociation could be more challenging, it is possible that any reduced ability to dissociate/digest the tissue was compensated for by the increased numbers of ductal progenitor cells seen in cirrhotic tissue (as indicated in Figure 3.8). Interestingly, the addition of a red blood cell (RBC) lysis step to the isolation protocol resulted in poorer cell yield when performed in parallel without a lysis step. This may be due to the RBCs having a positive effect and releasing factors supportive of growth (as they have been shown to be reservoirs for a range of different cytokines and growth factors such as VEGF and HGF(347)), or lysis buffer negatively impacting the progenitor cells(348). This question was not pursued as RBC contamination was quickly lost with passage, but could possibly offer another potential advantage of pursuing $EpCAM^+$ sorting or further investigation the influence of RBCs in co-culture.

One of the most significant adaptions to this protocol was the successful growth of organoids from cryopreserved tissue. Tsai *et al* demonstrated this technique with human gut biopsies, and highlighted the potential for utilising biopsy samples that may otherwise go unused due to the time and labour required to generate organoid cultures(274). This has also been demonstrated in cryopreserved biobanked endometrial biopsies, where results were comparable to fresh tissue(349). While not pursued for this project, this offers an exciting new avenue for organoid research in institutions that lack access to primary tissue. Culturing from cryopreserved tissue also offers a solution to issues with standardisation in source material,

where samples could be frozen within a much smaller time window from arrival and isolated in parallel.

4.3.4 Limitations of source material

An important limitation of this project and all studies using material from human donors, is that the tissue samples that we received were highly variable; an issue that is furthered by the low sample numbers in this study. While all ALD livers are from end stage alcohol related cirrhosis, the condition of the tissue was not consistent (which is exemplified in the IHC imaging shown in Figure 3.9). There was variation in levels of scarring and altered architecture, as well as the number of cells with progenitor markers. Clinical trials investigating sampling variability in NASH biopsies have highlighted that there is such range even within the cirrhotic liver that some biopsies can lead to a missed diagnosis, despite secondary biopsies confirming key features of NASH(350). Our tissue pieces were intentionally considerably larger than biopsies to account for this, however it emphasises the range of potential samples. Liver ECM has also been shown to be highly immunomodulatory(351), and it is well established *in vitro* that ECM stiffness alters liver cell function(352); this suggests that variable levels of scarring and ECM deposits as seen in Figure 3.7 could mean that we are isolating cells from quite different liver environments. Alongside this, there was variation in cold storage time of tissue samples before isolation. This is possibly most significant in the case of donor material, where there are additional delays between collection from the donor, to decision not to use for transplantation, and allocation to the CLGR(221). An additional consideration regarding donor livers is reason for rejection; unsuitability for transplant could be due to a number of factors (such as donor age or donation after cardiac death)(353) which makes the donor pool highly

variable. In particular, rejected donors with high levels of steatosis can result in poorer cell isolations (which is acknowledged both in our in-house protocols and in the literature(221, 354)), and for this reason I did not attempt to isolate from samples with visibly high fat accumulation. Both donors and ALD patients may also have a range of co-morbidities that we are not always informed of. Furthermore, HCC is common in patients with cirrhosis, and while every effort was made not to include samples where tumours were present elsewhere in the liver in donor-ALD comparisons, pre-neoplastic changes throughout the cirrhotic ALD liver may contribute to changes in organoid phenotype (355, 356). The low sample numbers in this study mean that it is hard to account for any effects that this variability may have, and in cases such as organoid growth patterns where ranges were particularly high, we may be missing differences between ALD and donor tissue. Organoid culture was successfully completed on samples from an ALD/HCC liver explant and on healthy resected tissue from patients with liver cancer, however they were not included in comparisons due to unknown impacts of disease or treatments. This could be investigated at a later date, as tumour organoids are a well-established and informative tool. Being able to utilise the samples that weren't included in this study to grow organoids from tumours and surrounding tissue in parallel could offer a unique insight into the development of HCC in ALD cirrhosis.

4.3.5 Summary

In this chapter, we have demonstrated our ability to grow and differentiate organoids from donor and cirrhotic livers. Our findings suggest that we are successfully isolating a progenitor-like cell, and we see indicators of hepatocyte function with differentiation such as expression of albumin and lipid droplet formation. This, alongside the presence of detox enzymes,

support the potential use of this model to replicate alcohol injury from donor and cirrhotic samples. The differences in gene expression between both tissue types suggest that samples may be retaining characteristics from the diseased liver, which is advantageous for studying AH which most commonly occurs on a background of chronic liver damage. While there is still characterisation to be done on organoid phenotype and function, these findings supported progression to the investigation of injury responses.

Chapter 5 – Modelling injury in 3D cultures

5.1 Introduction

After establishing the function and phenotype of our cultured organoids, the next step was to attempt to recreate the injury we have seen in our patient groups – thus permitting understanding of not only the inherent differences between donor and ALD derived organoids, but also how they respond depending on the state of maturity (ductal or hepatocyte-like). Alongside response to alcohol, we also considered the additional stimulation from exposure to bacterial products as is frequently seen in all ARLD patients(174, 177). One particularly damaging effect of this is the increase in circulating LPS – a molecule found on the outer capsule of gram negative bacteria such as *E.coli*(73). In homeostasis, the liver would usually contribute to clearance of these molecules from commensal bacteria(74), however loss of hepatocyte function and increased concentrations of circulating LPS in ARLD can lead to endotoxemia and systemic immune activation. For this reason, we consider it an important additional stimulus in our model alongside alcohol.

As discussed in the introduction to this thesis, the liver also has a number of key immune functions, and the production of inflammatory cytokines and proteins required for the acute phase response influence systemic immune behaviour(62, 82). In this chapter we investigate whether we are capturing those functions in our organoid model, and whether we can recapitulate *in vivo* responses to injury. Furthermore, based on our findings regarding neutrophil behaviour in both AH and ALD, the next question was to assess the effect of organoid conditioned media on neutrophil function in order for us to begin to dissect the

mechanisms underpinning neutrophil response to liver injury *in vivo*. As shown in Chapter 3, there is significant increase in neutrophil number and infiltration into the liver in AH, but an overall decrease in function. Here we hope to investigate the impact of both injured and uninjured organoids on primary isolated neutrophils to see if damage signalling alters their phenotype.

In this chapter, I aimed to do the following:

- Measure organoid responses to alcohol and bacterial products
- Investigate different outputs and pathways to better understand how this model might be utilised to study liver-neutrophil crosstalk
- Gather pilot data describing the effect of injured and uninjured organoid supernatants on neutrophil function

5.2 Results

5.2.1 Selecting appropriate injurious stimuli

Now that we understood more about the difference in phenotype between ALD and donor derived organoids, as well as how this changed with differentiation, the next step was to assess how they would respond to injurious stimuli designed to recreate the hepatic environment in alcoholic hepatitis. The first step in this process was a titration of ethanol into the media of ductal and differentiated organoids (Figure 5.1). I selected a concentration range between 1 and 100mM to reflect the exposure range *in vivo(357)*. When I measured gene expression for ADH1 and CYP2E1 in ductal and differentiated cells from an ALD liver there was a differential response (Figure 5.1). Whilst there was a dose dependent variation in expression of both genes in ductal cells with a peak at 5mM this was not replicated in matched differentiated samples, however this was only performed on cells from a single donor. To ensure that ethanol evaporation over the culture period was not impacting on response, I trialled a different dose regime using two separate higher doses of 200mM ethanol over 24 hours on differentiated organoids (Figure 5.2A). This led to a more dramatic decrease in expression of ADH1A, CYP2E1 and also albumin gene expression. We therefore questioned whether we were observing a toxic effect of ethanol or possibly a de-differentiation of our hepatocytes. The alcohol titration was therefore repeated on two new donor and two ALD-derived sets of differentiated organoids. Figure 5.2B shows that there was no significant change in either EpCAM or CYP2E1 with increasing concentrations of ethanol for these patient samples. Importantly I compared the Ct values for four common housekeeping genes in response to injurious stimuli. These were stable across treatments, and subsequent qPCR experiments were completed relative to SRSF4 only. This was chosen due to published data

showing it to be the most stable housekeeping in ALD samples(358) alongside it having similar Ct values to our genes of interest (Figure 5.3).

We chose to continue with a treatment of 100mM ethanol plus LPS at 100ng/ml for 24 hours. This caused no obvious changes in appearance or morphology after treatment in ductal or differentiated organoids (Figure 5.4A-D). Adenylate kinase activity in cell supernatant was measured to assess levels of injury. Overall, while some samples showed slight increases in this marker of cell damage, levels were inconsistent with no reliable injury in response to treatment with ethanol and LPS (Figure 5.4E) overall. Only samples from undifferentiated donor derived organoids appeared to show credible levels of cell damage, however repeats are necessary to confirm this pattern.

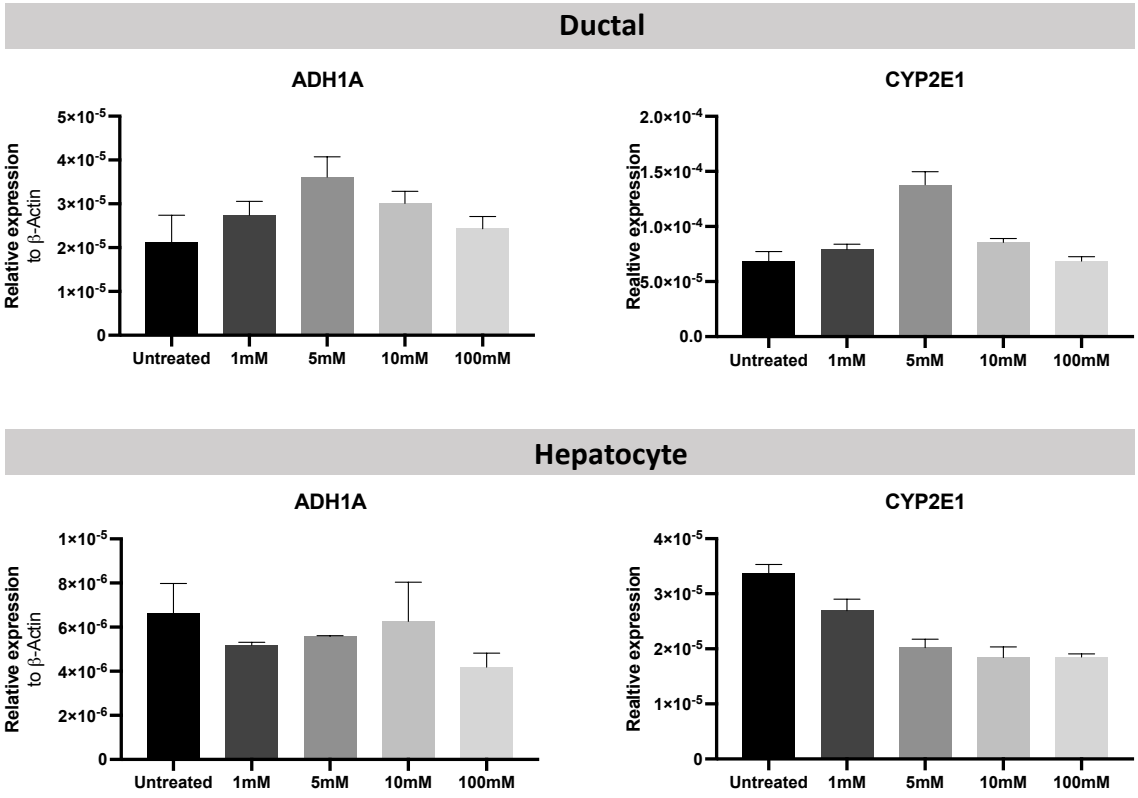


Figure 5.1: Ductal and hepatocyte-like organoids express alcohol metabolizing enzymes, which may be altered in the presence of ethanol. Ductal and hepatocyte-like organoids derived from an ALD liver were treated with increasing concentrations of ethanol (EtOH) for 24 hours. Expression of genes related to ethanol metabolism were assessed via qPCR relative to β-Actin housekeeping gene and displayed as relative expression. Error bars show ±relative expression error for 3 technical repeats within each condition for n=1.

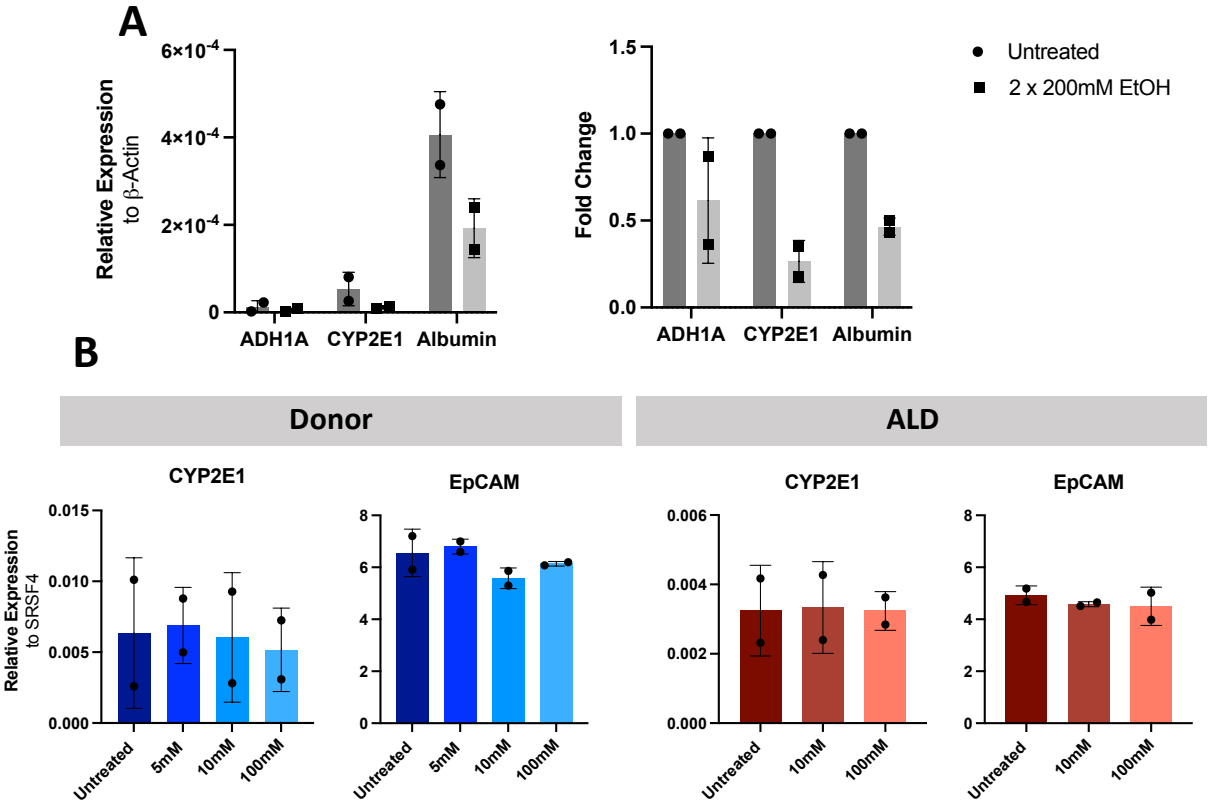


Figure 5.2: Single dose of ethanol does not alter expression of CYP2E1 or EpCAM in differentiated organoids. Hepatocyte-like organoids were either given two doses of 200mM ethanol (EtOH) over the course of 24 hours (A) or treated with increasing concentrations of EtOH for 24 hours (B). Samples in (A) were isolated from ALD livers, and samples in (B) from donor (blue) or ALD (red) livers as indicated. Expression of genes related to ethanol metabolism were assessed via qPCR relative to either β-Actin (A) or SRSF4 (B) housekeeping genes and displayed as relative expression or fold change in relative expression as indicated. Error bars show ±SD for n=2 biological repeats.

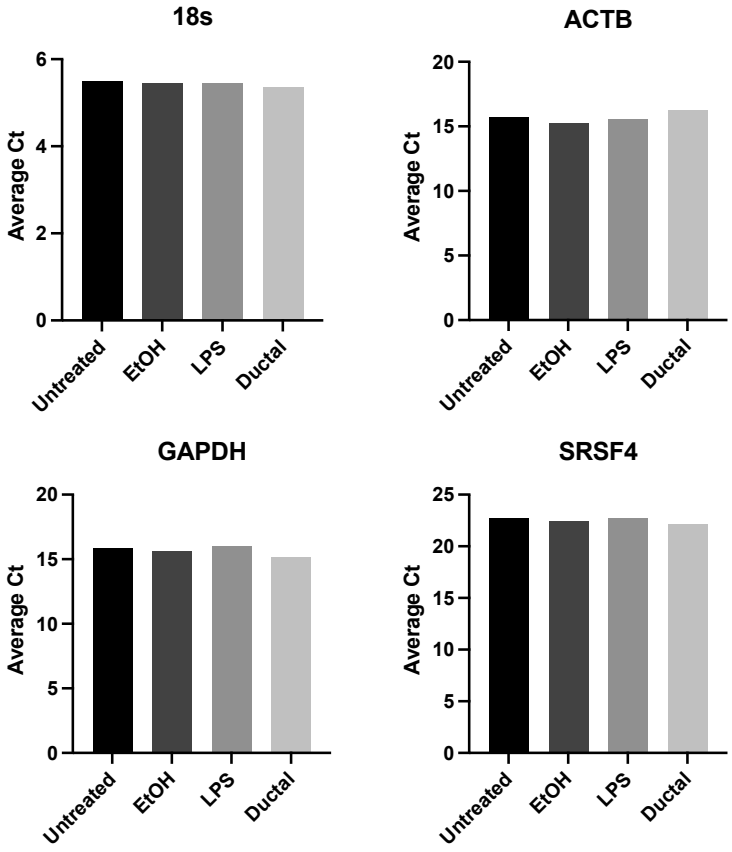


Figure 5.3: Common housekeeping gene Cycle threshold (Ct) values are not altered with treatment or differentiation state. Differentiated organoids derived from an ALD liver were treated with either 100mM ethanol (EtOH) or 100ng/ml LPS, alongside untreated undifferentiated (ductal) organoids. The Cycle threshold (Ct) values of the four different housekeeping genes indicated when measured using qPCR were compared between treatment conditions. Data is presented as average Ct for n=1 biological repeat completed in triplicate.

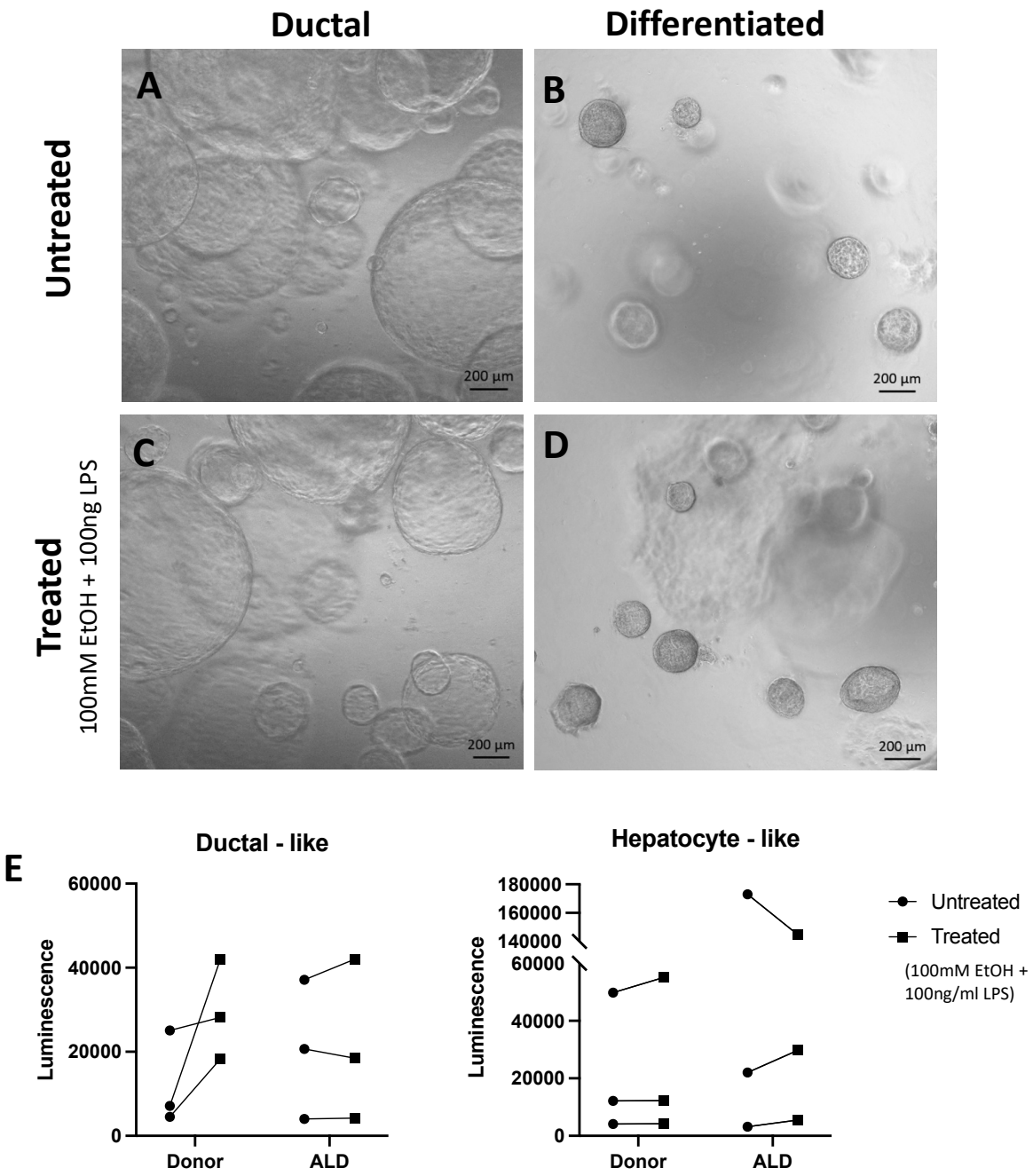


Figure 5.4: Exposure to ethanol and LPS does not alter organoid morphology or size, but may induce some release of cell damage marker adenylate kinase. Ductal (A and C) and hepatocyte-like (B and D) organoids were treated with 100mM ethanol (EtOH) and 100ng/ml LPS for 24 hours and imaged using a ZEISS brightfield microscope. Release of adenylate kinase (AK) as a marker of cell damage was measured via luminescence (E) in ductal-like and hepatocyte-like organoids derived from both donor and ALD livers, with and without 24 hour treatment with 100mM EtOH and 100ng/ml LPS. n=3 per condition with square symbols represented treated matched samples. Data points represent average luminescence reading for 3 technical replicates.

5.2.2 Understanding organoid response to injury

A key element of the immune-liver crosstalk is the production of cytokines and chemokines by hepatic cells, which recruit and retain inflammatory cells(62). As we have previously highlighted the importance of infiltrating neutrophils in liver injury in AH, I investigated organoid chemokine production using a proteome profiler kit on supernatants from organoid cultures (Figures 5.5 and 5.6). Ductal organoids from both cirrhotic and donor livers produced multiple chemokines, many of which are associated with neutrophil activation and migration. These included CXCL8 (IL-8), CXCL5 (ENA-78 – Epithelial derived Neutrophil Activating Peptide-78), CXCL7 (NAP-2 - Neutrophil Activating Peptide - 2), CXCL1 (Groα), MidKine, and CCL20. Of particular note, the most highly produced chemokine in all samples was IL-8, a key neutrophil chemoattractant(359). Based on normalised Mean Pixel Density, the levels of chemokine produced were similar in both ALD and donor derived ductal organoids, and overall did not change markedly after ethanol and LPS treatment. There was a small increase in IL-8 and CXCL7 production by donor ductal organoids (Figure 5.5C) after stimulation, alongside a reduction in CXCL16 and Midkine. Whilst ALD organoids produced a similar level of the same chemokine proteins in general, there seemed to be a lower effect of treatment.

A similar pattern appears when differentiated organoid supernatant was assessed using the same methodology (Figure 5.6). We see the same proteins present in the samples, with a slight trend towards lower production in those derived from cirrhotic liver (Figure 5.6B). Once stimulated with ethanol and LPS there also appeared to be fewer changes compared to treated ductal organoids. There were slight increases in MidKine and CXCL7 by both donor and ALD organoids, and a notable increase in CCL20 production by ALD derived cells.

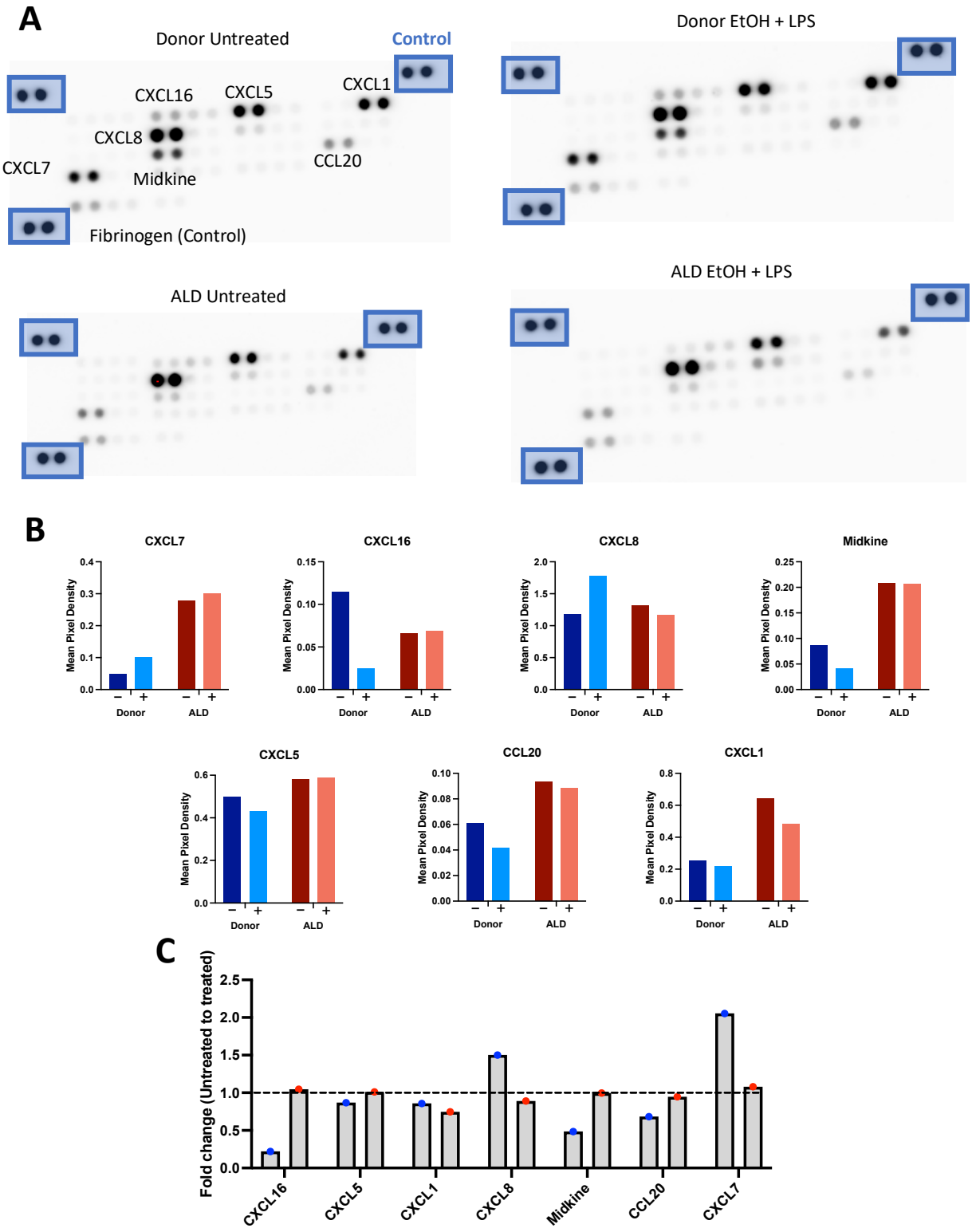


Figure 5.5: Chemokine production by Ductal-like organoids in response to treatment with ethanol and LPS. Ductal-like organoids were treated with 100mM ethanol (EtOH) and 100ng/ml LPS for 24 hours. Supernatants were collected and chemokine production was assessed using a Proteome Profiler ™ Human Chemokine Array. Blots were measured using a ChemiDoc ™ MP Imaging System (A). Positive results for chemokines are labelled and control dots are indicated with a blue rectangle. Mean Pixel Intensity (MPI) was calculated relative to the average of control dots using FIJI image analysis software (B). Results were then displayed as fold change from untreated to treated MPI for positive results (C). n=1 for each condition, dotted line indicates no fold change.

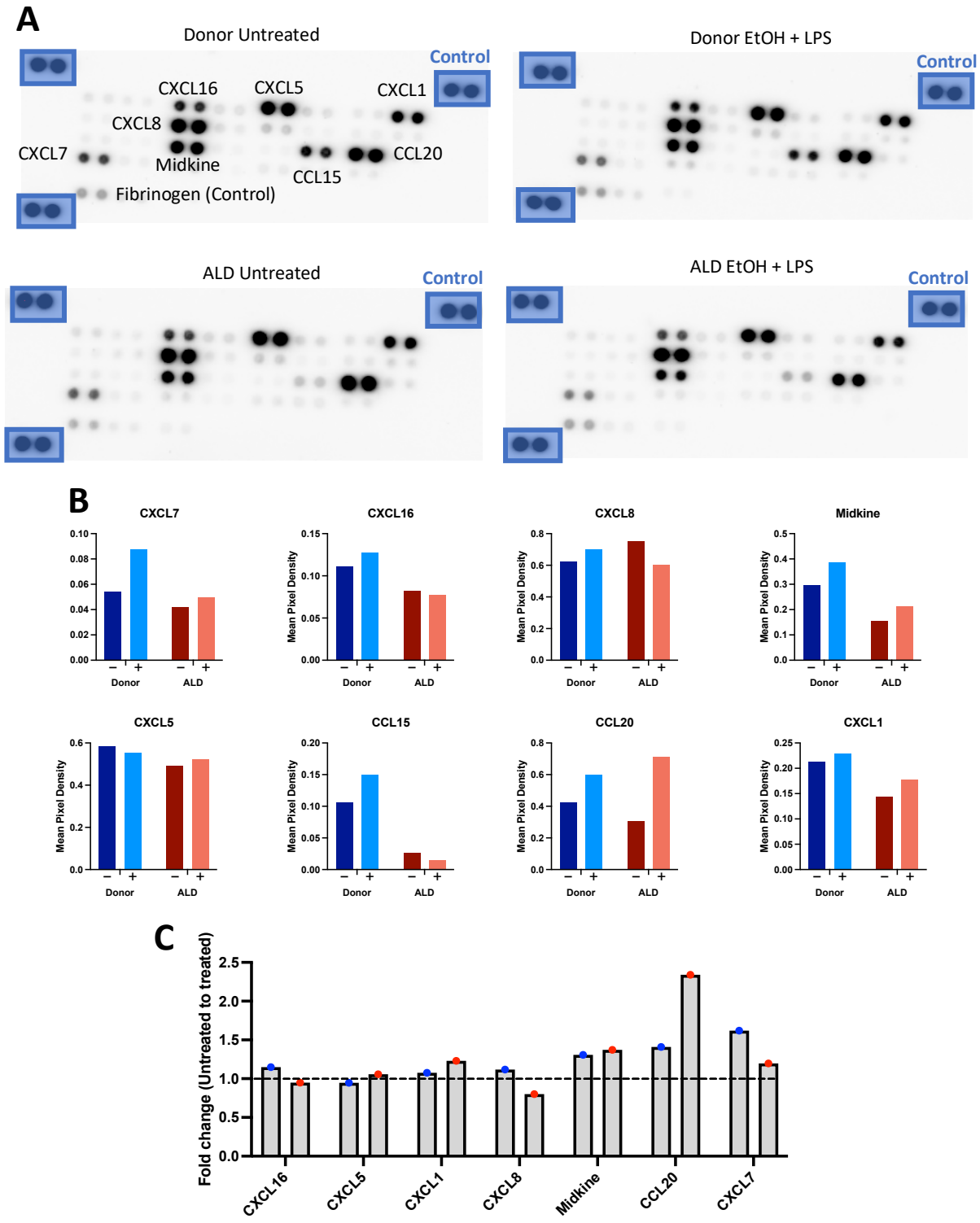


Figure 5.6: Chemokine production by hepatocyte-like organoids in response to treatment with ethanol and LPS. Hepatocyte-like organoids were treated with 100mM ethanol (EtOH) and 100ng/ml LPS for 24 hours. Supernatants were collected and chemokine production was assessed using a Proteome Profiler™ Human Chemokine Array. Blots were measured using a ChemiDoc™ MP Imaging System (A). Positive results for chemokines are labelled and control dots are indicated with a blue rectangle. Mean Pixel Intensity (MPI) was calculated relative to the average of control dots using FIJI image analysis software (B). Results were then displayed as fold change from untreated to treated MPI for positive results (C). n=1 for each condition, dotted line indicates no fold change.

As the proteome profiler assays are only semi-quantitative, I next wanted to assess the levels of IL-8 production in more detail (Figure 5.7). An IL-8 ELISA performed on organoid supernatants from multiple donors showed production of this chemokine in the range of nanograms per ml, which is similar to the levels seen in the plasma of patients with septic shock(360). In agreement with the proteome profiler data (Figure 5.5 and 5.6) production levels were similar between ALD and donor derived organoids, as well as between ductal and differentiated samples from the same patients. However, it was clear that interpatient variability was high.

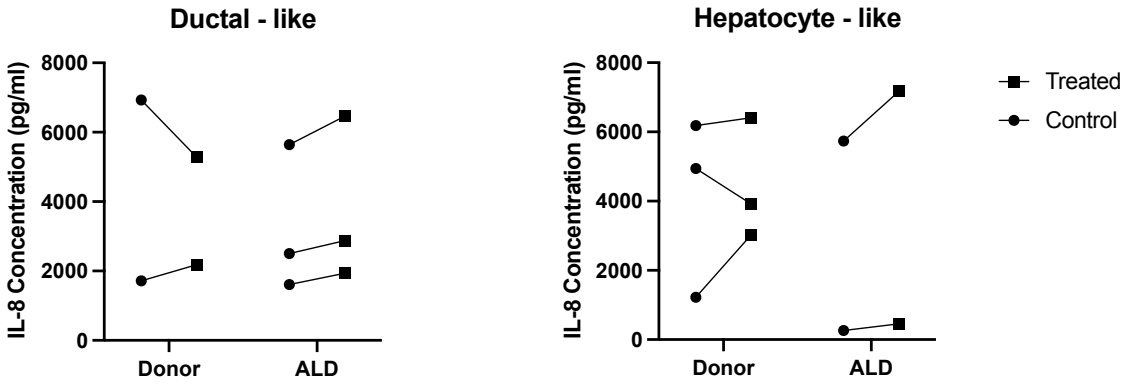


Figure 5.7: Both ductal and hepatocyte-like organoids produce IL-8 under basal and stimulated conditions. Ductal and hepatocyte-like organoids derived from both ALD and donor livers were treated for 24 hours with 100mM ethanol and 100ng/ml LPS. Supernatants were then collected and IL-8 concentration was measured using a Human IL-8/CXCL8 DuoSet® ELISA, and quantified using an IL-8 standard curve of known concentration. n=2-3 samples per condition with square symbols indicating matched treated samples.

I next wanted to assess whether the combination of ethanol and LPS was impacting expression of our phenotypic marker genes. Our initial investigations looked at ethanol only titrations and EpCAM expression in differentiated samples (Figure 5.2). I therefore compared expression of ductal markers such as EpCAM and Cytokeratin 19 alongside hepatocyte markers such as HNF4a and Albumin in organoids treated with both ethanol and LPS (Figure 5.8). There were no notable changes in expression after treatment of ductal or differentiated samples, alongside no changes in expression of CYP2E1 which supports our previous findings from separate patient cases in Figure 5.2. I also wanted to investigate whether the addition of ethanol and LPS was regulating TLR4 at the mRNA level. Whilst there was no change in response to treatment, relative expression was approximately 10-fold higher in hepatocyte-like organoids compared to ductal-like samples, indicating an increase with differentiation (Figure 5.8).

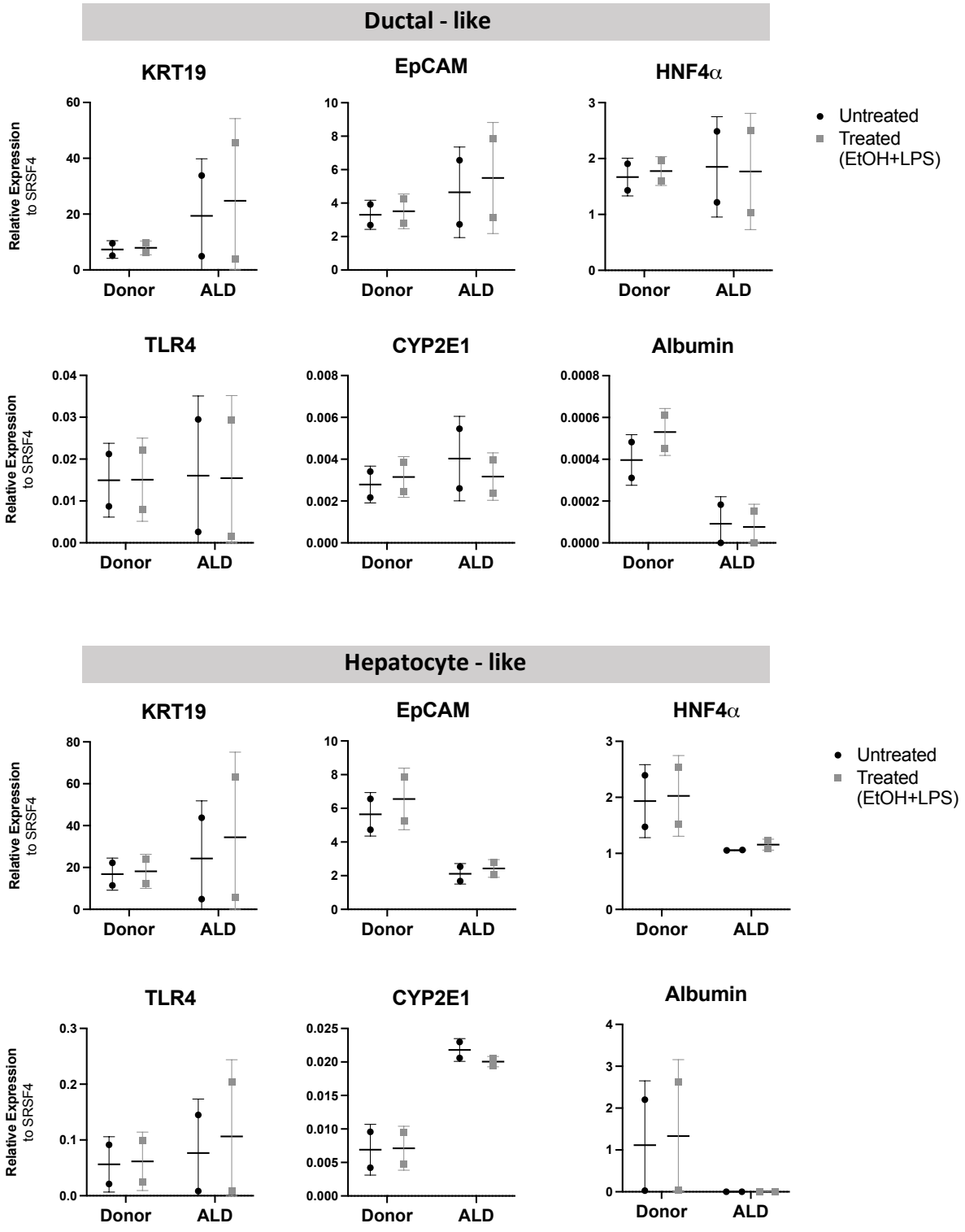


Figure 5.8: Acute treatment with ethanol and LPS does not cause changes to key organoid markers. Both ductal and hepatocyte-like organoids derived from donor and ALD livers were treated with 100mM ethanol (EtOH) and 100ng/ml LPS for 24 hours. Expression of key ductal and hepatocyte genes was assessed by qPCR and is displayed as mean relative expression to SRSF4 housekeeping gene ± SD. Values were generated from n=2 biological repeats for each condition, with square data points representing matched treated samples.

Given that I had observed that albumin expression was lower in differentiated ALD derived organoids than donor cells, and that there were differences in chemokine protein production between donor and cirrhotic cells, I wanted to perform a more detailed gene expression analysis. As part of a separate project, members of our lab were using a NanoString nCounter gene expression panel able to compare expression of over 700 genes in a dedicated fibrosis pathway set. Whilst many genes were perhaps less relevant for ductal cells and hepatocytes, the panel included a number of key inflammatory markers which would be helpful to assess the organoid response to ethanol and LPS treatment. I was therefore able to load RNA from a single matched set of donor and ALD differentiated organoids onto the kit as it was processed. Analysis of gene changes that were increased or decreased by a minimum of 2-fold showed a considerably reduced response in ALD organoids (2 changed genes) compared to donor derived organoids (80 changed genes) (Figure 5.9). Alongside this, many of the genes in the donor organoids increased or decreased by around 10-fold in response to treatment, compared to 2-fold in ALD. The most downregulated genes in the donor cells included NOTCH3 (associated with development), CETP (involved in lipoprotein transport) and MMP3 (associated with ECM breakdown). The most highly upregulated genes in the donor cells were the adhesion molecule VCAM-1, and LRP2 (associated with albumin binding). In contrast, only the classical complement binding protein C4BPA was downregulated and platelet activating factor receptor (PTAFR) was upregulated in ALD organoids after treatment (gene descriptions were investigated using the National Center for Biotechnology Information Gene Molecular Database(361)). Given the comparatively low response of ALD derived organoids we performed separate qPCR analysis to check for genes that would indicate cellular senescence (Figure 5.10). There was no significant difference in expression of P16 or P21 between donor

and ALD derived organoids at the ductal or differentiated stage, however there was an expected increase in both of these markers with differentiation.

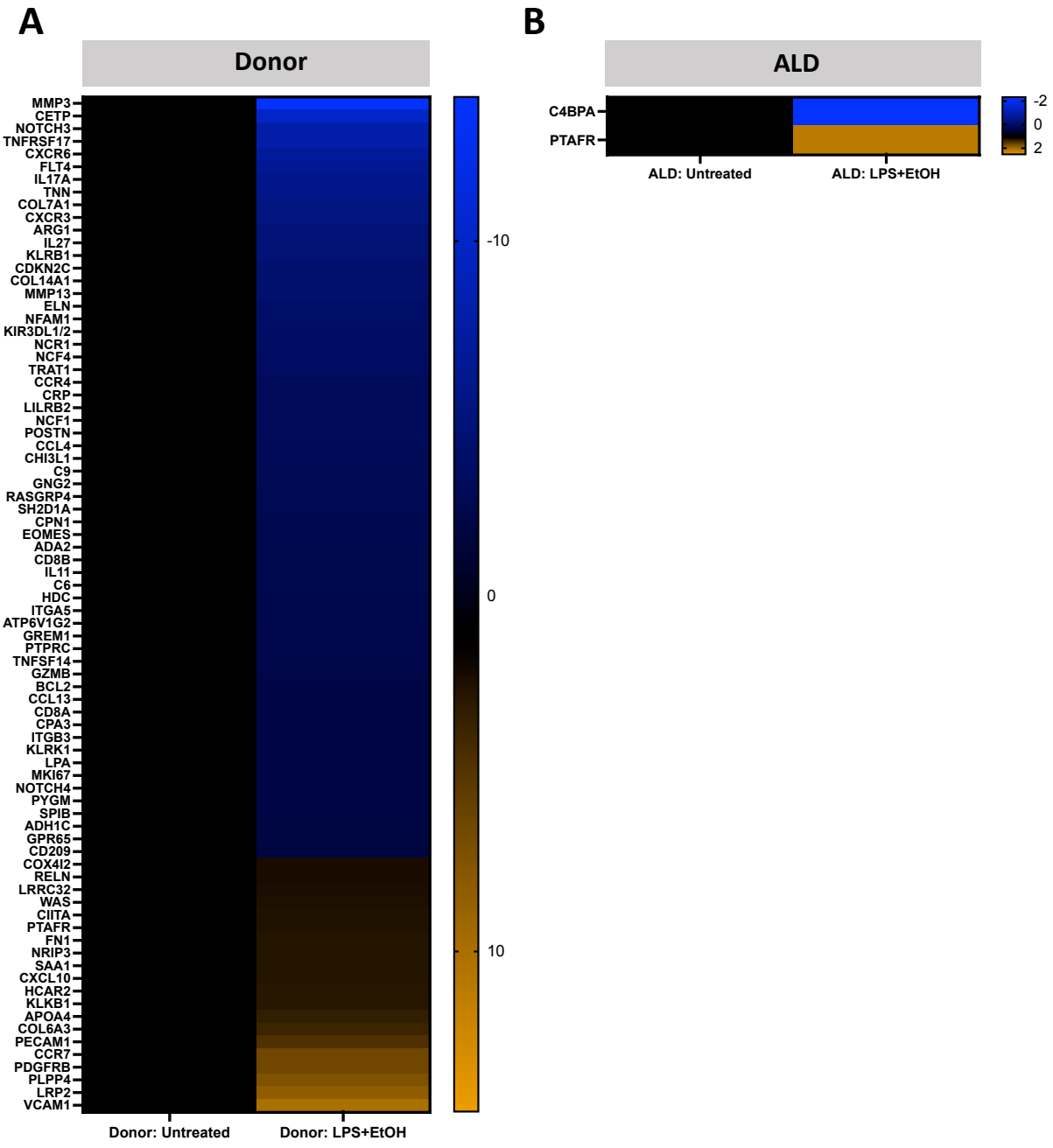


Figure 5.9: Donor liver derived organoids show a robust genomic response to treatment which is not recreated in cirrhotic liver derived organoids. RNA was extracted from differentiated hepatocyte-like organoids, RNA purity was assessed via TapeStation and samples were loaded onto a NanoString nCounter Fibrosis Panel by Ellie Northall. The panel was run by Birmingham Tissue Analytics and resulting data was analysed by Dr Emma Shepherd using nCounter software to investigate differential gene expression in response to treatment. Values were generated from n=1 set of donor (A) and ALD derived (B) hepatocyte-like organoids, with or without treatment with 100mM ethanol and 100ng/ml LPS for 24 hours, with minimum cut off of 2-fold gene change.

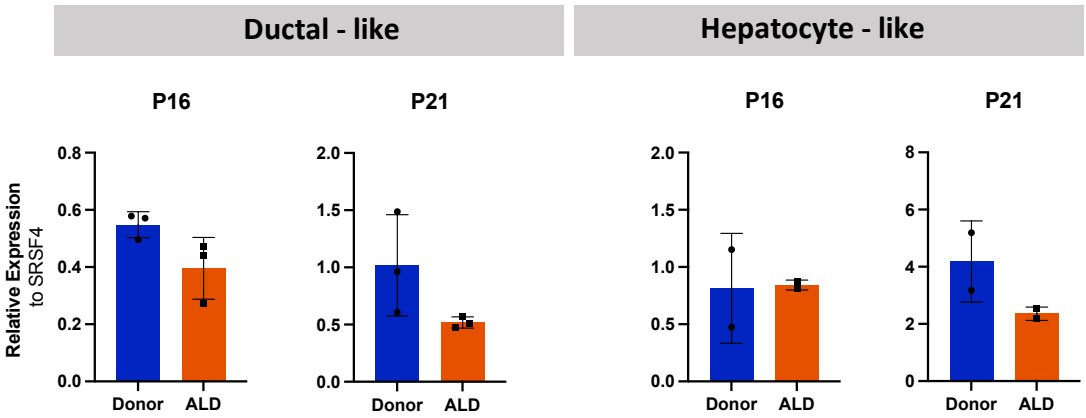


Figure 5.10: Diminished response to treatment is not due to increased senescence markers in ALD compared to donor derived organoids. Organoids were grown from both donor and ALD liver tissue, and RNA was isolated from both ductal and differentiated stage samples. Relative expression of P16 and P21 senescence markers were analysed using qPCR, and data is displayed as mean relative expression to SRSF4 housekeeping gene ± SD. Data points represent individual samples for n=2-3. Unpaired t test showed no significant difference between donor and ALD derived organoids.

One of the most significant contributions of the liver to immune function is the production of compliment proteins. These are essential to the function of the innate immune response, including the activation and recruitment of neutrophils(362). I therefore used a TaqMan® Array for the Human Complement Pathway to check for mRNA expression for a large number of complement proteins. As the array enabled investigation of three samples, I chose to look at expression in differentiated organoids from one ALD liver (both untreated and treated with 100mM ethanol and 100ng/ml LPS) and one donor liver (treated only) and saw expression of several key complement proteins (Figure 5.11). Overall, expression of most genes was higher in the donor sample, most notably for proteins C5 and C8A. MBL2 appeared to be expressed in treated but not untreated ALD organoids, and slight changes with treatment were also seen in C2, C3, Complement Factor B (CFB), and Complement factor D (CFD). We did not see any expression of C1Q, C6, C7, C8B, C8G, C9 or MASP2.

Based on these results, I chose the proteins C3, C5, C8 and MBL2 to pursue and assess their expression in different conditions (Figure 5.12). Both C3 and C8 showed no or extremely low expression in ductal organoids but increased notably with differentiation, whereas levels of C5 were similar in both ductal and hepatocyte-like samples, and C8 appeared to be slightly lower in ALD derived differentiated organoids. Interestingly, while expression in ALD organoids was lower for most proteins (in line with our previous findings), expression of C3 was considerably higher in differentiated organoids derived from diseased livers. Overall treatment with LPS and ethanol does not seem to alter expression of any of the complement proteins investigated above untreated levels.

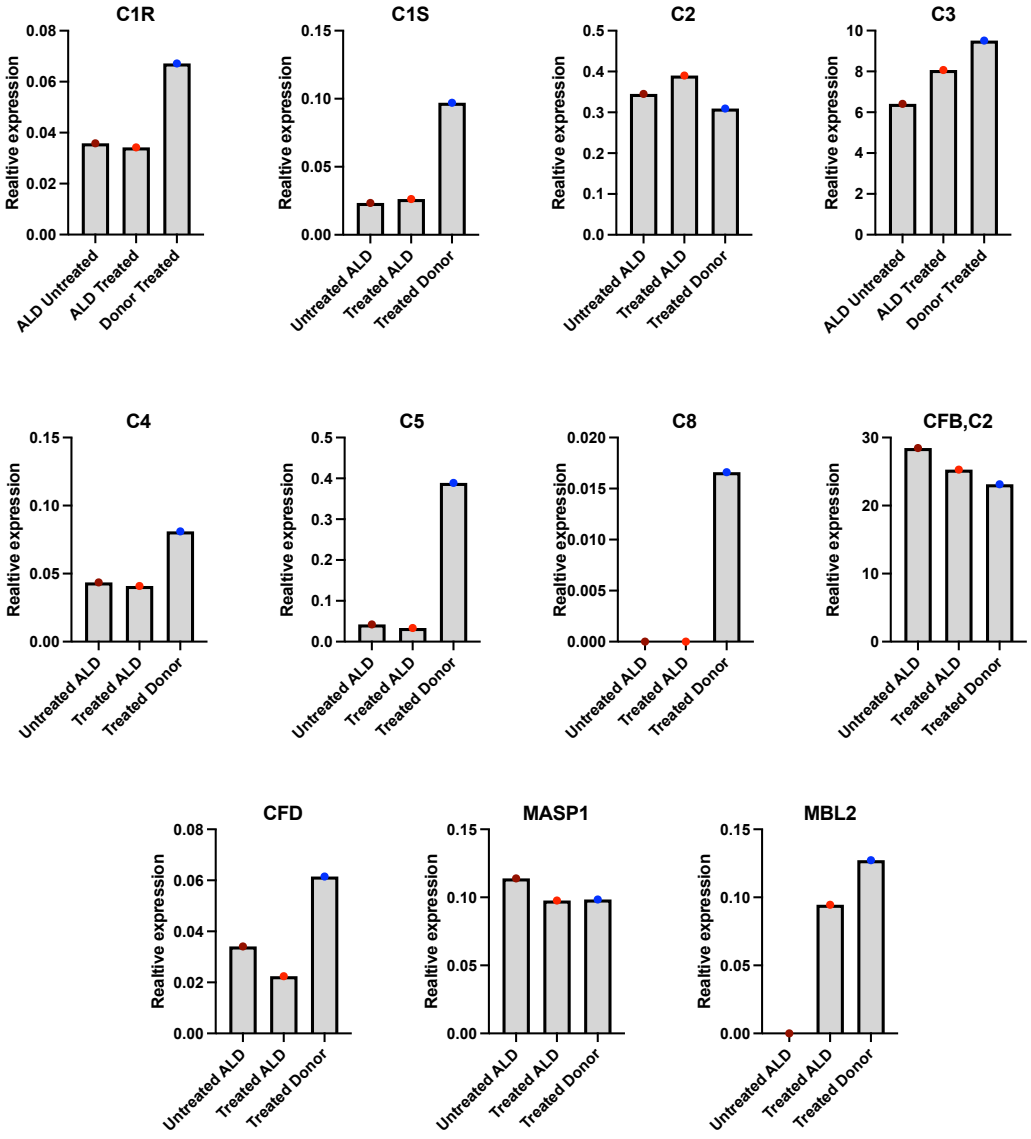


Figure 5.11: Differentiated organoids express the genes for several complement proteins. Differentiated organoids from both ALD and donor livers were treated for 24 hours with 100mM ethanol and 100ng/ml LPS. Expression of indicated complement genes was then investigated by qPCR using a TaqMan® Array for the Human Complement Pathway on matched untreated and treated ALD samples, and a single treated donor sample. Data points are relative expression to TBP for n=1 biological and technical repeat.

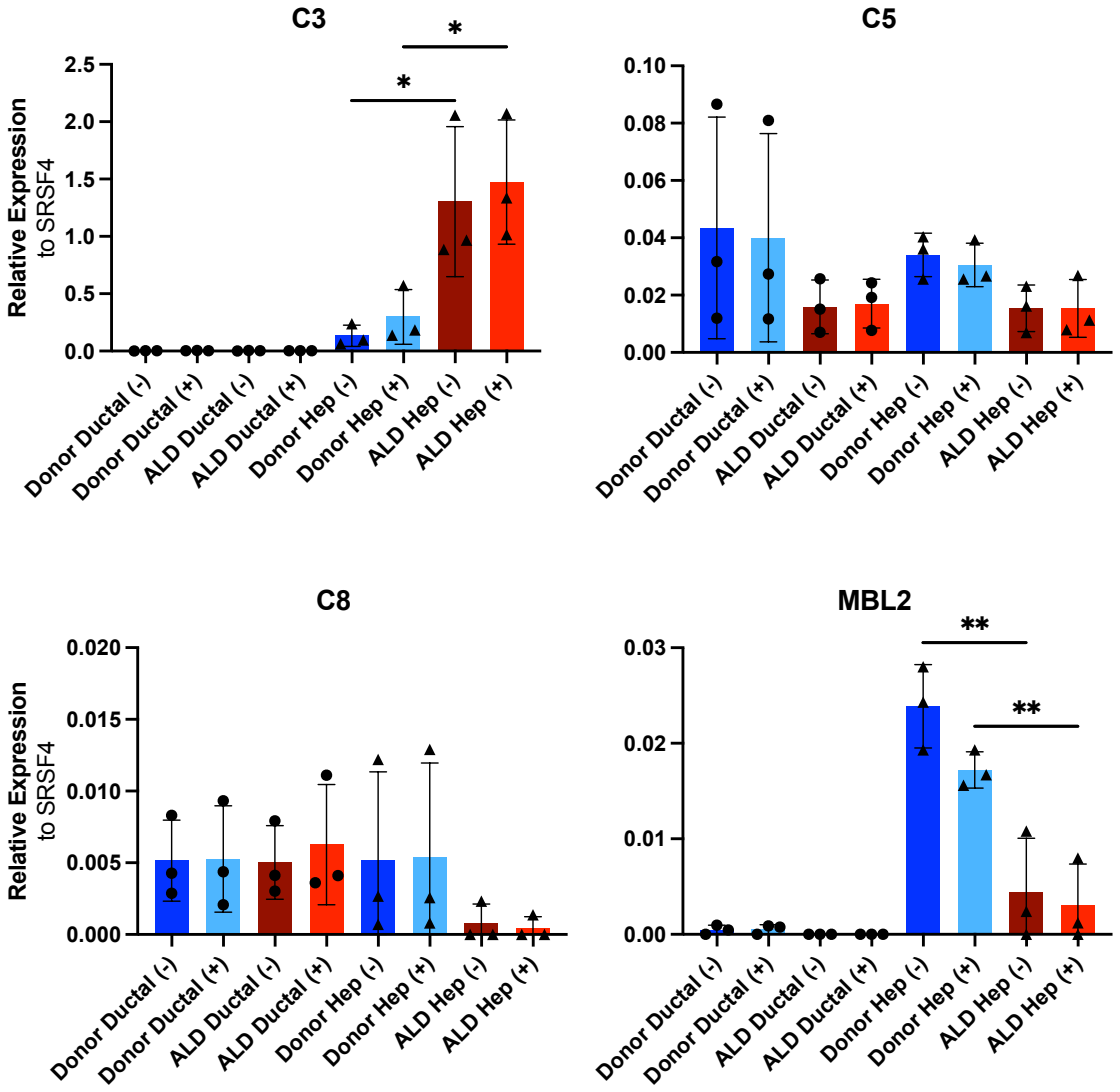


Figure 5.12: Organoid expression of complement proteins changes with differentiation and is altered in disease. Both ductal and hepatocyte-like (Hep) organoids derived from donor and ALD livers were treated with 100mM ethanol (EtOH) and 100ng/ml LPS for 24 hours. Values were generated from n=3 samples per condition with (+) or without (-) treatment, with triangular data points indicating differentiated samples. Expression of indicated complement genes was assessed by qPCR and is displayed as mean relative expression to SRSF4 housekeeping gene ±SD. Statistical comparison of relative expression was performed using unpaired t-test where P values are P≤0.05 (*), P≤0.01 (**).

5.2.3 Do supernatants from hepatic organoids influence neutrophil function?

Following on from the results of the chemokine profiler shown in Figures 5.5 and 5.6, it was suspected that organoid supernatant would act as a chemoattractant. This was confirmed using a CytoSelect™ 96 well migration assay, which allowed semi-quantitative measurement of neutrophil migration based on total DNA from lysed migrated cells. We demonstrated that isolated neutrophils from healthy donors migrated an average of approximately 5-fold more towards organoid supernatant (Figure 5.13B) when compared to media controls. As highlighted previously, organoid cultures were not controlled for cell number, however normalising fold change in chemotaxis to total protein per well of organoids did not alter the outcome of this analysis (data not shown). Pilot experiments with neutrophil-organoid co-culture also suggest a potential for neutrophil migration into organoids. Confocal microscopy was used to assess whether labelled neutrophils could migrate into organoids resident within the Matrigel support. Figure 5.13C suggests possible migration of isolated donor neutrophils (blue) into a ductal organoid in culture (yellow).

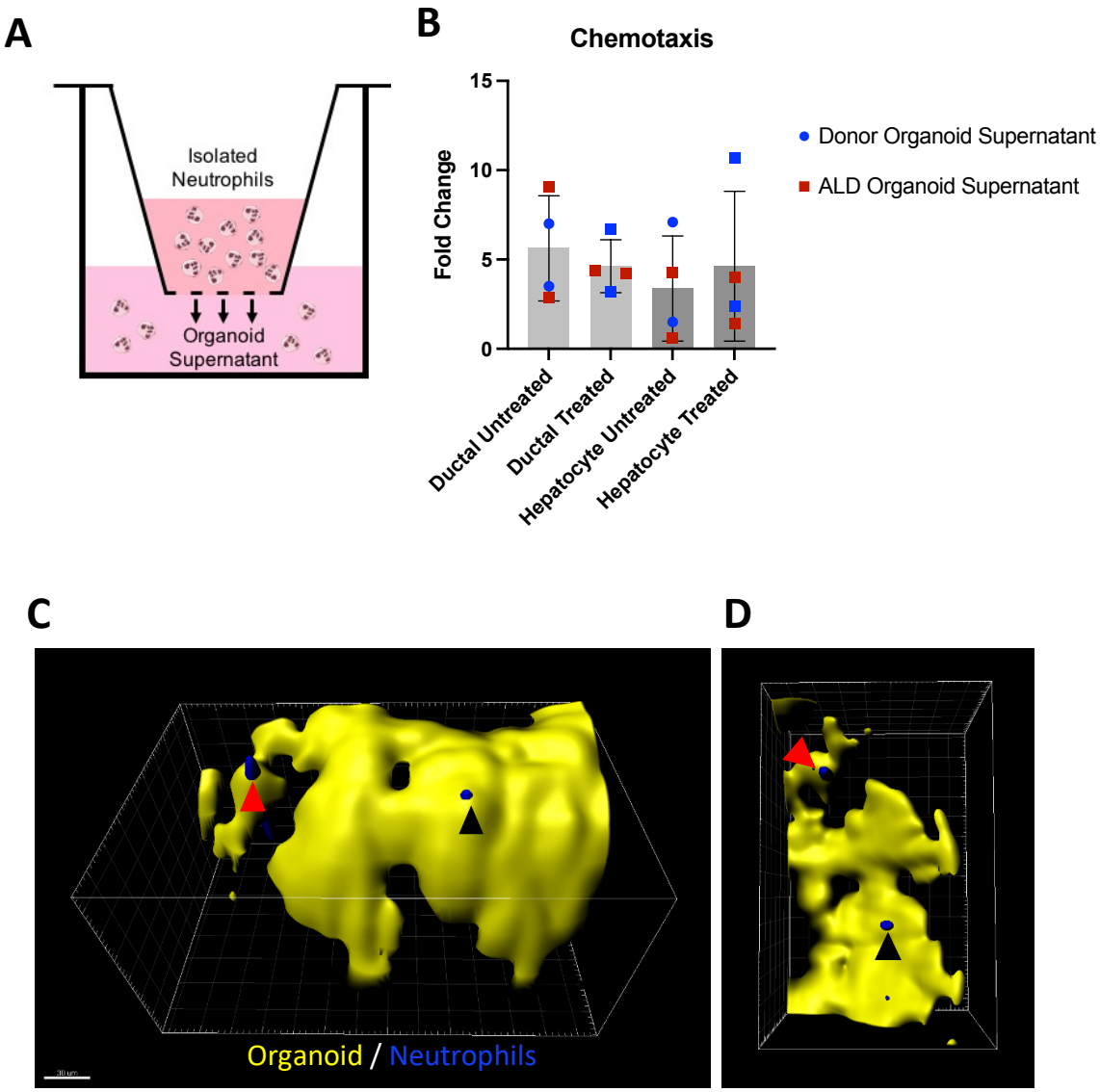


Figure 5.13: Organoids are able to induce neutrophil chemotaxis. Blood from healthy volunteers was collected into EDTA containing vacutainers and neutrophils were isolated using a density gradient. Neutrophil migration was then assessed using a CytoSelect™ cell migration assay. Cells were incubated for 2 hours on top of a 3-micron semi-permeable membrane above supernatants (A) from donor and ALD derived organoids, both in ductal-like and hepatocyte-like stages of development, with or without treatment with 100mM ethanol and 100ng/ml LPS for 24 hours. Migration was quantified by lysing cells that had passed through the membrane, staining with a fluorescent DNA dye and measuring using a fluorescent plate reader (B). Data was generated from n=2 blood donors and is presented as fold change in migration from treatment-matched control medium ± SD, where data points differentiate between donor (blue circle) and ALD (red square) samples. Isolated neutrophils (blue) were also stained using CellTracker™ Dye and incubated for 1 hour 30 minutes with ductal organoids in culture stained with DRAQ5™ Fluorescent Probe Solution (yellow). Organoids were then imaged using a ZEISS LSM880 confocal microscope, and 3D images were rendered using Imaris software by Dr Scott Davies (C-D) to show neutrophil location. Red and black arrows indicate the same neutrophils viewed from outside (C) and inside (D) the organoid.

It was also important to understand whether organoid supernatant altered the antimicrobial functions of neutrophils. As demonstrated in Chapter 3**,** neutrophil phenotype and function is altered in both chronic and acute alcohol injury. There is also significant recruitment to the liver in alcoholic hepatitis that is not seen in donor or chronically diseased liver tissue (Figure 3.13). I have already demonstrated that my organoids produce chemotactic factors which are known to influence neutrophil recruitment (Figure 5.5-6), so my next step was to investigate the effect of organoid supernatant on a range of neutrophil functions.

I began by using the PHAGOTEST kit to determine the ability of neutrophils to phagocytose fluorescently labelled *E. coli*. I have previously shown that there is a significant reduction in phagocytic capacity in peripheral patient neutrophils compared to healthy donors (Figure 3.6). Here I found that incubation with supernatants from differentiated ALD organoids did not alter phagocytic capacity of healthy donor neutrophils (Figure 5.14). Mean Fluorescence Intensity (MFI) values were similar for cells exposed to media alone vs supernatants from treated or untreated cells.

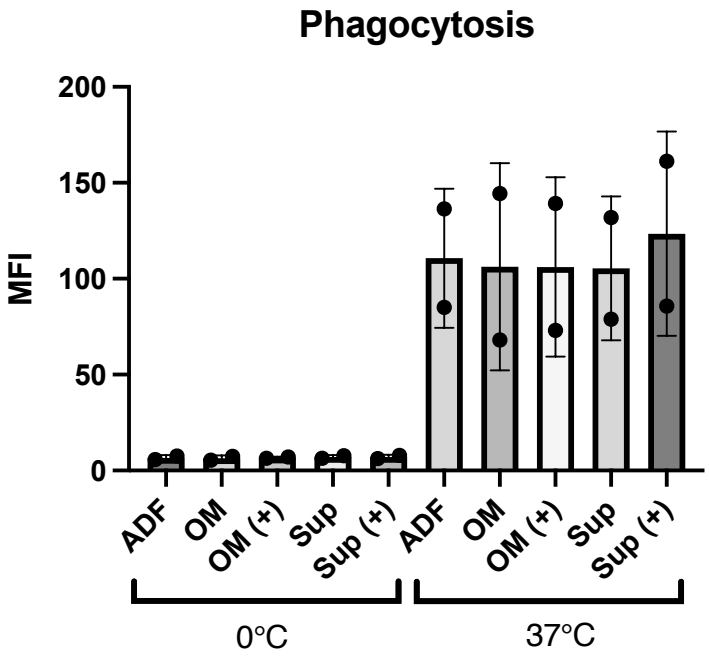


Figure 5.14: Neutrophil phagocytosis is not altered by incubation with basal or conditioned organoid medium. Blood from healthy volunteers was collected in heparin containing vacutainers and diluted 1:1 with either; Advanced DMEM F/12 (ADF), organoid media (OM), organoid media with the addition of 100mM ethanol and 100ng/ml LPS (OM+), or supernatant from a set of differentiated ALD derived organoids with (Sup+) or without (Sup) 24 hour treatment with ethanol and LPS. Samples were incubated for 3 hours at 37℃ and then phagocytosis was investigated using the PHAGOTEST kit. Opsonised and fluorescently labelled E.coli was added for 10 minutes at 37℃, followed by quenching of any non-phagocytosed external bacteria. Mean fluorescence Intensity (MFI) of the neutrophils in each condition was then measured using a CyAn™ ADP Analyzer to quantify the level of phagocytosed bacteria. Data was generated from n=2 blood donors and is presented as ± SD alongside 0℃ control samples.

Finally, I performed NETosis assays by incubating isolated neutrophils from healthy donors and AH patients with ductal and differentiated organoid supernatants, derived from donor and ALD livers. Strikingly, supernatants from ductal organoids were able to induce an average of approximately 9-fold increase in NETosis in healthy donor neutrophils, compared to very minimal responses from differentiated organoids (Figure 5.15). While this difference was significant in experiments testing healthy neutrophils, this was not the case when tested on neutrophils derived from patients with alcoholic hepatitis, despite similarly dramatic differences between ductal and hepatocyte-like supernatants. The impact of ductal supernatants was similar for both donor and ALD derived organoids with a slight trend for increased activity of the ALD supernatants, although samples were not normalised for cell number. Total protein measurements per well showed that the differences between ductal and differentiated supernatant was not due to organoid number as the notable difference in NETosis was seen even when total protein values were similar between both ductal and hepatocyte-like samples. As with previous experiments, we saw no additional response after treatment with LPS and ethanol, and have displayed the response to treated samples in Figure 5.15.

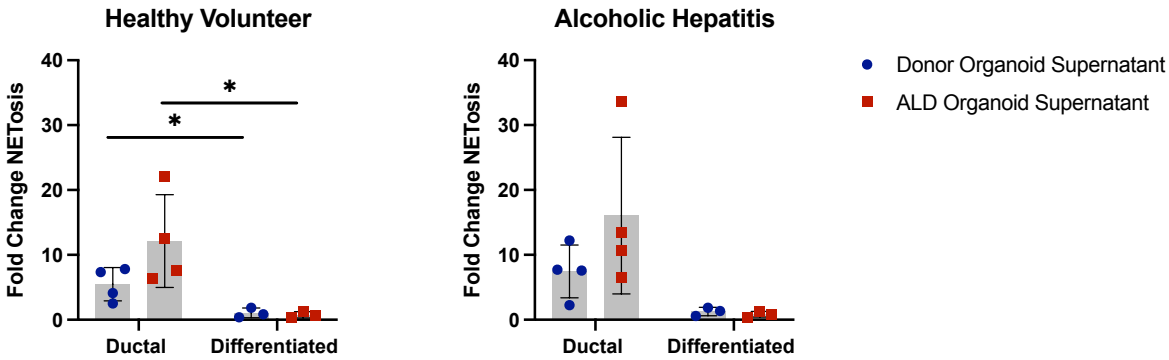


Figure 5.15: Ductal - but not hepatocyte-like - organoids induce NETosis in healthy and diseased human neutrophils. Blood from healthy volunteers and patients with alcoholic hepatitis was collected into EDTA containing blood tubes, and primary neutrophils were isolated using a density gradient. Cells were resuspended in supernatants from ductal and hepatocyte-like (differentiated) organoids, derived from both donor and ALD livers, which had been treated for 24 hours with 100mM ethanol and 100ng/ml LPS. Neutrophils and supernatant were incubated at 37℃ for 3 hours, and extracellular DNA was stained using SYTOX™ Green as an indicator of NETosis. Total fluorescence was quantified using a BioTek Synergy™ 2 fluorescent plate reader. Data was generated from n=3-4 blood donors per condition, each incubated with supernatants from organoids derived from different ALD and donor livers. Data points represent fold change in fluorescence from treatment matched medium controls ± SD. Statistical comparison was performed using unpaired t-test where P values are P≤0.05 (*).

5.3 Discussion

5.3.1 Alcohol metabolism

One of our first questions was whether our organoids would be responsive to ethanol. In the previous chapter, we demonstrated organoid expression of CYP2E1 and ADH1A which suggested there may be a functional ability to metabolise alcohol. Interestingly, we did not see mRNA expression of ADH1B in our initial testing, and therefore did not continue to look for expression of this marker. In hindsight, further investigation should be performed as polymorphisms in ADH1B are associated with a significant reduction in susceptibility to AUD and reduced alcohol intake(363). If the genetic phenotype in organoids derived from these livers is retained as suggested in the literature(214), this could become a valuable tool when investigating genetic contributions to AUD when compared to expression in donor livers and other chronic liver diseases. As initial testing was done on ALD derived samples, we may have also missed potential expression differences when compared to donor livers. Conversely, if this gene is not expressed at all in organoids, then we are missing an influential component of the ethanol metabolic pathway. Moving forward, matched gene expression experiments should be completed on both organoids and the whole tissue samples from which they were derived. This would give valuable context to our gene expression data and help to confirm whether we were replicating patterns seen *in vivo,* although in this instance the influence of other cell types should be considered and comparisons to isolated PHH used as an additional control.

Based on *in vivo* function, we might expect an increase in CYP2E1 expression with ethanol treatment, but see either no significant change or a reduction in differentiated organoids. As

mentioned previously, changes in CYP2E1 expression are less informative at the mRNA level as it is largely regulated post-translationally(332). Understanding expression at the protein level in this model could therefore offer more explanation as to how this enzyme is responding to treatments. Overall, CYP2E1 expression is 10-20 fold higher in chronic drinkers(159), and this may be recapitulated in organoids with a longer term ethanol treatment. We see inconsistent results as to whether CYP2E1 expression is higher or lower in our ALD derived organoids, which could be due to a number of factors. We may not be capturing the increased expression seen in chronic drinkers as patients who have been transplanted for ALD have been abstinent for at least 6 months. The changes in this group compared to those with active alcohol injury are demonstrated by the differences in peripheral blood biochemistry and cell counts shown in Chapter 3.

Overall, we see surprisingly few changes in the organoids in response to ethanol treatment. It is unclear whether this is due to over or under exposure, or other factors entirely, and there is evidence that ethanol induced gene changes in 2D HepG2 cultures were widespread but minimal (364). The notable reduction in general gene expression with a double dose of 200mM ethanol suggests more extreme cell toxicity, and is in keeping with literature suggesting doses over 100mM are cytotoxic(365). Our initial testing showed a dose response in ALD derived ductal organoids that was not reflected in matched differentiated samples. Brief investigations were completed at 5mM doses based on the data from ductal organoids, but this was inconclusive and did not suggest that lower doses induced a more significant response. There were also additional concerns regarding evaporation and potentially reduced cell exposure due to the Matrigel, therefore we selected a 100mM ethanol treatment, which

has also been utilised in several other studies of 3D liver models(366-368). Alongside the dose, the timing of our treatments may mean we are missing key responses. Several of these studies treat samples over several days, and this more "chronic" injury may be required to see significant changes in expression. Based on our results and the alcohol consumption patterns often seen in patients who present with AH, a more representative alcohol injury should perhaps include a lower dose injury over several days, followed by a more acute injury using high dose ethanol. The equivalent blood alcohol levels for a 100mM ethanol dose are extremely high and are associated with patients becoming comatose and death (greater than 400mg/dL). However, blood alcohol levels within this range are seen more regularly in those with AUD, and these patients show a level of tolerance that leads to fewer signs of intoxication(369). As shown in Chapter 3, our AH patients consumed an average of 176.5 units per week with the highest value being over 400, compared to the recommended 14 units per week. Our dosing, while high, is representative of concentrations seen in our patient cohorts. Conversely, while a more chronic injury model could be key, we may also be missing the more "acute" damage responses by collecting samples 24 hours after high concentration ethanol exposure. Measuring responses and cytokine production over several shorter time points could offer insight into the organoid inflammatory response to alcohol injury.

Another interesting consideration for why we see a lack of response in hepatocyte-like organoids is the possible de-differentiation of our cells. There is evidence that ethanol exposure significantly changes lineage and increases stem cell marker expression in gut derived organoids(370). It is important for us to acknowledge that expansion of these ductular reactions is initiated by liver injury *in vivo*, and that there is potential that by causing damage

to these highly plastic cells, especially “differentiated” ones, we may well be seeing a shift in phenotype that we haven’t characterised. When investigating stability of expression of key markers such as EpCAM and Albumin in treated cells, we see no changes that would suggest dedifferentiation. However, this is far from an extensive assessment of phenotype, and knowing whether ethanol treatment is reverting cells to a more progenitor-like phenotype is important for understanding how well we are replicating alcohol injury. It may also be that while we see signs of differentiation, we have not pushed these cells into a full hepatocyte-like phenotype. When investigating the phenomenon of hepatic progenitor cells differentiating into hepatocytes in liver “buds”, Stueck *et al* described progressive differentiation that resulted in a reduction of EpCAM and Cytokeratin 19 expression – markers that were still present in our hepatocyte like cells(371). It may be that while we have taken advantage of the potential for these cells to differentiate into hepatocyte-like cells, we have not managed to induce this change completely.

What these results show overall is that this model would benefit from a more conclusive marker of ethanol metabolism. Measuring acetaldehyde is complex, due to residual levels in many common lab reagents and high volatility. It is most commonly measured using Headspace gas chromatography (HS-GC) and reverse phase high-performance liquid chromatography (RP-HPLC), which is not easily translatable for our model(372). Work in lung epithelial cells has shown promise of a fluorescent probe which can indicate conversion of ethanol to acetaldehyde(373). More crudely, frequent time point measurements of ethanol concentration within wells may give an indication of ethanol metabolism, as long as evaporation was suitably controlled for. As we indicated in Chapter 4, our differentiated

organoids are capable of accumulating lipids. Therefore, the use of lipid dyes on treated organoids may also offer insight as to whether alcohol was being metabolised this way. A pilot study of this experiment was inconclusive, but could potentially be more effective with a longer-term ethanol treatment as explained above. While we saw an increase in ADK with treatment in some samples in our cell damage assay, which implies ethanol and LPS exposure could induce injury, these levels are not consistent and in many cases are surprisingly low. While the assay used does state that cryopreserved samples are suitable, the storage time of our samples was not consistent and repeating this assay on fresh supernatants could help to confirm injury responses.

It is well established that 3D culture improves how well liver cells replicate *in vivo* function(374), but understanding whether we are achieving the level of sensitivity required to justify complex and expensive organoid technology over other 3D models is important going forward. More clinically relevant measures of injury, such as the production of liver enzymes ALT and AST, would help us to establish whether we see the same patterns of injury in this model as in our patients. Low organoid cell number meant that these outputs were not measurable by traditional clinical equipment, so other technologies should be considered going forward.

5.3.2 Inflammatory responses to injury

When investigating production of chemokines in response to treatment with ethanol and LPS, we see a baseline production of many chemokines but surprisingly small change in both ductal and differentiated organoid supernatants once exposed to alcohol. Experiments investigating

the production of IL-8 by LPS stimulated human intrahepatic biliary epithelial cells (HIBECs) showed constitutive IL-8 production which did not change with LPS treatment, but did show induction of IL-6 and MCP-1(375) – interestingly, a different study showed increased gene expression and cytokine production of IL-8 in HIBEC with a 10-fold higher LPS treatment(376). However, our findings were in keeping with similar experiments completed by Aguilar-Bravo *et al* on ductal organoids derived from ARLD livers(52). When measuring gene expression changes for cytokines such as CXCL1, CXCL5 and CXCL20, they also showed that LPS alone does not induce any change, whereas a significant increase was seen with TNFα and IL-1β stimulation(52). Alongside this, they also showed that neutrophil conditioned media did change the inflammatory profile of their organoids, and this was increased significantly if the neutrophils had been activated with LPS(52). This paper not only supports our findings that responses to LPS were minimal, but also that our planned co-culture model utilising liver tissue and peripheral neutrophils from both donor and ARLD patients has potential. It is surprising additional treatment with ethanol alongside the LPS did not have an additive effect, but this could be for a number of reasons including insufficient ethanol metabolism. Investigating the influence of neutrophil conditioned media on this model should be an important next step in this project.

Before treating with LPS we demonstrated expression of TLR4 in our ductal and differentiated organoids. In Chapter 3 we show that IHC staining for TLR4 appears to be higher in cholangiocytes than hepatocytes, however in our organoid model we see an increase in TLR4 at an mRNA level with differentiation to a more hepatocyte-like phenotype. This reassures that lack of response to LPS is not due to absence of receptor, at least at the mRNA level.

Further investigation into the TLR4 pathway in this model and how this corresponds to ductular reactions *in vivo* could offer interesting insight into the increased sensitivity to gut antigen exposure in patients with ARLD. TLR4 ablation has been shown to protect against alcohol induced fatty liver disease in animal models(313), and understanding the impact of this pathway on injury is an important piece of the puzzle when investigating the immunocompromised phenotype in ARLD patients. Adopting the organoid gene editing techniques discussed in Chapter 6 could also provide an opportunity to see if TLR4 ablation is also protective in human 3D cell culture models. Furthermore, while TLR4 expression at the mRNA level does not change with LPS exposure, TLR2 expression has been shown to increase in response to inflammatory stimuli(377). This could therefore be an interesting target to investigate moving forward with regards to TLR responses in human hepatic organoids.

It is clear that the organoid cultures are producing a large number of chemotactic and potentially inflammatory cytokines even without injury. As our focus was on neutrophil chemotaxis, we chose to focus on IL-8 for quantification as this is an established neutrophil chemoattractant and has been associated with neutrophil infiltration around bile ductules(376). However, other factors in the organoid supernatant such as Groα and CXCL5 are all strongly associated with neutrophil activation and chemotaxis(378, 379). The production of these factors is also in keeping with the findings of Aguilar-Bravo *et al*, which further suggests potential for organoid responsiveness to immune stimuli(52). Interestingly, we only saw expression of CCL15 in one sample (differentiated donor). This chemokine has a number of associations with HCC, including the recruitment of suppressive monocytes(380) .

While it was not further pursued in this study, this could also be an interesting marker to investigate in organoid samples in the context of immune-liver crosstalk.

We have seen several indications that ALD derived organoids are not as responsive as those from donor livers. I had the opportunity to include a single sample from each differentiated organoid condition on a NanoString nCounter Fibrosis Panel. The analysis of this work was completed by Dr. Emma Shepherd, and shows a distinct difference in responsiveness from ALD and donor derived organoids. Importantly, with only a single sample it is essential to be cautious regarding conclusions drawn from the individual gene changes, however these results do support our earlier findings of lower expression of genes such as albumin in organoids derived from cirrhotic liver. What this also highlights is the importance of a much wider investigation into organoid gene expression. This will be discussed further in Chapters 6 and 7, but it is clear that with our limited qPCR panel we are potentially missing many different genes and pathways of interest.

The seemingly reduced responsiveness of ALD organoids prompted an investigation into cell cycle inhibitors P16 and P21, which are commonly used as a marker of cell senescence *in vitro*(381). We show in Chapter 3 that P16 is significantly upregulated in ALD liver tissue, but see no differences between donor and ALD derived organoids in ductal or differentiated states. The notable increase in expression of these markers with differentiation is in keeping with transition to a more quiescent hepatocyte-like cell type. There are a number of ways to investigate cell senescence *in vitro*(382) and baseline expression of P16 and P21 does not give a definitive answer as to whether this is influencing organoid behaviour. We did not pursue

this further due to the challenges of adapting assays to the organoid model, but in the context of these markers we do not see altered expression levels in cells derived from cirrhotic livers.

As highlighted in the introduction, the liver is responsible for a majority of complement protein production(82). Expression of these proteins at the mRNA level in our organoids is an exciting finding that supports both hepatocyte function and the potential for their use in immune-liver crosstalk studies. The initial array showed expression of a majority of liver derived complement proteins, but C3, C5, C8 and MBL2 were chosen to be investigated in more detail due to their interesting patterns in expression and appearance in the literature. When studied in further detail, the differences we see between donor and ALD derived organoids are mixed with regards to replicating other published studies. C3 appears to be notably higher in our ALD derived organoids, and high serum levels of C3a (the activated form of C3) has been associated with liver damage and steatosis in patients with high alcohol consumption(383). Conversely, in patients with NASH there is an inverse correlation between circulating C3 and clinical scores for liver cirrhosis(384). Studies utilising C3 knockout mice have also shown this protein to contribute to ethanol induced liver injury(385, 386). Alongside this, reduction in production of MBL in a cohort of cirrhotic patients was associated with increased infection risk(387). Reliable expression of these proteins at the mRNA level is promising, but as complement components circulate in an inactive state *in vivo* it is important for us to determine whether we can induce activation in produced proteins and see functional activity. In biopsies from patients with AH, C1q, C3 and C5 expression was shown to be increased when analysed by IHC, but only C1q and C5 showed increases by qPCR(388). This further emphasises the importance of measuring complement production at the protein level,

and also the potential changes we could induce in these proteins with optimised injury models.

A large proportion of complement components are also produced by immune cells(389). These cells also express a range of complement receptors, and their response to complement activation is integral to the acute phase response. Regarding neutrophils in particular, the alternative pathway acts as a positive feedback loop for neutrophil activation(390), and rodent C3 knockout models have demonstrated reduced neutrophil infiltration and activation in cholestatic liver injury(391). Furthermore, neutrophils are a significant contributor to serum levels of C7(392). There is evidence that circulating levels of C7 are an effective marker of fibrosis in NASH(393), and this could therefore be an interesting marker to investigate in our ARLD cohorts. A recent study investigating circulating complement proteins in patients with AH showed a significant alteration in disease, and highlighted how these findings could have diagnostic and prognostic value(394). This further emphasises the importance of understanding the influence of the complement pathway in our model, and in ARLD overall. These proteins could potentially act as a novel biomarker or therapeutic target in ARLD, and their expression in our organoids shows promise as a tool to investigate their mechanisms in disease.

5.3.3 Neutrophil – liver crosstalk

The changes in neutrophil number, function, and infiltration that we demonstrated in Chapter 3 are a key characteristic of acute liver injury. It is therefore essential that we understand whether this relationship can be replicated in our model, and if our “injured” organoids can

induce the neutrophil phenotype seen *in vivo*. Our next steps were therefore to try and recreate the results we had seen in peripheral blood neutrophils with exposure to our organoid supernatant. Initial investigations began looking at phagocytosis in isolated whole blood neutrophils. Based on our expectations of the model, this pilot data was collected after neutrophil incubation with differentiated ALD organoid supernatant as we believed this was likely to be the most activating condition. Now seeing our data collectively, it appears that not only are differentiated ALD organoids less responsive overall, but ductal-like organoids are potentially more pro-inflammatory. Considering our findings in the NETosis assays, it is likely that repeating these experiments with ductal supernatant may show a difference.

Our chemokine profilers strongly suggested that all of our organoid conditions would induce neutrophil migration due to production of chemoattractants such as IL-8. Reliably confirming this was challenging in common chemotaxis assays that utilise Transwells, due to low volumes of supernatant in organoid experiments (250μl/well). By utilising a commercial kit we were able to at least confirm that the supernatants were chemotactic compared to organoid medium alone, and that levels were similar across conditions as suggested by the proteome profilers. This assay did however have a number of limitations, including the fact that logistical limitations of multiple blood donors and conditions meant that repeats had to be completed over several days, whereas the equipment was designed to be single use. Leakage between wells on later repeats indicated that this had affected the functionality of the kit, so a number of results were excluded where this caused contamination between conditions. Furthermore, we were measuring the total fluorescence of DNA from lysed migrated cells rather than a total cell count, which could have been influenced by a number of factors such as NETosis early in

the assay and is therefore challenging to quantify. Overall, to fully understand the chemotactic effects of our organoids, it is essential to employ more sophisticated technology such as an Insall chamber(395). As our NETosis assays have shown production of NETs in response to ductal supernatants, being able to visualise migration in response to our stimuli would offer better insight into how this is affecting neutrophil behaviour. This would also offer more detail on differences when comparing responses of patient neutrophils to organoid supernatant, such as effect on directionality and efficiency of migration. What this assay did offer however is confirmation that organoids produce factors that are able to induce organoid migration, and that this avenue of investigation is worth pursuing in this model. The images taken of neutrophil migration into organoids in culture also suggest that they are able to potentially interact with organoids while they are still embedded in Matrigel, which offers interesting options for co-culture experiments moving forward. However, this was a single experiment and requires further validation. As discussed above and in more detail in Chapters 6 and 7, it is essential to consider how to incorporate neutrophils into this model to fully test responses to injurious stimuli.

There are a number of publications implicating interactions between neutrophils and cholangiocytes/ductular reactions in liver injury(52, 396), and the impact of ductal organoid supernatant on neutrophil NETosis is undoubtedly one of the most interesting findings of this project. We did not identify any notable differences between ductal and differentiated organoids in the Proteome Profiler, which would suggest that the increase in NETosis is not likely to be due to any of the cytokines listed. Alongside this, complement factors (with C3, C5 and C1q in particular) are associated with the induction of NETosis(397). When investigating

mRNA expression of C3 and C5, we saw almost no expression in ductal organoids, or expression similar to differentiated samples. One thing we are not capturing by qPCR is the functionality of the complement cascade, as complement factors usually circulate in an inactive state. The active form of C5 (C5a) has been used experimentally as an inducer of NETosis after neutrophil priming with interferon(398), and therefore emphasises the need to understand the context of the gene expression. In future experiments, it would beneficial to also consider the potential influence of extracellular vesicles (EVs) - membrane-bound carriers of cargo, released from cells as a form of intercellular communication(399). Recent studies have shown that the release of liver EVs after partial hepatectomy alters neutrophil phenotype and function(400), and liver derived EVs are able to induce NETosis in mouse models of *S. japonicum* infection(401). The production of EVs has already been studied in a number of organoid systems and extensively reviewed(402), and is an important mechanism to consider when analysing the crosstalk between liver organoids and neutrophils in co-culture.

In Chapter 3, I discussed technical issues we encountered with our NETosis assay. Considering these and the lower than expected responses seen to PMA treatment, it makes the influence of ductal organoid supernatant on NET production even more striking. Furthermore, as highlighted in the methodology ductal supernatants were added at a higher dilution than differentiated ones. Despite challenges in normalisation of cell number, comparisons between ductal and differentiated samples with similar levels of total protein retained this difference, which supports these results. However, lack of normalisation means it is not possible to draw conclusions between ALD and donor derived samples. While total protein measurements offer

some crude quantification of supernatant measurements, by varying cell number between experiments we are not ensuring consistency with regards to the severity of our injury. This is one of the most significant limitations of this project, and may mean that we are missing differences between samples derived from healthy and cirrhotic tissue. To some degree, the donor variation seen in organoid number and growth may be accounted for with higher sample number which could give a more reliable indication of changes, however our low number of repeats makes it challenging to draw conclusions.

5.3.4 Conclusions

The results in this chapter raise several questions, and it is evident that our treatment protocol was not inducing responses that we might expect in organoid cultures. However, despite low sample numbers we show some promising data that can help guide improvisation of this model towards potential application in the investigation of neutrophil-liver crosstalk. We have confirmed that our organoids produce multiple chemokines and factors which could influence neutrophil recruitment and function even when unstimulated. The lack of response to injury may well reflect the lack of interplay between parenchymal cells and other stromal or immune cell components in our organoid models, or a need for improvement in the injury model itself. While the constraints of this project did not enable progression to co-culture, our neutrophil studies show promising results and the production of inflammatory cytokines and expression of complement protein genes by organoids suggest exciting potential for this model.

It is important however to understand whether the slight trend towards higher responsiveness in donor derived organoids is due to an inherent functional difference in

progenitor cells derived from cirrhotic tissue, a level of exhaustion due to disease or if we are potentially isolating a different cell subset that affects responses. Our challenges with organoid number normalisation and low biological repeats make drawing conclusions difficult. Total protein offered some way of showing that differences between ductal and hepatocyte-like samples were real and not just as an artefact of cell number, but there is a chance we are missing potential differences that are subtler between donor and ALD derived samples.

Chapter 6 – General Discussion

There is no doubt that the rising impact of liver disease in the UK demands progress in both our understanding of the condition and our ability to treat it. In recent years, there has been a notable increase in alcoholic liver disease in particular, with 2021 seeing the highest number of alcohol specific deaths since these records began in 2001(403). This project has utilised privileged access to human tissue and blood samples to try and develop a tool that can contribute towards this field, and hopefully in the future help to improve outcomes for patients. There are many limitations to the work that have been discussed throughout the previous results chapters, and combined with additional challenges due to the timing of this project we leave many questions unanswered. However, I believe that the pilot data we have generated shows the exciting potential of this model, along with key findings regarding the changes in peripheral immune response that further highlight the importance of understanding neutrophil-liver crosstalk in ARLD.

We were able to demonstrate altered phenotype and function of neutrophils in patients with ARLD. These were most pronounced in patients with alcoholic hepatitis (AH), where immature granulocyte number correlated with several markers of poor prognosis in liver disease. We successfully isolated, cultured and differentiated human liver organoids from both donor and ALD cirrhotic liver tissue, which demonstrated hepatocyte functions such as lipid storage. While many characteristics were similar between donor and diseased tissue, there were recurring findings that ALD derived organoids exhibited reduced function – be this in changes in response to differentiation or injury. Organoid responses to injury overall were lower than expected, but cultures generated a number of key chemokines and cytokines linked to

immune function, and express genes for a range of complement proteins. Ductal, but not hepatocyte-like, organoids significantly increased NETosis in human neutrophils – further supporting the potential for this tool to help us understand how alcoholic liver injury affects cell populations in the liver, which in turn may be altering the systemic immune environment.

6.1 Modelling ARLD *in vitro*: where do we stand?

As discussed in the introduction to this thesis, the argument for pursuing organoid technology despite its many challenges is that it captures elements of human disease that traditional *in vitro* cell culture models do not. Alongside this, it offers a potential alternative to rodent models which do not recreate many elements of human ARLD. As reviewed by Wilkin *et al*, careful selections must be made regarding mouse strain, alcohol administration method, length of model, age and sex in order to capture the element of ARLD that is of interest(404). In particular, chronic injury and fibrosis are difficult to recreate in murine models(405) (although there is progress in acute-on-chronic models(406)), whereas this organoid model provides the opportunity to culture cells directly from ALD cirrhotic tissue environment.

There is still a lot to be explored when studying organoids derived from primary human liver tissue, particularly in the context of alcohol injury. I have previously highlighted work by Aguilar-Bravo *et al* which utilises ductal organoids derived from ARLD patients, but does not involve additional alcohol injury(52). Impressive ALD organoid models have also been derived from primary human pluripotent stem cells which were differentiated into mature cholangiocyte and hepatocyte like cells *in vitro*, and even co-cultured with foetal liver mesenchymal cells. These organoid co-cultures exhibited impressive functional responses to

ethanol injury(366), but are not utilising the progenitor population within the liver and therefore not capturing potentially imprinted phenotypes from patient liver environments.

There are several indicators that our cells are able to perform the tasks we would expect from them *in vivo*. From expression of complement genes to the formation of lipid droplets, these results suggest that what we are growing and differentiating is able to perform the role of a hepatocyte. However, our functional testing is limited, and while we see gene changes that would reliably suggest that we are pushing our organoids to a more hepatocyte-like phenotype with differentiation, there is the question of how "hepatocyte-like" they really are. In the context of this project, this potentially plastic intermediate phenotype does have merit, because the push of progenitor cells into hepatocyte-like and ductal-like cells is a hallmark of liver disease and injury(43). The ductular reactions that appear so frequently in injured liver tissue (as demonstrated with our IHC staining in Chapter 3) and the ability of other cell types to transition to hepatocytes in order to recover lost liver mass is highly associated with ARLD and liver inflammation(44). Furthermore, in alcoholic hepatitis liver progenitor cell markers correlate positively with disease severity and short term mortality(323), as well as impaired hepatocyte regeneration and disproportionate differentiation to cholangiocytes(407). This is therefore representative of the environment that we are trying to model to some degree, but organoids at both the undifferentiated and differentiated stage of development need further characterisation to really understand how well we are replicating these cells. Organoids derived from primary human hepatocytes rather than bi-potential progenitor cells have shown function comparable to primary human hepatocytes(408), and while our "ductular" response is relevant for our injury, other cell sources should be considered depending on the

exact research question. However, our work demonstrates exciting potential especially regarding the expression of genes involved in the acute phase response. As highlighted previously, the acute phase response – particularly the complement cascade – is one of the most notable ways that the liver influences the systemic immune response(81, 82). As discussed in Chapter 5, proteins from this pathway have been implicated in the pathology of ARLD, but also have potential as novel biomarkers of liver injury. While it is important to confirm that the gene expression we have seen in our organoids translates to functional protein production, our findings suggest that this model could be used to investigate complement production in ARLD. This could be an exciting opportunity to look at mechanistic differences between normal and cirrhotic liver derived organoid cultures, and whether their capacity to respond to injurious stimuli is altered in this context. The baseline differences between ALD and donor derived organoids (such as significantly higher production of C3 in ALD organoids, or MBL2 in donor derived) already indicate interesting avenues to investigate.

It is important to note that irrespective of how well we replicate hepatocyte function, we cannot ignore the contribution of cell types we are lacking. In the introduction to this thesis I highlighted how the liver's complexity is integral to its function. By growing our cells in 3D space, we allow cell-cell contact that is more representative of what we would see *in vivo*, but we are also not capturing key features of liver disease such as fibrosis, changes in the vasculature and the influence of resident immune cells. For example, the influence of the extracellular matrix environment (and in the case of ALD, fibrosis and scarring) is discussed further in Section 6.2 in the context of the gels in which we culture our organoids; this does not however account for complex role of hepatic stellate cells (HSCs) *in vivo*. These cells

contribute to alcoholic liver injury via a number of mechanisms including steatosis, inflammation, and ECM deposits(409, 410), and while simplified models allow us to address specific questions in isolation, it is important to consider how signalling is different *in vivo*. Our work with peripheral blood neutrophils was our stepping stone into multi-cell cultures. We demonstrate a change in neutrophil behaviour with ductal organoid conditioned media that is not replicated by differentiated cells. This suggests an active response to organoid signalling, and our chemotaxis data implies that it could be possible to use this model to recreate elements of the classic polymorphonuclear cell infiltration seen in AH. Developing an organoid-neutrophil co-culture method could start to recreate some of the important interactions we see *in vivo*, particularly if we also included endothelial cells and other stromal compartments. Using pharmacological tools such as chemokine antagonists would allow us to study the impact of specific pathways and potentially identify new therapeutic modalities.

6.2 Organoid technology in liver research: how far have we come?

In January 2017, organoids were crowned as the Method of the Year(411). Over the course of that year there were 761 Pubmed search results for the term “organoid”; in 2022 there were over 3000. We have seen a self-perpetuating increase in the application of this technology, as the higher the number of available protocols and publications, the more accessible this technique becomes. Furthermore, its surge in popularity has been accompanied by commercial interest - meaning a wider range of more affordable products have become available, and made it feasible for many groups to incorporate organoids into their work. Our access to human liver tissue allowed us to investigate the potential of this model as a tool to study ARLD, utilising primary human liver progenitor cells from healthy and cirrhotic samples.

Early in this project we demonstrated the ability to grow viable organoids from cryopreserved tissue. This has previously been achieved with other organoid models such as those derived from gut(274) and endometrial tissue(349). Isolation from cryopreserved samples makes this model viable for centres that do not have access to human tissue, as well as removing variation in sample processing; freezing all samples immediately and isolating in parallel circumvents challenges with unpredictable clinical samples and batch variability during isolation. By the end of this project, STEMCELL Technologies were providing easily accessible protocols for a range of liver organoid techniques, including cryopreserving tissue for organoid isolation(412), isolating RNA and immunofluorescent staining. In just a few years, the resources available have changed the landscape for working with this technology.

It is now well established that primary hepatocyte function is improved with 3D culture compared to traditional 2D culture, resulting in better metabolic function and cell-cell interactions, and 3D culture techniques are rapidly evolving(413). Over recent decades, extensive research has been performed into how to utilise 3D culture gels to mimic the *in vivo* ECM environment (414), and our understanding of how to apply this has markedly improved(415). Matrigel is one of the most popular hydrogels used for 3D cell cultures(415, 416), however, it has a number of disadvantages such as batch to batch variation, lack of clarity as to chemical characterisation of the matrix constituents and rodent tumorigenic origin (343). It is therefore hard to standardise - even within growth factor reduced Matrigel, there is a wide variation of growth factors and cytokine content that could be influencing this environment. In the liver in particular, it is well established that altered ECM composition affects cell phenotype(352, 417), and that increased mechanical stiffness of matrix can

promote hepatocyte death *in vitro*(418). Significant improvements have been made regarding the replication of the diseased liver environment in culture, and this holds exciting promise for future organoid models. Das *et al* demonstrated improved response of primary hepatocytes to alcohol injury in a 3D electrospun matrix, which could be modified to contain different ECM proteins(419). Focus on optimising these gels for 3D culture has also led to the development of impressive systems utilising decellularized tissue. Ravichandran *et al* derived an adaptable ECM gel from porcine liver that allowed variation in mechanical properties(420), and furthers studies showing porcine derived ECM to be a promising culture tool for organoids(421). More recently, successful hepatic organoid culture has also been demonstrated using decellularized human liver tissue – paving the way for exciting possibilities for donor or disease status matched cells and culture matrix(422). This is undoubtedly one of the most exciting improvements that could be made to our model in the future. Our access to large samples of both donor and cirrhotic tissue at the CLGR provides a unique opportunity to establish an organoid system that allows us to understand the impact of the liver matrix on organoid function, and capture the essential contribution of the fibrotic tissue environment(423). Liver ECM has been shown to be immunomodulatory via a number of mechanisms, including via direct interactions with a range of pro and anti-inflammatory ECM proteins – excellently reviewed by McQuitty *et al*(351). Changes in ECM composition in chronic disease alter the immune environment, and utilising this resource in culture could help us to better investigate both local and systemic effects.

The other experimental parameter which has a significant impact on cell function and phenotype is the choice of media used for cell differentiation and culture. In Chapter 4, I

described my attempts to “humanise” the commercially available STEMCELL Technologies HepatiCult™ mouse liver organoid medium, with limited success. The improvements in commercially available tools for organoid culture are exemplified by recent availability of the HepatiCult™ Human Organoid Kit. This contains all necessary components for the establishment, growth and differentiation of human liver organoids from primary tissue, along with advice and associated protocols. This is an exciting advancement, as it removes a level of variability from a technique where there is still very little standardisation across the literature. Even when simply considering the phrase “liver organoid” we see descriptions of models from cell line derived spheroids(424) to a range of cell types from liver progenitors, and advancements with this technology are hindered by a lack of consensus in the field(425). An impressive publication from Marsee *et al* aims to standardise nomenclature concerning hepatic, pancreatic and biliary organoids, and sets a precedent for collaboration within the organoid research field that could benefit the community as a whole. The launch of the Organoid Cell Atlas(426) also aims to address many of these challenges, and provide a resource that will help to characterise and validate human organoid models such that their potential may be realised.

6.3 Capturing liver disease in a dish: where could we go?

With advances in 3D modelling technology, we are starting to be able to capture some of the complexities of human biology *in vitro* in a way we have never been able to before. Organoids are a valuable tool, and the possibilities for applications both in research and therapy are only just being understood. The fact that organoids have been shown to retain the genetic phenotype of the organ from which they are derived is one of their most exciting

features(342). In the context of disease modelling, this offers some advantage over animal models where at least some understanding of the mechanism and genes responsible is required to recapitulate disease, which is not the case when samples can be isolated directly from patients(427). Furthermore, it offers a unique opportunity to investigate both mechanism and therapy. There has been a huge focus on utilising this feature in the context of tumour derived organoids not only for understanding mechanisms, but personalising treatment and predicting outcome(428, 429). Extensive sequencing has taken place in HCC tumours(430), and the potential for understanding what mechanisms result in progression to HCC from ALD would be invaluable, alongside the opportunity to predict treatment response and test novel therapeutics. As well as tumour organoids, 3D cultures from patients with cystic fibrosis have been used to effectively tailor treatment(431), and Huch *et al* demonstrated retention of phenotype in liver organoids derived from patients with Alpha-1-anti-trypsin deficiency(214). Our results consistently showed "reduced" responsiveness in ALD derived organoids compared to donor derived (such as lower expression of albumin genes post-differentiation, and fewer gene changes to injury in our NanoString array). Furthermore, we saw different patterns in complement gene expression in ALD derived vs donor derived livers. This suggests that even after many weeks in culture and exposure to differentiation cues, there is some level of imprinted phenotype from the tissue that is being retained. This is also emphasised by the variation between samples; we saw wide ranges in elements such as growth rates, gene expression and cytokine production which implies that donor variability is still a factor even in long term culture. I have highlighted previously that while over 90% of those who drink heavily develop steatosis, only a third of these go on to develop cirrhosis and even fewer to HCC. The retention of genetic phenotype in liver patient derived organoids may

offer a new research tool in helping to understand what dictates the outcome for these patients. We already know that factors such as sex and ethnicity contribute significantly to ARLD susceptibility(119), and have examples of influential polymorphisms in alcohol metabolising enzymes(363). Being able to investigate factors like this in living patient cultures could help to identify currently unknown risk factors. This adds additional value, as issues such as racial disparity in clinical trials is still a significant concern(432), and platforms like this may help to improve development of therapeutics that meet the needs of underrepresented patient groups. Furthermore, due to liver toxicity in novel therapeutics being such a challenge, drug development for patients with cirrhosis is made difficult as risk of liver failure is significantly increased. Being able to study responses to treatment in organoids derived from cirrhotic liver may help to overcome some of these challenges. Alongside capturing patient genetic properties in organoids, it is also possible to edit them to investigate specific mechanisms. The CRISPR-Cas9 gene editing system has revolutionised the worlds of research and medicine(433). This has already been demonstrated with great effect in human liver organoids, with successful production of fluorescently tagged Cytokeratin 19 reporter lines or tumour suppressor gene knockouts to study tumorigenesis(434-436). This allows application of some of the more advantageous features of animal models, such as fluorescent reporter cells, to a system that is derived directly from human tissue. This offers exciting opportunities for understanding mechanistic effects of therapeutics, toxins, and immune signalling in liver tissue.

The field of drug discovery is limited by available models of the liver, largely due to the fact that hepatotoxicity is the most common reason for drugs being withdrawn from the

market(88). Common rodent models are poor predictors of human drug hepatotoxicity(437), and while CYP2E1 is fairly well conserved, activities of other metabolic enzymes vary between species(438). A lack of effective models of chronic liver disease also limits capability to investigate potential treatments for these conditions. Organoids have the potential to sit at an ideal interface where realistic patient variation is represented in a high-throughput system. We demonstrated the challenges of heterogeneous culture in this project, and unlike organoids derived from other sources such as the gut(266), bi-potential progenitor derived liver organoids do not spontaneously differentiate and require intervention to become hepatocyte-like. However, the development of high throughput, standardisable midbrain organoid systems presents exciting potential for the adaption of organoid technology in toxicity screening(439).

Organoids have not only demonstrated themselves to be valuable in the context of drug discovery and personalised medicine, but also as a therapeutic themselves. The potential for organoids as transplantable material is already showing exciting results(440). In the context of liver specifically, we know that while the liver is extremely tolerant to transplantation, demand far outweighs available organs. In decompensated liver disease, symptoms such as jaundice, hepatic encephalopathy and increased bleed risk are all due to loss of hepatocyte function, which could be restored with this type of technology. There is already discussion of human organoids as transplantable material in the liver(441), and exciting advances have been made with this technique where intestinal grafts have been developed using both patient derived organoids and scaffolds(442). This study, along with advances in hydrogel development as discussed above remove the necessity for animal derived products such as

Matrigel and transition this into a much more clinically relevant approach. Mouse models have demonstrated that transplanted hepatic progenitor cells have huge regenerative capacity in liver injury(443). The potential for developing a liver repair model with patient derived hepatic organoids, grown within matrix derived from decellularized human tissue, is an exciting concept not far from reach.

The work in this thesis only touches on the very edge of co-culture potential. There are established protocols for the co-culture of organoids with T cell derived from both peripheral blood and local tissue(444, 445). Cultures with innate immune cells, including neutrophils, have also been demonstrated in gut derived organoids (although neutrophil co-culture was limited by their short lifespan)(446). Furthermore, neutrophil migration and antimicrobial responses were seen in a polarised monolayer co-culture adapted from patient derived gut organoids(447). Early work by Takebe *et al*, developed a vascularised human liver bud from iPSCs(448), and lung organoid co-culture with mesenchymal stem cells has demonstrated potential as a model of airway injury and repair(449). The inclusion of fibroblasts in organoid models of oral tumours(450) and mammary glands(451) also show how other key cells within the liver could be incorporated into these models. While hepatocyte function is important to understand in ARLD, much of the liver damage incurred with chronic alcohol use is due to inflammation. Without modelling the liver-immune crosstalk, we lack the ability to understand both local and systemic effects of alcohol injury. In this project we have looked briefly at the role of neutrophils in this context, but incorporating both innate and adaptive liver resident immune cells (such as Kupffer and resident T cells), alongside key non-

parenchymal cells such as fibroblasts, is essential to identify what mechanisms are leaving patients at such high risk of infection.

Continuing on from multiple cell-type cultures to multiple organs, there are several 3D culture studies investigating the impact of alcohol on the brain or gut(452-454). Being able to capture the crosstalk between these systems and the liver could offer a valuable *in vitro* tool. In particular, the influence of alcohol consumption on gut permeability and the changes this then induces within the liver could offer insight into key signalling events that influence systemic immune responses. The gut-liver axis has already been highlighted as an essential crosstalk to investigate in organoid models(455), and recent multi-organ-on-a-chip technology has advanced to multiple tissue types all linked by vascular flow(456). Liver-on-a-chip models have also demonstrated key features of ALD, showing steatosis and epithelial remodelling with alcohol injury under flow conditions(457), and hepatocyte-like cell lines have showed improved functionality in microfluidic devices(458). This highlights the importance of including this biological feature, and may also be an answer to longer culture of differentiated hepatocyte-like organoids. A recent study on the Emulate Liver Chip identified that it was able to predict drug hepatotoxicity with 87% accuracy and 100% sensitivity, offering huge technical and economic improvements in the drug discovery pipeline(459). The importance of such models is exemplified by drugs such as Fialuridine; a therapeutic developed for the treatment of Hepatitis B which was promising in animal models, but caused severe toxicity and liver failure in clinical trials(245). Modelling alcohol injury in these 3D multi-organ systems offer an early stage warning system for drug toxicity, as well as valuable mechanistic insight.

6.4 “How much do you know about your liver?”

One of the greatest privileges I had during this project was the work I was able to undertake in public engagement and outreach. As part of this, I completed an additional qualification in Research Communication and Public Engagement, which provided the opportunity to create a piece of digital engagement focused on liver health. This was a continuation of work done with Pint of Science, where I had the opportunity to discuss liver health with members of the public, and these conversations clearly highlighted how the importance of liver health is underestimated. According to the British Liver Trust, only 5% of British adults consider their liver health to be of “great concern” compared to 72% for their heart(101). On evaluation of my project, 96% of participants said they had learned something new about their liver, half of which learned “lots more” than they knew before. Considering that over three quarters of patients with ARLD are diagnosed after a point when intervention could have prevented disease progression, it shows that improving awareness is an essential part of our toolkit to improve the outcomes of liver disease in the UK, and I feel that this work was an important contribution to the project and my skills as a scientific communicator.

Chapter 7 – Future work

Throughout this thesis, I have highlighted areas where further investigation would be beneficial. Here I discuss are some key experiments that if completed in the more immediate future would add value to our findings, alongside how the project could develop with further time and funding.

7.1 The next steps

Overall, the greatest limitation of this project is sample size and low number of repeats. While we can identify some patterns in our results and even see some statistical significance, few results were repeated more than 3-4 times, and in some cases (such as the NanoString array or neutrophil-organoid co-culture) samples were tested only once. Due to constrictions both in sample availability and time, many results need to be repeated and confirmed. Several assays were chosen to provide pilot data as to whether certain avenues of investigation were worth pursuing, which now informs many of the key questions for future work.

Regarding the organoid model itself, there are two main limitations – normalisation of organoid output, and functional responses to treatment. Published comparisons have highlighted the challenges of standardising products from organoids derived from adult human tissue compared to iPSCs(460). The optimisation of a cell count or seeding method that allows a more consistent and reproducible measure of organoid output would help us to clarify differences between donor and ALD derived organoids, especially in applications such as NETosis and chemotaxis. In particular, standardised supernatants would enable the use of technologies such as the Insall chamber(395). This would provide visualisation of neutrophil

migratory behaviour, and could help us to decipher the influence of organoid signalling cues in more detail. Given our findings regarding increased circulation of immature granulocyte number in patients with ARLD, it is also important to investigate whether they are significantly contributing to overall immune dysfunction and sepsis risk. Investigation of these cells as a fraction of "low density" neutrophils in Behçet's disease shows that despite higher numbers they did not explain neutrophil functional differences compared to healthy controls, and would be an interesting parameter to assess in our patients(461).

Our findings are in keeping with published work showing that LPS treatment alone was not sufficient to induce inflammatory responses in organoid cultures(52). However, it is important to confirm that we were able to replicate the responses seen with IL-1β and neutrophil conditioned media, with the intention of moving towards neutrophil co-culture. This creates the opportunity to study the neutrophil-organoid crosstalk in a multidirectional way, as well as whether there is a retained inflammatory phenotype in ARLD derived samples. Understanding the mechanisms by which the injured liver signals to increase leukocyte traffic, be this beneficial or detrimental, would aid the design of specific chemokine or integrin targeting therapies for example. Furthermore, fully understanding the extent of ethanol metabolism is key, and replicating our steatosis imaging experiments with more "chronic" alcohol treatment may indicate whether this model could be used to recreate alcoholic steatohepatitis *in vitro*. A pilot experiment with 24-hour treatment of ethanol and LPS was inconclusive (data not shown) but the droplet formation seen with lipid treatment holds promise for this function. Ethanol treatment for up to one week has been demonstrated in

other 3D models(366, 367), and it is important to understand the impact of this injury over time when moving forward with our organoid platform.

Many of our results rely on studying gene expression at the mRNA level, and it is key to understand whether this translates to protein production. Using methods such as immunofluorescent imaging or ELISA (particularly in the case of albumin and complement proteins) could offer more definitive answers on organoid function. While our confocal imaging was informative, it was limited by the 3D structure and size of the organoids, particularly in ductal stages. Light sheet microscopy has been shown to be particularly advantageous when imaging 3D cultures and samples suspended within gels(462), and highlighted as a useful tool in imaging organoid cultures(463, 464). This could offer more detailed information on elements such as TLR expression and localisation within 3D space in our model. Once these questions have been answered, it would be possible to more confidently investigate the neutrophil-liver crosstalk in ARLD using our organoid model. Furthermore, we may be able start to investigate which parameters make the difference as to whether neutrophils are a help or a hindrance in liver injury (209, 211) (202).

7.2 Looking further ahead

One lesson that is clear from our NanoString data is that the genes we focus on in this project do not tell the whole story. Understanding changes on a wider scale by utilising technology such as single cell RNA sequencing will help to characterise not only baseline differences between healthy and donor derived organoids, but also how they respond to injury. There has been many advancements of the application of this technology in organoid models (338), and

replicating the comparisons made in whole liver tissue by Dr Paul Horn (Chapter 3) would allow us to make vital comparisons between organoids from different tissue types, at different stages of differentiation, and in response to injury. As mentioned above, it is also essential not to restrict these studies to gene expression. Our proteome profilers show interesting baseline expression of many cytokines and chemokines, but these are likely a small snapshot of what is actually being produced. Mass spectrometry based proteomics have been used to decipher protein changes in response to ischemia reperfusion injury in intestinal organoids, and could offer insight into functional responses to alcohol exposure in our system(465).

I have also highlighted above the exciting developments in organ-on-a-chip technology. It cannot be ignored that an advantage of animal models is being able to understand the systemic changes in response to disease and injury. Being able to utilise the advances not only in culture techniques but also individual organoid systems could offer an opportunity to develop *in vitro* models of ARLD that capture more of the systemic disease. Our access to whole liver tissue also offers the opportunity to culture multiple cell types such as fibroblasts and Kupffer cells from matched tissue donors when investigating a multi-cell platform. When describing ARLD at the start of this thesis, I listed the key stages of disease: steatosis, steatohepatitis, fibrosis, cirrhosis, and HCC. Here we have demonstrated the ability to form lipid droplets, and are working towards replicating at least part of the inflammatory response seen in acute hepatitis. However, for us to really move away from animal models and towards organoid culture it is essential to capture all stages of disease development. Recent studies have shown distinct disease features from different stages of NASH in organoids derived from a mouse model(466), which shows promise for capturing the stages of ARLD in vitro. Advances

in ECM gels help towards recreating the mechanical properties of an injured liver, but until we can incorporate essential cell-cell crosstalk from LSEC, HSCs and resident immune cells, we lack the necessary pieces of the puzzle to understand why patients with ARLD present with such severe immune deficit.

7.3 Final thoughts

There are clear unmet clinical needs in terms of ARLD diagnosis and treatment that are only growing. In the first few months of the COVID-19 pandemic, there was a 50% increase in AH related admissions in the USA(467). As AH mortality has not improved significantly since the 1970s(122) and alcohol related deaths are rising in the UK, it is evident that our current models are limited. Recent advances in *in vitro* modelling technology could offer a tool not only for therapeutic investigations, but also as potential treatments in the form of transplantable tissues. While this project sits at the very early stages of model development, it has shown promising pilot data and highlights some exciting avenues for further investigation. Firstly, being able to grow organoids from ALD cirrhotic tissue holds great value. It appears that at least some level of phenotype is retained from chronic injury, and understanding whether there is a level of senescence, exhaustion, or immaturity in these cells could help us to understand altered liver regeneration in ARLD. Furthermore, if drug metabolism is altered due to this fact, it could offer a first pass model for novel therapeutics in cirrhosis which are challenging to test due to risks of hepatotoxicity in these patients and difficulty recreating fibrosis in animal models. Our findings on neutrophil phenotype and number, and the ability of ductal organoid supernatant to increase NETosis highlight some interesting questions about how the increased number of progenitor cells in ALD cirrhotic tissue could be contributing to

the sepsis-like phenotype of high neutrophil activation but low effectiveness. Furthermore, the differences in complement gene expression between ALD and donor derived organoids also indicate that this model could have potential to investigate another way in which alcoholic liver injury is altering systemic immune signalling.

Possibly most excitingly, the advances in the organoid field over the last few years have been phenomenal, and it is possible to address many of these future work questions with new resources, protocols and techniques. I hope that this project has provided the first steps towards a valuable model of ARLD *in vitro*.

Supplementary data

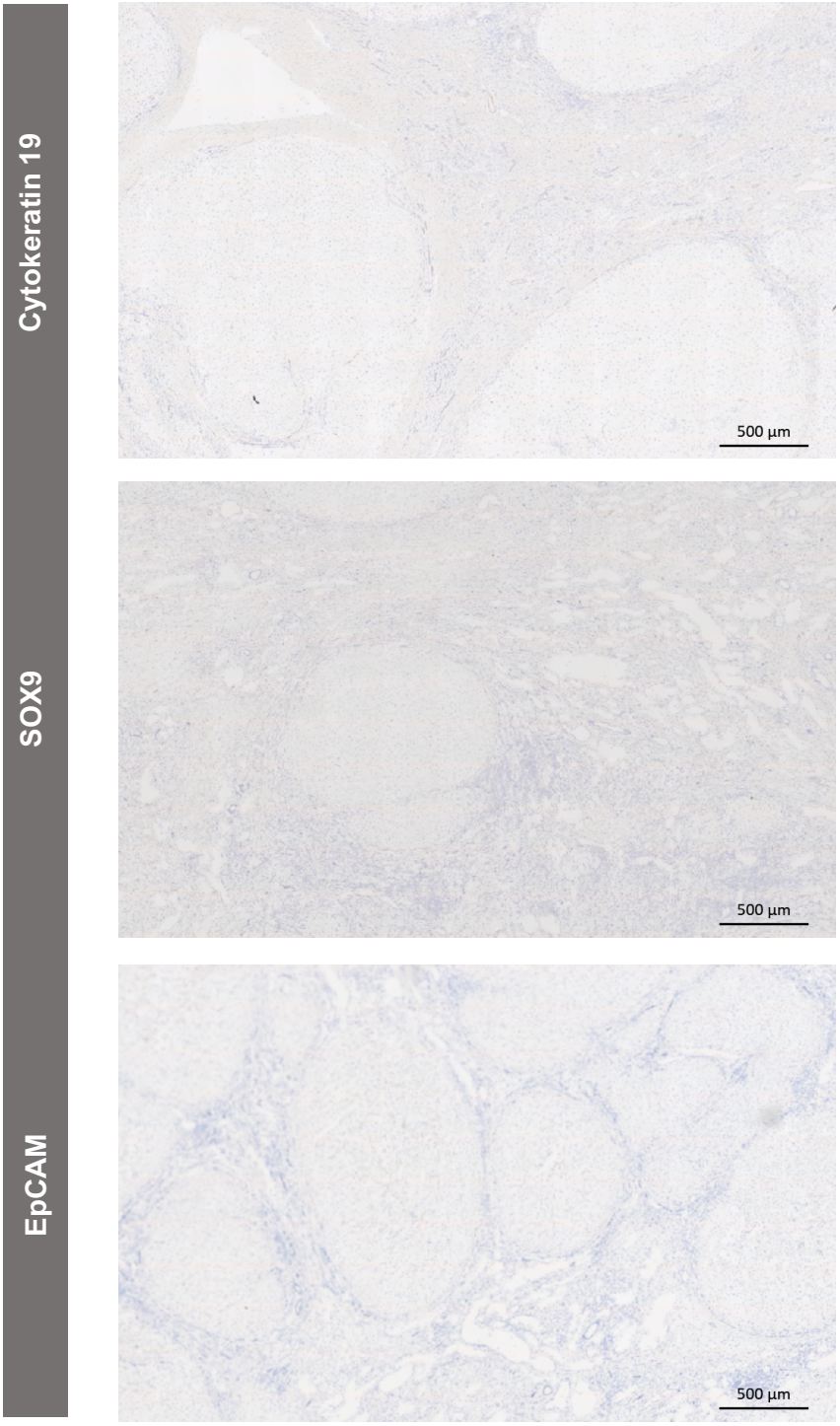


Figure S.1: Isotype Matched Control (IMC) images for Immunohistochemical staining of Cytokeratin 19, SOX9 and EpCAM in human liver. Images showing representative fields of view from whole liver tissue for isotype matched control staining for the antibodies indicated. All immunohistochemical staining was completed alongside an isotype matched control (assay dependent) to confirm specific staining. Isotype matched controls were used at matched concentrations to their corresponding antibody. Scale bar is 500µm.

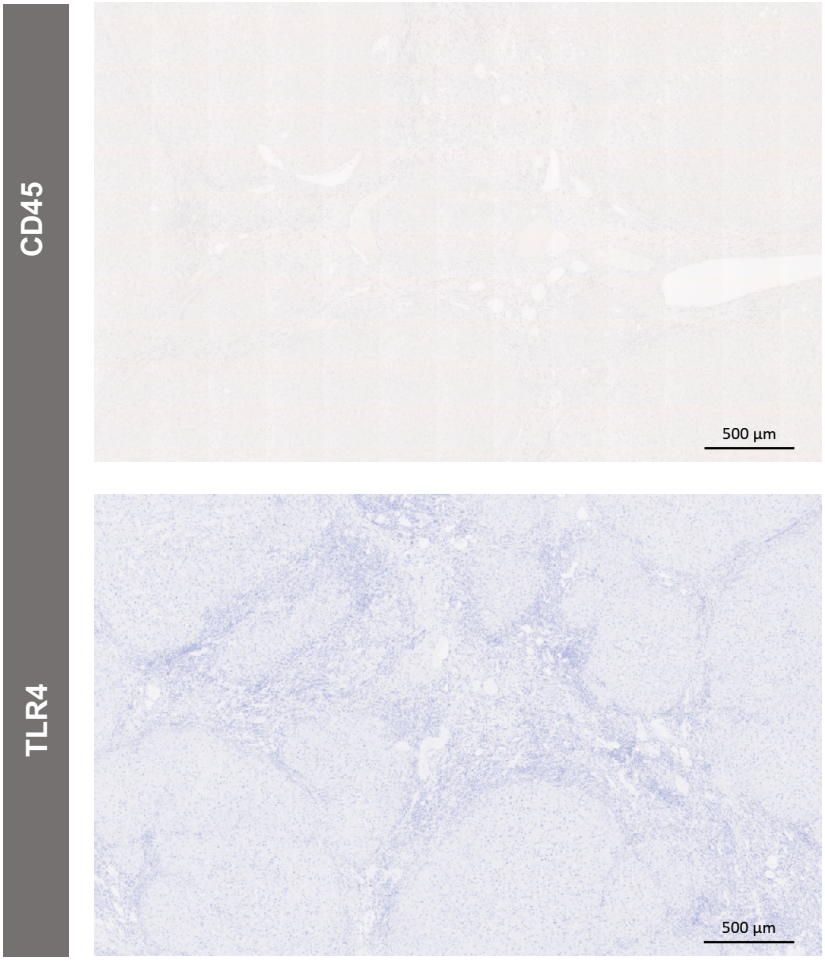


Figure S.2: Isotype Matched Control (IMC) images for Immunohistochemical staining of CD45 and TLR4 in human liver. Images showing representative fields of view from whole liver tissue for isotype matched control staining for the antibodies indicated. All immunohistochemical staining was completed alongside an isotype matched control (assay dependent) to confirm specific staining. Isotype matched controls were used at matched concentrations to their corresponding antibody. Scale bar is 500µm.

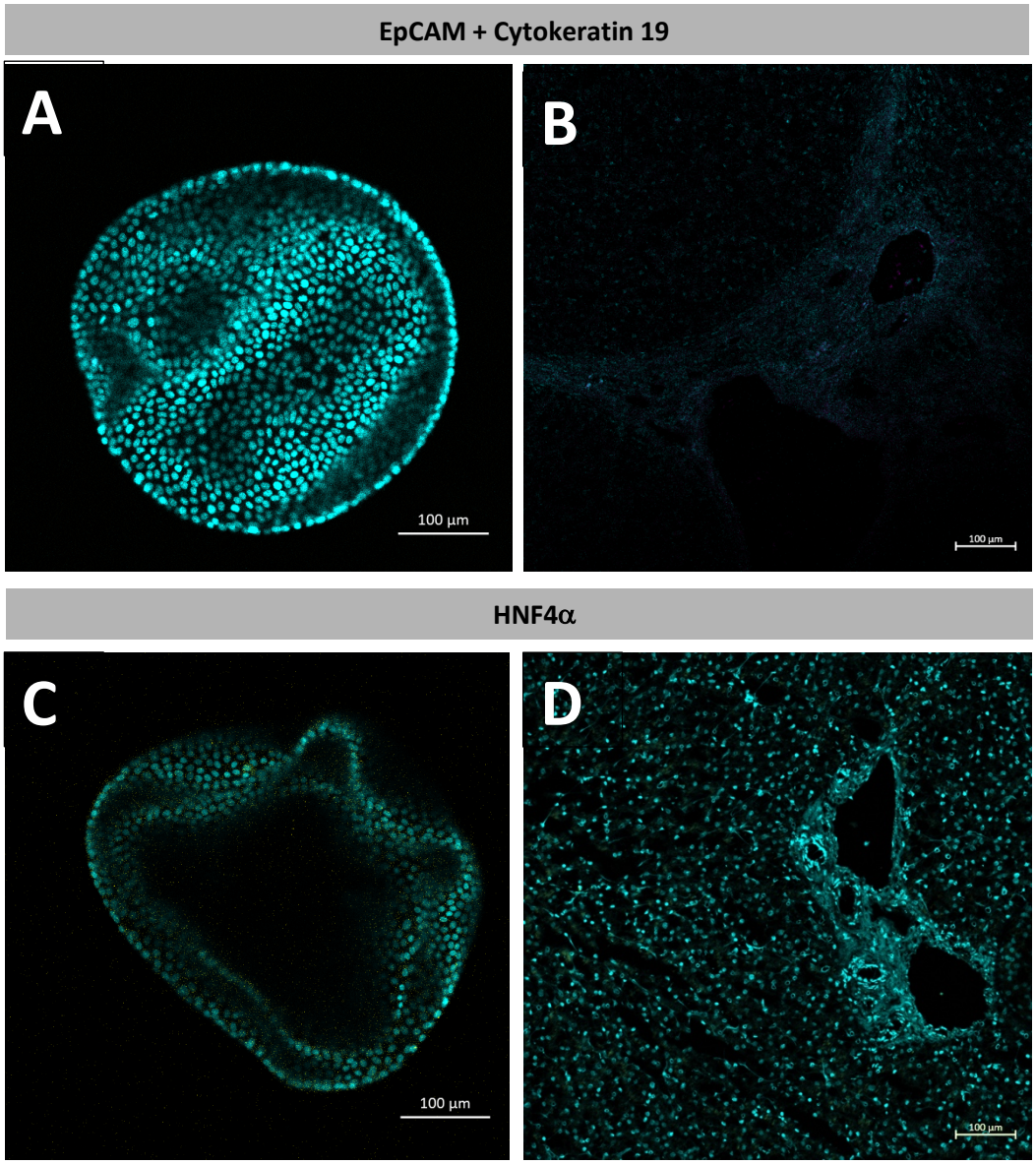


Figure S.3: Isotype Matched Control (IMC) images for Immunofluorescent staining of whole tissue and organoids. Images showing representative fields of view from organoids (A and C) and whole liver tissue (B and D) which have been stained with isotype matched control antibodies for either EpCAM and Cytokeratin 19 (A and B) or HNF4α (C and D), and counterstained with DAPI. All immunofluorescent staining was completed alongside an isotype matched control (assay dependent) to confirm specific staining. Isotype matched controls were used at matched concentrations to their corresponding antibody. Scale bar is 100μm.

References

1. Williams R, Aspinall R, Bellis M, Camps-Walsh G, Cramp M, Dhawan A, et al. Addressing liver disease in the UK: a blueprint for attaining excellence in health care and reducing premature mortality from lifestyle issues of excess consumption of alcohol, obesity, and viral hepatitis. The Lancet. 2014;384(9958):1953-97.
2. Bhatia SN, Underhill GH, Zaret KS, Fox IJ. Cell and tissue engineering for liver disease. Sci Transl Med. 2014;6(245):245sr2.
3. Eipel C, Abshagen K, Vollmar B. Regulation of hepatic blood flow: the hepatic arterial buffer response revisited. World J Gastroenterol. 2010;16(48):6046-57.
4. Albillos A, de Gottardi A, Rescigno M. The gut-liver axis in liver disease: Pathophysiological basis for therapy. J Hepatol. 2020;72(3):558-77.
5. Lorente S, Hautefeuille M, Sanchez-Cedillo A. The liver, a functionalized vascular structure. Scientific Reports. 2020;10(1):16194.
6. Damania A, Jain E, Kumar A. Advancements in in vitro hepatic models: application for drug screening and therapeutics. Hepatol Int. 2014;8(1):23-38.
7. Schulze RJ, Schott MB, Casey CA, Tuma PL, McNiven MA. The cell biology of the hepatocyte: A membrane trafficking machine. J Cell Biol. 2019;218(7):2096-112.
8. Rui L. Energy metabolism in the liver. Compr Physiol. 2014;4(1):177-97.
9. Seebacher F, Zeigerer A, Kory N, Krahmer N. Hepatic lipid droplet homeostasis and fatty liver disease. Seminars in Cell & Developmental Biology. 2020;108:72-81.
10. Boyer JL, Soroka CJ. Bile formation and secretion: An update. Journal of Hepatology. 2021;75(1):190-201.
11. Quinlan GJ, Martin GS, Evans TW. Albumin: Biochemical properties and therapeutic potential. Hepatology. 2005;41(6):1211-9.
12. Garcia-Martinez R, Caraceni P, Bernardi M, Gines P, Arroyo V, Jalan R. Albumin: Pathophysiologic basis of its role in the treatment of cirrhosis and its complications. Hepatology. 2013;58(5):1836-46.
13. Bernardi M, Maggioli C, Zaccherini G. Human albumin in the management of complications of liver cirrhosis. Crit Care. 2012;16(2):211.
14. Dixon LJ, Barnes M, Tang H, Pritchard MT, Nagy LE. Kupffer cells in the liver. Compr Physiol. 2013;3(2):785-97.
15. Li P, He K, Li J, Liu Z, Gong J. The role of Kupffer cells in hepatic diseases. Molecular Immunology. 2017;85:222-9.
16. Nguyen-Lefebvre AT, Horuzsko A. Kupffer Cell Metabolism and Function. J Enzymol Metab. 2015;1(1).
17. Knoll P, Schlaak J, Uhrig A, Kempf P, zum Büschenfelde K-HM, Gerken G. Human Kupffer cells secrete IL-10 in response to lipopolysaccharide (LPS) challenge. Journal of Hepatology. 1995;22(2):226-9.
18. Ju C, Tacke F. Hepatic macrophages in homeostasis and liver diseases: from pathogenesis to novel therapeutic strategies. Cellular & Molecular Immunology. 2016;13(3):316-27.
19. Tacke F. Targeting hepatic macrophages to treat liver diseases. J Hepatol. 2017;66(6):1300-12.

20. Yang Y, Bazhin AV, Werner J, Karakhanova S. Reactive Oxygen Species in the Immune System. International Reviews of Immunology. 2013;32(3):249-70.
21. Wang C, Ma C, Gong L, Guo Y, Fu K, Zhang Y, et al. Macrophage Polarization and Its Role in Liver Disease. Front Immunol. 2021;12:803037.
22. Shetty S, Lalor PF, Adams DH. Liver sinusoidal endothelial cells — gatekeepers of hepatic immunity. Nature Reviews Gastroenterology & Hepatology. 2018;15(9):555-67.
23. Knolle PA, Wohlleber D. Immunological functions of liver sinusoidal endothelial cells. Cell Mol Immunol. 2016;13(3):347-53.
24. Poisson J, Lemoinne S, Boulanger C, Durand F, Moreau R, Valla D, et al. Liver sinusoidal endothelial cells: Physiology and role in liver diseases. Journal of Hepatology. 2017;66(1):212-27.
25. Kamm DR, McCommis KS. Hepatic stellate cells in physiology and pathology. J Physiol. 2022;600(8):1825-37.
26. Roehlen N, Crouchet E, Baumert TF. Liver Fibrosis: Mechanistic Concepts and Therapeutic Perspectives. Cells. 2020;9(4).
27. Poisson J, Lemoinne S, Boulanger C, Durand F, Moreau R, Valla D, et al. Liver sinusoidal endothelial cells: Physiology and role in liver diseases. J Hepatol. 2017;66(1):212-27.
28. Banales JM, Huebert RC, Karlsen T, Strazzabosco M, LaRusso NF, Gores GJ. Cholangiocyte pathobiology. Nat Rev Gastroenterol Hepatol. 2019;16(5):269-81.
29. Tabibian JH, Masyuk AI, Masyuk TV, O'Hara SP, LaRusso NF. Physiology of cholangiocytes. Compr Physiol. 2013;3(1):541-65.
30. Alvaro D, Mancino MG, Glaser S, Gaudio E, Marzioni M, Francis H, et al. Proliferating Cholangiocytes: A Neuroendocrine Compartment in the Diseased Liver. Gastroenterology. 2007;132(1):415-31.
31. Popper H, Kent G, Stein R. Ductular cell reaction in the liver in hepatic injury. J Mt Sinai Hosp N Y. 1957;24(5):551-6.
32. O'Hara SP, Tabibian JH, Splinter PL, LaRusso NF. The dynamic biliary epithelia: Molecules, pathways, and disease. Journal of Hepatology. 2013;58(3):575-82.
33. Roskams TA, Theise ND, Balabaud C, Bhagat G, Bhathal PS, Bioulac-Sage P, et al. Nomenclature of the finer branches of the biliary tree: Canals, ductules, and ductular reactions in human livers. Hepatology. 2004;39(6):1739-45.
34. Chen X-M, O'Hara SP, Nelson JB, Splinter PL, Small AJ, Tietz PS, et al. Multiple TLRs Are Expressed in Human Cholangiocytes and Mediate Host Epithelial Defense Responses to *Cryptosporidium parvum* via Activation of NF-κB. The Journal of Immunology. 2005;175(11):7447-56.
35. Ankoma-Sey V. Hepatic Regeneration—Revisiting the Myth of Prometheus. Physiology. 1999;14(4):149-55.
36. Mao SA, Glorioso JM, Nyberg SL. Liver regeneration. Transl Res. 2014;163(4):352-62.
37. Olthoff KM, Emond JC, Shearon TH, Everson G, Baker TB, Fisher RA, et al. Liver regeneration after living donor transplantation: adult-to-adult living donor liver transplantation cohort study. Liver Transpl. 2015;21(1):79-88.
38. Fausto N, Campbell JS. The role of hepatocytes and oval cells in liver regeneration and repopulation. Mechanisms of Development. 2003;120(1):117-30.

39. Overturf K, al-Dhalimy M, Ou CN, Finegold M, Grompe M. Serial transplantation reveals the stem-cell-like regenerative potential of adult mouse hepatocytes. Am J Pathol. 1997;151(5):1273-80.
40. So J, Kim A, Lee SH, Shin D. Liver progenitor cell-driven liver regeneration. Exp Mol Med. 2020;52(8):1230-8.
41. Farber E. Similarities in the sequence of early histological changes induced in the liver of the rat by ethionine, 2-acetylamino-fluorene, and 3'-methyl-4-dimethylaminoazobenzene. Cancer Res. 1956;16(2):142-8.
42. Zhang Y, Bai XF, Huang CX. Hepatic stem cells: existence and origin. World J Gastroenterol. 2003;9(2):201-4.
43. Chaudhari P, Tian L, Deshmukh A, Jang YY. Expression kinetics of hepatic progenitor markers in cellular models of human liver development recapitulating hepatocyte and biliary cell fate commitment. Exp Biol Med (Maywood). 2016;241(15):1653-62.
44. Sato K, Marzioni M, Meng F, Francis H, Glaser S, Alpini G. Ductular Reaction in Liver Diseases: Pathological Mechanisms and Translational Significances. Hepatology. 2019;69(1):420-30.
45. Theise ND, Saxena R, Portmann BC, Thung SN, Yee H, Chiriboga L, et al. The canals of hering and hepatic stem cells in humans. Hepatology. 1999;30(6):1425-33.
46. Tarlow BD, Pelz C, Naugler WE, Wakefield L, Wilson EM, Finegold MJ, et al. Bipotential adult liver progenitors are derived from chronically injured mature hepatocytes. Cell Stem Cell. 2014;15(5):605-18.
47. Alison MR, Poulsom R, Jeffery R, Dhillon AP, Quaglia A, Jacob J, et al. Hepatocytes from non-hepatic adult stem cells. Nature. 2000;406(6793):257.
48. Theise ND, Nimmakayalu M, Gardner R, Illei PB, Morgan G, Teperman L, et al. Liver from bone marrow in humans. Hepatology. 2000;32(1):11-6.
49. Crosby HA, Strain AJ. Adult liver stem cells: bone marrow, blood, or liver derived? Gut. 2001;48(2):153.
50. Gouw ASH, Clouston AD, Theise ND. Ductular reactions in human liver: Diversity at the interface. Hepatology. 2011;54(5):1853-63.
51. Azad AI, Krishnan A, Troop L, Li Y, Katsumi T, Pavelko K, et al. Targeted Apoptosis of Ductular Reactive Cells Reduces Hepatic Fibrosis in a Mouse Model of Cholestasis. Hepatology. 2020;72(3):1013-28.
52. Aguilar-Bravo B, Rodrigo-Torres D, Ariño S, Coll M, Pose E, Blaya D, et al. Ductular Reaction Cells Display an Inflammatory Profile and Recruit Neutrophils in Alcoholic Hepatitis. Hepatology. 2019;69(5):2180-95.
53. Zhao J, Zhang S, Liu Y, He X, Qu M, Xu G, et al. Single-cell RNA sequencing reveals the heterogeneity of liver-resident immune cells in human. Cell Discovery. 2020;6(1):22.
54. Liaskou E, Wilson DV, Oo YH. Innate Immune Cells in Liver Inflammation. Mediators of Inflammation. 2012;2012:949157.
55. Marra F, Tacke F. Roles for Chemokines in Liver Disease. Gastroenterology. 2014;147(3):577-94.e1.
56. Chaudhry S, Emond J, Griesemer A. Immune Cell Trafficking to the Liver. Transplantation. 2019;103(7):1323-37.

57. Lalor PF, Edwards S, McNab G, Salmi M, Jalkanen S, Adams DH. Vascular adhesion protein-1 mediates adhesion and transmigration of lymphocytes on human hepatic endothelial cells. J Immunol. 2002;169(2):983-92.
58. Crispe IN. Liver antigen-presenting cells. J Hepatol. 2011;54(2):357-65.
59. Koyama Y, Brenner DA. Liver inflammation and fibrosis. J Clin Invest. 2017;127(1):55-64.
60. Calne RY, Sells RA, Pena JR, Davis DR, Millard PR, Herbertson BM, et al. Induction of Immunological Tolerance by Porcine Liver Allografts. Nature. 1969;223(5205):472-6.
61. Dai H, Zheng Y, Thomson AW, Rogers NM. Transplant Tolerance Induction: Insights From the Liver. Front Immunol. 2020;11:1044.
62. Robinson MW, Harmon C, O'Farrelly C. Liver immunology and its role in inflammation and homeostasis. Cellular & Molecular Immunology. 2016;13(3):267-76.
63. Horst AK, Neumann K, Diehl L, Tiegs G. Modulation of liver tolerance by conventional and nonconventional antigen-presenting cells and regulatory immune cells. Cellular & Molecular Immunology. 2016;13(3):277-92.
64. Xia S, Guo Z, Xu X, Yi H, Wang Q, Cao X. Hepatic microenvironment programs hematopoietic progenitor differentiation into regulatory dendritic cells, maintaining liver tolerance. Blood. 2008;112(8):3175-85.
65. Takeuchi O, Akira S. Pattern Recognition Receptors and Inflammation. Cell. 2010;140(6):805-20.
66. Kawasaki T, Kawai T. Toll-Like Receptor Signaling Pathways. Frontiers in Immunology. 2014;5.
67. Seki E, Brenner DA. Toll-like receptors and adaptor molecules in liver disease: Update. Hepatology. 2008;48(1):322-35.
68. de Oliviera Nascimento L, Massari P, Wetzler LM. The Role of TLR2 in Infection and Immunity. Frontiers in Immunology. 2012;3(79).
69. Schwabe RF, Seki E, Brenner DA. Toll-Like Receptor Signaling in the Liver. Gastroenterology. 2006;130(6):1886-900.
70. Guo J, Friedman SL. Toll-like receptor 4 signaling in liver injury and hepatic fibrogenesis. Fibrogenesis Tissue Repair. 2010;3:21.
71. Jirillo E, Caccavo D, Magrone T, Piccigallo E, Amati L, Lembo A, et al. The role of the liver in the response to LPS: experimental and clinical findings. J Endotoxin Res. 2002;8(5):319-27.
72. Jenne CN, Kubes P. Immune surveillance by the liver. Nature Immunology. 2013;14(10):996-1006.
73. Guerville M, Boudry G. Gastrointestinal and hepatic mechanisms limiting entry and dissemination of lipopolysaccharide into the systemic circulation. American Journal of Physiology-Gastrointestinal and Liver Physiology. 2016;311(1):G1-G15.
74. Mimura Y, Sakisaka S, Harada M, Sata M, Tanikawa K. Role of hepatocytes in direct clearance of lipopolysaccharide in rats. Gastroenterology. 1995;109(6):1969-76.
75. Yao Z, Mates JM, Cheplowitz AM, Hammer LP, Maiseyeu A, Phillips GS, et al. Blood-Borne Lipopolysaccharide Is Rapidly Eliminated by Liver Sinusoidal Endothelial Cells via High-Density Lipoprotein. J Immunol. 2016;197(6):2390-9.

76. Fox ES, Thomas P, Broitman SA. Clearance of gut-derived endotoxins by the liver. Release and modification of 3H, 14C-lipopolysaccharide by isolated rat Kupffer cells. Gastroenterology. 1989;96(2 Pt 1):456-61.
77. Topchiy E, Cirstea M, Kong HJ, Boyd JH, Wang Y, Russell JA, et al. Lipopolysaccharide Is Cleared from the Circulation by Hepatocytes via the Low Density Lipoprotein Receptor. PLoS One. 2016;11(5):e0155030.
78. Mandrekar P, Szabo G. Signalling pathways in alcohol-induced liver inflammation. J Hepatol. 2009;50(6):1258-66.
79. Gruys E, Toussaint MJ, Niewold TA, Koopmans SJ. Acute phase reaction and acute phase proteins. J Zhejiang Univ Sci B. 2005;6(11):1045-56.
80. Jain S, Gautam V, Naseem S. Acute-phase proteins: As diagnostic tool. J Pharm Bioallied Sci. 2011;3(1):118-27.
81. Thorgersen EB, Barratt-Due A, Haugaa H, Harboe M, Pischke SE, Nilsson PH, et al. The Role of Complement in Liver Injury, Regeneration, and Transplantation. Hepatology. 2019;70(2):725-36.
82. Qin X, Gao B. The complement system in liver diseases. Cell Mol Immunol. 2006;3(5):333-40.
83. Dunkelberger JR, Song W-C. Complement and its role in innate and adaptive immune responses. Cell Research. 2010;20(1):34-50.
84. Zhou Y, Yuan G, Zhong F, He S. Roles of the complement system in alcohol-induced liver disease. Clin Mol Hepatol. 2020;26(4):677-85.
85. Moshage HJ, Janssen JA, Franssen JH, Hafkenscheid JC, Yap SH. Study of the molecular mechanism of decreased liver synthesis of albumin in inflammation. J Clin Invest. 1987;79(6):1635-41.
86. Kaysen GA, Dubin JA, Müller H-G, Rosales L, Levin NW, Mitch WE, et al. Inflammation and reduced albumin synthesis associated with stable decline in serum albumin in hemodialysis patients. Kidney International. 2004;65(4):1408-15.
87. Sevior DK, Pelkonen O, Ahokas JT. Hepatocytes: the powerhouse of biotransformation. Int J Biochem Cell Biol. 2012;44(2):257-61.
88. Onakpoya IJ, Heneghan CJ, Aronson JK. Post-marketing withdrawal of 462 medicinal products because of adverse drug reactions: a systematic review of the world literature. BMC Med. 2016;14:10.
89. Zanger UM, Turpeinen M, Klein K, Schwab M. Functional pharmacogenetics/genomics of human cytochromes P450 involved in drug biotransformation. Analytical and Bioanalytical Chemistry. 2008;392(6):1093-108.
90. Zhao M, Ma J, Li M, Zhang Y, Jiang B, Zhao X, et al. Cytochrome P450 Enzymes and Drug Metabolism in Humans. Int J Mol Sci. 2021;22(23).
91. Woolbright BL, Jaeschke H. Xenobiotic and Endobiotic Mediated Interactions Between the Cytochrome P450 System and the Inflammatory Response in the Liver. Adv Pharmacol. 2015;74:131-61.
92. Gu X, Manautou JE. Molecular mechanisms underlying chemical liver injury. Expert Rev Mol Med. 2012;14:e4.
93. Cederbaum AI. Alcohol metabolism. Clin Liver Dis. 2012;16(4):667-85.

94. Jung Y-c, Namkoong K. Chapter 7 - Alcohol: intoxication and poisoning – diagnosis and treatment. In: Sullivan EV, Pfefferbaum A, editors. Handbook of Clinical Neurology. 125: Elsevier; 2014. p. 115-21.
95. Yin SJ, Liao CS, Wu CW, Li TT, Chen LL, Lai CL, et al. Human stomach alcohol and aldehyde dehydrogenases: comparison of expression pattern and activities in alimentary tract. Gastroenterology. 1997;112(3):766-75.
96. Setshedi M, Wands JR, Monte SM. Acetaldehyde adducts in alcoholic liver disease. Oxid Med Cell Longev. 2010;3(3):178-85.
97. Osna NA, Donohue TM, Jr., Kharbanda KK. Alcoholic Liver Disease: Pathogenesis and Current Management. Alcohol Res. 2017;38(2):147-61.
98. Leung T-M, Nieto N. CYP2E1 and oxidant stress in alcoholic and non-alcoholic fatty liver disease. Journal of Hepatology. 2013;58(2):395-8.
99. Zakhari S. Overview: how is alcohol metabolized by the body? Alcohol Res Health. 2006;29(4):245-54.
100. Office for National Statistics (ONS). Alcohol-specific deaths in the UK: registered in 2020 [Internet]. 2021 [[cited 2023 February 4]. Available from: https://www.ons.gov.uk/peoplepopulationandcommunity/healthandsocialcare/causesofdeath/bulletins/alcoholrelateddeathsintheunitedkingdom/registeredin2020.
101. British Liver Trust. The alarming impact of liver disease in the UK - Facts and statistics. [Internet]. 2019. [cited 2023 February 4] Available from: https://britishlivertrust.org.uk/wp-content/uploads/The-alarming-impact-of-liver-disease-FINAL-June-2019.pdf.
102. Marsano LS, Mendez C, Hill D, Barve S, McClain CJ. Diagnosis and treatment of alcoholic liver disease and its complications. Alcohol Res Health. 2003;27(3):247-56.
103. Sharma P, Arora A. Clinical presentation of alcoholic liver disease and non-alcoholic fatty liver disease: spectrum and diagnosis. Transl Gastroenterol Hepatol. 2020;5:19.
104. Aithal GP, Palaniyappan N, China L, Härmälä S, Macken L, Ryan JM, et al. Guidelines on the management of ascites in cirrhosis. Gut. 2021;70(1):9-29.
105. Northup PG, Caldwell SH. Coagulation in Liver Disease: A Guide for the Clinician. Clinical Gastroenterology and Hepatology. 2013;11(9):1064-74.
106. Roche SP, Kobos R. Jaundice in the adult patient. Am Fam Physician. 2004;69(2):299-304.
107. Butterworth RF. Hepatic encephalopathy--a serious complication of alcoholic liver disease. Alcohol Res Health. 2003;27(2):143-5.
108. Torruellas C, French SW, Medici V. Diagnosis of alcoholic liver disease. World J Gastroenterol. 2014;20(33):11684-99.
109. Kwo PY, Cohen SM, Lim JK. ACG Clinical Guideline: Evaluation of Abnormal Liver Chemistries. Official journal of the American College of Gastroenterology | ACG. 2017;112(1):18-35.
110. Newsome PN, Cramb R, Davison SM, Dillon JF, Foulerton M, Godfrey EM, et al. Guidelines on the management of abnormal liver blood tests. Gut. 2018;67(1):6-19.
111. Friedman LS. Surgery in the patient with liver disease. Trans Am Clin Climatol Assoc. 2010;121:192-204; discussion 5.
112. Seitz HK, Bataller R, Cortez-Pinto H, Gao B, Gual A, Lackner C, et al. Alcoholic liver disease. Nat Rev Dis Primers. 2018;4(1):16.

113. Lieber CS. Alcoholic fatty liver: its pathogenesis and mechanism of progression to inflammation and fibrosis. Alcohol. 2004;34(1):9-19.
114. Lian C-Y, Zhai Z-Z, Li Z-F, Wang L. High fat diet-triggered non-alcoholic fatty liver disease: A review of proposed mechanisms. Chemico-Biological Interactions. 2020;330:109199.
115. Naveau S, Giraud V, Borotto E, Aubert A, Capron F, Chaput JC. Excess weight risk factor for alcoholic liver disease. Hepatology. 1997;25(1):108-11.
116. Hart CL, Morrison DS, Batty GD, Mitchell RJ, Davey Smith G. Effect of body mass index and alcohol consumption on liver disease: analysis of data from two prospective cohort studies. Bmj. 2010;340:c1240.
117. Tsukamoto H, Machida K, Dynnyk A, Mkrtchyan H. "Second hit" models of alcoholic liver disease. Semin Liver Dis. 2009;29(2):178-87.
118. O'Shea RS, Dasarathy S, McCullough AJ, Practice Guideline Committee of the American Association for the Study of Liver Diseases, Practice Parameters Committee of the American College of Gastroenterology. Alcoholic liver disease. Hepatology. 2010;51(1):307-28.
119. European Association for the Study of the Liver. EASL Clinical Practice Guidelines: Management of alcohol-related liver disease. Journal of Hepatology. 2018;69(1):154-81.
120. Lefkowitch JH. Morphology of alcoholic liver disease. Clin Liver Dis. 2005;9(1):37-53.
121. Thursz M, Morgan TR. Treatment of Severe Alcoholic Hepatitis. Gastroenterology. 2016;150(8):1823-34.
122. Hughes E, Hopkins LJ, Parker R. Survival from alcoholic hepatitis has not improved over time. PLoS One. 2018;13(2):e0192393.
123. Basra G, Basra S, Parupudi S. Symptoms and signs of acute alcoholic hepatitis. World J Hepatol. 2011;3(5):118-20.
124. Singal AK, Bataller R, Ahn J, Kamath PS, Shah VH. ACG Clinical Guideline: Alcoholic Liver Disease. Am J Gastroenterol. 2018;113(2):175-94.
125. Wynn TA. Cellular and molecular mechanisms of fibrosis. J Pathol. 2008;214(2):199-210.
126. Lackner C, Tiniakos D. Fibrosis and alcohol-related liver disease. J Hepatol. 2019;70(2):294-304.
127. Ekstedt M, Hagström H, Nasr P, Fredrikson M, Stål P, Kechagias S, et al. Fibrosis stage is the strongest predictor for disease-specific mortality in NAFLD after up to 33 years of follow-up. Hepatology. 2015;61(5):1547-54.
128. Lackner C, Spindelboeck W, Haybaeck J, Douschan P, Rainer F, Terracciano L, et al. Histological parameters and alcohol abstinence determine long-term prognosis in patients with alcoholic liver disease. Journal of Hepatology. 2017;66(3):610-8.
129. Ellis EL, Mann DA. Clinical evidence for the regression of liver fibrosis. Journal of Hepatology. 2012;56(5):1171-80.
130. Puche JE, Saiman Y, Friedman SL. Hepatic stellate cells and liver fibrosis. Compr Physiol. 2013;3(4):1473-92.
131. Ginès P, Krag A, Abraldes JG, Solà E, Fabrellas N, Kamath PS. Liver cirrhosis. The Lancet. 2021;398(10308):1359-76.
132. Moreau R, Jalan R, Gines P, Pavesi M, Angeli P, Cordoba J, et al. Acute-on-chronic liver failure is a distinct syndrome that develops in patients with acute decompensation of cirrhosis. Gastroenterology. 2013;144(7):1426-37, 37.e1-9.

133. Ganne-Carrié N, Chaffaut C, Bourcier V, Archambeaud I, Perarnau J-M, Oberti F, et al. Estimate of hepatocellular carcinoma incidence in patients with alcoholic cirrhosis. Journal of Hepatology. 2018;69(6):1274-83.
134. West J, Card TR, Aithal GP, Fleming KM. Risk of hepatocellular carcinoma among individuals with different aetiologies of cirrhosis: a population-based cohort study. Aliment Pharmacol Ther. 2017;45(7):983-90.
135. Hagström H, Thiele M, Sharma R, Simon TG, Roelstraete B, Söderling J, et al. Risk of Cancer in Biopsy-Proven Alcohol-Related Liver Disease: A Population-Based Cohort Study of 3410 Persons. Clinical Gastroenterology and Hepatology. 2022;20(4):918-29.e8.
136. Ganne-Carrié N, Nahon P. Hepatocellular carcinoma in the setting of alcohol-related liver disease. Journal of Hepatology. 2019;70(2):284-93.
137. Seitz HK, Stickel F. Molecular mechanisms of alcohol-mediated carcinogenesis. Nature Reviews Cancer. 2007;7(8):599-612.
138. Gao B, Bataller R. Alcoholic liver disease: pathogenesis and new therapeutic targets. Gastroenterology. 2011;141(5):1572-85.
139. Department of Health and Social Care, the Welsh Government, the Department of Health Northern Ireland, Public Health England, NHS England and NHS Improvement, the British Association for the Study of Community Dentistry,. Delivering better oral health: an evidence-based toolkit for prevention - Chapter 12: Alcohol [Internet]. 2021 [updated 9 November 2021];[cited 2023 February 4]. Available from: https://www.gov.uk/government/publications/delivering-better-oral-health-an-evidence-based-toolkit-for-prevention/chapter-12-alcohol#resources.
140. Schomerus G, Leonhard A, Manthey J, Morris J, Neufeld M, Kilian C, et al. The stigma of alcohol-related liver disease and its impact on healthcare. Journal of Hepatology.77(2):P516-24.
141. Singh S, Osna NA, Kharbanda KK. Treatment options for alcoholic and non-alcoholic fatty liver disease: A review. World J Gastroenterol. 2017;23(36):6549-70.
142. Xie YD, Feng B, Gao Y, Wei L. Effect of abstinence from alcohol on survival of patients with alcoholic cirrhosis: A systematic review and meta-analysis. Hepatol Res. 2014;44(4):436-49.
143. Jesse S, Bråthen G, Ferrara M, Keindl M, Ben-Menachem E, Tanasescu R, et al. Alcohol withdrawal syndrome: mechanisms, manifestations, and management. Acta Neurologica Scandinavica. 2017;135(1):4-16.
144. Crabb DW, Im GY, Szabo G, Mellinger JL, Lucey MR. Diagnosis and Treatment of Alcohol-Associated Liver Diseases: 2019 Practice Guidance From the American Association for the Study of Liver Diseases. Hepatology. 2020;71(1):306-33.
145. Heckley GA, Jarl J, Asamoah BO, U GG. How the risk of liver cancer changes after alcohol cessation: a review and meta-analysis of the current literature. BMC Cancer. 2011;11:446.
146. Mitchell MC, Friedman LS, McClain CJ. Medical Management of Severe Alcoholic Hepatitis: Expert Review from the Clinical Practice Updates Committee of the AGA Institute. Clin Gastroenterol Hepatol. 2017;15(1):5-12.
147. Singal AK, Louvet A, Shah VH, Kamath PS. Grand Rounds: Alcoholic Hepatitis. J Hepatol. 2018;69(2):534-43.

148. Thursz MR, Richardson P, Allison M, Austin A, Bowers M, Day CP, et al. Prednisolone or Pentoxifylline for Alcoholic Hepatitis. New England Journal of Medicine. 2015;372(17):1619-28.
149. Louvet A, Naveau S, Abdelnour M, Ramond MJ, Diaz E, Fartoux L, et al. The Lille model: a new tool for therapeutic strategy in patients with severe alcoholic hepatitis treated with steroids. Hepatology. 2007;45(6):1348-54.
150. Mathurin P, O'Grady J, Carithers RL, Phillips M, Louvet A, Mendenhall CL, et al. Corticosteroids improve short-term survival in patients with severe alcoholic hepatitis: meta-analysis of individual patient data. Gut. 2011;60(2):255-60.
151. Lv S, Han M, Yi R, Kwon S, Dai C, Wang R. Anti-TNF-α therapy for patients with sepsis: a systematic meta-analysis. Int J Clin Pract. 2014;68(4):520-8.
152. Reinhart K, Karzai W. Anti-tumor necrosis factor therapy in sepsis: Update on clinical trials and lessons learned. Critical Care Medicine. 2001;29(7):S121-S5.
153. Akriviadis E, Botla R, Briggs W, Han S, Reynolds T, Shakil O. Pentoxifylline improves short-term survival in severe acute alcoholic hepatitis: a double-blind, placebo-controlled trial. Gastroenterology. 2000;119(6):1637-48.
154. Blendis L, Dotan I. Anti-TNF therapy for severe acute alcoholic hepatitis: What went wrong? Gastroenterology. 2004;127(5):1637-9.
155. Nguyen-Khac E, Thevenot T, Piquet M-A, Benferhat S, Goria O, Chatelain D, et al. Glucocorticoids plus N-Acetylcysteine in Severe Alcoholic Hepatitis. New England Journal of Medicine. 2011;365(19):1781-9.
156. Shasthry SM, Sharma MK, Shasthry V, Pande A, Sarin SK. Efficacy of Granulocyte Colony-stimulating Factor in the Management of Steroid-Nonresponsive Severe Alcoholic Hepatitis: A Double-Blind Randomized Controlled Trial. Hepatology. 2019;70(3):802-11.
157. Singh V, Sharma AK, Narasimhan RL, Bhalla A, Sharma N, Sharma R. Granulocyte colony-stimulating factor in severe alcoholic hepatitis: a randomized pilot study. Am J Gastroenterol. 2014;109(9):1417-23.
158. Marot A, Singal AK, Moreno C, Deltenre P. Granulocyte colony-stimulating factor for alcoholic hepatitis: A systematic review and meta-analysis of randomised controlled trials. JHEP Rep. 2020;2(5):100139.
159. Stickel F, Datz C, Hampe J, Bataller R. Pathophysiology and Management of Alcoholic Liver Disease: Update 2016. Gut Liver. 2017;11(2):173-88.
160. Marroni CA, Fleck AM, Jr., Fernandes SA, Galant LH, Mucenic M, de Mattos Meine MH, et al. Liver transplantation and alcoholic liver disease: History, controversies, and considerations. World J Gastroenterol. 2018;24(26):2785-805.
161. Burra P, Senzolo M, Adam R, Delvart V, Karam V, Germani G, et al. Liver Transplantation for Alcoholic Liver Disease in Europe: A Study from the ELTR (European Liver Transplant Registry). American Journal of Transplantation. 2010;10(1):138-48.
162. European Association for the Study of the Liver. EASL Clinical Practice Guidelines: Liver transplantation. Journal of Hepatology. 2016;64(2):433-85.
163. Herrick-Reynolds KM, Punchhi G, Greenberg RS, Strauss AT, Boyarsky BJ, Weeks-Groh SR, et al. Evaluation of Early vs Standard Liver Transplant for Alcohol-Associated Liver Disease. JAMA Surg. 2021;156(11):1026-34.

164. NHS Blood and Transplant. How long is the wait for a liver? [Internet]. unknown [[cited 2023 February 4]. Available from: https://www.nhsbt.nhs.uk/organ-transplantation/liver/receiving-a-liver/how-long-is-the-wait-for-a-liver/.
165. Laing RW, Mergental H, Yap C, Kirkham A, Whilku M, Barton D, et al. Viability testing and transplantation of marginal livers (VITTAL) using normothermic machine perfusion: study protocol for an open-label, non-randomised, prospective, single-arm trial. BMJ Open. 2017;7(11):e017733.
166. NHS Blood and Transplant. Annual Report on Liver Transplantation - Report for 2020/2021 (1 April 2011 – 31 March 2021). [Internet]. 2021. [cited 2023 February 4] Available from: https://nhsbtdbe.blob.core.windows.net/umbraco-assets-corp/24593/nhsbt-liver-transplant-report-2021-final.pdf.
167. NHS Blood and Transplant. POL195/14 – Liver Transplantation: Selection Criteria and Recipient Registration. [Internet]. 2022. [cited 2023 February 4] Available from: https://nhsbtdbe.blob.core.windows.net/umbraco-assets-corp/27372/pol195-120822.pdf.
168. Bunchorntavakul C, Chamroonkul N, Chavalitdhamrong D. Bacterial infections in cirrhosis: A critical review and practical guidance. World J Hepatol. 2016;8(6):307-21.
169. Wyke RJ. Problems of bacterial infection in patients with liver disease. Gut. 1987;28(5):623-41.
170. Fernández J, Navasa M, Gómez J, Colmenero J, Vila J, Arroyo V, et al. Bacterial infections in cirrhosis: epidemiological changes with invasive procedures and norfloxacin prophylaxis. Hepatology. 2002;35(1):140-8.
171. Albillos A, Lario M, Álvarez-Mon M. Cirrhosis-associated immune dysfunction: Distinctive features and clinical relevance. Journal of Hepatology. 2014;61(6):1385-96.
172. Gustot T, Fernandez J, Szabo G, Albillos A, Louvet A, Jalan R, et al. Sepsis in alcohol-related liver disease. Journal of Hepatology. 2017;67(5):1031-50.
173. Michelena J, Altamirano J, Abraldes JG, Affò S, Morales-Ibanez O, Sancho-Bru P, et al. Systemic inflammatory response and serum lipopolysaccharide levels predict multiple organ failure and death in alcoholic hepatitis. Hepatology. 2015;62(3):762-72.
174. Bode C, Christian Bode J. Effect of alcohol consumption on the gut. Best Practice & Research Clinical Gastroenterology. 2003;17(4):575-92.
175. Bode JC, Bode C, Heidelbach R, Dürr HK, Martini GA. Jejunal microflora in patients with chronic alcohol abuse. Hepatogastroenterology. 1984;31(1):30-4.
176. Mutlu EA, Gillevet PM, Rangwala H, Sikaroodi M, Naqvi A, Engen PA, et al. Colonic microbiome is altered in alcoholism. Am J Physiol Gastrointest Liver Physiol. 2012;302(9):G966-78.
177. Dubinkina VB, Tyakht AV, Odintsova VY, Yarygin KS, Kovarsky BA, Pavlenko AV, et al. Links of gut microbiota composition with alcohol dependence syndrome and alcoholic liver disease. Microbiome. 2017;5(1):141.
178. Samuelson DR, Shellito JE, Maffei VJ, Tague ED, Campagna SR, Blanchard EE, et al. Alcohol-associated intestinal dysbiosis impairs pulmonary host defense against Klebsiella pneumoniae. PLoS Pathog. 2017;13(6):e1006426.
179. Bellinghausen C, Pletz MW, Rupp J, Witzenrath M, Welsch C, Zeuzem S, et al. Chronic liver disease negatively affects outcome in hospitalised patients with community-acquired pneumonia. Gut. 2021;70(1):221-2.

180. Simet SM, Sisson JH. Alcohol's Effects on Lung Health and Immunity. Alcohol Res. 2015;37(2):199-208.
181. Bunchorntavakul C, Chavalitdhamrong D. Bacterial infections other than spontaneous bacterial peritonitis in cirrhosis. World J Hepatol. 2012;4(5):158-68.
182. Arvaniti V, D'Amico G, Fede G, Manousou P, Tsochatzis E, Pleguezuelo M, et al. Infections in patients with cirrhosis increase mortality four-fold and should be used in determining prognosis. Gastroenterology. 2010;139(4):1246-56, 56.e1-5.
183. Arroyo V, Moreau R, Kamath PS, Jalan R, Ginès P, Nevens F, et al. Acute-on-chronic liver failure in cirrhosis. Nature Reviews Disease Primers. 2016;2(1):16041.
184. Fernández J, Acevedo J, Wiest R, Gustot T, Amoros A, Deulofeu C, et al. Bacterial and fungal infections in acute-on-chronic liver failure: prevalence, characteristics and impact on prognosis. Gut. 2018;67(10):1870-80.
185. Clària J, Stauber RE, Coenraad MJ, Moreau R, Jalan R, Pavesi M, et al. Systemic inflammation in decompensated cirrhosis: Characterization and role in acute-on-chronic liver failure. Hepatology. 2016;64(4):1249-64.
186. Molina PE, Happel KI, Zhang P, Kolls JK, Nelson S. Focus on: Alcohol and the immune system. Alcohol Res Health. 2010;33(1-2):97-108.
187. Lin C-Y, Tsai IF, Ho Y-P, Huang C-T, Lin Y-C, Lin C-J, et al. Endotoxemia contributes to the immune paralysis in patients with cirrhosis. Journal of Hepatology. 2007;46(5):816-26.
188. Kolaczkowska E, Kubes P. Neutrophil recruitment and function in health and inflammation. Nature Reviews Immunology. 2013;13(3):159-75.
189. Lakshman R, Finn A. Neutrophil disorders and their management. Journal of Clinical Pathology. 2001;54(1):7-19.
190. An International Group. Alcoholic Liver Disease: Morphological Manifestations. The Lancet. 1981;317(8222):707-11.
191. Brinkmann V, Reichard U, Goosmann C, Fauler B, Uhlemann Y, Weiss DS, et al. Neutrophil extracellular traps kill bacteria. Science. 2004;303(5663):1532-5.
192. Gierlikowska B, Stachura A, Gierlikowski W, Demkow U. Phagocytosis, Degranulation and Extracellular Traps Release by Neutrophils—The Current Knowledge, Pharmacological Modulation and Future Prospects. Frontiers in Pharmacology. 2021;12.
193. Tak T, Tesselaar K, Pillay J, Borghans JAM, Koenderman L. What's your age again? Determination of human neutrophil half-lives revisited. Journal of Leukocyte Biology. 2013;94(4):595-601.
194. Mayadas TN, Cullere X, Lowell CA. The multifaceted functions of neutrophils. Annu Rev Pathol. 2014;9:181-218.
195. Furze RC, Rankin SM. Neutrophil mobilization and clearance in the bone marrow. Immunology. 2008;125(3):281-8.
196. Ballard HS. The hematological complications of alcoholism. Alcohol Health Res World. 1997;21(1):42-52.
197. Shi X, DeLucia AL, Bao J, Zhang P. Alcohol abuse and disorder of granulopoiesis. Pharmacol Ther. 2019;198:206-19.
198. Forrest EH, Storey N, Sinha R, Atkinson SR, Vergis N, Richardson P, et al. Baseline neutrophil-to-lymphocyte ratio predicts response to corticosteroids and is associated with infection and renal dysfunction in alcoholic hepatitis. Aliment Pharmacol Ther. 2019;50(4):442-53.

199. Maas SL, Soehnlein O, Viola JR. Organ-Specific Mechanisms of Transendothelial Neutrophil Migration in the Lung, Liver, Kidney, and Aorta. Front Immunol. 2018;9:2739.
200. Steinhoff G, Behrend M, Schrader B, Duijvestijn AM, Wonigeit K. Expression patterns of leukocyte adhesion ligand molecules on human liver endothelia. Lack of ELAM-1 and CD62 inducibility on sinusoidal endothelia and distinct distribution of VCAM-1, ICAM-1, ICAM-2, and LFA-3. Am J Pathol. 1993;142(2):481-8.
201. Weston CJ, Shepherd EL, Claridge LC, Rantakari P, Curbishley SM, Tomlinson JW, et al. Vascular adhesion protein-1 promotes liver inflammation and drives hepatic fibrosis. J Clin Invest. 2015;125(2):501-20.
202. Kono H, Uesugi T, Froh M, Rusyn I, Bradford BU, Thurman RG. ICAM-1 is involved in the mechanism of alcohol-induced liver injury: studies with knockout mice. American Journal of Physiology-Gastrointestinal and Liver Physiology. 2001;280(6):G1289-G95.
203. von Meijenfeldt FA, Stravitz RT, Zhang J, Adelmeijer J, Zen Y, Durkalski V, et al. Generation of neutrophil extracellular traps in patients with acute liver failure is associated with poor outcome. Hepatology. 2022;75(3):623-33.
204. Mookerjee RP, Stadlbauer V, Lidder S, Wright GAK, Hodges SJ, Davies NA, et al. Neutrophil dysfunction in alcoholic hepatitis superimposed on cirrhosis is reversible and predicts the outcome. Hepatology. 2007;46(3):831-40.
205. Sônego F, Castanheira FV, Ferreira RG, Kanashiro A, Leite CA, Nascimento DC, et al. Paradoxical Roles of the Neutrophil in Sepsis: Protective and Deleterious. Front Immunol. 2016;7:155.
206. Bukong TN, Cho Y, Iracheta-Vellve A, Saha B, Lowe P, Adejumo A, et al. Abnormal neutrophil traps and impaired efferocytosis contribute to liver injury and sepsis severity after binge alcohol use. J Hepatol. 2018;69(5):1145-54.
207. Tritto G, Bechlis Z, Stadlbauer V, Davies N, Francés R, Shah N, et al. Evidence of neutrophil functional defect despite inflammation in stable cirrhosis. J Hepatol. 2011;55(3):574-81.
208. Taïeb J, Delarche C, Ethuin F, Selloum S, Poynard T, Gougerot-Pocidalo MA, et al. Ethanol-induced inhibition of cytokine release and protein degranulation in human neutrophils. J Leukoc Biol. 2002;72(6):1142-7.
209. Lu Y, Chang N, Zhao X, Xue R, Liu J, Yang L, et al. Activated Neutrophils Secrete Chitinase-Like 1 and Attenuate Liver Inflammation by Inhibiting Pro-Inflammatory Macrophage Responses. Front Immunol. 2022;13:824385.
210. Yang W, Tao Y, Wu Y, Zhao X, Ye W, Zhao D, et al. Neutrophils promote the development of reparative macrophages mediated by ROS to orchestrate liver repair. Nat Commun. 2019;10(1):1076.
211. Mattos MS, Lopes ME, de Araujo AM, Alvarenga DM, Nakagaki BN, Mafra K, et al. Prolonged neutrophil survival at necrotic sites is a fundamental feature for tissue recovery and resolution of hepatic inflammation. J Leukoc Biol. 2020;108(4):1199-213.
212. Wang J, Hossain M, Thanabalasuriar A, Gunzer M, Meininger C, Kubes P. Visualizing the function and fate of neutrophils in sterile injury and repair. Science. 2017;358(6359):111-6.
213. Cunningham RP, Porat-Shliom N. Liver Zonation – Revisiting Old Questions With New Technologies. Frontiers in Physiology. 2021;12.

214. Huch M, Gehart H, van Boxtel R, Hamer K, Blokzijl F, Verstegen M, et al. Long-term Culture of Genome-Stable Bipotent Stem Cells From Adult Human Liver. Cell. 2015;160(1-2).
215. Berry MN, Friend DS. High-Yield Preparation Of Isolated Rat Liver Parenchymal Cells: A Biochemical and Fine Structural Study. J Cell Biol. 1969;43(3):506-20.
216. Guguen-Guillouzo C, Campion JP, Brissot P, Glaise D, Launois B, Bourel M, et al. High yield preparation of isolated human adult hepatocytes by enzymatic perfusion of the liver. Cell Biology International Reports. 1982;6(6):625-8.
217. Bissell DM, Guzelian PS. Phenotypic Stability of Adult Rat Hepatocytes in Primary Monolayer Culture. 1980;349(1):85-98.
218. Guguen-Guillouzo C, Guillouzo A. Modulation of functional activities in cultured rat hepatocytes. Mol Cell Biochem. 1983;53-54(1-2):35-56.
219. Clement B, Guguen-Guillouzo C, Campion J-P, Glaise D, Bourel M, Guillouzo A. Long-Term Co-Cultures of Adult Human Hepatocytes with Rat Liver Epithelial Cells: Modulation of Albumin Secretion and Accumulation of Extracellular Material. Hepatology. 1984;4(3):373-80.
220. Dunn JC, Tompkins RG, Yarmush ML. Long-term in vitro function of adult hepatocytes in a collagen sandwich configuration. Biotechnol Prog. 1991;7(3):237-45.
221. Bhogal RH, Hodson J, Bartlett DC, Weston CJ, Curbishley SM, Haughton E, et al. Isolation of Primary Human Hepatocytes from Normal and Diseased Liver Tissue: A One Hundred Liver Experience. PLoS ONE. 2011;6(3):e18222.
222. Maurice M, Rogier E, Cassio D, Feldmann G. Formation of Plasma Membrane Domains in Rat Hepatocytes and Hepatoma Cell Lines in Culture. Journal of cell science. 1988;90 (Pt 1).
223. Moghe PV, Berthiaume F, Ezzell RM, Toner M, Tompkins RG, Yarmush ML. Culture matrix configuration and composition in the maintenance of hepatocyte polarity and function. Biomaterials. 1996;17(3):373-85.
224. Tuschl G, Mueller S. Effects of cell culture conditions on primary rat hepatocytes—Cell morphology and differential gene expression. 2006;218(2-3):205-15.
225. Heslop JA, Rowe C, Walsh J, Sison-Young R, Jenkins R, Kamalian L, et al. Mechanistic evaluation of primary human hepatocyte culture using global proteomic analysis reveals a selective dedifferentiation profile. Arch Toxicol. 2017;91(1):439-52.
226. Webber EM, Godowski PJ, Fausto N. In vivo response of hepatocytes to growth factors requires an initial priming stimulus. 1994;19(2):489-97.
227. Michalopoulos GK. Liver Regeneration. Science. 1997;276(5309):60-6.
228. Levy G, Bomze D, Heinz S, Ramachandran SD, Noerenberg A, Cohen M, et al. Long-term culture and expansion of primary human hepatocytes. Nature Biotechnology. 2015;33(12):1264-71.
229. Eva R, Bram DC, Joery DK, Tamara V, Geert B, Vera R, et al. Strategies for immortalization of primary hepatocytes. J Hepatol. 2014;61(4):925-43.
230. Knowles B, Howe C, Aden D. Human hepatocellular carcinoma cell lines secrete the major plasma proteins and hepatitis B surface antigen. Science. 1980;209(4455):497-9.
231. Sefried S, Häring HU, Weigert C, Eckstein SS. Suitability of hepatocyte cell lines HepG2, AML12 and THLE-2 for investigation of insulin signalling and hepatokine gene expression. Open Biol. 82018.
232. Guo L, Dial S, Shi L, Branham W, Liu J, Fang J-L, et al. Similarities and Differences in the Expression of Drug-Metabolizing Enzymes between Human Hepatic Cell Lines and Primary Human Hepatocytes. Drug Metabolism and Disposition. 2011;39(3):528-38.

233. Westerink WMA, Schoonen WGEJ. Phase II enzyme levels in HepG2 cells and cryopreserved primary human hepatocytes and their induction in HepG2 cells. Toxicology in Vitro. 2007;21(8):1592-602.
234. Cederbaum A, Wu D, Mari M, Bai J. CYP2E1-dependent Toxicity and Oxidative Stress in HepG2 Cells. Free radical biology & medicine. 2001;31(12).
235. Zanelli U, Caradonna NP, Hallifax D, Turlizzi E, Houston JB. Comparison of Cryopreserved HepaRG Cells with Cryopreserved Human Hepatocytes for Prediction of Clearance for 26 Drugs. Drug Metabolism and Disposition. 2012;40(1):104-10.
236. Yokoyama Y, Sasaki Y, Terasaki N, Kawataki T, Takekawa K, Iwase Y, et al. Comparison of Drug Metabolism and Its Related Hepatotoxic Effects in HepaRG, Cryopreserved Human Hepatocytes, and HepG2 Cell Cultures. Biological and Pharmaceutical Bulletin. 2018;41(5):722-32.
237. Bucher S, Tête A, Podechard N, Liamin M, Le Guillou D, Chevanne M, et al. Co-exposure to benzo[a]pyrene and ethanol induces a pathological progression of liver steatosis in vitro and in vivo. Scientific Reports. 2018;8(1).
238. Gerets HHJ, Tilmant K, Gerin B, Chanteux H, Depelchin BO, Dhalluin S, et al. Characterization of primary human hepatocytes, HepG2 cells, and HepaRG cells at the mRNA level and CYP activity in response to inducers and their predictivity for the detection of human hepatotoxins. Cell Biology and Toxicology. 2012;28(2):69-87.
239. Cerec V, Glaise D, Garnier D, Morosan S, Turlin B, Drenou B, et al. Transdifferentiation of hepatocyte-like cells from the human hepatoma HepaRG cell line through bipotent progenitor. Hepatology. 2007;45(4):957-67.
240. Tian L, Prasad N, Jang Y-Y. In Vitro Modeling of Alcohol-Induced Liver Injury Using Human-Induced Pluripotent Stem Cells. In: Nagy A, Turksen K, editors. Patient-Specific Induced Pluripotent Stem Cell Models: Generation and Characterization. New York, NY: Springer New York; 2016. p. 271-83.
241. Baxter M, Withey S, Harrison S, Segeritz C-P, Zhang F, Atkinson-Dell R, et al. Phenotypic and functional analyses show stem cell-derived hepatocyte-like cells better mimic fetal rather than adult hepatocytes. Journal of Hepatology. 2015;62(3):581-9.
242. Goldring C, Antoine DJ, Bonner F, Crozier J, Denning C, Fontana RJ, et al. Stem cell-derived models to improve mechanistic understanding and prediction of human drug-induced liver injury. Hepatology. 2017;65(2):710-21.
243. Waterston RH, Lindblad-Toh K, Birney E, Rogers J, Abril JF, Agarwal P, et al. Initial sequencing and comparative analysis of the mouse genome. Nature. 2002;420(6915):520-62.
244. Perlman RL. Mouse models of human disease: An evolutionary perspective. Evol Med Public Health. 2016;2016(1):170-6.
245. McKenzie R, Fried M, Sallie R, Conjeevaram H, Di Bisceglie A, Park Y, et al. Hepatic Failure and Lactic Acidosis Due to Fialuridine (FIAU), an Investigational Nucleoside Analogue for Chronic Hepatitis B. The New England journal of medicine. 1995;333(17).
246. Xu D, Nishimura T, Nishimura S, Zhang H, Zheng M, Guo Y-Y, et al. Fialuridine Induces Acute Liver Failure in Chimeric TK-NOG Mice: A Model for Detecting Hepatic Drug Toxicity Prior to Human Testing. PLoS Medicine. 2014;11(4):e1001628.
247. Brol MJ, Rösch F, Schierwagen R, Magdaleno F, Uschner FE, Manekeller S, et al. Combination of CCl(4) with alcoholic and metabolic injuries mimics human liver fibrosis. Am J Physiol Gastrointest Liver Physiol. 2019;317(2):G182-g94.

248. Lieber CS, Decarli LM, Sorrell MF. Experimental methods of ethanol administration. Hepatology. 1989;10(4):501-10.
249. Ghosh Dastidar S, Warner JB, Warner DR, McClain CJ, Kirpich IA. Rodent Models of Alcoholic Liver Disease: Role of Binge Ethanol Administration. Biomolecules. 2018;8(1).
250. Bertola A, Mathews S, Ki SH, Wang H, Gao B. Mouse model of chronic and binge ethanol feeding (the NIAAA model). Nature Protocols. 2013;8(3):627-37.
251. Sheriff L, Khan RS, Saborano R, Wilkin R, Luu NT, Gunther UL, et al. Alcoholic hepatitis and metabolic disturbance in female mice: a more tractable model than Nrf2 (-/-) animals. Dis Model Mech. 2020;13(12).
252. Holmes RS, Duley JA, Algar EM, Mather PB, Rout UK. Biochemical and Genetic Studies on Enzymes of Alcohol Metabolism: The Mouse as a Model Organism for Human Studies. Alcohol and Alcoholism. 1986;21(1):41-56.
253. Heit C, Dong H, Chen Y, Shah YM, Thompson DC, Vasiliou V. Transgenic Mouse Models for Alcohol Metabolism, Toxicity and Cancer. Adv Exp Med Biol. 2015;815:375-87.
254. Liu Y, Meyer C, Xu C, Weng H, Hellerbrand C, Dijke Pt, et al. Animal models of chronic liver diseases. American Journal of Physiology-Gastrointestinal and Liver Physiology. 2013;304(5):G449-G68.
255. Landry J, Bernier D, Ouellet C, Goyette R, Marceau N. Spheroidal aggregate culture of rat liver cells: histotypic reorganization, biomatrix deposition, and maintenance of functional activities. The Journal of Cell Biology. 1985;101(3):914-23.
256. Li A, Colburn S, Beck D. A Simplified Method for the Culturing of Primary Adult Rat and Human Hepatocytes as Multicellular Spheroids. In vitro cellular & developmental biology : journal of the Tissue Culture Association. 1992;28A(9-10).
257. Bell CC, Hendriks DFG, Moro SML, Ellis E, Walsh J, Renblom A, et al. Characterization of primary human hepatocyte spheroids as a model system for drug-induced liver injury, liver function and disease. Scientific Reports. 2016;6(1):25187.
258. Ramaiahgari SC, den Braver MW, Herpers B, Terpstra V, Commandeur JNM, van de Water B, et al. A 3D in vitro model of differentiated HepG2 cell spheroids with improved liver-like properties for repeated dose high-throughput toxicity studies. Archives of Toxicology. 2014;88(5):1083-95.
259. Luckert C, Schulz C, Lehmann N, Thomas M, Hofmann U, Hammad S, et al. Comparative Analysis of 3D Culture Methods on Human HepG2 Cells. Archives of toxicology. 2017;91(1).
260. Gunness P, Mueller D, Shevchenko V, Heinzle E, Ingelman-Sundberg M, Noor F. 3D Organotypic Cultures of Human HepaRG Cells: A Tool for In Vitro Toxicity Studies. Toxicological Sciences. 2013;133(1):67-78.
261. Baze A, Parmentier C, Hendriks DFG, Hurrell T, Heyd B, Bachellier P, et al. Three-Dimensional Spheroid Primary Human Hepatocytes in Monoculture and Coculture with Nonparenchymal Cells. Tissue Engineering Part C: Methods. 2018;24(9):534-45.
262. Simian M, Bissell MJ. Organoids: A historical perspective of thinking in three dimensions. J Cell Biol. 2017;216(1):31-40.
263. Clevers H. Modeling Development and Disease with Organoids. Cell. 2016;165(7):1586-97.
264. Qian X, Song H, Ming G-l. Brain organoids: advances, applications and challenges. Development. 2019;146(8).

265. Post Y, Puschhof J, Beumer J, Kerkkamp H, de Bakker M, Slagboom J, et al. Snake Venom Gland Organoids. Cell. 2020;180(2).
266. Sato T, Vries RG, Snippert HJ, Wetering Mvd, Barker N, Stange DE, et al. Single Lgr5 stem cells build crypt-villus structures in vitro without a mesenchymal niche. Nature. 2009;459(7244):262-5.
267. Huch M, Dorrell C, Boj SF, van Es JH, Li VS, van de Wetering M, et al. In vitro expansion of single Lgr5+ liver stem cells induced by Wnt-driven regeneration. Nature. 2013;494(7436):247-50.
268. Singal AK, Kamath PS. Model for End-stage Liver Disease. J Clin Exp Hepatol. 2013;3(1):50-60.
269. Barber K, Madden S, Allen J, Collett D, Neuberger J, Gimson A, et al. Elective Liver Transplant List Mortality: Development of a United Kingdom End-Stage Liver Disease Score. Transplantation. 2011;92(4):469-76.
270. Forrest EH, Evans CD, Stewart S, Phillips M, Oo YH, McAvoy NC, et al. Analysis of factors predictive of mortality in alcoholic hepatitis and derivation and validation of the Glasgow alcoholic hepatitis score. Gut. 2005;54(8):1174-9.
271. Alcohol Change UK. Unit calculator [Internet]. date unknown [[cited 2023 March 4]. Available from: https://alcoholchange.org.uk/alcohol-facts/interactive-tools/unit-calculator.
272. Hazeldine J, Harris P, Chapple IL, Grant M, Greenwood H, Livesey A, et al. Impaired neutrophil extracellular trap formation: a novel defect in the innate immune system of aged individuals. Aging Cell. 2014;13(4):690-8.
273. Fernando EH, Dicay M, Stahl M, Gordon MH, Vegso A, Baggio C, et al. A simple, cost-effective method for generating murine colonic 3D enteroids and 2D monolayers for studies of primary epithelial cell function. American Journal of Physiology-Gastrointestinal and Liver Physiology. 2017;313(5):G467-G75.
274. Tsai YH, Czerwinski M, Wu A, Dame MK, Attili D, Hill E, et al. A Method for Cryogenic Preservation of Human Biopsy Specimens and Subsequent Organoid Culture. Cell Mol Gastroenterol Hepatol. 2018;6(2):218-22.e7.
275. STEMCELL Technologies. How to Thaw Intestinal Organoids [Internet]. 2021 [updated March 2021];[cited 2023 March 11]. Version 1.0.0. Available from: https://www.stemcell.com/how-to-thaw-intestinal-organoids.html.
276. Ramachandran P, Dobie R, Wilson-Kanamori JR, Dora EF, Henderson BEP, Luu NT, et al. Resolving the fibrotic niche of human liver cirrhosis at single-cell level. Nature. 2019;575(7783):512-8.
277. Amezquita R, Lun A, Hicks S, Gottardo R, O'Callaghan A. Orchestrating Single-Cell Analysis with Bioconductor [Internet]: Bioconductor; 2022 [cited; 2023 February 25]. Available from: https://bioconductor.org/books/release/OSCA/
278. Liberzon A, Birger C, Thorvaldsdóttir H, Ghandi M, Mesirov JP, Tamayo P. The Molecular Signatures Database (MSigDB) hallmark gene set collection. Cell Syst. 2015;1(6):417-25.
279. Subramanian A, Tamayo P, Mootha VK, Mukherjee S, Ebert BL, Gillette MA, et al. Gene set enrichment analysis: A knowledge-based approach for interpreting genome-wide expression profiles. Proceedings of the National Academy of Sciences. 2005;102(43):15545-50.

280. Public Health England. Monitoring alcohol consumption and harm during the COVID-19 pandemic: summary [Internet]. 2022 [[cited 2022 July 24]. Available from: https://www.gov.uk/government/publications/alcohol-consumption-and-harm-during-the-covid-19-pandemic/monitoring-alcohol-consumption-and-harm-during-the-covid-19-pandemic-summary.
281. Public Health England. Working years of life lost due to alcohol mortality. [Internet]. 2020. [cited 2022 July 24] Available from: https://assets.publishing.service.gov.uk/government/uploads/system/uploads/attachment_data/file/901239/Working_years_of_life_lost_due_to_alcohol_mortality.pdf.
282. Hosseini N, Shor J, Szabo G. Alcoholic Hepatitis: A Review. Alcohol Alcohol. 2019;54(4):408-16.
283. Innes H, Morling JR, Aspinall EA, Goldberg DJ, Hutchinson SJ, Guha IN. Late diagnosis of chronic liver disease in a community cohort (UK biobank): determinants and impact on subsequent survival. Public Health. 2020;187:165-71.
284. Mansour D, McPherson S. Management of decompensated cirrhosis. Clin Med (Lond). 2018;18(Suppl 2):s60-s5.
285. Chan C, Levitsky J. Infection and Alcoholic Liver Disease. Clin Liver Dis. 2016;20(3):595-606.
286. Noor MT, Manoria P. Immune Dysfunction in Cirrhosis. J Clin Transl Hepatol. 2017;5(1):50-8.
287. Xu R, Huang H, Zhang Z, Wang FS. The role of neutrophils in the development of liver diseases. Cell Mol Immunol. 2014;11(3):224-31.
288. Piotrowski D, Sączewska-Piotrowska A, Jaroszewicz J, Boroń-Kaczmarska A. Lymphocyte-To-Monocyte Ratio as the Best Simple Predictor of Bacterial Infection in Patients with Liver Cirrhosis. Int J Environ Res Public Health. 2020;17(5).
289. Maruyama S, Hirayama C, Yamamoto S, Koda M, Udagawa A, Kadowaki Y, et al. Red blood cell status in alcoholic and non-alcoholic liver disease. Journal of Laboratory and Clinical Medicine. 2001;138(5):332-7.
290. Weiskopf D, Weinberger B, Grubeck-Loebenstein B. The aging of the immune system. Transpl Int. 2009;22(11):1041-50.
291. Erol A, Karpyak VM. Sex and gender-related differences in alcohol use and its consequences: Contemporary knowledge and future research considerations. Drug and Alcohol Dependence. 2015;156:1-13.
292. Office for National Statistics (ONS). Alcohol-specific deaths in the UK: registered in 2020 [Internet]. 2021 [[cited 2022 June 16]. Available from: https://www.ons.gov.uk/peoplepopulationandcommunity/healthandsocialcare/causesofdeath/bulletins/alcoholrelateddeathsintheunitedkingdom/registeredin2020.
293. Bhala N, Cézard G, Ward HJT, Bansal N, Bhopal R, Health obotS, et al. Ethnic Variations in Liver- and Alcohol-Related Disease Hospitalisations and Mortality: The Scottish Health and Ethnicity Linkage Study. Alcohol and Alcoholism. 2016;51(5):593-601.
294. Basra S, Anand BS. Definition, epidemiology and magnitude of alcoholic hepatitis. World J Hepatol. 2011;3(5):108-13.
295. McCormick KA, Cochran NE, Back AL, Merrill JO, Williams EC, Bradley KA. How primary care providers talk to patients about alcohol: a qualitative study. J Gen Intern Med. 2006;21(9):966-72.

296. Cylwik B, Chrostek L. Disturbances of folic acid and homocysteine metabolism in alcohol abuse. Pol Merkur Lekarski. 2011;30(178):295-9.
297. Gonzalez-Casas R, Jones EA, Moreno-Otero R. Spectrum of anemia associated with chronic liver disease. World J Gastroenterol. 2009;15(37):4653-8.
298. Raka J, Aishwariya Brigit G, Shubham N. Haematological Changes in Alcohol and Substance Use Disorders- An Overview. International Archives of Substance Abuse and Rehabilitation. 2020;2(1).
299. Hampson P, Dinsdale RJ, Wearn CM, Bamford AL, Bishop JRB, Hazeldine J, et al. Neutrophil Dysfunction, Immature Granulocytes, and Cell-free DNA are Early Biomarkers of Sepsis in Burn-injured Patients: A Prospective Observational Cohort Study. Annals of Surgery. 2017;265(6).
300. Ayres LS, Sgnaolin V, Munhoz TP. Immature granulocytes index as early marker of sepsis. Int J Lab Hematol. 2019;41(3):392-6.
301. Levine RF, Spivak JL, Meagher RC, Sieber F. Effect of ethanol on thrombopoiesis. British Journal of Haematology. 1986;62(2):345-54.
302. Afdhal N, McHutchison J, Brown R, Jacobson I, Manns M, Poordad F, et al. Thrombocytopenia associated with chronic liver disease. Journal of Hepatology. 2008;48(6):1000-7.
303. Chauhan A, Adams DH, Watson SP, Lalor PF. Platelets: No longer bystanders in liver disease. Hepatology. 2016;64(5):1774-84.
304. Blériot C, Dupuis T, Jouvion G, Eberl G, Disson O, Lecuit M. Liver-resident macrophage necroptosis orchestrates type 1 microbicidal inflammation and type-2-mediated tissue repair during bacterial infection. Immunity. 2015;42(1):145-58.
305. Drifte G, Dunn-Siegrist I, Tissières P, Pugin J. Innate immune functions of immature neutrophils in patients with sepsis and severe systemic inflammatory response syndrome. Crit Care Med. 2013;41(3):820-32.
306. Matos LC, Batista P, Monteiro N, Ribeiro J, Cipriano MA, Henriques P, et al. Lymphocyte subsets in alcoholic liver disease. World J Hepatol. 2013;5(2):46-55.
307. Sarin S, Pamecha V, Sinha PK, Patil N, Mahapatra N. Neutrophil Lymphocyte Ratio can Preempt Development of Sepsis After Adult Living Donor Liver Transplantation. J Clin Exp Hepatol. 2022;12(4):1142-9.
308. Swain P, Romero N, Dranka BP. Modulation of oxidative burst with exposure to cytokines in neutrophil cell activation. The Journal of Immunology. 2018;200(1 Supplement):49.26-49.26.
309. Aljohani W, Chan BPH, Yaghoobi M. Role of N-Acetylcysteine in the Treatment of Acute Nonacetaminophen, Nonalcoholic and Nonviral Hepatitis: A Meta-analysis. Journal of the Canadian Association of Gastroenterology. 2020;4(3):125-30.
310. Yoon SM, Gerasimidou D, Kuwahara R, Hytiroglou P, Yoo JE, Park YN, et al. Epithelial cell adhesion molecule (EpCAM) marks hepatocytes newly derived from stem/progenitor cells in humans. Hepatology. 2011;53(3):964-73.
311. Ferreira-Gonzalez S, Rodrigo-Torres D, Gadd VL, Forbes SJ. Cellular Senescence in Liver Disease and Regeneration. Semin Liver Dis. 2021;41(1):50-66.
312. Odena G, Chen J, Lozano JJ, Altamirano J, Rodrigo-Torres D, Affo S, et al. LPS-TLR4 Pathway Mediates Ductular Cell Expansion in Alcoholic Hepatitis. Scientific Reports. 2016;6(1):35610.

313. Jia L, Chang X, Qian S, Liu C, Lord CC, Ahmed N, et al. Hepatocyte toll-like receptor 4 deficiency protects against alcohol-induced fatty liver disease. Mol Metab. 2018;14:121-9.
314. Holt AP, Salmon M, Buckley CD, Adams DH. Immune interactions in hepatic fibrosis. Clin Liver Dis. 2008;12(4):861-82, x.
315. Haydon G, Lalor PF, Hubscher SG, Adams DH. Lymphocyte recruitment to the liver in alcoholic liver disease. Alcohol. 2002;27(1):29-36.
316. Celli R, Zhang X. Pathology of Alcoholic Liver Disease. J Clin Transl Hepatol. 2014;2(2):103-9.
317. Dominguez M, Miquel R, Colmenero J, Moreno M, García–Pagán JC, Bosch J, et al. Hepatic Expression of CXC Chemokines Predicts Portal Hypertension and Survival in Patients With Alcoholic Hepatitis. Gastroenterology. 2009;136(5):1639-50.
318. Lalor PF, Adams DH. Adhesion of lymphocytes to hepatic endothelium. Mol Pathol. 1999;52(4):214-9.
319. Afford SC, Fisher NC, Neil DA, Fear J, Brun P, Hubscher SG, et al. Distinct patterns of chemokine expression are associated with leukocyte recruitment in alcoholic hepatitis and alcoholic cirrhosis. J Pathol. 1998;186(1):82-9.
320. McDonald B, McAvoy EF, Lam F, Gill V, de la Motte C, Savani RC, et al. Interaction of CD44 and hyaluronan is the dominant mechanism for neutrophil sequestration in inflamed liver sinusoids. J Exp Med. 2008;205(4):915-27.
321. McDonald B, Jenne CN, Zhuo L, Kimata K, Kubes P. Kupffer cells and activation of endothelial TLR4 coordinate neutrophil adhesion within liver sinusoids during endotoxemia. American Journal of Physiology-Gastrointestinal and Liver Physiology. 2013;305(11):G797-G806.
322. Theise ND. Histopathology of alcoholic liver disease. Clinical Liver Disease. 2013;2(2):64-7.
323. Sancho-Bru P, Altamirano J, Rodrigo-Torres D, Coll M, Millán C, José Lozano J, et al. Liver progenitor cell markers correlate with liver damage and predict short-term mortality in patients with alcoholic hepatitis. Hepatology. 2012;55(6):1931-41.
324. Sugimoto H, Yang C, LeBleu VS, Soubasakos MA, Giraldo M, Zeisberg M, et al. BMP-7 functions as a novel hormone to facilitate liver regeneration. The FASEB Journal. 2007;21(1):256-64.
325. Coltman N, Coke B, Chatzi K, Shepherd E, Lalor P, Schulz-Utermoehl T, et al. Application of HepG2/C3A liver spheroids as a model system for genotoxicity studies. Toxicology Letters. 2021;345.
326. Moravcová A, Červinková Z, Kučera O, Mezera V, Rychtrmoc D, Lotková H. The effect of oleic and palmitic acid on induction of steatosis and cytotoxicity on rat hepatocytes in primary culture. Physiol Res. 2015;64(Suppl 5):S627-36.
327. Shepherd EL, Karim S, Newsome PN, Lalor PF. Inhibition of vascular adhesion protein-1 modifies hepatic steatosis in vitro and in vivo. World J Hepatol. 2020;12(11):931-48.
328. Limaye PB, Alarcón G, Walls AL, Nalesnik MA, Michalopoulos GK, Demetris AJ, et al. Expression of specific hepatocyte and cholangiocyte transcription factors in human liver disease and embryonic development. Lab Invest. 2008;88(8):865-72.
329. Walesky C, Apte U. Role of hepatocyte nuclear factor 4α (HNF4α) in cell proliferation and cancer. Gene Expr. 2015;16(3):101-8.

330. Jetter A, Kullak-Ublick GA. Drugs and hepatic transporters: A review. Pharmacological Research. 2020;154:104234.
331. Olsavsky Goyak KM, Laurenzana EM, Omiecinski CJ. Hepatocyte differentiation. Methods Mol Biol. 2010;640:115-38.
332. Lu Y, Cederbaum AI. Cytochrome P450s and Alcoholic Liver Disease. Curr Pharm Des. 2018;24(14):1502-17.
333. Gaskell H, Sharma P, Colley HE, Murdoch C, Williams DP, Webb SD. Characterization of a functional C3A liver spheroid model. Toxicol Res (Camb). 2016;5(4):1053-65.
334. Štampar M, Sedighi Frandsen H, Rogowska-Wrzesinska A, Wrzesinski K, Filipič M, Žegura B. Hepatocellular carcinoma (HepG2/C3A) cell-based 3D model for genotoxicity testing of chemicals. Science of The Total Environment. 2021;755:143255.
335. Cederbaum AI. Methodology to assay CYP2E1 mixed function oxidase catalytic activity and its induction. Redox Biol. 2014;2:1048-54.
336. Förster F, Volz A, Fricker G. Compound profiling for ABCC2 (MRP2) using a fluorescent microplate assay system. European Journal of Pharmaceutics and Biopharmaceutics. 2008;69(1):396-403.
337. Huch M, Dollé L. The plastic cellular states of liver cells: Are EpCAM and Lgr5 fit for purpose? Hepatology. 2016;64(2):652-62.
338. Brazovskaja A, Treutlein B, Camp JG. High-throughput single-cell transcriptomics on organoids. Current Opinion in Biotechnology. 2019;55:167-71.
339. Yang F, Zhang F, Ji X, Jiang X, Xue M, Yu H, et al. Secretory galectin-3 induced by glucocorticoid stress triggers stemness exhaustion of hepatic progenitor cells. Journal of Biological Chemistry. 2020;295(49):16852-62.
340. Hsu DK, Dowling CA, Jeng K-CG, Chen J-T, Yang R-Y, Liu F-T. Galectin-3 expression is induced in cirrhotic liver and hepatocellular carcinoma. International Journal of Cancer. 1999;81(4):519-26.
341. Hara A, Niwa M, Noguchi K, Kanayama T, Niwa A, Matsuo M, et al. Galectin-3 as a Next-Generation Biomarker for Detecting Early Stage of Various Diseases. Biomolecules. 2020;10(3).
342. Kopper O, de Witte CJ, Lõhmussaar K, Valle-Inclan JE, Hami N, Kester L, et al. An organoid platform for ovarian cancer captures intra- and interpatient heterogeneity. Nat Med. 2019;25(5):838-49.
343. Hughes CS, Postovit LM, Lajoie GA. Matrigel: a complex protein mixture required for optimal growth of cell culture. Proteomics. 2010;10(9):1886-90.
344. Francis H, Glaser S, Ueno Y, LeSage G, Marucci L, Benedetti A, et al. cAMP stimulates the secretory and proliferative capacity of the rat intrahepatic biliary epithelium through changes in the PKA/Src/MEK/ERK1/2 pathway. Journal of Hepatology. 2004;41(4):528-37.
345. Chomczynski P, Sacchi N. Single-step method of RNA isolation by acid guanidinium thiocyanate-phenol-chloroform extraction. Anal Biochem. 1987;162(1):156-9.
346. Yoon S-M, Gerasimidou D, Kuwahara R, Hytiroglou P, Yoo JE, Park YN, et al. Epithelial cell adhesion molecule (EpCAM) marks hepatocytes newly derived from stem/progenitor cells in humans. Hepatology. 2011;53(3):964-73.
347. Karsten E, Breen E, Herbert BR. Red blood cells are dynamic reservoirs of cytokines. Scientific Reports. 2018;8(1):3101.

348. Li Z, Mu D, Liu C, Xin M, Fu S, Li S, et al. The Impact of Ammonium Chloride-Based Erythrocyte Lysis Process on Banked Adipose-Derived Stem Cells. Biopreserv Biobank. 2022;20(3):229-37.
349. Bui BN, Boretto M, Kobayashi H, van Hoesel M, Steba GS, van Hoogenhuijze N, et al. Organoids can be established reliably from cryopreserved biopsy catheter-derived endometrial tissue of infertile women. Reproductive BioMedicine Online. 2020;41(3):465-73.
350. Ratziu V, Charlotte F, Heurtier A, Gombert S, Giral P, Bruckert E, et al. Sampling Variability of Liver Biopsy in Nonalcoholic Fatty Liver Disease. Gastroenterology. 2005;128(7):1898-906.
351. McQuitty CE, Williams R, Chokshi S, Urbani L. Immunomodulatory Role of the Extracellular Matrix Within the Liver Disease Microenvironment. Frontiers in Immunology. 2020;11.
352. Wells RG. The role of matrix stiffness in regulating cell behavior. Hepatology. 2008;47(4):1394-400.
353. Orman ES, Barritt IV AS, Wheeler SB, Hayashi PH. Declining liver utilization for transplantation in the United States and the impact of donation after cardiac death. Liver Transplantation. 2013;19(1):59-68.
354. Alexandrova K, Griesel C, Barthold M, Heuft HG, Ott M, Winkler M, et al. Large-scale isolation of human hepatocytes for therapeutic application. Cell Transplant. 2005;14(10):845-53.
355. Boyd NM, Reade PC. Differences between preneoplastic cells, neoplastic cells and their normal counterparts. Journal of Oral Pathology & Medicine. 1988;17(6):257-65.
356. Desjonqueres E, Campani C, Marra F, Zucman-Rossi J, Nault J-C. Preneoplastic lesions in the liver: Molecular insights and relevance for clinical practice. Liver International. 2022;42(3):492-506.
357. Dasgupta A. 1 - Alcohol a double-edged sword: Health benefits with moderate consumption but a health hazard with excess alcohol intake. In: Dasgupta A, editor. Alcohol, Drugs, Genes and the Clinical Laboratory: Academic Press; 2017. p. 1-21.
358. Boujedidi H, Bouchet-Delbos L, Cassard-Doulcier AM, Njiké-Nakseu M, Maitre S, Prévot S, et al. Housekeeping gene variability in the liver of alcoholic patients. Alcohol Clin Exp Res. 2012;36(2):258-66.
359. Baggiolini M, Walz A, Kunkel SL. Neutrophil-activating peptide-1/interleukin 8, a novel cytokine that activates neutrophils. J Clin Invest. 1989;84(4):1045-9.
360. Endo S, Inada K, Ceska M, Takakuwa T, Yamada Y, Nakae H, et al. Plasma interleukin 8 and polymorphonuclear leukocyte elastase concentrations in patients with septic shock. J Inflamm. 1995;45(2):136-42.
361. National Library of Medicine (US), National Center for Biotechnology Information. Gene [Internet]. Bethesda (MD)2004 [[cited 2023 March 16]. Available from: https://www.ncbi.nlm.nih.gov/gene/.
362. Markiewski MM, Lambris JD. The Role of Complement in Inflammatory Diseases From Behind the Scenes into the Spotlight. The American Journal of Pathology. 2007;171(3):715-27.
363. Bierut LJ, Goate AM, Breslau N, Johnson EO, Bertelsen S, Fox L, et al. ADH1B is associated with alcohol dependence and alcohol consumption in populations of European and African ancestry. Molecular Psychiatry. 2012;17(4):445-50.

364. Pochareddy S, Edenberg HJ. Chronic Alcohol Exposure Alters Gene Expression in HepG2 Cells. Alcohol: Clinical and Experimental Research. 2012;36(6):1021-33.
365. Dolganiuc A, Szabo G. In vitro and in vivo models of acute alcohol exposure. World J Gastroenterol. 2009;15(10):1168-77.
366. Wang S, Wang X, Tan Z, Su Y, Liu J, Chang M, et al. Human ESC-derived expandable hepatic organoids enable therapeutic liver repopulation and pathophysiological modeling of alcoholic liver injury. Cell Res. 2019;29(12):1009-26.
367. Angireddy R, Chowdhury AR, Zielonka J, Ruthel G, Kalyanaraman B, Avadhani NG. Alcohol-induced CYP2E1, mitochondrial dynamics and retrograde signaling in human hepatic 3D organoids. Free Radical Biology and Medicine. 2020;159:1-14.
368. Tian L, Prasad N, Jang Y-Y. In Vitro Modeling of Alcohol-Induced Liver Injury Using Human-Induced Pluripotent Stem Cells. Methods Mol Biol: Springer New York; 2014. p. 271-83.
369. Olson KN, Smith SW, Kloss JS, Ho JD, Apple FS. Relationship Between Blood Alcohol Concentration and Observable Symptoms of Intoxication in Patients Presenting to an Emergency Department. Alcohol and Alcoholism. 2013;48(4):386-9.
370. Forsyth CB, Shaikh M, Bishehsari F, Swanson G, Voigt RM, Dodiya H, et al. Alcohol Feeding in Mice Promotes Colonic Hyperpermeability and Changes in Colonic Organoid Stem Cell Fate. Alcohol Clin Exp Res. 2017;41(12):2100-13.
371. Stueck AE, Wanless IR. Hepatocyte buds derived from progenitor cells repopulate regions of parenchymal extinction in human cirrhosis. Hepatology. 2015;61(5):1696-707.
372. Guan X, Rubin E, Anni H. An optimized method for the measurement of acetaldehyde by high-performance liquid chromatography. Alcohol Clin Exp Res. 2012;36(3):398-405.
373. Reeves AG, Subbarao M, Lippert AR. Imaging acetaldehyde formation during ethanol metabolism in living cells using a hydrazinyl naphthalimide fluorescent probe. Analytical Methods. 2017;9(23):3418-21.
374. Bell CC, Dankers ACA, Lauschke VM, Sison-Young R, Jenkins R, Rowe C, et al. Comparison of Hepatic 2D Sandwich Cultures and 3D Spheroids for Long-term Toxicity Applications: A Multicenter Study. Toxicol Sci. 2018;162(2):655-66.
375. Yokoyama T, Komori A, Nakamura M, Takii Y, Kamihira T, Shimoda S, et al. Human intrahepatic biliary epithelial cells function in innate immunity by producing IL-6 and IL-8 via the TLR4-NF-kappaB and -MAPK signaling pathways. Liver Int. 2006;26(4):467-76.
376. Isse K, Harada K, Nakanuma Y. IL-8 expression by biliary epithelial cells is associated with neutrophilic infiltration and reactive bile ductules. Liver International. 2007;27(5):672-80.
377. Matsumura T, Ito A, Takii T, Hayashi H, Onozaki K. Endotoxin and cytokine regulation of toll-like receptor (TLR) 2 and TLR4 gene expression in murine liver and hepatocytes. J Interferon Cytokine Res. 2000;20(10):915-21.
378. Geiser T, Dewald B, Ehrengruber MU, Clark-Lewis I, Baggiolini M. The interleukin-8-related chemotactic cytokines GRO alpha, GRO beta, and GRO gamma activate human neutrophil and basophil leukocytes. J Biol Chem. 1993;268(21):15419-24.
379. Walz A, Burgener R, Car B, Baggiolini M, Kunkel SL, Strieter RM. Structure and neutrophil-activating properties of a novel inflammatory peptide (ENA-78) with homology to interleukin 8. J Exp Med. 1991;174(6):1355-62.

380. Liu LZ, Zhang Z, Zheng BH, Shi Y, Duan M, Ma LJ, et al. CCL15 Recruits Suppressive Monocytes to Facilitate Immune Escape and Disease Progression in Hepatocellular Carcinoma. Hepatology. 2019;69(1):143-59.
381. Hernandez-Segura A, Nehme J, Demaria M. Hallmarks of Cellular Senescence. Trends in Cell Biology. 2018;28(6):436-53.
382. González-Gualda E, Baker AG, Fruk L, Muñoz-Espín D. A guide to assessing cellular senescence in vitro and in vivo. The FEBS Journal. 2021;288(1):56-80.
383. Wlazlo N, van Greevenbroek MM, Ferreira I, Jansen EH, Feskens EJ, van der Kallen CJ, et al. Activated complement factor 3 is associated with liver fat and liver enzymes: the CODAM study. Eur J Clin Invest. 2013;43(7):679-88.
384. Baumann M, Witzke O, Canbay A, Patschan S, Treichel U, Gerken G, et al. Serum C3 complement concentrations correlate with liver function in patients with liver cirrhosis. Hepatogastroenterology. 2004;51(59):1451-3.
385. Bykov I, Junnikkala S, Pekna M, Lindros KO, Meri S. Complement C3 contributes to ethanol-induced liver steatosis in mice. Annals of Medicine. 2006;38(4):280-6.
386. Pritchard MT, McMullen MR, Stavitsky AB, Cohen JI, Lin F, Edward Medof M, et al. Differential contributions of C3, C5, and decay-accelerating factor to ethanol-induced fatty liver in mice. Gastroenterology. 2007;132(3):1117-26.
387. Altorjay I, Vitalis Z, Tornai I, Palatka K, Kacska S, Farkas G, et al. Mannose-binding lectin deficiency confers risk for bacterial infections in a large Hungarian cohort of patients with liver cirrhosis. J Hepatol. 2010;53(3):484-91.
388. Shen H, French BA, Liu H, Tillman BC, French SW. Increased activity of the complement system in the liver of patients with alcoholic hepatitis. Exp Mol Pathol. 2014;97(3):338-44.
389. Lubbers R, van Essen MF, van Kooten C, Trouw LA. Production of complement components by cells of the immune system. Clin Exp Immunol. 2017;188(2):183-94.
390. Camous L, Roumenina L, Bigot S, Brachemi S, Frémeaux-Bacchi V, Lesavre P, et al. Complement alternative pathway acts as a positive feedback amplification of neutrophil activation. Blood. 2011;117(4):1340-9.
391. Guo Z, Chen J, Zeng Y, Wang Z, Yao M, Tomlinson S, et al. Complement Inhibition Alleviates Cholestatic Liver Injury Through Mediating Macrophage Infiltration and Function in Mice. Frontiers in Immunology. 2022;12.
392. Høgåsen AK, Würzner R, Abrahamsen TG, Dierich MP. Human polymorphonuclear leukocytes store large amounts of terminal complement components C7 and C6, which may be released on stimulation. J Immunol. 1995;154(9):4734-40.
393. Hou W, Janech MG, Sobolesky PM, Bland AM, Samsuddin S, Alazawi W, et al. Proteomic screening of plasma identifies potential noninvasive biomarkers associated with significant/advanced fibrosis in patients with nonalcoholic fatty liver disease. Biosci Rep. 2020;40(1).
394. Fan X, McCullough RL, Huang E, Bellar A, Kim A, Poulsen KL, et al. Diagnostic and Prognostic Significance of Complement in Patients With Alcohol-Associated Hepatitis. Hepatology. 2021;73(3):983-97.
395. Muinonen-Martin AJ, Veltman DM, Kalna G, Insall RH. An improved chamber for direct visualisation of chemotaxis. PLoS One. 2010;5(12):e15309.

396. Takeuchi M, Vidigal PT, Guerra MT, Hundt MA, Robert ME, Olave-Martinez M, et al. Neutrophils interact with cholangiocytes to cause cholestatic changes in alcoholic hepatitis. Gut. 2021;70(2):342-56.
397. de Bont CM, Boelens WC, Pruijn GJM. NETosis, complement, and coagulation: a triangular relationship. Cell Mol Immunol. 2019;16(1):19-27.
398. Martinelli S, Urosevic M, Daryadel A, Oberholzer PA, Baumann C, Fey MF, et al. Induction of genes mediating interferon-dependent extracellular trap formation during neutrophil differentiation. J Biol Chem. 2004;279(42):44123-32.
399. Zaborowski MP, Balaj L, Breakefield XO, Lai CP. Extracellular Vesicles: Composition, Biological Relevance, and Methods of Study. Bioscience. 2015;65(8):783-97.
400. Brandel V, Schimek V, Göber S, Hammond T, Brunnthaler L, Schrottmaier WC, et al. Hepatectomy-induced apoptotic extracellular vesicles stimulate neutrophils to secrete regenerative growth factors. J Hepatol. 2022;77(6):1619-30.
401. Wang L, Zhu Z, Liao Y, Zhang L, Yu Z, Yang R, et al. Host liver-derived extracellular vesicles deliver miR-142a-3p induces neutrophil extracellular traps via targeting WASL to block the development of Schistosoma japonicum. Mol Ther. 2022;30(5):2092-107.
402. Abdollahi S. Extracellular vesicles from organoids and 3D culture systems. Biotechnol Bioeng. 2021;118(3):1029-49.
403. Office for National Statistics (ONS). Alcohol-specific deaths in the UK: registered in 2021 [Internet]. 2022 [[cited 2023 January 21]. Available from: https://www.ons.gov.uk/peoplepopulationandcommunity/birthsdeathsandmarriages/deaths/bulletins/alcoholspecificdeathsintheuk/2021registrations.
404. Wilkin RJW, Lalor PF, Parker R, Newsome PN. Murine Models of Acute Alcoholic Hepatitis and Their Relevance to Human Disease. The American Journal of Pathology. 2016;186(4):748-60.
405. Woolbright BL, Jaeschke H. Alcoholic Hepatitis: Lost in Translation. J Clin Transl Hepatol. 2018;6(1):89-96.
406. Furuya S, Argemi J, Uehara T, Katou Y, Fouts DE, Schnabl B, et al. A Novel Mouse Model of Acute-on-Chronic Cholestatic Alcoholic Liver Disease: A Systems Biology Comparison With Human Alcoholic Hepatitis. Alcohol Clin Exp Res. 2020;44(1):87-101.
407. Dubuquoy L, Louvet A, Lassailly G, Truant S, Boleslawski E, Artru F, et al. Progenitor cell expansion and impaired hepatocyte regeneration in explanted livers from alcoholic hepatitis. Gut. 2015;64(12):1949-60.
408. Hu H, Gehart H, Artegiani B, LÖpez-Iglesias C, Dekkers F, Basak O, et al. Long-Term Expansion of Functional Mouse and Human Hepatocytes as 3D Organoids. Cell. 2018;175(6):1591-606.e19.
409. Suh YG, Jeong WI. Hepatic stellate cells and innate immunity in alcoholic liver disease. World J Gastroenterol. 2011;17(20):2543-51.
410. Arab JP, Cabrera D, Sehrawat TS, Jalan-Sakrikar N, Verma VK, Simonetto D, et al. Hepatic stellate cell activation promotes alcohol-induced steatohepatitis through Igfbp3 and SerpinA12. Journal of Hepatology. 2020;73(1):149-60.
411. Method of the Year 2017: Organoids. Nature Methods. 2018;15(1):1.
412. STEMCELL Technologies. Cryopreserving Human Liver Tissue for Organoid Culture [Internet]. 2021 [[cited 2023 February 25]. Available from:

https://www.stemcell.com/technical-resources/cryopreserving-hepatic-tissue-for-organoid-culture.html.
413. Lauschke VM, Shafagh RZ, Hendriks DFG, Ingelman-Sundberg M. 3D Primary Hepatocyte Culture Systems for Analyses of Liver Diseases, Drug Metabolism, and Toxicity: Emerging Culture Paradigms and Applications. Biotechnology Journal. 2019;14(7):1800347.
414. Tibbitt MW, Anseth KS. Hydrogels as extracellular matrix mimics for 3D cell culture. Biotechnol Bioeng. 2009;103(4):655-63.
415. Caliari SR, Burdick JA. A practical guide to hydrogels for cell culture. Nature Methods. 2016;13(5):405-14.
416. Kleinman HK, Martin GR. Matrigel: Basement membrane matrix with biological activity. Seminars in Cancer Biology. 2005;15(5):378-86.
417. Kang N. Mechanotransduction in Liver Diseases. Semin Liver Dis. 2020;40(1):84-90.
418. Xia T, Zhao R, Feng F, Yang L. The Effect of Matrix Stiffness on Human Hepatocyte Migration and Function-An In Vitro Research. Polymers (Basel). 2020;12(9).
419. Das P, DiVito MD, Wertheim JA, Tan LP. Bioengineered 3D electrospun nanofibrous scaffold with human liver cells to study alcoholic liver disease in vitro. Integrative Biology. 2021;13(7):184-95.
420. Ravichandran A, Murekatete B, Moedder D, Meinert C, Bray LJ. Photocrosslinkable liver extracellular matrix hydrogels for the generation of 3D liver microenvironment models. Sci Rep. 2021;11(1):15566.
421. Giobbe GG, Crowley C, Luni C, Campinoti S, Khedr M, Kretzschmar K, et al. Extracellular matrix hydrogel derived from decellularized tissues enables endodermal organoid culture. Nature Communications. 2019;10(1):5658.
422. Willemse J, van Tienderen G, van Hengel E, Schurink I, van der Ven D, Kan Y, et al. Hydrogels derived from decellularized liver tissue support the growth and differentiation of cholangiocyte organoids. Biomaterials. 2022;284:121473.
423. Shepherd EL, Northall E, Papakyriacou P, Safranska K, Sorensen K, Lalor PF. Hepatic Stellate Cells: Methods and Protocols. In: Ralf Weiskirchen and Scott L. Friedman, editor. Methods in Molecular Biology: Springer Nature; (In Press).
424. Au SH, Chamberlain MD, Mahesh S, Sefton MV, Wheeler AR. Hepatic organoids for microfluidic drug screening. Lab Chip. 2014;14(17):3290-9.
425. Marsee A, Roos FJM, Verstegen MMA, Marsee A, Roos F, Verstegen M, et al. Building consensus on definition and nomenclature of hepatic, pancreatic, and biliary organoids. Cell Stem Cell. 2021;28(5):816-32.
426. Bock C, Boutros M, Camp JG, Clarke L, Clevers H, Knoblich JA, et al. The Organoid Cell Atlas. Nat Biotechnol. 2021;39(1):13-7.
427. Kim J, Koo BK, Knoblich JA. Human organoids: model systems for human biology and medicine. Nat Rev Mol Cell Biol. 2020;21(10):571-84.
428. Berg HF, Hjelmeland ME, Lien H, Espedal H, Fonnes T, Srivastava A, et al. Patient-derived organoids reflect the genetic profile of endometrial tumors and predict patient prognosis. Communications Medicine. 2021;1(1):20.
429. Narasimhan V, Wright JA, Churchill M, Wang T, Rosati R, Lannagan TRM, et al. Medium-throughput Drug Screening of Patient-derived Organoids from Colorectal Peritoneal Metastases to Direct Personalized Therapy. Clin Cancer Res. 2020;26(14):3662-70.

430. Schulze K, Nault J-C, Villanueva A. Genetic profiling of hepatocellular carcinoma using next-generation sequencing. Journal of Hepatology. 2016;65(5):1031-42.
431. Berkers G, van Mourik P, Vonk AM, Kruisselbrink E, Dekkers JF, de Winter-de Groot KM, et al. Rectal Organoids Enable Personalized Treatment of Cystic Fibrosis. Cell Rep. 2019;26(7):1701-8.e3.
432. Jan J, Osho A, Murphy CC, Mazure CM, Singal AG, Rich NE. Gender, Age, Racial and Ethnic Disparities in Clinical Trial Enrollment for Primary Liver Cancer. Gastroenterology. 2022;163(1):14-20.e2.
433. Jinek M, Chylinski K, Fonfara I, Hauer M, Doudna JA, Charpentier E. A programmable dual-RNA-guided DNA endonuclease in adaptive bacterial immunity. Science. 2012;337(6096):816-21.
434. Hendriks D, Artegiani B, Hu H, Chuva de Sousa Lopes S, Clevers H. Establishment of human fetal hepatocyte organoids and CRISPR–Cas9-based gene knockin and knockout in organoid cultures from human liver. Nature Protocols. 2021;16(1):182-217.
435. Artegiani B, Hendriks D, Beumer J, Kok R, Zheng X, Joore I, et al. Fast and efficient generation of knock-in human organoids using homology-independent CRISPR–Cas9 precision genome editing. Nature Cell Biology. 2020;22(3):321-31.
436. Ramakrishna G, Babu PE, Singh R, Trehanpati N. Application of CRISPR-Cas9 based gene editing to study the pathogenesis of colon and liver cancer using organoids. Hepatology International. 2021;15(6):1309-17.
437. Olson H, Betton G, Robinson D, Thomas K, Monro A, Kolaja G, et al. Concordance of the toxicity of pharmaceuticals in humans and in animals. Regul Toxicol Pharmacol. 2000;32(1):56-67.
438. Martignoni M, Groothuis GM, de Kanter R. Species differences between mouse, rat, dog, monkey and human CYP-mediated drug metabolism, inhibition and induction. Expert Opin Drug Metab Toxicol. 2006;2(6):875-94.
439. Renner H, Grabos M, Becker KJ, Kagermeier TE, Wu J, Otto M, et al. A fully automated high-throughput workflow for 3D-based chemical screening in human midbrain organoids. eLife. 2020;9:e52904.
440. Hsia GSP, Esposito J, da Rocha LA, Ramos SLG, Okamoto OK. Clinical Application of Human Induced Pluripotent Stem Cell-Derived Organoids as an Alternative to Organ Transplantation. Stem Cells Int. 2021;2021:6632160.
441. Reza HA, Okabe R, Takebe T. Organoid transplant approaches for the liver. Transplant International. 2021;34(11):2031-45.
442. Meran L, Massie I, Campinoti S, Weston AE, Gaifulina R, Tullie L, et al. Engineering transplantable jejunal mucosal grafts using patient-derived organoids from children with intestinal failure. Nature Medicine. 2020;26(10):1593-601.
443. Lu WY, Bird TG, Boulter L, Tsuchiya A, Cole AM, Hay T, et al. Hepatic progenitor cells of biliary origin with liver repopulation capacity. Nat Cell Biol. 2015;17(8):971-83.
444. Schreurs R, Baumdick ME, Drewniak A, Bunders MJ. In vitro co-culture of human intestinal organoids and lamina propria-derived CD4(+) T cells. STAR Protoc. 2021;2(2):100519.
445. Cattaneo CM, Dijkstra KK, Fanchi LF, Kelderman S, Kaing S, van Rooij N, et al. Tumor organoid-T-cell coculture systems. Nat Protoc. 2020;15(1):15-39.

446. Staab JF, Lemme-Dumit JM, Latanich R, Pasetti MF, Zachos NC. Co-Culture System of Human Enteroids/Colonoids with Innate Immune Cells. Curr Protoc Immunol. 2020;131(1):e113.
447. Lemme-Dumit JM, Doucet M, Zachos NC, Pasetti MF. Epithelial and Neutrophil Interactions and Coordinated Response to Shigella in a Human Intestinal Enteroid-Neutrophil Coculture Model. mBio. 2022;13(3):e0094422.
448. Takebe T, Sekine K, Enomura M, Koike H, Kimura M, Ogaeri T, et al. Vascularized and functional human liver from an iPSC-derived organ bud transplant. Nature. 2013;499(7459):481-4.
449. Leeman KT, Pessina P, Lee JH, Kim CF. Mesenchymal Stem Cells Increase Alveolar Differentiation in Lung Progenitor Organoid Cultures. Sci Rep. 2019;9(1):6479.
450. Zhao H, Jiang E, Shang Z. 3D Co-culture of Cancer-Associated Fibroblast with Oral Cancer Organoids. J Dent Res. 2021;100(2):201-8.
451. Koledova Z, Lu P. A 3D Fibroblast-Epithelium Co-culture Model for Understanding Microenvironmental Role in Branching Morphogenesis of the Mammary Gland. Methods Mol Biol. 2017;1501:217-31.
452. Park JH, Jung IK, Lee Y, Jin S, Yun HJ, Kim BW, et al. Alcohol stimulates the proliferation of mouse small intestinal epithelial cells via Wnt signaling. Biochem Biophys Res Commun. 2021;534:639-45.
453. Lu R, Voigt RM, Zhang Y, Kato I, Xia Y, Forsyth CB, et al. Alcohol Injury Damages Intestinal Stem Cells. Alcohol Clin Exp Res. 2017;41(4):727-34.
454. Arzua T, Yan Y, Jiang C, Logan S, Allison RL, Wells C, et al. Modeling alcohol-induced neurotoxicity using human induced pluripotent stem cell-derived three-dimensional cerebral organoids. Transl Psychiatry. 2020;10(1):347.
455. Shek D, Chen D, Read SA, Ahlenstiel G. Examining the gut-liver axis in liver cancer using organoid models. Cancer Lett. 2021;510:48-58.
456. Ronaldson-Bouchard K, Teles D, Yeager K, Tavakol DN, Zhao Y, Chramiec A, et al. A multi-organ chip with matured tissue niches linked by vascular flow. Nature Biomedical Engineering. 2022;6(4):351-71.
457. Nawroth JC, Petropolis DB, Manatakis DV, Maulana TI, Burchett G, Schlünder K, et al. Modeling alcohol-associated liver disease in a human Liver-Chip. Cell Rep. 2021;36(3):109393.
458. Prot JM, Aninat C, Griscom L, Razan F, Brochot C, Guillouzo CG, et al. Improvement of HepG2/C3a cell functions in a microfluidic biochip. Biotechnol Bioeng. 2011;108(7):1704-15.
459. Ewart L, Apostolou A, Briggs SA, Carman CV, Chaff JT, Heng AR, et al. Performance assessment and economic analysis of a human Liver-Chip for predictive toxicology. Communications Medicine. 2022;2(1):154.
460. Sakabe K, Takebe T, Asai A. Organoid Medicine in Hepatology. Clinical Liver Disease. 2020;15(1):3-8.
461. Murad M, Low L, Davidson M, Murray PI, Rauz S, Wallace GR. Low density neutrophils are increased in patients with Behçet's disease but do not explain differences in neutrophil function. Journal of Inflammation. 2022;19(1):5.
462. Schoppmeyer R, Zhao R, Hoth M, Qu B. Light-sheet Microscopy for Three-dimensional Visualization of Human Immune Cells. J Vis Exp. 2018(136):e57651.
463. Rios AC, Clevers H. Imaging organoids: a bright future ahead. Nat Methods. 2018;15(1):24-6.

464. Dekkers JF, Alieva M, Wellens LM, Ariese HCR, Jamieson PR, Vonk AM, et al. High-resolution 3D imaging of fixed and cleared organoids. Nature Protocols. 2019;14(6):1756-71.
465. Kip AM, Soons Z, Mohren R, Duivenvoorden AAM, Röth AAJ, Cillero-Pastor B, et al. Proteomics analysis of human intestinal organoids during hypoxia and reoxygenation as a model to study ischemia-reperfusion injury. Cell Death & Disease. 2021;12(1):95.
466. Elbadawy M, Yamanaka M, Goto Y, Hayashi K, Tsunedomi R, Hazama S, et al. Efficacy of primary liver organoid culture from different stages of non-alcoholic steatohepatitis (NASH) mouse model. Biomaterials. 2020;237:119823.
467. Gonzalez HC, Zhou Y, Nimri FM, Rupp LB, Trudeau S, Gordon SC. Alcohol-related hepatitis admissions increased 50% in the first months of the COVID-19 pandemic in the USA. Liver International. 2022;42(4):762-4.